ROLE OF MITOCHONDRIA-ASSOCIATED NON-CODING RNAs IN INTRACELLULAR COMMUNICATION

EDITED BY: Samarjit Das, Eleonora Leucci, Eric Barrey, Nina Entelis, John Hollander and Veronica Andrea Burzio

PUBLISHED IN: Frontiers in Physiology and Frontiers in Cell and Developmental Biology

frontiers Research Topics

ISSN 1664-8714
ISBN 978-2-83250-131-3
DOI 10.3389/978-2-83250-131-3

About Frontiers

Frontiers is more than just an open-access publisher of scholarly articles: it is a pioneering approach to the world of academia, radically improving the way scholarly research is managed. The grand vision of Frontiers is a world where all people have an equal opportunity to seek, share and generate knowledge. Frontiers provides immediate and permanent online open access to all its publications, but this alone is not enough to realize our grand goals.

Frontiers Journal Series

The Frontiers Journal Series is a multi-tier and interdisciplinary set of open-access, online journals, promising a paradigm shift from the current review, selection and dissemination processes in academic publishing. All Frontiers journals are driven by researchers for researchers; therefore, they constitute a service to the scholarly community. At the same time, the Frontiers Journal Series operates on a revolutionary invention, the tiered publishing system, initially addressing specific communities of scholars, and gradually climbing up to broader public understanding, thus serving the interests of the lay society, too.

Dedication to Quality

Each Frontiers article is a landmark of the highest quality, thanks to genuinely collaborative interactions between authors and review editors, who include some of the world's best academicians. Research must be certified by peers before entering a stream of knowledge that may eventually reach the public - and shape society; therefore, Frontiers only applies the most rigorous and unbiased reviews.
Frontiers revolutionizes research publishing by freely delivering the most outstanding research, evaluated with no bias from both the academic and social point of view. By applying the most advanced information technologies, Frontiers is catapulting scholarly publishing into a new generation.

What are Frontiers Research Topics?

Frontiers Research Topics are very popular trademarks of the Frontiers Journals Series: they are collections of at least ten articles, all centered on a particular subject. With their unique mix of varied contributions from Original Research to Review Articles, Frontiers Research Topics unify the most influential researchers, the latest key findings and historical advances in a hot research area! Find out more on how to host your own Frontiers Research Topic or contribute to one as an author by contacting the Frontiers Editorial Office: frontiersin.org/about/contact

ROLE OF MITOCHONDRIA-ASSOCIATED NON-CODING RNAs IN INTRACELLULAR COMMUNICATION

Topic Editors:
Samarjit Das, Johns Hopkins University, United States
Eleonora Leucci, KU Leuven, Belgium
Eric Barrey, INRA UMR1313 Genetique Animale et Biologie Integrative, France
Nina Entelis, Génomique et Microbiologie (GMGM), France
John Hollander, West Virginia University, United States
Veronica Andrea Burzio, Andres Bello University, Chile

Citation: Das, S., Leucci, E., Barrey, E., Entelis, N., Hollander, J., Burzio, V. A., eds. (2022). Role of Mitochondria-Associated Non-Coding RNAs in Intracellular Communication. Lausanne: Frontiers Media SA. doi: 10.3389/978-2-83250-131-3

Table of Contents

frontiers | Frontiers in Physiology

TYPE Editorial
PUBLISHED 22 August 2022
DOI 10.3389/fphys.2022.980674

OPEN ACCESS

EDITED AND REVIEWED BY
Amadou K. S. Camara,
Medical College of Wisconsin,
United States

*CORRESPONDENCE
Samarjit Das,
sdas11@jhmi.edu

SPECIALTY SECTION
This article was submitted to Mitochondrial Research, a section of the journal Frontiers in Physiology

RECEIVED 28 June 2022
ACCEPTED 26 July 2022
PUBLISHED 22 August 2022

CITATION
Burzio VA, Barrey E, Leucci E, Entelis N, Hollander JM and Das S (2022), Editorial: Role of mitochondria-associated non-coding RNAs in intracellular communication. *Front. Physiol.* 13:980674. doi: 10.3389/fphys.2022.980674

Editorial: Role of mitochondria-associated non-coding RNAs in intracellular communication

Veronica A. Burzio[1], Eric Barrey[2], Eleonora Leucci[3], Nina Entelis[4], John M. Hollander[5] and Samarjit Das[6,7]*

[1]Centro Ciencia and Vida, Andes Biotechnologies SpA, Universidad Andrés Bello, Santiago, Chile, [2]Université Paris-Saclay, AgroParisTech, INRAE, GABI, Jouy-en-Josas, France, [3]Laboratory for RNA Cancer Biology, Department of Oncology, Katholieke Universiteit Leuven, Leuven, Belgium, [4]UMR 7156 GMGM Strasbourg University–CNRS, Strasbourg, France, [5]Division of Exercise Physiology, and Mitochondria, Metabolism & Bioenergetics Working Group, West Virginia University School of Medicine, Morgantown, WV, United States, [6]Department of Pathology and Critical Care Medicine, Johns Hopkins School of Medicine, Baltimore, MD, United States, [7]Department of Anesthesiology and Critical Care Medicine, Johns Hopkins School of Medicine, Baltimore, MD, United States

KEYWORDS

non-coding RNAs, microRNA, LncRNA–long noncoding RNA, mitochondria, intracellular communication, human health

Editorial on the Research Topic
Role of mitochondria-associated non-coding RNAs in intracellular communication

Once considered solely as the powerhouse of eukaryotic cells, the mitochondrion is now known to be a hub for several other important cellular processes such as apoptosis, calcium homeostasis, regulation of innate immunity, amino acid metabolism, stem cell regulation and the cellular regulome, among others (Murphy and Steenbergen, 2011). Some of these functions are accounted for by the minimal circular 16,569-bp genome of human mitochondria (mtDNA), which contains the genes for 2 rRNAs, 22 tRNAs and 13 polypeptides (Chen et al., 2009). However, most mitochondrial proteins are nuclear-encoded and imported from the cytosol (Neupert and Herrmann, 2007). Lately, there is increasing evidence of bidirectional communication between mitochondria and the nucleus, coordinating multiple cellular functions (Soledad et al., 2019). This connection, nonetheless, is not limited to mitochondrial import of nuclear-encoded proteins and export of metabolites, but has also been shown to involve noncoding RNAs (ncRNAs) connecting both cellular compartments (Baradan et al., 2017; Macgregor-Das and Das, 2018; Soledad et al., 2019). Long noncoding RNAs (lncRNAs), as well as microRNAs (miRNAs) have been found inside mitochondria, both originating from the mtDNA (Mach et al., 2016; Fitzpatrick et al., 2019) and from the nucleus (Bandiera et al., 2011; Barrey et al., 2011). These mitochondria-associated ncRNAs have been shown to participate in intracellular communication, not only with the nucleus, but also with other

cellular compartments (Srinivasan and Das, 2015; Baradan et al., 2017). Elucidation of the communication between mitochondria and the rest of the cell will constitute a very important piece in the grand puzzle of cellular homeostasis and pathogenesis.

Since the identification of miRNAs in the mitochondrial compartment in early 2011 (Barrey et al., 2011; Das et al., 2012), a myriad of publications on this Research Topic were produced in many cellular models and several mammalian species including human, mouse, rat and horse. Most of these reports provide novel information about how these ncRNAs within mitochondria modulate cellular function. Recent advancements in RNA-sequencing technology have enticed new researchers to begin investigating mitochondrial ncRNAs. Therefore, there is a great need for basic information and standardized guidelines, such as normalization controls and mitochondrial isolation procedures, to conduct rigorous research in this field. Here, we have gathered a great Research Topic of studies and review articles for the broader community, including areas that require further research and validation.

For this Research Topic, Liu and Shan presented a comprehensive review on mtDNA-encoded ncRNAs where they discussed the roles that ncRNAs play in cellular pathophysiology and the bi-directional communication between mitochondria and the nucleus. In another review, Giordani et al. have focused on small ncRNAs (mainly microRNAs) that are present in the mitochondrial compartment. These microRNAs are called "mitomiRs." The authors discussed the emerging roles of mitomiRs in the bi-directional communication between mitochondria and the nucleus. In this article, the authors mainly focused on the role of mitomiRs in cellular metabolism, dynamics, and bioenergetics and how this could lead to the production of considerable amounts of reactive oxygen species (ROS) and increased mitochondrial permeability, which are among the hallmarks of cellular senescence. Huang et al. authored another review article where they discussed the cross-talk between mitochondria and other cellular organelles using ncRNAs as mediators. These authors summarized the implications of mitochondria-centric ncRNA trafficking with respects to cellular function.

This unique Research Topic of articles focusing on mitochondria-associated ncRNAs also includes original research articles which show the therapeutic potential of RNA transcripts that alter mitochondrial function as a means to provide protection against disease. For example, Rodrigues et al., demonstrate that intramuscular delivery of miR-1 reduces insulin resistance during obesity. It has been previously shown that miR-1 can translocate into the mitochondrion and alter mitochondrial gene expression. Furthermore, depending on the level of stress in skeletal myocytes, miR-1 can translocate into the mitochondrion from the cytoplasm and target mitochondrial mRNA (Zhang et al., 2014). These data could provide insight into the therapeutic potential of ncRNAs for obesity-induced skeletal muscle dysfunction (Rodrigues et al.). In another original study, Duroux-Richard et al. show that mitomiR therapeutics can be beneficial for macrophage differentiation, polarization, and function. The regulation of macrophage inflammatory pathways is governed specifically by mitomiRs and the implications in immune-mediated inflammatory disorders remain poorly understood. This study also suggests that this mitomiR-dependent control could be further enhanced through the transfer of mitochondria from donor to target cells, as a new strategy for mitomiR delivery. Mathuram et al. report that synthetic overexpression of a small ncRNA, mito-ncR-805, can increase Krebs cycle activity and mitochondrial OXPHOS, stabilize mitochondrial potential, accelerate cell division, and reduce the levels of the pro-apoptotic pseudokinase TRIB3. Previously, the same group identified mito-ncR-805 as being conserved in mammalian mitochondrial genomes, however there are shorter versions of mouse and human transcripts (mmu-CR805 and hsa-LDL1, respectively). Mito-ncR-805 acts as a retrograde signal between mitochondria to the nucleus (Blumental-Perry et al., 2020). In the present study, Mathuram et al. altered a functional sequence of the D-loop transcript, mito-ncR-805, and demonstrated that this could have a significant effect on cellular function. Nandi et al., using a rat model, both *in vitro* (H9c2 cell line) and *in vivo*, demonstrated that enhanced sympatho-excitation to the heart elicits cardiac miR-18a-5p/HIF-1α signaling that leads to mitochondrial abnormalities and consequential pathological cardiac remodeling. The goal of this study was to find a therapeutic option against hypertension-induced heart failure, as the hallmark of hypertensive heart disease are sympatho-excitation and cardiac mitochondrial abnormality. In this study, the authors identified the mechanism whereby miR-18a-5p can regulate ROS-induced mitochondrial transition pore opening via activation of pro-hypertrophy/fibrosis/inflammatory factors that induce pathological cardiac hypertrophy and fibrosis commonly observed in neurogenic hypertension (Nandi et al.).

Another interesting subject covered in this Research Topic is mitochondria-derived tRNA fragments (tRFs). This family of molecules was observed many years ago and were first thought to be degradation products of transcripts. However, with the advancement in sequencing technologies and meta-analysis of data, several groups have confirmed both the existence of tRFs in the cytoplasm and mitochondria, and more importantly, that they carry out biological functions. The review paper by Shaukat et al. provides general information on the types of tRF and their biological functions, with special focus on mitochondrial tRNA-derived fragments (mt-tRFs). The recent data on biogenesis of mt-tRFs and their putative functions are discussed in detail, taking into account the possible role of mt-tRNA modification patterns. Correlation of some mt-tRFs with specific human

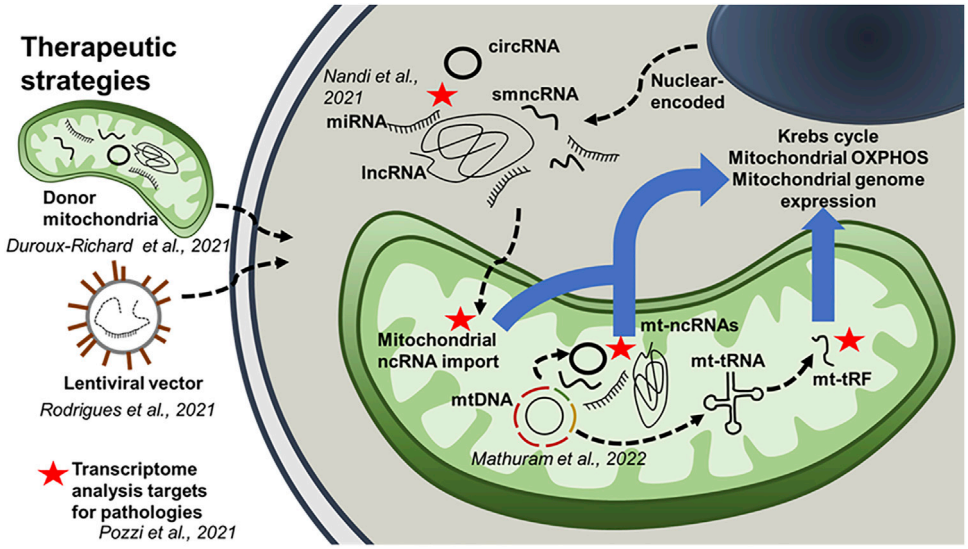

FIGURE 1
The role of mitochondria-associated ncRNAs. This schematic diagram integrates results obtained from the Research Topic of articles in this special edition. It highlights the potential role of mitochondria-associated ncRNAs in intracellular communication. The diagram also outlines several therapeutic strategies using ncRNAs.

disorders raises their potential as biomarkers for several types of cancer, some infections and neurodegenerative diseases caused by mtDNA mutations. To further validate the importance of point mutations on mt-tRFs, Meseguer and Rubio published an original research article, where they demonstrated that MELAS (mitochondrial encephalomyopathy, lactic acidosis, and stroke-like episodes) disease, caused by the m.3243A>G mutation in the mitochondrial tRNALeu (UUR) gene, is associated with changes in the expression levels of several mt-tRFs. Importantly, mt-tRF Leu (UUR) mimic partially restored mitochondrial respiration in MELAS cybrid cells, which indicates the therapeutic and diagnostic potential of mt-tRFs. The authors also identified that Dicer and Ago2, two essential proteins in miRNA maturation and function, play an important role in mt-tRF biogenesis.

Finally, this Research Topic also incorporates a study related to the current ongoing SARS-CoV-2 pandemic. Pozzi performed an *in silico* analysis (Pozzi) and identified potential mitochondrial ncRNAs that could play an important role in the pathogenesis of SARS-CoV-2 replication and propagation, which could potentially underlie the basis for long COVID syndrome. More research is needed to better understand whether mitochondrial ncRNA(s) may lead to potential therapeutics for SARS-CoV-2 infection but this study serves as a basis for understanding the pathological mechanisms of SARS-CoV-2.

We hope the reader finds this editorial and the articles it references to be useful in understanding the current state of the field regarding mitochondria-associated ncRNAs and their roles in intracellular communication, undoubtedly mediated by a myriad of long and small ncRNAs (Figure 1). Further studies into these processes will shed light on which pathways are involved in the mechanisms underlying normal and pathological involvement of ncRNAs in the communication between mitochondria and other organelles, particularly the nucleus. Ultimately, the expansion of our knowledge on these cellular events will lay the groundwork for the development of potential therapeutic strategies for different human pathologies.

Author contributions

All authors listed have made a substantial, direct, and intellectual contribution to the work and approved it for publication.

Funding

This work was supported by NIH grants U54AG062333 and U18TR003780 (SD), HL128485 (JH) as well as the Community Foundation for the Ohio Valley Whipkey Trust (JH). Funding was also provided by ANID, Chile (Fondecyt 1140345 and BASAL/FB210008) and Universidad Andrés Bello, Chile (DI-05-20/REG) (VB). NE was supported by the IdEx Unistra (ANR-10-IDEX-0002) and EUR IMCBio (ANR17-EURE-0023).

Acknowledgments

We would like to acknowledge Andrew Taylor who contributed the artwork for the figure in the manuscript.

Conflict of interest

The authors declare that the research was conducted in the absence of any commercial or financial relationships that could be construed as a potential conflict of interest.

Publisher's note

All claims expressed in this article are solely those of the authors and do not necessarily represent those of their affiliated organizations, or those of the publisher, the editors and the reviewers. Any product that may be evaluated in this article, or claim that may be made by its manufacturer, is not guaranteed or endorsed by the publisher.

References

Bandiera, S., Ruberg, S., Girard, M., Cagnard, N., Hanein, S., Chretien, D., et al. (2011). Nuclear outsourcing of RNA interference components to human mitochondria. *PLoS One* 6, e20746. doi:10.1371/journal.pone.0020746

Baradan, R., Hollander, J. M., and Das, S. (2017). Mitochondrial miRNAs in diabetes: Just the tip of the iceberg. *Can. J. Physiol. Pharmacol.* 95, 1156–1162. doi:10.1139/cjpp-2016-0580

Barrey, E., Saint-Auret, G., Bonnamy, B., Damas, D., Boyer, O., and Gidrol, X. (2011). Pre-microRNA and mature microRNA in human mitochondria. *PLoS One* 6, e20220. doi:10.1371/journal.pone.0020220

Blumental-Perry, A., Jobava, R., Bederman, I., Degar, A. J., Kenche, H., Guan, B. J., et al. (2020). Retrograde signaling by a mtDNA-encoded non-coding RNA preserves mitochondrial bioenergetics. *Commun. Biol.* 3, 626. doi:10.1038/s42003-020-01322-4

Chen, J. Q., Cammarata, P. R., Baines, C. P., and Yager, J. D. (2009). Regulation of mitochondrial respiratory chain biogenesis by estrogens/estrogen receptors and physiological, pathological and pharmacological implications. *Biochim. Biophys. Acta* 1793, 1540–1570. doi:10.1016/j.bbamcr.2009.06.001

Das, S., Ferlito, M., Kent, O. A., Fox-Talbot, K., Wang, R., Liu, D., et al. (2012). Nuclear miRNA regulates the mitochondrial genome in the heart. *Circ. Res.* 110, 1596–1603. doi:10.1161/CIRCRESAHA.112.267732

Fitzpatrick, C., Bendek, M. F., Briones, M., Farfan, N., Silva, V. A., Nardocci, G., et al. (2019). Mitochondrial ncRNA targeting induces cell cycle arrest and tumor growth inhibition of MDA-MB-231 breast cancer cells through reduction of key cell cycle progression factors. *Cell Death Dis.* 10, 423. doi:10.1038/s41419-019-1649-3

Macgregor-Das, A. M., and Das, S. (2018). A microRNA's journey to the center of the mitochondria. *Am. J. Physiol. Heart Circ. Physiol.* 315, H206–H215. doi:10.1152/ajpheart.00714.2017

Mach, N., Plancade, S., Pacholewska, A., Lecardonnel, J., Riviere, J., Moroldo, M., et al. (2016). Integrated mRNA and miRNA expression profiling in blood reveals candidate biomarkers associated with endurance exercise in the horse. *Sci. Rep.* 6, 22932. doi:10.1038/srep22932

Murphy, E., and Steenbergen, C. (2011). What makes the mitochondria a killer? Can we condition them to be less destructive? *Biochim. Biophys. Acta* 1813, 1302–1308. doi:10.1016/j.bbamcr.2010.09.003

Neupert, W., and Herrmann, J. M. (2007). Translocation of proteins into mitochondria. *Annu. Rev. Biochem.* 76, 723–749. doi:10.1146/annurev.biochem.76.052705.163409

Soledad, R. B., Charles, S., and Samarjit, D. (2019). The secret messages between mitochondria and nucleus in muscle cell biology. *Arch. Biochem. Biophys.* 666, 52–62. doi:10.1016/j.abb.2019.03.019

Srinivasan, H., and Das, S. (2015). Mitochondrial miRNA (MitomiR): A new player in cardiovascular health. *Can. J. Physiol. Pharmacol.* 93, 855–861. doi:10.1139/cjpp-2014-0500

Zhang, X., Zuo, X., Yang, B., Li, Z., Xue, Y., Zhou, Y., et al. (2014). MicroRNA directly enhances mitochondrial translation during muscle differentiation. *Cell* 158, 607–619. doi:10.1016/j.cell.2014.05.047

frontiers in Physiology

BRIEF RESEARCH REPORT
published: 06 July 2021
doi: 10.3389/fphys.2021.676265

Intramuscular Injection of miR-1 Reduces Insulin Resistance in Obese Mice

Alice C. Rodrigues[1], Alexandre R. Spagnol[1], Flávia de Toledo Frias[1], Mariana de Mendonça[1], Hygor N. Araújo[2,3], Dimitrius Guimarães[2,3], William J. Silva[4], Anaysa Paola Bolin[1], Gilson Masahiro Murata[5] and Leonardo Silveira[2,3]*

[1] Department of Pharmacology, Instituto de Ciencias Biomedicas, Universidade de São Paulo, São Paulo, Brazil, [2] Obesity and Comorbidities Research Center (OCRC), Campinas, Brazil, [3] Department of Structural and Functional Biology, Institute of Biology, University of Campinas (UNICAMP), Campinas, Brazil, [4] Department of Anatomy, Instituto de Ciencias Biomedicas, Universidade de São Paulo, São Paulo, Brazil, [5] Department of Medical Clinics, Faculty of Medicine, University of São Paulo, São Paulo, Brazil

The role of microRNAs in metabolic diseases has been recognized and modulation of them could be a promising strategy to treat obesity and obesity-related diseases. The major purpose of this study was to test the hypothesis that intramuscular miR-1 precursor replacement therapy could improve metabolic parameters of mice fed a high-fat diet. To this end, we first injected miR-1 precursor intramuscularly in high-fat diet-fed mice and evaluated glucose tolerance, insulin sensitivity, and adiposity. miR-1-treated mice did not lose weight but had improved insulin sensitivity measured by insulin tolerance test. Next, using an *in vitro* model of insulin resistance by treating C2C12 cells with palmitic acid (PA), we overexpressed miR-1 and measured p-Akt content and the transcription levels of a protein related to fatty acid oxidation. We found that miR-1 could not restore insulin sensitivity in C2C12 cells, as indicated by p-Akt levels and that miR-1 increased expression of *Pgc1a* and *Cpt1b* in PA-treated cells, suggesting a possible role of miR-1 in mitochondrial respiration. Finally, we analyzed mitochondrial oxygen consumption in primary skeletal muscle cells treated with PA and transfected with or without miR-1 mimic. PA-treated cells showed reduced basal respiration, oxygen consumption rate-linked ATP production, maximal and spare capacity, and miR-1 overexpression could prevent impairments in mitochondrial respiration. Our data suggest a role of miR-1 in systemic insulin sensitivity and a new function of miR-1 in regulating mitochondrial respiration in skeletal muscle.

Keywords: skeletal muscle, mitochondrial dysfunction, high-fat diet, obesity, microRNA

OPEN ACCESS

Edited by:
Samarjit Das,
Johns Hopkins University,
United States

Reviewed by:
P. Darrell Neufer,
East Carolina University, United States
Carlos Palmeira,
University of Coimbra, Portugal

****Correspondence:***
Alice C. Rodrigues
alice-rodrigues@usp.br

Specialty section:
This article was submitted to Mitochondrial Research, a section of the journal Frontiers in Physiology

Received: *04 March 2021*
Accepted: *11 June 2021*
Published: *06 July 2021*

Citation:
Rodrigues AC, Spagnol AR, Frias FT, de Mendonça M, Araújo HN, Guimarães D, Silva WJ, Bolin AP, Murata GM and Silveira L (2021) Intramuscular Injection of miR-1 Reduces Insulin Resistance in Obese Mice. Front. Physiol. 12:676265. doi: 10.3389/fphys.2021.676265

INTRODUCTION

Obesity, an abnormal or excessive fat accumulation that presents a risk to health, is strongly associated with type 2 diabetes mellitus (T2DM) (Boles et al., 2017). Being obese increases the risk of developing T2DM by at least six times, regardless of genetic predisposition to the disease (Schnurr et al., 2020). Intramyocellular lipid accumulation, resulting from enhanced adipose tissue lipolysis and impaired fatty acid beta-oxidation in skeletal muscle, induces insulin resistance, a major defect involved in the development of T2DM (Sergi et al., 2019). Mitochondrial reduced function in muscle has been associated with this metabolic inflexibility observed in T2DM patients

(Phielix et al., 2008). Therefore, enhancing mitochondrial function in skeletal muscle may be a strategy to improve insulin sensitivity.

MicroRNAs (miRNA or miR), small non-coding RNAs that negatively regulate gene expression, are increasingly being characterized as important regulators of mitochondrial function in obesity (Murri and El Azzouzi, 2018). As acknowledged by Bandiera et al. (2013), miRNA can be found in mitochondria acting within the organelle, while nuclear-encoded miRNAs can act at mitochondria or in the nucleus/cytosol on genes encoding mitochondrial proteins.

In skeletal muscle of high-fat diet -fed mice, mitochondrial function is impaired (Martins et al., 2018) and miR-1 is decreased in soleus and gastrocnemius muscles (Frias et al., 2016, 2018). Thus, miR-1 expression seems to be related to mitochondrial function.

MiR-1 is the most abundant microRNA in human skeletal muscle (Liang et al., 2007) and myomiR is recognized as an important regulator of skeletal muscle development (Chen et al., 2006). Experiments in skeletal muscle satellite cells and primary myoblasts have suggested that miR-1 promotes myoblast differentiation (Chen et al., 2010). Of note, miR-1, induced during myogenesis, efficiently enters the mitochondria where it unexpectedly stimulates, rather than represses, the translation of specific mitochondrial genome-encoded transcripts (Zhang et al., 2014).

Therefore, the purpose of this study was to investigate the role of miR-1 in skeletal muscle mitochondrial function and the potential of miR-1 to treat obesity-related disorders including insulin resistance. Our findings suggest miR-1 can increase muscle oxidative metabolism and mitochondrial content in primary mouse myotubes and *in vivo* improves peripheral insulin sensitivity, providing a new insight into miR-1 function in skeletal muscle.

MATERIALS AND METHODS

Ethics and Animals

The Experimental Animal Ethics Committees of ICB-USP and from the Institute of Biology of the University of Campinas approved the experimental procedure of this study. Male wild-type C57BL/6 J mice were obtained from the Facility for Mice Production at the Department of Pharmacology of the Institute of Biomedical Sciences (ICB) of the University of São Paulo (USP) and were maintained at 12:12-h light–dark cycle and 23°C ± 2°C. The animals were housed in cages (2–3 animals/cage) and received a standard diet (Nuvilab-Nuvital Nutrients Ltd., Parana, Brazil) and water *ad libitum* until the beginning of the experimental period.

Experimental Design

Eight-week-old male wild-type C57BL/6J mice (n = 35) were randomly divided into two groups: C- fed a balanced diet (C group n = 12) (cat.151, Pragsoluções Biociências, Jaú, SP, Brazil) and H- fed a high-fat diet (H group, n = 23) (cat.10, Pragsoluções). After 6 weeks of diet, part of the animals in the H group received intramuscularly miR-1 precursor plasmid (H + mir-1a-1, n = 12) or negative control (scrambled control, n = 11), as described in the next section. Animals in the C group received a scramble control plasmid. Body weight was measured every week and intraperitoneal glucose and insulin tolerance tests (ipGTT and ipITT) were performed 1 week before euthanasia. After 28 days of the injection, animals were euthanized (between 1 and 3pm) by decapitation, and gastrocnemius (GA) and soleus muscles (SO) were carefully dissected from the surrounding tissue; GA was frozen in liquid nitrogen and stored at −80°C until analyses and SO was freshly used for insulin incubation studies. Adipose tissue depots were dissected and weighed to evaluate adiposity levels.

In vivo miR-1 Therapy

In vivo experiments involving transfection of mouse pre-microRNA-1 expression construct (cat#MMIR-1a-1-PA-1, System biosciences) or Scramble negative control construct (cat#MMIR-000-PA-1) were conducted on GA muscle. Mice were submitted to a small incision in the skin to apply four injections (10 μl, 40U) of Hyaluronidase (Sigma #H3506, Germany). After 30 min, GA muscle received four injections (10 μL each) of the miR-1 precursor expression vector (1.25 μg/μL) in lateral and central sides of the muscle or negative control and the plasmid was introduced into muscle cells by electroporation, as described previously (Silva et al., 2019). Delivery of the plasmid was confirmed by visualization of GFP-positive fibers and DAPI, for nuclei identification, in GA sections using a fluorescence microscope Axio Scope.A1 (Carl Zeiss Microscopy GmbH, Göttingen, Germany). Contralateral non-injected GA muscle was used as a negative control.

ipGTT, ipITT, and Serum Insulin Measurement

GTT and ITT were performed in mice who had been fasted for 6 h, as previously described (de Mendonça et al., 2020b). The plasma glucose disappearance rate (K_{ITT}) during the 4- to 16-min period following the insulin injection was taken as a measure of insulin action (Bonora et al., 1989). During GTT, 20 μL of blood was also collected and homogenized with EDTA for insulin measurements. Serum insulin was measured using EZMRI- 13K kit (The Antibody Registry, 2021f).

Cell Culture Conditions and Treatments

Myoblast C2C12 cells (ATCC #: CRL-1772, RRID:CVCL_0188) (SciCrunch, 2021) were maintained in high glucose DMEM (SIGMA, St. Louis, MO, United States) supplemented with 10% fetal bovine serum and 1% penicillin/streptomycin (10,000 UI/mL streptomycin and 10,000 UI/mL penicillin) under humidified conditions with 5% CO2 at 37°C. After total confluence was achieved, the cells were differentiated using DMEM containing horse serum (HS) 2% for 5 days. Differentiated C2C12 cells were exposed to 500 μM palmitic acid (PA) or 1% bovine serum albumin (BSA) (vehicle control) for 24 h. After treatment, the cells were washed twice with cold

PBS, and total RNA was isolated using TRIzol reagent (Thermo Scientific) for analysis of miR-1 expression.

For gain-of-function experiment, undifferentiated C2C12 cells were transfected with LNA miR-1 mimic (miR-1 mimic; 472818-004 Exiqon) or scramble control (Scr; 199006-002 Exiqon), as previously described (Frias et al., 2018). Transfection media was replaced for differentiation media for 72 h and during the last 24 h, cells were treated with 500 μM PA or 1% BSA. Cells were washed with PBS and lysed in TRIzol reagent to measure mRNA expression by RT-qPCR. For quantification of p-AKT levels, the same procedure described above was done, however, after 96 h of the transfection, C2C12 cells were stimulated with 7 nM insulin for 15 min. Cells were lysed in a RIPA buffer containing protease inhibitors and western blot for p-AKT (Ser473) was performed.

Primary Muscle Cells Transfection and Mitochondrial Oxygen Consumption

Primary mouse skeletal muscle cells were obtained, as described in Araujo et al. (2020) and plated in a 24-well seahorse plate, and differentiated using DMEM containing HS 10% for 3 days ($n = 6$). miR-1 mimic (25 nM) or Scr (25 nM) was transfected in 100 μL OptiMEM medium containing 3 μL of Lipofectamine RNAiMAX (Life Technologies) for 48 h. After 24 h of transfection, cells were treated with 500 μM PA or 1% BSA. Mitochondrial oxygen consumption was evaluated, as previously described (Lima et al., 2019), using a Seahorse analysis (XF24; Agilent Technologies Inc., Santa Clara, CA, United States). Non-mitochondrial OCR values were subtracted from all data before being used for the analyses. After each assay, cells were fixed and crystal violet was stained for cell number normalization by measuring absorbance at 590 nm. For citrate synthase activity, cells were plated in 12-well, and the same protocol described above was performed.

Quantification of MicroRNA and mRNA Expression by RT-qPCR

Total RNA was extracted from GA muscle using miRVana Paris RNA Isolation kit (Thermo Fisher Scientific) according to the manufacturer's instructions. Quantification of miR-1 expression was performed as described in Frias et al. (2016). MicroRNA expression was normalized to sno234 levels.

For mRNA expression, cDNA synthesis was performed using the High Capacity kit (Thermo Fisher Scientific) from 500 ng of total RNA extracted from C2C12 cells. All PCR reactions were performed using diluted (1:10) cDNA template, forward and reverse primers (200 nM each) for Pdk4, Pgc1a, Cpt1b, Acot2 genes (Frias et al., 2018), and Power SYBR Green PCR Master Mix (Thermo Fisher Scientific). For normalization of expression, the constitutive gene Hprt1 was used.

Western Blot

The two mouse SO muscles were isolated, attached to stainless steel clips to maintain resting tension, and preincubated with Krebs-Ringer bicarbonate buffer containing glucose in the presence or absence of insulin 7 nM, as previously described (de Mendonça et al., 2020a). The muscles were briefly washed in cold KRBB at 4°C, dried on filter paper, and frozen in liquid N2. Proteins were extracted from SO and GA muscles and C2C12 frozen samples and loaded into polyacrylamide gels, separated by SDS-PAGE, and transferred to nitrocellulose membranes. Membranes were blotted with primary antibodies overnight at 4°C [p-AKT (Ser473) (The Antibody Registry, 2021e); AKT (The Antibody Registry, 2021a), AMPK (The Antibody Registry, 2021b), and p-AMPKα (Thr172) (The Antibody Registry, 2021c), Cell Signaling; GAPDH (The Antibody Registry, 2021d), Abcam] and after incubation with peroxidase-conjugated secondary antibodies for 1h at room temperature, the detection was performed by C-Digit Imager using Clarity^{TM} Western ECL (Bio-Rad).

Citrate Synthase Activity

Citrate synthase activity was measured in primary myotube cells and in gastrocnemius muscles (10 mg) homogenized in 1:100 (wt/vol) of extraction buffer, as previously described (Alp et al., 1976). Enzyme activities were assessed in duplicate and measurements were performed every 10 s over a 3 min period on Spectramax M5 spectrophotometer (Molecular devices, Sunnyvale, CA, United States). The results were expressed on a protein basis as determined by the BCA protein assay kit (Thermo Fisher Scientific, Waltham, MA, United States).

Statistical Analysis

Data are presented as mean ± S.D. The differences between the two groups were assessed by *t*-test and differences among three groups were assessed by one-way ANOVA, followed by Tukey's post-test. A *p*-value of less than 0.05 was considered statistically significant.

RESULTS

Intramuscular Injection of miR-1 Precursor Improves Insulin Resistance in Obese Mice

Mice were fed a high-fat diet (HFD) for 6 weeks and had increased body weight compared to control and intramuscular (i.m.) injection of miR-1 precursor (mir-1a-1), which did not affect weight gain in the following 4 weeks after injection (**Figure 1A**). An increment in fat mass, glucose intolerance, insulin resistance, and hyperinsulinemia were observed in obese mice after 10 weeks of high-fat diet (**Figures 1B–H**). Treatment with i.m. miR-1 precursor improved peripheral insulin resistance in obese mice as indicated by K_{ITT} (**Figure 1H**), but had no effect on fasting glycemia or glucose tolerance (**Figures 1C–E**).

mir-1a-1 and empty vector plasmids were effectively delivered in GA muscle as GFP-positive fibers are detected after 28 days of the injection of mir-1a-1 vector (miR-1 precursor) (**Figure 2A**). As expected in the muscle of the contralateral non-injected leg, there were no GPF-positive fibers (**Figure 2A**). We measure miR-1 levels in the GA muscle of obese and obese treated with mir-1a-1 vector and, as expected, miR-1 levels were decreased in the GA muscle of HFD-fed mice, and mir-1a-1 treatment restored miR-1 levels (**Figure 2B**). There was no difference in GA mass among the groups (**Figure 2C**). Interestingly, the levels of miR-1 in GA muscle positively correlated with K_{ITT} (**Figure 2D**).

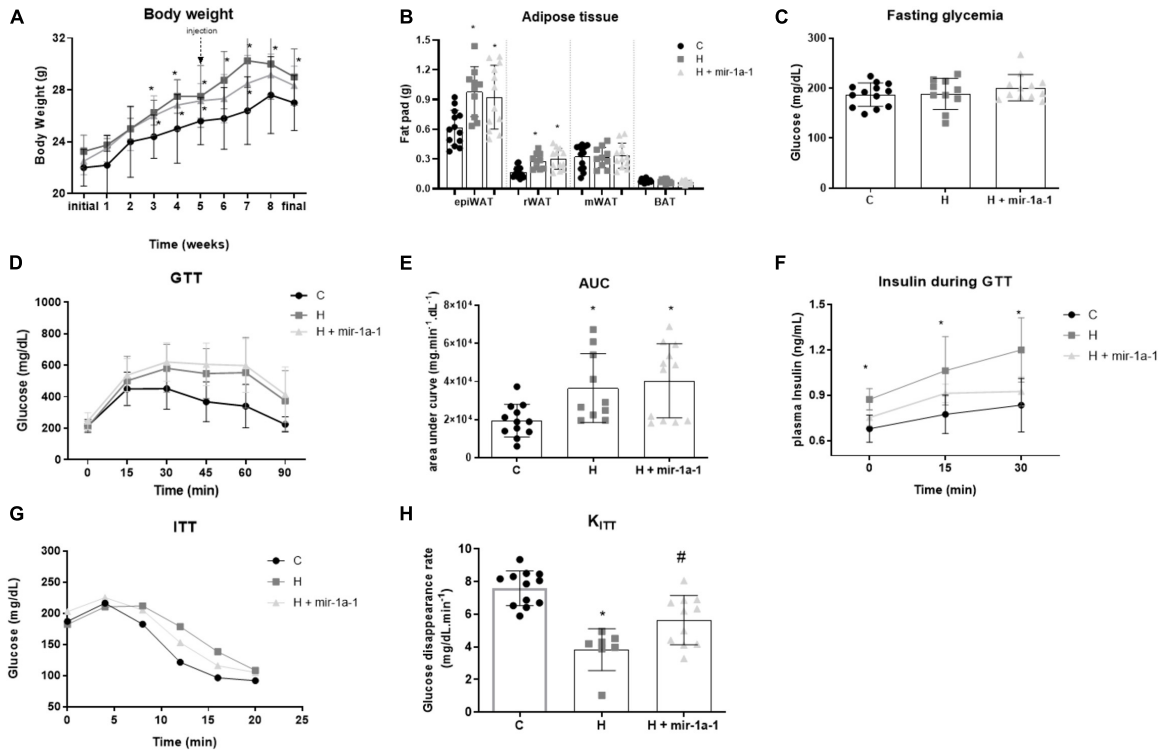

FIGURE 1 | Intramuscular miR-1 precursor (mir-1a-1) replacement therapy improves insulin resistance of obese mice. **(A)** Time-course of weight gain; **(B)** white adipose tissue (WAT) mass: epi = epididymal; r = retroperitoneal, m = mesenteric and brown adipose tissue (BAT) mass; **(C)** Glycemia after a 6h-fasting; **(D)** Glucose tolerance test (GTT) curve; **(E)** Area under the curve of GTT; **(F)** Serum insulin during GTT; **(G)** Insulin tolerance test (ITT) curve; **(H)** K_{ITT} calculated from ITT curve. *#$p < 0.05$ as indicated by one-way ANOVA followed by Tukey's post-test. (*) vs. control (C), (#) vs. obese (H); n = 7–12.

We next measured phospho/total Akt ratio in insulin-stimulated soleus muscle as an indicator of insulin sensitivity in skeletal muscle. Feeding a HFD decreases the ratio of p-Akt to total Akt, however, treatment with mir-1a-1 plasmid had no effect on p-AKT levels (**Figure 2E**). AMPK activation in skeletal muscle has beneficial effects on glucose uptake, independent of insulin sensitivity (Koistinen et al., 2003). Thus, we analyzed the levels of AMPK in mouse GA muscle. As predicted, p-AMPK is reduced in overweight mice and i.m. injection of mir-1a-1 plasmid restored p-AMPK to C group levels (**Figure 2F**). AMPK activation is related to increased mitochondrial biogenesis, therefore we measured citrate synthase (CS) activity, a marker of mitochondria content and muscle oxidative capacity (Larsen et al., 2012), in GA muscle of the animals. We observed a higher CS activity in mir-1a-1-treated GA muscle compared to those from control and HFD mice (**Figure 2G**).

Restoring miR-1 Expression in PA-Treated Cells Increases Expression of Genes Related to Mitochondrial Function

Using an *in vitro* model of obesity we investigated the effects of miR-1 specifically in myotubes. PA-treated cells had decreased levels of miR-1 (**Figure 3A**) and transfection of miR-1 mimic, effectively overexpressed miR-1 in myotubes treated with PA (**Figure 3B**).

According to *in vivo* results, overexpression of miR-1 in C2C12 myotubes and treatment with PA could not prevent the reduction of p-Akt levels in insulin-stimulated cells (**Figures 3C,D**).

AMPK activation is related to increased mitochondrial fatty acid oxidation. Remarkably, in C2C12 cells overexpression of miR-1 increases p-AMPK levels and miR-1 inhibition decreases p-AMPK levels (**Supplementary Figure 1**). Since p-AMPK levels and higher CS activity were associated with increased miR-1 levels in GA muscle of obese animals, we measured the transcript levels of proteins involved in mitochondrial β-oxidation in C2C12 cells treated with PA and transfected with miR-1. We found *Pgc1a*, *Cpt1b,* and *Acot2* were increased in PA-treated cells overexpressing miR-1 compared to PA-treated cells (**Figure 3E**) suggesting that miR-1 induces a more oxidative metabolism in C2C12 myotubes.

miR-1 Overexpression Protects PA-Treated Primary Skeletal Muscle Cells From Reducing Mitochondrial Oxidative Capacity

MiR-1 was overexpressed in primary myotubes (**Figure 3F**). After treatment with palmitic acid, CS activity (**Figure 3G**) and mitochondrial oxygen consumption, using a Seahorse analyzer

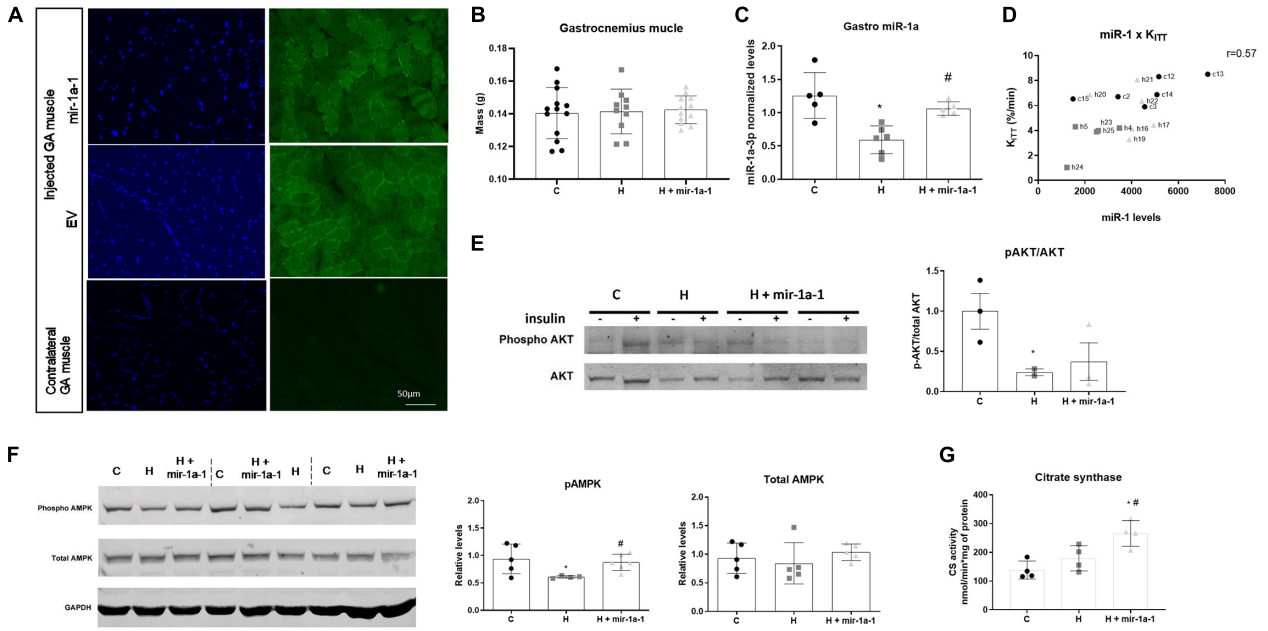

FIGURE 2 | Increased miR-1 levels in gastrocnemius muscle of obese mice restores pAMPK levels. **(A)** Representative fluorescence images of GFP-positive fibers in gastrocnemius (GA) sections after 28 days of transfection of the empty vector (EV) or miR-1 precursor (mir-1a-1) and contralateral non-injected GA. Blue = DAPI for nuclei identification; Green = GFP-positive fibers; **(B)** GA mass (n = 10–13); **(C)** miR-1 levels in GA muscle of control (C), obese (H) and miR-1 precursor-treated obese (H + mir-1a-1) mice (n = 5); **(D)** correlation analysis between miR-1 expression and K_{ITT} values (n = 5); **(E)** Representative blots of phospho and total AKT levels after stimulation of soleus muscle with insulin. Phospho and total AKT were normalized by ponceau-stained total protein content and phospho/total AKT ratio was calculated (n = 2–3); **(F)** Representative phospho and total AMPK and GAPDH levels. Relative phospho and total AMPK content was calculated after normalization with GAPDH (n = 5); **(G)** Citrate synthase activity in gastrocnemius muscle (n = 4). *#$p < 0.05$ as indicated by one-way ANOVA followed by Tukey's post-test. (*) vs. control (C), (#) vs. obese (H).

(**Figures 3H, I**), were measured. PA-treated myotubes had no difference in CS activity compared to the control, but overexpression of miR-1 increased CS activity in PA-treated cells (**Figure 3G**). Non-mitochondrial respiration was calculated, and it was not different in PA-treated cells compared to control cells. Significant differences were observed in basal, ATP-linked, and maximum mitochondrial oxygen consumption rate (OCR), in primary skeletal muscle cells treated with PA compared to control cells (**Figure 3I**). Mitochondrial oxidative capacity, as suggested by mitochondrial reserve capacity (spare capacity), was also reduced in palmitic acid, as compared to control cells. Transfection of miR-1 mimic prevents PA in decreasing mitochondrial basal and maximal OCR and spare capacity (**Figure 3I**). Notably, miR-1 also increases the proton leak compared to control and PA-treated cells, suggesting miR-1 uses other mechanisms to regulate mitochondrial ATP production (**Figure 3I**).

DISCUSSION

MiR-1 is a well-known myomiR that is crucial for myotube differentiation, which is dysregulated in the skeletal muscle of obese and diabetic individuals (Chen et al., 2012; Frias et al., 2016, 2018; Dahlmans et al., 2017). However, miR-1 functions in diabetes and obesity are still underexplored. As this study describes, miR-1 may have a role in mitochondrial function in the skeletal muscle of obese subjects and intramuscular miR-1 precursor replacement therapy improves peripheral insulin resistance in obese mice.

Strategies that can improve insulin sensitivity and glycemic control are used in the management of obesity-related T2DM. Current therapy in the management of T2DM has been shown to exert beneficial effects in T2DM by modulating mitochondrial function (Pinti et al., 2019; Apostolova et al., 2020; Fiorentino et al., 2021). Mitochondrial function has been associated with muscle insulin resistance and T2D in multiple studies (Petersen et al., 2004, 2005; Ritov et al., 2005, 2010; Befroy et al., 2007; Koves et al., 2008; Phielix et al., 2008; Minet and Gaster, 2010, 2011; Fiorentino et al., 2021). Mitochondrial function has been associated with deficient oxidative capacity, resulting in increased amounts of intramyocellular lipids. Lipotoxicity interferes with insulin signaling, causing insulin resistance (Petersen et al., 2004). Impaired mitochondrial substrate oxidation has both been shown in the insulin resistant offspring of T2D patients (Befroy et al., 2007) and exercising T2D patients *in vivo* (Schrauwen and Hesselink, 2008). Thus, a reduced TCA cycle flux is both a marker and a maker of the diabetic phenotype (Gaster et al., 2012). Even though mitochondrial function has been suggested to play an important role in the pathogenesis of insulin resistance and T2DM, some studies have observed normal mitochondrial function in diet-induced obesity models

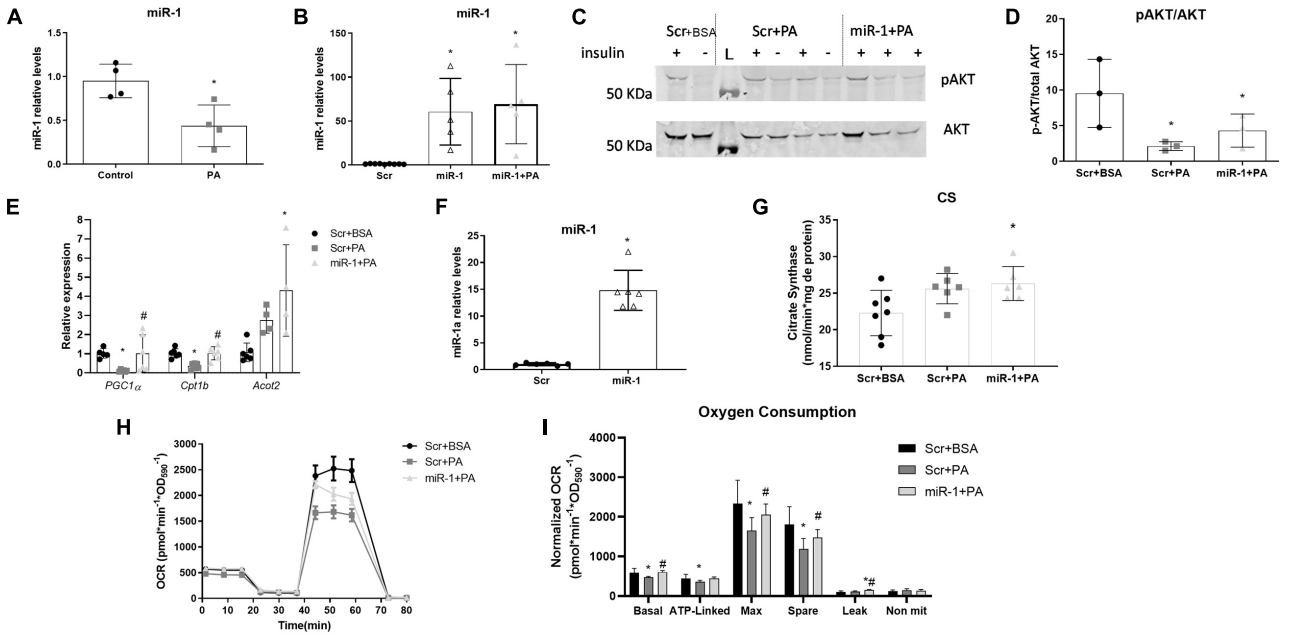

FIGURE 3 | Overexpression of miR-1 protects PA-treated primary skeletal muscle cells from reducing mitochondrial oxidative capacity. **(A)** miR-1 levels in PA-treated myotubes ($n = 4$), (*$p < 0.05$ vs. control); **(B)** overexpression of miR-1 in PA-treated cells ($n = 5$), (*$p < 0.05$ vs. Scr); **(C)** Representative blots of phospho and total AKT levels after insulin treatment of control (Scr), PA-treated (Scr + PA) and miR-1 overexpressing cells treated with PA ($n = 6$), L = protein ladder; **(D)** phospho and total AKT were normalized by total protein content stained with amido black and p/total AKT ratio was calculated in insulin-stimulated cells ($n = 3$) (*$p < 0.05$ vs. Scr + BSA); **(E)** mRNA expression of mitochondrial and beta-oxidation markers ($n = 6$), (*#$p < 0.05$: (*) vs. Scr + BSA, (#) vs. Scr + PA); **(F)** overexpression of miR-1 in primary myotubes ($n = 6$) (*$p < 0.05$ vs. Scr); **(G)** Citrate synthase activity in primary myotubes ($n = 6$), (*$p < 0.05$ vs. Scr); **(H)** Oxygen consumption rates (OCR) corrected by non-mitochondrial OCR; **(I)** Basal, ATP-linked, proton leak (leak), spare capacity (spare) and non-mitochondrial (non-mit) OCR from primary myotubes transfected with miR-1 or scrambled control and treated with palmitic acid or vehicle for 24 h ($n = 6$). *#$p < 0.05$: (*) vs. Scr + BSA (C), (#) vs. Scr + PA.

(Garcia-Roves et al., 2007; Brøns et al., 2012; Stephenson et al., 2012). Here, we show that palmitic acid impairs mitochondrial respiration and possibly fatty acid oxidation in mouse myotubes. Our findings corroborate previous studies demonstrating the increase in free fatty acids metabolites inhibits ATP synthesis in isolated mitochondria from mouse and human skeletal muscle (Abdul-Ghani et al., 2008) and that saturated free fatty acids decrease both mitochondrial hyperpolarization and ATP generation in C2C12 cells and primary myotubes (Hirabara et al., 2010).

These findings show that overexpression of miR-1 in myotubes prevents abnormalities in mitochondrial function induced by the saturated fatty acid in skeletal muscle. A relationship between miR-1 and mitochondria has been established. During skeletal muscle differentiation, miR-1, a nuclear-encoded miRNA, translocates into the mitochondrial compartment to induce the expression of mitochondrial genes (Zhang et al., 2014). Besides that, after an acute bout of endurance exercise, a well-known inducer of mitochondrial biogenesis in skeletal muscle, miR-1 expression is increased in the quadriceps of mice (Safdar et al., 2009).

Low levels of miR-1 have been described in the skeletal muscle of insulin resistant mice and patients (Chen et al., 2012; Frias et al., 2016, 2018; Dahlmans et al., 2017) and, as demonstrated by our data, in cultivated insulin resistant myotubes. Interestingly, treatment with PPARα agonist, an inducer of fatty acid oxidation, decreases lipid deposition and restores miR-1 levels in soleus muscle of obese mice (Frias et al., 2018). This suggests that up-regulation of miR-1 is associated with higher oxidative metabolism. In addition, exercise training, which helps restore mitochondrial function in T2DM patients (van Tienen et al., 2012), acutely up-regulates miR-1 expression in the skeletal muscle of obese mice (Safdar et al., 2009). Consistent with these results, our data show that miR-1 increases mitochondrial biogenesis and muscle oxidative metabolism in insulin resistant myotubes.

In the present study, peripheral insulin sensitivity was increased in obese mice treated with miR-1 precursor without weight loss. Studies have shown that the capacity for AMPK-mediated glucose uptake is intact in muscle cells from patients with T2DM, while insulin-induced glucose uptake is impaired (Koistinen et al., 2003). Accordingly, AMPK was restored in the gastrocnemius muscle of miR-1 treated mice and may have contributed to insulin-independent glucose transport in skeletal muscle of miR-1 precursor treated animals. A previous report from our group demonstrated that in C2C12 cells, overexpression of miR-1 increases basal glucose uptake (Frias et al., 2018). This study showed that AMPK phosphorylation is stimulated in C2C12 cells transfected with miR-1. Moreover, activation of liver AMPK by metformin, a first-line antidiabetic drug, improves mitochondrial respiratory activity along

with improved hyperglycemia in high-fat- diet-fed mice (Wang et al., 2019). Our study did not observe weight loss after miR-1 therapy. Our data corroborate previous findings that treatment of SVF cells from brown fat with LNA miR-1 inhibitor caused no effect on adipogenesis or brown fat enriched markers (Sun et al., 2011).

In conclusion, this study suggests that miR-1, through activation of AMPK, increases muscle oxidative metabolism and mitochondrial content in skeletal muscle, which in turn improves insulin sensitivity. Our data suggest a novel role of miR-1 in insulin resistance.

DATA AVAILABILITY STATEMENT

The raw data supporting the conclusions of this article will be made available by the authors, without undue reservation.

ETHICS STATEMENT

The animal study was reviewed and approved by the Ethics Committee on Animal Use of the Biomedical Sciences Institute (University of São Paulo) (CEUA-ICB/USP).

AUTHOR CONTRIBUTIONS

AR conceived and designed the research. AR, AB, AS, DG, FF, GM, HA, LS, MM, and WS acquired, analyzed, and interpreted data. AR wrote the manuscript. All authors contributed to the article and approved the submitted version.

FUNDING

This work was supported by funding from the São Paulo Research Foundation to AR (FAPESP, Grant numbers 20/08049-2; 18/07087-8, 15/24789-8 and 11/05876-6). This study was financed in part by the Coordenação de Aperfeiçoamento de Pessoal de Nível Superior-Brasil (CAPES) – finance code 001. AB and MM are recipients of fellowships from FAPESP (2018/07241-7 and 2017/19513-9).

SUPPLEMENTARY MATERIAL

The Supplementary Material for this article can be found online at: https://www.frontiersin.org/articles/10.3389/fphys.2021.676265/full#supplementary-material

REFERENCES

Abdul-Ghani, M. A., Muller, F. L., Liu, Y., Chavez, A. O., Balas, B., Zuo, P., et al. (2008). Deleterious action of FA metabolites on ATP synthesis: possible link between lipotoxicity, mitochondrial dysfunction, and insulin resistance. *Am. J. Physiol. Endocrinol. Metab.* 295, E678–E685.

Alp, P. R., Newsholme, E. A., and Zammit, V. A. (1976). Activities of citrate synthase and NAD+-linked and NADP + - linked isocitrate dehydrogenase in muscle from vertebrates and invertebrates. *Biochem. J.* 154, 689–700. doi: 10.1042/bj1540689

Apostolova, N., Iannantoni, F., Gruevska, A., Muntane, J., Rocha, M., and Victor, V. M. (2020). Mechanisms of action of metformin in type 2 diabetes: effects on mitochondria and leukocyte-endothelium interactions. *Redox Biol.* 34:101517. doi: 10.1016/j.redox.2020.101517

Araujo, H. N., Lima, T. I., Guimarães, D. S. P. S. F., Oliveira, A. G., Favero-Santos, B. C., Branco, R. C. S., et al. (2020). Regulation of Lin28a-miRNA *let-7b-5p* pathway in skeletal muscle cells by peroxisome proliferator-activated receptor delta. *Am. J. Physiol. Cell Physiol.* 319, C541–C551.

Bandiera, S., Matégot, R., Girard, M., Demongeot, J., and Henrion-Caude, A. (2013). MitomiRs delineating the intracellular localization of microRNAs at mitochondria. *Free Rad. Biol. Med.* 64, 12–19. doi: 10.1016/j.freeradbiomed.2013.06.013

Befroy, D. E., Petersen, K. F., Dufour, S., Mason, G. F., de Graaf, R. A., Rothman, D. L., et al. (2007). Impaired mitochondrial substrate oxidation in muscle of insulin-resistant offspring of type 2 diabetic patients. *Diabetes* 56, 1376–1381. doi: 10.2337/db06-0783

Boles, A., Kandimalla, R., and Reddy, P. H. (2017). Dynamics of diabetes and obesity: epidemiological perspective. *Biochim. Biophys. Acta Mol. Basis Dis.* 1863, 1026–1036. doi: 10.1016/j.bbadis.2017.01.016

Bonora, E., Moghetti, P., Zancanaro, C., Cigolini, M., Querena, M., Cacciatori, V., et al. (1989). Estimates of in vivo insulin action in man: comparison of insulin tolerance tests with euglycemic and hyperglycemic glucose clamp studies. *J. Clin. Endocrinol. Metab.* 68, 374–378. doi: 10.1210/jcem-68-2-374

Brøns, C., Jacobsen, S., Hiscock, N., White, A., Nilsson, E., Dunger, D., et al. (2012). Effects of high-fat overfeeding on mitochondrial function, glucose and fat metabolism, and adipokine levels in low-birth-weight subjects. *Am. J. Physiol. Endocrinol. Metab.* 302, E43–E51.

Chen, G.-Q., Lian, W.-J., Wang, G.-M., Wang, S., Yang, Y.-Q., and Zhao, Z.-W. (2012). Altered microRNA expression in skeletal muscle results from high-fat diet-induced insulin resistance in mice. *Mol. Med. Rep.* 5, 1362–1368.

Chen, J. F., Mandel, E. M., Thomson, J. M., Wu, Q., Callis, T. E., Hammond, S. M., et al. (2006). The role of microRNA-1 and microRNA-133 in skeletal muscle proliferation and differentiation. *Nat. Genet.* 38, 228–233. doi: 10.1038/ng1725

Chen, J. F., Tao, Y., Li, J., Deng, Z., Yan, Z., Xiao, X., et al. (2010). microRNA-1 and microRNA-206 regulate skeletal muscle satellite cell proliferation and differentiation by repressing Pax7. *J. Cell Biol.* 190, 867–879. doi: 10.1083/jcb.200911036

Dahlmans, D., Houzelle, A., Jörgensen, J. A., Phielix, E., Lindeboom, L., Hesselink, M. K. C., et al. (2017). Evaluation of muscle microRNA expression in relation to human peripheral insulin sensitivity: a cross-sectional study in metabolically distinct subject groups. *Front. Physiol.* 8:711. doi: 10.3389/fphys.2017.00711

de Mendonça, M., de Sousa, É, da Paixão, A. O., Araújo Dos Santos, B., Roveratti Spagnol, A., Murata, G. M., et al. (2020a). MicroRNA miR-222 mediates pioglitazone beneficial effects on skeletal muscle of diet-induced obese mice. *Mol. Cell. Endocrinol.* 501:110661. doi: 10.1016/j.mce.2019.110661

de Mendonça, M., Rocha, K. C., de Sousa, É, Pereira, B. M. V., Oyama, L. M., and Rodrigues, A. C. (2020b). Aerobic exercise training regulates serum extracellular vesicle miRNAs linked to obesity to promote their beneficial effects in mice. *Am. J. Physiol. Endocrinol. Metab.* 319, E579–E591.

Fiorentino, T. V., Monroy, A., Kamath, S., Sotero, R., Cas, M. D., Daniele, G., et al. (2021). Pioglitazone corrects dysregulation of skeletal muscle mitochondrial proteins involved in ATP synthesis in type 2 diabetes. *Metabolism* 114:154416. doi: 10.1016/j.metabol.2020.154416

Frias, F., de, T., de Mendonça, M., Martins, A. R., Gindro, A. F., Cogliati, B., et al. (2016). MyomiRs as markers of insulin resistance and decreased myogenesis in skeletal muscle of diet-induced obese mice. *Front. Endocrinol.* 7:76. doi: 10.3389/fendo.2016.00076

Frias, F., de, T., Rocha, K. C. E., de Mendonça, M., Murata, G. M., Araujo, H. N., et al. (2018). Fenofibrate reverses changes induced by high-fat diet on metabolism in mice muscle and visceral adipocytes. *J. Cell. Physiol.* 233, 3515–3528. doi: 10.1002/jcp.26203

Garcia-Roves, P., Huss, J. M., Han, D. H., Hancock, C. R., Iglesias- Gutierrez, E., Chen, M., et al. (2007). Raising plasma fatty acid concentration induces

increased biogenesis of mitochondria in skeletal muscle. *Proc. Natl. Acad. Sci. U.S.A* 104, 10709–10713. doi: 10.1073/pnas.0704024104

Gaster, M., Nehlin, J. O., and Minet, A. D. (2012). Impaired TCA cycle flux in mitochondria in skeletal muscle from type 2 diabetic subjects: marker or maker of the diabetic phenotype? *Arch. Physiol. Biochem.* 118, 156–189. doi: 10.3109/13813455.2012.656653

Hirabara, S. M., Curi, R., and Maechler, P. (2010). Saturated fatty acid-induced insulin resistance is associated with mitochondrial dysfunction in skeletal muscle cells. *J. Cell. Physiol.* 222, 187–194. doi: 10.1002/jcp.21936

Koistinen, H. A., Galuska, D., Chibalin, A. V., Yang, J., Zierath, J. R., Holman, G. D., et al. (2003). 5-amino-imidazole carboxamide riboside increases glucose transport and cell-surface GLUT4 content in skeletal muscle from subjects with type 2 diabetes. *Diabetes* 52, 1066–1072. doi: 10.2337/diabetes.52.5.1066

Koves, T. R., Ussher, J. R., Noland, R. C., Slentz, D., Mosedale, M., Ilkayeva, O., et al. (2008). Mitochondrial overload and incomplete fatty acid oxidation contribute to skeletal muscle insulin resistance. *Cell Metab.* 7, 45–56. doi: 10.1016/j.cmet.2007.10.013

Larsen, S., Nielsen, J., Hansen, C. N., Nielsen, L. B., Wibrand, F., Stride, N., et al. (2012). Biomarkers of mitochondrial content in skeletal muscle of healthy young human subjects. *J. Physiol.* 590, 3349–3360. doi: 10.1113/jphysiol.2012.230185

Liang, Y., Ridzon, D., Wong, L., and Chen, C. (2007). Characterization of microRNA expression profiles in normal human tissues. *BMC Genomics.* 8:166. doi: 10.1186/1471-2164-8-166

Lima, T. I., Guimarães, D., Sponton, C. H., Bajgelman, M. C., Palameta, S., Toscaro, J. M., et al. (2019). Essential role of the PGC-1α/PPARβ axis in Ucp3 gene induction. *J. Physiol.* 597, 4277–4291. doi: 10.1113/jp278006

Martins, A. R., Crisma, A. R., Masi, L. N., Amaral, C. L., Marzuca-Nassr, G. N., Bomfim, L. H. M., et al. (2018). Attenuation of obesity and insulin resistance by fish oil supplementation is associated with improved skeletal muscle mitochondrial function in mice fed a high-fat diet. *J. Nutr. Biochem.* 55, 76–88. doi: 10.1016/j.jnutbio.2017.11.012

Minet, A. D., and Gaster, M. (2010). ATP synthesis is impaired in isolated mitochondria from myotubes established from type 2 diabetic subjects. *Biochem. Biophys. Res. Commun.* 402, 70–74. doi: 10.1016/j.bbrc.2010.09.115

Minet, A. D., and Gaster, M. (2011). The dynamic equilibrium between ATP synthesis and ATP consumption is lower in isolated mitochondria from myotubes established from type 2 diabetic subjects compared to lean control. *Biochem. Biophys. Res. Commun.* 409, 591–595. doi: 10.1016/j.bbrc.2011.04.028

Murri, M., and El Azzouzi, H. (2018). MicroRNAs as regulators of mitochondrial dysfunction and obesity. *Am. J. Physiol. Heart Circ. Physiol.* 315, H291–H302.

Petersen, K. F., Dufour, S., Befroy, D., Garcia, R., and Shulman, G. I. (2004). Impaired mitochondrial activity in the insulin-resistant offspring of patients with type 2 diabetes. *N. Engl. J. Med.* 350, 664–671. doi: 10.1056/NEJMoa031314

Petersen, K. F., Dufour, S., and Shulman, G. I. (2005). Decreased insulin-stimulated ATP synthesis and phosphate transport in muscle of insulin-resistant offspring of type 2 diabetic parents. *PLoS Med.* 2:e233. doi: 10.1371/journal.pmed.0020233

Phielix, E., Schrauwen-Hinderling, V. B., Mensink, M., Lenaers, E., Meex, R., Hoeks, J., et al. (2008). Lower intrinsic ADP-stimulated mitochondrial respiration underlies in vivo mitochondrial dysfunction in muscle of male Type 2 diabetic patients. *Diabetes* 57, 2943–2949. doi: 10.2337/db08-0391

Pinti, M. V., Fink, G. K., Hathaway, Q. A., Durr, A. J., Kunovac, A., and Hollander, J. M. (2019). Mitochondrial dysfunction in type 2 diabetes mellitus: an organ-based analysis. *Am. J. Physiol. Endocrinol. Metab.* 316, E268–E285.

Ritov, V. B., Menshikova, E. V., Azuma, K., Wood, R., Toledo, F. G. S., Goodpaster, B. H., et al. (2010). Deficiency of electron transport chain in human skeletal muscle mitochondria in type 2 diabetes mellitus and obesity. *Am. J. Physiol. Endocrinol. Metab.* 298, E49–E58.

Ritov, V. B., Menshikova, E. V., He, J., Ferrell, R. E., Goodpaster, B. H., and Kelley, D. E. (2005). Deficiency of subsarcolemmal mitochondria in obesity and type 2 diabetes. *Diabetes* 54, 8–14. doi: 10.2337/diabetes.54.1.8

Safdar, A., Abadi, A., Akhtar, M., Hettinga, B. P., and Tarnopolsky, M. A. (2009). miRNA in the regulation of skeletal muscle adaptation to acute endurance exercise in C57Bl/6J male mice. *PLoS One* 4:e5610. doi: 10.1371/journal.pone.0005610

Schnurr, T. M., Jakupović, H., Carrasquilla, G. D., Ängquist, L., Grarup, N., Sørensen, T. I. A., et al. (2020). Obesity, unfavourable lifestyle and genetic risk of type 2 diabetes: a case-cohort study. *Diabetologia* 63, 1324–1332. doi: 10.1007/s00125-020-05140-5

Schrauwen, P., and Hesselink, M. K. (2008). Reduced tricarboxylic acid cycle flux in type 2 diabetes mellitus? *Diabetologia* 51, 1694–1697. doi: 10.1007/s00125-008-1069-x

SciCrunch (2021). *FDI Lab: SciCrunch Infrastructure*. Available online at: https://scicrunch.org/resolver/CVCL_0188 (accessed February 6, 2021).

Sergi, D., Naumovski, N., Heilbronn, L. K., Abeywardena, M., O'Callaghan, N., Lionetti, L., et al. (2019). Mitochondrial (Dys)function and insulin resistance: from pathophysiological molecular mechanisms to the impact of diet. *Front. Physiol.* 10:532. doi: 10.3389/fphys.2019.00532

Silva, W. J., Graça, F. A., Cruz, A., Silvestre, J. G., Labeit, S., Miyabara, E. H., et al. (2019). miR-29c improves skeletal muscle mass and function throughout myocyte proliferation and differentiation and by repressing atrophy-related genes. *Acta Physiol.* 226:e13278.

Stephenson, E. J., Camera, D. M., Jenkins, T. A., Kosari, S., Lee, J. S., Hawley, J. A., et al. (2012). Skeletal muscle respiratory capacity is enhanced in rats consuming an obesogenic Western diet. *Am. J. Physiol. Endocrinol. Metab.* 302, E1541–E1549. doi: 10.1152/ajpendo.00590.2011

Sun, L., Xie, H., Mori, M. A., Alexander, R., Yuan, B., Hattangadi, S. M., et al. (2011). Mir193b-365 is essential for brown fat differentiation. *Nat. Cell Biol.* 13, 958–965. doi: 10.1038/ncb2286

The Antibody Registry (2021a). *AB_329827 Search - The Antibody Registry*. Available online at: https://antibodyregistry.org/search.php?q=AB_329827 (accessed February 6, 2021).

The Antibody Registry (2021b). *AB_330331 Search - The Antibody Registry*. Available online at: https://antibodyregistry.org/search?q=AB_330331 (accessed February 6, 2021).

The Antibody Registry (2021c). *AB_331250 Search - The Antibody Registry*. Available online at: https://antibodyregistry.org/search?q=AB_331250ti (accessed February 6, 2021).

The Antibody Registry (2021d). *RRID:AB_2630358 Search – The Antibody Registry*. Available online at: https://www.antibodyregistry.org/search?q=RRID:AB_2630358 (accessed February 17, 2021).

The Antibody Registry (2021e). *AB_2629283 Search - The Antibody Registry*. Available online at: https://antibodyregistry.org/search.php?q=AB_2629283 (accessed February 6, 2021).

The Antibody Registry (2021f). *AB_2783856 Search - The Antibody Registry*. Available online at: https://antibodyregistry.org/search.php?q=AB_2783856 (accessed February 6, 2021).

van Tienen, F. H. J., Praet, S. F. E., de Feyter, H. M., van den Broek, N. M., Lindsey, P. J., Schoonderwoerd, K. G. C., et al. (2012). Physical activity is the key determinant of skeletal muscle mitochondrial function in type 2 diabetes. *J. Clin. Endocrinol. Metab.* 97, 3261–3269. doi: 10.1210/jc.2011-3454

Wang, Y., An, H., Liu, T., Qin, C., Sesaki, H., Guo, S., et al. (2019). Metformin improves mitochondrial respiratory activity through activation of AMPK. *Cell Rep.* 29, 1511–1523.e5.

Zhang, X., Zuo, X., Yang, B., Li, Z., Xue, Y., Zhou, Y., et al. (2014). MicroRNA directly enhances mitochondrial translation during muscle differentiation. *Cell* 158, 607–619. doi: 10.1016/j.cell.2014.05.047

Conflict of Interest: The authors declare that the research was conducted in the absence of any commercial or financial relationships that could be construed as a potential conflict of interest.

frontiers in Cell and Developmental Biology

REVIEW
published: 30 July 2021
doi: 10.3389/fcell.2021.713729

Mitochondria Encoded Non-coding RNAs in Cell Physiology

*Xu Liu and Ge Shan**

Hefei National Laboratory for Physical Sciences at Microscale, The CAS Key Laboratory of Innate Immunity and Chronic Disease, Division of Life Science and Medicine, Department of Clinical Laboratory, The First Affiliated Hospital of USTC, School of Basic Medical Sciences, University of Science and Technology of China, Hefei, China

Mitochondria are the powerhouses of mammalian cells, which participate in series of metabolic processes and cellular events. Mitochondria have their own genomes, and it is generally acknowledged that human mitochondrial genome encodes 13 proteins, 2 rRNAs and 22 tRNAs. However, the complexity of mitochondria derived transcripts is just starting to be envisaged. Currently, there are at least 8 lncRNAs, some dsRNAs, various small RNAs, and hundreds of circRNAs known to be generated from mitochondrial genome. These non-coding RNAs either translocate into cytosol/nucleus or reside in mitochondria to play various biological functions. Here we present an overview of regulatory non-coding RNAs encoded by the mammalian mitochondria genome. For overall understandings of non-coding RNAs in mitochondrial function, a brief summarization of nuclear-encoded non-coding RNAs in mitochondria is also included. We discuss about roles of these non-coding RNAs in cellular physiology and the communication between mitochondria and the nucleus.

Keywords: mitochondria, mitochondria-encoded non-coding RNA, lncRNA, dsRNA, small ncRNA, circRNA

OPEN ACCESS

Edited by:
Veronica Andrea Burzio, Andres Bello University, Chile

Reviewed by:
Amaresh Chandra Panda, Institute of Life Sciences (ILS), India
Chandrasekhar Kanduri, University of Gothenburg, Sweden
Piotr Stepien, University of Warsaw, Poland

***Correspondence:**
Ge Shan
shange@ustc.edu.cn

Specialty section:
This article was submitted to Signaling, a section of the journal Frontiers in Cell and Developmental Biology

Received: *24 May 2021*
Accepted: *12 July 2021*
Published: *30 July 2021*

Citation:
Liu X and Shan G (2021) Mitochondria Encoded Non-coding RNAs in Cell Physiology. Front. Cell Dev. Biol. 9:713729. doi: 10.3389/fcell.2021.713729

INTRODUCTION

Mitochondria are vital to cells and are involved in multiple essential cellular events. On top of generating ATP, mitochondria also produce reactive oxygen species (ROS), redox molecules, and intermediates required for the synthesis of biomolecules. Furthermore, they are key hubs of intracellular signaling pathways and participate in response to external environmental changes (McBride et al., 2006).

Mitochondria have independent circular genomes (mtDNA) (**Figure 1**). Human mtDNA is mostly coding (more than 90%) and transcribed entirely in a bidirectional, polycistronic manner. Both strands of mtDNA harbor coding information. The heavy strand encodes 12 protein genes which are all subunits of the oxidative phosphorylation system (OXPHOS), two ribosomal RNAs (12S and 16S), and 14 tRNAs. The light strand encodes for a single mRNA (ND6) and 8 tRNAs (Scarpulla, 2008; Gustafsson et al., 2016; Barshad et al., 2018). Transcription is initiated from two heavy-strand promoters (HSP1, HSP2) and one light-strand promoter (LSP), located in the major non-coding region named "D-loop". Two long polycistronic RNAs produced from HSP2 and LSP cover almost the full-length of each strand and another transcript transcribed from HSP1 consists of the two rRNA genes (Taanman, 1999; Asin-Cayuela and Gustafsson, 2007). The long mitochondrial precursor transcripts undergo the generally accepted "tRNA punctuations" processing by RNase P and RNase Z (ELAC2) cleavage to generate individual mRNAs, rRNAs, and tRNAs (Ojala et al., 1981; Holzmann et al., 2008; Lopez Sanchez et al., 2011; Barchiesi and Vascotto, 2019).

Recent years have witnessed the fast growing in understanding the great complexity of transcripts from the nuclear genome (Djebali et al., 2012; Iyer et al., 2015), and growing evidence has also demonstrated the presence of mitochondria-encoded non-coding RNAs (ncRNAs) such as long non-coding RNA (lncRNA) (Jusic and Devaux, 2020), circular RNAs (circRNAs) (Liu et al., 2020; Wu et al., 2020; Zhao et al., 2020), small non-coding RNAs (sncRNAs) (Mercer et al., 2011; Jusic and Devaux, 2020), and double-stranded RNAs (dsRNAs) (Dhir et al., 2018) with potential regulatory functions, respectively (**Figure 1**).

In this review we will focus on known regulatory non-coding RNAs encoded by the mitochondrial genome, and we also present a summarization of nuclear-encoded non-coding RNAs found in mitochondria for overall understandings about ncRNAs in mitochondria-nucleus communication. We highlight and discuss about their functional relevance in biomedicine, and in the context of cross-talk between mitochondria and the nucleus.

MITOCHONDRIA-ENCODED lncRNAs

LncRNA is a major class of non-coding RNAs that is widely expressed in cells. Nuclear-encoded lncRNAs play diverse regulatory roles in mammalian cells, including transcriptional regulation, translational regulation, protein scaffolding, chromosome remodeling etc. (Gomes et al., 2013; Rashid et al., 2016; Marchese et al., 2017; Chen and Shan, 2020). A series of lncRNAs transcribed from the mtDNA have been recently reported, and these lncRNAs may also participate in multiple biological processes (**Figure 2** and **Table 1**).

Three lncRNAs (lnc*ND5*, lnc*Cyt b*, lnc*ND6*) generated from the mitochondrial genome were identified by Rackham et al. (2011) from deep sequencing data of human HeLa mitochondria (Rackham et al., 2011). The positions of these three lncRNAs corresponded to the regions complementary to the mitochondrial ND5, ND6, and Cyt b genes. There was no significant open reading frame present in them. It was shown that the three lncRNAs might play a functional role to stabilize ND5, ND6, and Cyt b mRNAs or to regulate the expression of the three genes in mitochondria through forming RNA-RNA duplexes (Rackham et al., 2011). The abundance of the three lncRNAs was cell and tissue-specific, indicating that they might be subjected to cell specific regulation and to play physiological roles.

Villegas et al. (2007) reported a 2,374 nt human mitochondrial transcript containing an inverted repeat (IR) of 820 nt linked to the 5′ end of the 16S mt-rRNA and named it SncmtRNA (sense non-coding mitochondrial RNA) (Villegas et al., 2007). In SncmtRNA, the IR generates a stem-loop structure with a double stranded region and a 40 nt loop. SncmtRNA was over-expressed in several tumor cell lines but not in resting cells (Villegas et al., 2007). The same researcher team later identified 2 transcripts containing IRs linked to the 5′ region of the antisense transcript of 16S mt-rRNA gene in the L-strand of the mtDNA, and designated them antisense ncmtRNA-1 (ASncmtRNA-1, 310 nt IR) and antisense ncmtRNA-2 (ASncmtRNA-2, 545 nt IR) (Burzio et al., 2009). AsncmtRNAs were expressed in normal proliferating cells but were down-regulated in different types of human tumor cells (Burzio et al., 2009). The subcellular location of SncmtRNA and ASncmtRNAs seemed to be nucleus (Landerer et al., 2011). Knockdown of ASncmtRNAs (ASK for short) by antisense oligonucleotide (ASO-1537S) targeting the single-stranded loop region resulted in Dicer-mediated release of hsa-miR-4485. hsa-miR-4485 in combination with nuclear miRNAs (mainly hsa-miR-5096 and hsa-miR-3609), which were induced by ASK, inhibited translation of 5 important cell cycle proteins (Cyclin B1, Cyclin D1, CDK1, CDK4, Survivin), and thereby induced growth inhibition of breast cancer cells (Fitzpatrick et al., 2019). The same researcher group later reported that exosomes derived from ASO-1537S-treated MDA-MB-231 breast cancer cells inhibited tumorigenesis of recipient cells (Lobos-González et al., 2020). And they also observed ASK induced bladder cancer cell death and inhibition of tumor growth (Borgna et al., 2020). The above results indicated that ASncmtRNAs could be potential therapeutic targets for breast cancer and bladder cancer.

Global transcriptomic profiling of human left ventricular (LV) from heart failing patients and controls revealed that in LV, relatively high abundance (71%) of lncRNAs were encoded by mitochondrial genome (mito-lncRNAs), and the abundance of mito-lncRNAs showed some but not statistically significant reduction in both non-ischemic and ischemic human failing hearts (Yang et al., 2014). A mitochondria-encoded chimeric transcript, long intergenic non-coding RNA predicting cardiac remodeling (LIPCAR) with the 5′-half (1–392 nt) mapped to lnc*Cyt b* and 3′-half (385–781 nt) mapped to antisense of mt-COX2 gene was identified in plasma from myocardial infarction patients (Kumarswamy et al., 2014). The expression level of LIPCAR was downregulated at the early stage of myocardial infarction but upregulated during later stages; in addition, high LIPCAR levels were associated with future cardiovascular death. The circulating LIPCAR has a potential to be a risk-free biomarker of LV remodeling and a predictor of patient survival of heart failure (Kumarswamy et al., 2014).

Using a PacBio full-length third-generation sequencing transcriptome dataset, Gao et al. (2018) discovered two polycistronic transcripts hsa-MDL1 (Mitochondrial D-loop 1) and hsa-MDL1AS (Mitochondrial D-loop 1 antisense) generated from the region covering the $tRNA^{Pro}$ gene and full length of the human D-loop region (Gao et al., 2018). The presence of these transcripts was further confirmed by pan RNA-seq analysis (Xu et al., 2019). The mature hsa-MDL1 was generated from the H-strand polycistronic transcript, and hsa-MDLAS was antisense to hsa-MDL1 with much lower expression level. A great number of small RNAs reversely aligned to the mitochondrial D-loop region and a relatively lower abundant forwardly aligned small RNA (5% of reversely aligned ones) were obtained by searching public small RNA-sequencing data. hsa-MDL1 and hsa-MDL1AS were believed to be precursors of some of these small RNAs (Gao et al., 2018). Pan RNA-seq analysis also revealed the ubiquitous existence of 5′ and 3′ end small RNAs of MDL1 and MDL1AS (Xu et al., 2019).

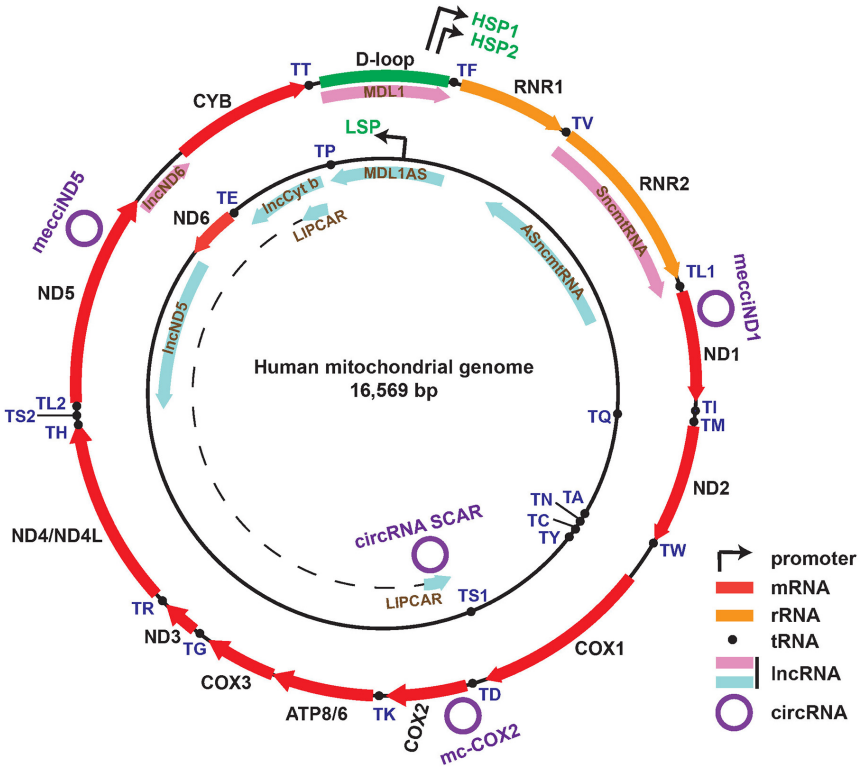

FIGURE 1 | Map of the human mitochondrial genome with the following features: Genes corresponding to 13 mRNAs, 2 rRNAs, and 22 tRNAs within heavy (outer track) and light (inner track) strands; D-loop region and promoters (HSP1, HSP2, LSP) of both strands; eight mitochondria-encoded lncRNAs shown in the inner side of each ring (lnc*ND5*, lnc*Cyt b*, lnc*ND6*, MDL1S, MDL1AS, SmtncRNA, ASmtncRNA, and LIPCAR); four recently reported functional circRNAs (mecciND1, mecciND5, mc-COX2, circRNA SCAR).

MITOCHONDRIA-ENCODED dsRNAs

Dhir et al. (2018) discovered highly unstable mitochondrial double-stranded RNA (mt-dsRNA) in HeLa cells, which was supposed to be the natural outcomes of the nearly complete transcription of both heavy and light strands of mtDNA. It has been known that almost the entire L-strand transcript undergoes rapid RNA turnover by the mitochondrial RNA degradosome (Borowski et al., 2013), and indeed the level of mt-dsRNAs was restricted by the RNA degradosome components SUV3 and PNPT1 (Dhir et al., 2018). Pathological PNPT1 mutations led to abnormal mt-dsRNA accumulation. The Bax-Bak dependent release of mt-dsRNAs into cytoplasm triggered the upregulation of interferon-stimulated genes and the activation of innate immune defenses through the MDA5–MAVS axis (Dhir et al., 2018). In Trp53 mutant mouse embryonic fibroblasts, mitochondrial dsRNAs cleaved by RNase L were immunogenic, and could activate the type I interferon (IFN) pathway via RIG-I-like receptors (Wiatrek et al., 2019).

MITOCHONDRIA-ENCODED circRNAs

circRNAs encoded by mammalian mitochondrial genome had not been revealed until recent report about the identification of hundreds of mitochondria encoded circRNAs (mecciRNAs) in human and murine cells through second-generation sequencing of mitochondrial RNAs (Liu et al., 2020, 2021). In three cell lines and one tumor tissue (hepatocellular carcinoma) from human and two cell lines together with two tissues (skeletal muscle and heart) from mice, 248 human mecciRNAs and 268 murine mecciRNAs were identified, respectively (Liu et al., 2020). Actually, the presence of large amount of mecciRNAs was not mammalian specific, as over one hundred mecciRNAs were also identified in zebrafish (Liu et al., 2020). mecciRNAs were encoded by both the light and heavy strands of the mtDNA, although the heavy strand of mtDNA encoded the majority (Liu et al., 2020). The presence of mitochondria encoded circRNAs in human HEK293 cells was examined by RT-PCR assay to amplify over one hundred individual mecciRNAs (Mance et al., 2020). With third-generation sequencing, mecciRNAs from murine brain were also analyzed for their junctions and full length (Zhang et al., 2021).

It was found that some mecciRNAs distributed both inside the mitochondria and outside in the cytosol (Liu et al., 2020). Functional studies of two mecciRNAs, mecciND1 (encoded by the mitochondrial ND1 gene) and mecciND5 (encoded by the mitochondrial ND5 gene) demonstrated that these mecciRNAs conducted essential physiological functions. mecciND1 bound to RPA1 and RPA2 proteins, which were

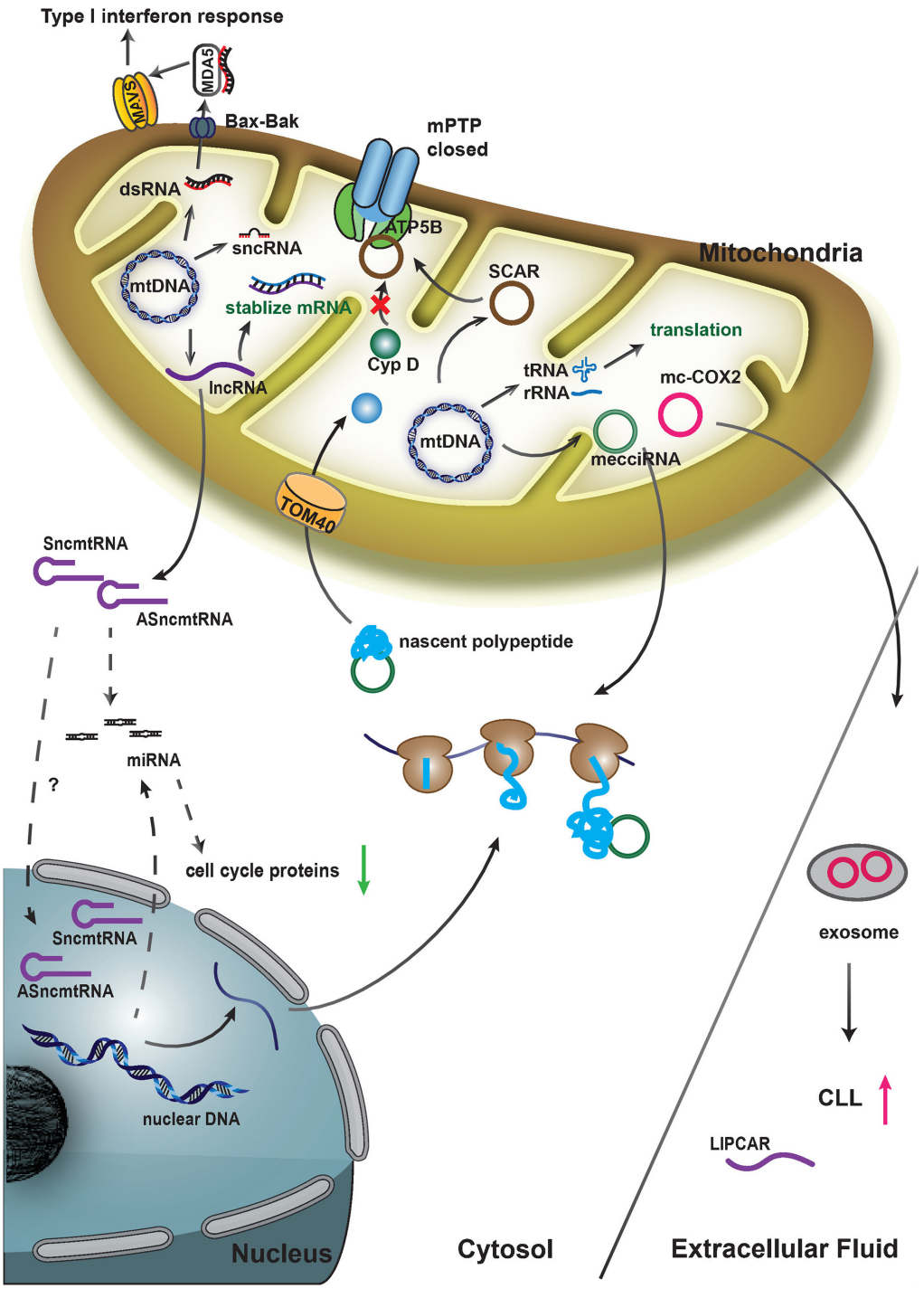

FIGURE 2 | Proposed functions and functional mechanisms of mitochondria-encoded noncoding RNAs.

involved in mtDNA replication. The expression level of mecciND1 was positively related to mitochondrial RPA protein levels and mtDNA copy numbers. mtDNA copy numbers were increased after mecciND1 overexpression and decreased under mecciND1 knockdown. mecciND5 interacted with hnRNPA1, hnRNPA2B1 and hnRNPA3 and promoted their mitochondrial importation (Liu et al., 2020). Both *in vivo* and *in vitro* evidence showed that the two mecciRNAs, mecciND1 and mecciND5, could interact with TOM40 and PNPASE, and function as molecular chaperons to facilitate the mitochondrial entry of newly synthesized polypeptides encoded by the nuclear genome (Liu et al., 2020; **Figure 2**). mecciND1 and

TABLE 1 | Mitochondria-encode non-coding RNAs.

mt-ncRNAs	Type	Distribution	Proposed function	References
tRNAs	tRNA	Mitochondria	Mitochondrial mRNA translation	Taanman, 1999
16S rRNA 12S rRNA	rRNA	Mitochondria	Components of mitochondrial ribosome	Taanman, 1999
lnc*ND5*, lnc*Cyt b*, lnc*ND6*	lncRNA	Mitochondria	Stabilization of ND5, ND6, and Cyt b mRNAs through forming RNA-RNA duplexes	Rackham et al., 2011
SncmtRNA, ASncmtRNAs	lncRNA	Ubiquitous	Cell-cycle regulation in cancer cells	Villegas et al., 2007; Burzio et al., 2009; Landerer et al., 2011; Fitzpatrick et al., 2019; Lobos-González et al., 2020; Borgna et al., 2020
LIPCAR	lncRNA	Plasma	A risk-free biomarker for cardiac remodeling	Kumarswamy et al., 2014; Yang et al., 2014;
MDL1, MDL1AS	lncRNA	Mitochondria	Precursors of some tiRNAs	Gao et al., 2018; Xu et al., 2019
dsRNAs	dsRNA	Mitochondria Cytosol	Participate in the activation of innate immune defenses through MDA5–MAVS antiviral signaling axis	Dhir et al., 2018; Wiatrek et al., 2019
mecciND1, mecciND5	circRNA	Mitochondria Cytosol	Promote mitochondrial protein import	Liu et al., 2020
mc-COX2	circRNA	Exosome	Promotes CLL cell proliferation	Wu et al., 2020
circRNA SCAR	circRNA	Mitochondria	Binds to ATP5B and inhibits mitochondrial ROS output and fibroblast activation	Zhao et al., 2020
mitosRNAs	sRNA	Mitochondria	Might be involved in the regulation of normal expression of mitochondrial genes	Mercer et al., 2011; Ro et al., 2013
hsa-miR-4461, hsa-miR-4463, hsa-miR-4484, hsa-miR-4485	sRNA	Mitochondria	May regulate site-specific turnover of target mRNAs	Sripada et al., 2012
hsa-tir-MDL1AS-18	sRNA	Mitochondria	Highly expressed in normal tissues than in Hepatocellular Carcinoma (HCC) tissues	Gao et al., 2018
piRNAs	sRNA	Mitochondria	Unknown	Esteller, 2011; Larriba et al., 2018

mecciND5 were upregulated in hepatocellular carcinoma (HCC) tissues, and moreover, mecciRNA levels were regulated in stress conditions, suggesting that they were critical for cells to cope with physiological and pathological changes (Liu et al., 2020).

When investigating the role of mitochondria-located circRNAs in metaflammation, Zhao et al. (2020) observed that 3 mitochondria-encoded circRNAs were downregulated in liver fibroblasts from patients with non-alcoholic steatohepatitis (NASH). One of the three mecciRNAs, termed SCAR (Steatohepatitis-associated circRNA ATP5B Regulator), was an antisense RNA from the locus COX2. SCAR bound directly to ATP5B, a mitochondrial permeability transition pore (mPTP) regulator. The interaction of ATP5B and SCAR shut down mPTP by blocking Cyclophilin D-mPTP interaction, and therefore, inhibited mitochondrial ROS (mROS) output (Zhao et al., 2020; **Figure 2**). mROS output was required for liver fibroblast activation, and this circRNA had a potential to serve as a therapeutic target for NASH (Zhao et al., 2020). Another highly expressed mecciRNA, mc-COX2, a sense RNA from the locus COX2, was found in the plasma exosomes of chronic lymphocytic leukemia (CLL) patients (Wu et al., 2020). mc-COX2 was closely correlated to prognosis of CLL, and moreover, it seemed that higher expression levels of mc-COX2 could promote cell proliferation and protect cells from apoptosis (Wu et al., 2020; **Figure 2**).

MITOCHONDRIA-ENCODED sncRNAs

In mammalian cells, small non-coding RNAs (sncRNAs) are diverse and abundant, mainly including microRNAs (miRNAs), endogenous-short interfering RNA (siRNAs), PIWI-interacting RNAs (piRNAs), and other types of small RNAs derived from tRNAs, rRNAs, and snoRNAs (Gomes et al., 2013). Recent studies have identified several types of sncRNAs that are generated from mammalian mitochondrial genome (**Table 1**).

Mercer et al. (2011) provided a comprehensive description of the human mitochondrial transcriptome. They sequenced mitochondrial small RNAs (sRNAs) isolated from human bone osteosarcoma cell line 143B and revealed 31 sRNAs of two distinct classes of 21 and 26 nt from 17 loci of mtDNA. The majority (84%) of them were produced from tRNA genes. Expression of these mitochondria-encoded sncRNAs changed dynamically in different cell types, however, the expression of sncRNAs did not seem to correlate significantly with the expression of overlapping genes (Mercer et al., 2011). Ro et al. (2013) reported that thousands of small RNAs were encoded

from murine and human mitochondrial genomes, and major size of these sRNAs ranged between 30 and 39 nt (mouse) and 20 and 29 nt (human). These RNAs were mainly transcribed from the sense direction of the mitochondrial genes (host genes), and only a small portion were from the antisense direction of their host genes. Those sRNAs appeared to target antisense transcripts and promoted the expression of their host genes *in vitro* (Ro et al., 2013). Interestingly, all these researches provided evidence that these mitochondria-encoded sncRNAs were generated in a Dicer-independent manner, and might be products of some unknown ribonucleases within the mitochondria (Mercer et al., 2011; Ro et al., 2013).

In human HEK293 and HeLa mitochondria, 4 known miRNAs (hsa-miR-4461, hsa-miR-4463, hsa-miR-4484, and hsa-miR-4485) and 24 putative novel miRNAs could be aligned to mitochondrial genome at the positions corresponding to 16S rRNA, tRNA, and mRNA (Sripada et al., 2012). These miRNAs might regulate site-specific turnover of target mRNAs. However, it was not conclusive that whether these microRNAs were actually transcribed from mitochondrial genome (Sripada et al., 2012). A series of small RNAs that aligned to the D-loop region of mtDNA were discovered by Gao et al. (2018). These small RNAs might be generated from mitochondrial lncRNAs hsa-MDL1AS and hsa-MDL1. The most abundant small RNA was hsa-tir-MDL1AS-18, derived from lncRNA hsa-MDL1AS. It belonged to transcription initial RNAs (tiRNAs), as 18 nucleotides from its 5′ end precisely overlapped with transcription initiation (IT) sites of the L-strand promoter. hsa-tir-MDL1AS-18 was down-regulated in hepatocellular carcinoma (HCC) tissues, suggesting that the balance of tiRNAs/lncRNAs regulation might be abnormal in cancer cells (Gao et al., 2018).

Through mapping known piRNA sequences to the human mtDNA, Kwon et al. (2014) identified 29 piRNAs, and 12 out of these 29 piRNAs matched to the stem-loop fragments of seven mitochondrial tRNAs with asymmetric tRNA fragment usage and cell type specific expression. They also reported the presence of PIWI through Western blots and three abundant mature piRNAs by RT-PCR in the mitochondria of HeLa-S3 cells (Kwon et al., 2014). Mitochondria-encoded piRNAs might also be present in mouse (Larriba et al., 2018). Among all the small RNA reads from oocytes and zygotes of mice, about 20% of the reads were mapped to mitochondrial DNA, and 80–90% of the reads were classified as piRNAs based on the size; these piRNAs were encoded by both strands of the mouse mitochondrial genome, and were highly expressed from the loci corresponding to mitochondrial tRNAs, 16S rRNA, and D-loop region (Larriba et al., 2018). Functional study of mitochondrial piRNAs is lacking, and these piRNAs are speculated to function in stress responses (Kwon et al., 2014), gamete differentiation, and fertilization (Larriba et al., 2018).

NUCLEAR-ENCODED ncRNAs IN MITOCHONDRIA

In mammalian mitochondria, besides some well-known nuclear encoded tRNAs ($tRNA^{Leu}UAA$, $tRNA^{Gln}UUG$, and $tRNA^{Gln}CUG$) (Rubio et al., 2008; Mercer et al., 2011; Gowher et al., 2013), 5S rRNA (Yoshionari et al., 1994; Magalhães et al., 1998; Entelis et al., 2001; Mercer et al., 2011; Zelenka et al., 2014; Autour et al., 2018), RMRP RNA (Chang and Clayton, 1987; Li et al., 1994; Wang et al., 2010; Noh et al., 2016), some nuclear-encoded ncRNAs including miRNAs and lncRNAs were also found to play critical roles in mitochondria (Kim et al., 2017; Jeandard et al., 2019; **Table 2**). miRNAs were described in purified mitochondria of rat and mouse through miRNA microarray analysis (Kren et al., 2009; Bian et al., 2010). Bandiera et al. (2011) identified 13 nuclear-encoded miRNAs enriched in mitochondria of HeLa cells, and defined these mitochondria-located miRNAs as mitomiRs. Meanwhile, Barrey et al. (2011) predicted 25 pre-miRNAs and 33 miRNAs in human mitochondrial *in silico* sequencing analysis, and a set of them were demonstrated to be present in the mitochondria of skeletal muscular cells by *in situ* hybridization and RT-PCR (Barrey et al., 2011). Moreover, both studies revealed that these miRNAs might post-transcriptionally regulate mt-RNAs in mitochondria through RNA interfering pathway (Bandiera et al., 2011; Barrey et al., 2011). Nuclear DNA-encoded miR-18c was found to be translocated into the mitochondria of rat cardiac myocytes (Das et al., 2012). miR-18c loaded in AGO2n bound to the 3′ UTR of mt-COX1, and inhibited mt-COX1 translation, ultimately leading to complex IV remodeling and mitochondrial dysfunction (Das et al., 2012). mitomiR-378 conducted a similar function that downregulated mt-ATP6 translation in mouse HL-1 cells (Jagannathan et al., 2015). Fan and co-workers identified mitomiR-2392 was upregulated in cisplatin-resistant tongue squamous cell carcinoma (TSCC) cells and TSCC tumors (Fan et al., 2019). Surprisingly, mitomiR-2392 was found to partially repress the transcription of mtDNA rather than the translation, through miRNA:mtDNA base pairing with an AGO2-dependent manner (Fan et al., 2019). The downstream genes regulated by mitomiR-2392 were different between two TSCC cell lines, suggesting a cell-specific regulation (Fan et al., 2019). In addition to inhibitory effects, some mitomiRs were found playing positive regulatory functions. For example, miR-1 was induced and imported into mitochondria during myogenesis to stimulate the translation of mt-ND1 and mt-COX1, through specific miRNA:mRNA base-pairing with the participation of AGO2 in mouse heart and C2C12 cells (Zhang et al., 2014). Most mitomiRs with demonstrated functions played AGO2-dependent roles, and an array of evidence showed that AGO2 was present in mitochondria (Bandiera et al., 2011, 2013; Zhang et al., 2014; Vendramin et al., 2017).

The malignant lncRNA SAMMSON (survival associated mitochondrial melanoma specific oncogenic non-coding RNA) was predominantly localized in the cytoplasm of human melanoblasts and melanoma cells, and interestingly, a large fraction of cytoplasmic SAMMSON was found to co-localize and co-purify with mitochondria (Leucci et al., 2016). SAMMSON played pro-oncogenic roles in mitochondrial homeostasis and metabolism by interacting with and stabilizing p32 protein, a regulator of the maturation of mitochondrial 16S rRNA (Leucci et al., 2016; Vendramin et al., 2018). Human nuclear RNase P RNA component (H1 RNA) was reported in mitochondria of HeLa cells (Bartkiewicz et al., 1989; Puranam and Attardi, 2001).

TABLE 2 | Nuclear-encoded non-coding RNAs in mitochondria.

ncRNAs	Type	Function in cytosol/nucleus	Proposed function in mitochondria	References
tRNAs ($tRNA^{Leu}$UAA, $tRNA^{Gln}$UUG, $tRNA^{Gln}$CUG)	tRNA	Translation	May participate in translation	Rubio et al., 2008; Gowher et al., 2013
Various miRNAs (hsa-miR-494, hsa-miR-1275, hsa-miR-1974, miR18c, miR-378 etc.) and pre-miRNAs	miRNA	RNA interfering pathway	Translation inhibition	Bandiera et al., 2011; Barrey et al., 2011; Das et al., 2012; Jagannathan et al., 2015
mitomiR-2392	miRNA	RNA interfering pathway	Transcription repression	Fan et al., 2019
miR-1	miRNA	RNA interfering pathway	Translation activation	Zhang et al., 2014
5S rRNA	rRNA	Component of the cytosolic ribosome	May participate in translation	Yoshionari et al., 1994; Magalhães et al., 1998; Entelis et al., 2001; Autour et al., 2018; Mercer et al., 2011; Zelenka et al., 2014
RMRP	lncRNA	5.8S rRNA processing	Mitochondrial RNA processing	Chang and Clayton, 1987; Li et al., 1994; Wang et al., 2010; Noh et al., 2016
SAMMSON	lncRNA	Interacts with p32 and facilitates its targeting to the mitochondria	Unknown	Leucci et al., 2016; Vendramin et al., 2018
H1 RNA	lncRNA	RNA component of nuclear RNase P	May participate in mitochondrial RNA processing	Bartkiewicz et al., 1989; Puranam and Attardi, 2001
hTERC	lncRNA	RNA component of Telomerase	May be processed in mitochondria and transported back to cytosol	Cheng et al., 2018

However, as human mitochondrial RNase P was a protein-only complex and a trans-acting RNA component was not required for catalysis (Holzmann et al., 2008), the role of H1 RNA in mitochondria was still unclear. Cheng et al. (2018) found that human telomerase RNA component (hTERC) was imported into mitochondria, processed to a shorter form hTERC-53, and then exported back to the cytosol (Cheng et al., 2018). The underlaying mechanism and cellular significance of this cytosol and mitochondria import-export process of hTERC-hTERC-53 is elusive and needs further investigation.

DISCUSSION

It is apparent that the known complexity of mitochondrial transcriptome of human and mammals has been greatly expanded. Mitochondrial genome encodes not only very limited numbers of mRNAs, rRNAs and tRNAs as previously understood, but also a variety of non-coding RNAs such as lncRNAs, circRNAs, sncRNAs, and dsRNAs with diverse regulatory functions. Mitochondria seem to have sacrificed the protein coding ability, although maintained the capacity of generating their "own" complex ncRNA profiles, with the small size but highly utilized genome.

Mitochondria-encoded lncRNAs seem function through RNA-RNA interaction or as precursors of small RNAs to regulate the stabilization or expression of their corresponding mt-RNAs in mitochondria (Rackham et al., 2011; Gao et al., 2018). Several mt-lncRNAs can be detected outside the mitochondria, such as LIPCAR in plasma, SncmtRNA and ASncmtRNAs in nucleus, but the mechanisms of their transport or function are still elusive (Landerer et al., 2011; Kumarswamy et al., 2014). circRNAs encoded by the mammalian nuclear genome are known to function as microRNA sponges, transcriptional regulators, protein binding partners, and templates for protein translation (Chen et al., 2015; Li et al., 2015; Kristensen et al., 2019; Chen and Shan, 2021). Mitochondria-encoded circRNAs may reside in or shuttle in and out of the mitochondria to play critical roles, and the functions and functional mechanisms of mecciRNAs are waiting for further in-depth investigation (Liu et al., 2020; Zhao et al., 2020). The sRNAs, miRNAs, piRNAs, and other snRNAs encoded by mitochondrial genome are generally classified by their size, and the functions of these non-coding RNAs need further elucidation. Some nuclear genome encoded miRNAs (mitomiRs) can also function in mitochondria. Studies of these mitomiRs may provide some implications for future investigation on mitochondria-encoded sncRNAs. The presence of AGO2 in mitochondria makes it reasonable to speculate that certain sncRNAs can also function through RNAi machinery in mitochondria (Bandiera et al., 2011; Bandiera et al., 2013; Zhang et al., 2014; Vendramin et al., 2017). The functional characterizations of mitochondria-encoded ncRNAs are just emerging, and the biogenesis and metabolism of mitochondria-encoded ncRNAs, including circRNAs, lncRNAs, and sncRNAs, remain largely obscure.

Due to the limited coding capacity of mitochondrial genome, it is known that a large number of proteins encoded by the nuclear genome are imported into mitochondria from cytosol to sustain the biogenesis and function of these organelles (Harbauer et al., 2014; Wiedemann and Pfanner, 2017). Mitochondria

generate energy, ROS, and other metabolic molecules for multiple essential cellular events, and also participate in multiple pathways regulating nuclear gene expression, cell death, proliferation, differentiation, etc. (McBride et al., 2006). The growing evidence and examples reviewed in this article have shown that non-coding RNAs are engaged in the bidirectional communication between mitochondria and the nucleus (Vendramin et al., 2017; Gusic and Prokisch, 2020). Nuclear DNA-encoded miRNAs and lncRNAs can also be transported into mitochondria and regulate mitochondrial gene expression transcriptionally and post-transcriptionally. However, the import mechanisms are still poorly understood. Several lines of evidence show that tRNAs are imported into mitochondria by an ATP dependent mechanism that is distinct from protein import (Rubio et al., 2008; Gowher et al., 2013). Disruption of the mitochondrial membrane potential, which is crucial for protein import, has no effect on tRNA import (Rubio et al., 2008). There is only one protein PNPT1 (also named PNPASE), which locates in the intermembrane space (IMS) of mitochondria, known to facilitate the transport of RMRP, H1 RNA, and hTERC through binding to small stem-loops of these RNAs (Wang et al., 2010; Kim et al., 2017; Jeandard et al., 2019). Mitochondria-encoded ncRNAs contribute to the nucleus-mitochondria communication, and some of them not only function inside the mitochondria but also play roles outside of the mitochondria. For example, mecciRNAs shuttle between mitochondria and cytosol to facilitate the mitochondrial entry of newly synthesized polypeptides encoded by the nuclear genome (Liu et al., 2020). ASncmtRNAs are reported with nuclear and cytosolic localization, and regulate the translation of cell cycle proteins (Landerer et al., 2011; Fitzpatrick et al., 2019). But how these ncRNAs get transported through the bilayer membrane of mitochondria is still unclear, and further investigations about the mechanisms will contribute to a deeper understanding of mitochondria-nucleus communication.

Mitochondrial dysfunction relates to a series of diseases, such as cardiovascular diseases, cancers, and neurodegeneration (Herst et al., 2017; Jusic and Devaux, 2020). The cell/tissue specific expression of mt-ncRNAs also suggests that they may take part in mitochondria-related diseases. The investigations of mitochondrial ncRNAs regulatory network would contribute to better understanding of etiology, and lead to novel diagnostic and therapeutic approaches for mitochondrial dysfunction-related diseases. Mitochondria-encoded non-coding RNAs have no doubt pointed to a new direction for the study of mitochondria-nucleus communication, and study about these RNAs is an important field of biomedicine.

AUTHOR CONTRIBUTIONS

GS and XL conceived the scope of the manuscript and wrote the manuscript. Both authors contributed to the article and approved the submitted version.

FUNDING

This work was supported by grants from the National Key R&D Program of China (2019YFA0802600 and 2018YFC1004500), the National Natural Science Foundation of China (32000438, 31725016, 31930019, and 91940303), and the Strategic Priority Research Program "Biological basis of aging and therapeutic strategies" of the Chinese Academy of Sciences (XDB39010400).

REFERENCES

Asin-Cayuela, J., and Gustafsson, C. M. (2007). Mitochondrial transcription and its regulation in mammalian cells. *Trends Biochem. Sci.* 32, 111–117. doi: 10.1016/j.tibs.2007.01.003

Autour, A., C Y Jeng, S., D Cawte, A., Abdolahzadeh, A., Galli, A., Panchapakesan, S. S. S., et al. (2018). Fluorogenic RNA Mango aptamers for imaging small non-coding RNAs in mammalian cells. *Nat. Commun.* 9:656. doi: 10.1038/s41467-018-02993-8

Bandiera, S., Matégot, R., Girard, M., Demongeot, J., and Henrion-Caude, A. (2013). MitomiRs delineating the intracellular localization of microRNAs at mitochondria. *Free Radic. Biol. Med.* 64, 12–19. doi: 10.1016/j.freeradbiomed.2013.06.013

Bandiera, S., Rüberg, S., Girard, M., Cagnard, N., Hanein, S., Chrétien, D., et al. (2011). Nuclear outsourcing of RNA interference components to human mitochondria. *PLoS One* 6:e20746. doi: 10.1371/journal.pone.0020746

Barchiesi, A., and Vascotto, C. (2019). Transcription, processing, and decay of mitochondrial RNA in health and disease. *Int. J. Mol. Sci.* 20:2221. doi: 10.3390/ijms20092221

Barrey, E., Saint-Auret, G., Bonnamy, B., Damas, D., Boyer, O., and Gidrol, X. (2011). Pre-microRNA and mature microRNA in human mitochondria. *PLoS One* 6:e20220. doi: 10.1371/journal.pone.0020220

Barshad, G., Marom, S., Cohen, T., and Mishmar, D. (2018). Mitochondrial DNA transcription and its regulation: an evolutionary perspective. *Trends Genet.* 34, 682–692. doi: 10.1016/j.tig.2018.05.009

Bartkiewicz, M., Gold, H., and Altman, S. (1989). Identification and characterization of an RNA molecule that copurifies with RNase P activity from HeLa cells. *Genes Dev.* 3, 488–499. doi: 10.1101/gad.3.4.488

Bian, Z., Li, L., Tang, R., Hou, D., Chen, X., Zhang, C., et al. (2010). Identification of mouse liver mitochondria-associated miRNAs and their potential biological functions. *Cell Res.* 20, 1076–1078. doi: 10.1038/cr.2010.119

Borgna, V., Lobos-González, L., Guevara, F., Landerer, E., Bendek, M., Ávila, R., et al. (2020). Targeting antisense mitochondrial noncoding RNAs induces bladder cancer cell death and inhibition of tumor growth through reduction of survival and invasion factors. *J. Cancer* 11, 1780–1791. doi: 10.7150/jca.38880

Borowski, L. S., Dziembowski, A., Hejnowicz, M. S., Stepien, P. P., and Szczesny, R. J. (2013). Human mitochondrial RNA decay mediated by PNPase–hSuv3 complex takes place in distinct foci. *Nucleic Acids Res.* 41, 1223–1240. doi: 10.1093/nar/gks1130

Burzio, V. A., Villota, C., Villegas, J., Landerer, E., Boccardo, E., Villa, L. L., et al. (2009). Expression of a family of noncoding mitochondrial RNAs distinguishes normal from cancer cells. *Proc. Natl. Acad. Sci. U.S.A.* 106, 9430–9434. doi: 10.1073/pnas.0903086106

Chang, D. D., and Clayton, D. A. (1987). A mammalian mitochondrial RNA processing activity contains nucleus-encoded RNA. *Science* 235, 1178–1184. doi: 10.1126/science.2434997

Chen, H., and Shan, G. (2020). The physiological function of long-noncoding RNAs. *Noncoding RNA Res.* 5, 178–184. doi: 10.1016/j.ncrna.2020.09.003

Chen, L., and Shan, G. (2021). CircRNA in cancer: fundamental mechanism and clinical potential. *Cancer Lett.* 505, 49–57. doi: 10.1016/j.canlet.2021.02.004

Chen, L., Huang, C., Wang, X. L., and Shan, G. (2015). Circular RNAs in eukaryotic cells. *Curr. Genomics* 16, 312–318. doi: 10.2174/1389202916666150707161554

Cheng, Y., Liu, P. P., Zheng, Q., Gao, G., Yuan, J. P., Wang, P. F., et al. (2018). Mitochondrial trafficking and processing of telomerase RNA TERC. *Cell Rep.* 24, 2589–2595. doi: 10.1016/j.celrep.2018.08.003

Das, S., Ferlito, M., Kent, O. A., Fox-Talbot, K., Wang, R., Liu, D., et al. (2012). Nuclear miRNA regulates the mitochondrial genome in the heart. *Circ. Res.* 110, 1596–1603. doi: 10.1161/circresaha.112.267732

Dhir, A., Dhir, S., Borowski, L. S., Jimenez, L., Teitell, M., Rötig, A., et al. (2018). Mitochondrial double-stranded RNA triggers antiviral signalling in humans. *Nature* 560, 238–242. doi: 10.1038/s41586-018-0363-0

Djebali, S., Davis, C. A., Merkel, A., Dobin, A., Lassmann, T., Mortazavi, A., et al. (2012). Landscape of transcription in human cells. *Nature* 489, 101–108. doi: 10.1038/nature11233

Entelis, N. S., Kolesnikova, O. A., Dogan, S., Martin, R. P., and Tarassov, I. A. (2001). 5 S rRNA and tRNA import into human mitochondria. comparison of in vitro requirements. *J. Biol. Chem.* 276, 45642–45653. doi: 10.1074/jbc.M103906200

Esteller, M. (2011). Non-coding RNAs in human disease. *Nat. Rev. Genet.* 12, 861–874. doi: 10.1038/nrg3074

Fan, S., Tian, T., Chen, W., Lv, X., Lei, X., Zhang, H., et al. (2019). Mitochondrial miRNA determines chemoresistance by reprogramming metabolism and regulating mitochondrial transcription. *Cancer Res.* 79, 1069–1084. doi: 10.1158/0008-5472.can-18-2505

Fitzpatrick, C., Bendek, M. F., Briones, M., Farfán, N., Silva, V. A., Nardocci, G., et al. (2019). Mitochondrial ncRNA targeting induces cell cycle arrest and tumor growth inhibition of MDA-MB-231 breast cancer cells through reduction of key cell cycle progression factors. *Cell Death Dis.* 10:423. doi: 10.1038/s41419-019-1649-3

Gao, S., Tian, X., Chang, H., Sun, Y., Wu, Z., Cheng, Z., et al. (2018). Two novel lncRNAs discovered in human mitochondrial DNA using PacBio full-length transcriptome data. *Mitochondrion* 38, 41–47. doi: 10.1016/j.mito.2017.08.002

Gomes, A. Q., Nolasco, S., and Soares, H. (2013). Non-coding RNAs: multi-tasking molecules in the cell. *Int. J. Mol. Sci.* 14, 16010–16039. doi: 10.3390/ijms140816010

Gowher, A., Smirnov, A., Tarassov, I., and Entelis, N. (2013). Induced tRNA import into human mitochondria: implication of a host aminoacyl-tRNA-synthetase. *PLoS One* 8:e66228. doi: 10.1371/journal.pone.0066228

Gusic, M., and Prokisch, H. (2020). ncRNAs: new players in mitochondrial health and disease? *Front. Genet.* 11:95. doi: 10.3389/fgene.2020.00095

Gustafsson, C. M., Falkenberg, M., and Larsson, N. G. (2016). Maintenance and expression of mammalian mitochondrial DNA. *Annu. Rev. Biochem.* 85, 133–160. doi: 10.1146/annurev-biochem-060815-014402

Harbauer, A. B., Zahedi, R. P., Sickmann, A., Pfanner, N., and Meisinger, C. (2014). The protein import machinery of mitochondria-a regulatory hub in metabolism, stress, and disease. *Cell Metab.* 19, 357–372. doi: 10.1016/j.cmet.2014.01.010

Herst, P. M., Rowe, M. R., Carson, G. M., and Berridge, M. V. (2017). Functional mitochondria in health and disease. *Front. Endocrinol.* 8:296. doi: 10.3389/fendo.2017.00296

Holzmann, J., Frank, P., Löffler, E., Bennett, K. L., Gerner, C., and Rossmanith, W. (2008). RNase P without RNA: identification and functional reconstitution of the human mitochondrial tRNA processing enzyme. *Cell* 135, 462–474. doi: 10.1016/j.cell.2008.09.013

Iyer, M. K., Niknafs, Y. S., Malik, R., Singhal, U., Sahu, A., Hosono, Y., et al. (2015). The landscape of long noncoding RNAs in the human transcriptome. *Nat. Genet.* 47, 199–208. doi: 10.1038/ng.3192

Jagannathan, R., Thapa, D., Nichols, C. E., Shepherd, D. L., Stricker, J. C., Croston, T. L., et al. (2015). Translational regulation of the mitochondrial genome following redistribution of mitochondrial MicroRNA in the diabetic heart. *Circ. Cardiovasc. Genet.* 8, 785–802. doi: 10.1161/circgenetics.115.001067

Jeandard, D., Smirnova, A., Tarassov, I., Barrey, E., Smirnov, A., and Entelis, N. (2019). Import of non-coding RNAs into human mitochondria: a critical review and emerging approaches. *Cells* 8:286. doi: 10.3390/cells8030286

Jusic, A., and Devaux, Y. (2020). Mitochondrial noncoding RNA-regulatory network in cardiovascular disease. *Basic. Res. Cardiol.* 115:23. doi: 10.1007/s00395-020-0783-5

Kim, K. M., Noh, J. H., Abdelmohsen, K., and Gorospe, M. (2017). Mitochondrial noncoding RNA transport. *BMB Rep.* 50, 164–174. doi: 10.5483/bmbrep.2017.50.4.013

Kren, B. T., Wong, P. Y. P., Sarver, A., Zhang, X., Zeng, Y., and Steer, C. J. (2009). MicroRNAs identified in highly purified liver-derived mitochondria may play a role in apoptosis. *RNA Biol.* 6, 65–72. doi: 10.4161/rna.6.1.7534

Kristensen, L. S., Andersen, M. S., Stagsted, L. V., Ebbesen, K. K., Hansen, T. B., and Kjems, J. (2019). The biogenesis, biology and characterization of circular RNAs. *Nat. Rev. Genet.* 20, 675–691. doi: 10.1038/s41576-019-0158-7

Kumarswamy, R., Bauters, C., Volkmann, I., Maury, F., Fetisch, J., Holzmann, A., et al. (2014). Circulating long noncoding RNA, LIPCAR, predicts survival in patients with heart failure. *Circ. Res.* 114, 1569–1575. doi: 10.1161/CIRCRESAHA.114.303915

Kwon, C., Tak, H., Rho, M., Chang, H. R., Kim, Y. H., Kim, K., et al. (2014). Detection of PIWI and piRNAs in the mitochondria of mammalian cancer cells. *Biochem. Biophys. Res. Commun.* 446, 218–223. doi: 10.1016/j.bbrc.2014.02.112

Landerer, E., Villegas, J., Burzio, V. A., Oliveira, L., Villota, C., Lopez, C., et al. (2011). Nuclear localization of the mitochondrial ncRNAs in normal and cancer cells. *Cell. Oncol.* 34, 297–305. doi: 10.1007/s13402-011-0018-8

Larriba, E., Rial, E., and Del Mazo, J. (2018). The landscape of mitochondrial small non-coding RNAs in the PGCs of male mice, spermatogonia, gametes and in zygotes. *BMC Genomics* 19:634. doi: 10.1186/s12864-018-5020-3

Leucci, E., Vendramin, R., Spinazzi, M., Laurette, P., Fiers, M., Wouters, J., et al. (2016). Melanoma addiction to the long non-coding RNA SAMMSON. *Nature* 531, 518–522. doi: 10.1038/nature17161

Li, K., Smagula, C. S., Parsons, W. J., Richardson, J. A., Gonzalez, M., Hagler, H. K., et al. (1994). Subcellular partitioning of MRP RNA assessed by ultrastructural and biochemical analysis. *J. Cell Biol.* 124, 871–882. doi: 10.1083/jcb.124.6.871

Li, Z., Huang, C., Bao, C., Chen, L., Lin, M., Wang, X., et al. (2015). Exon-intron circular RNAs regulate transcription in the nucleus. *Nat. Struct. Mol. Biol.* 22, 256–264. doi: 10.1038/nsmb.2959

Liu, X., Wang, X., Li, J., Hu, S., Deng, Y., Yin, H., et al. (2020). Identification of mecciRNAs and their roles in the mitochondrial entry of proteins. *Sci. China Life Sci.* 63, 1429–1449. doi: 10.1007/s11427-020-1631-9

Liu, X., Yang, Y., and Shan, G. (2021). Identification and detection of mecciRNAs. *Methods* 21, 43–48. doi: 10.1016/j.ymeth.2021.02.006

Lobos-González, L., Bustos, R., Campos, A., Silva, V., Silva, V., Jeldes, E., et al. (2020). Exosomes released upon mitochondrial ASncmtRNA knockdown reduce tumorigenic properties of malignant breast cancer cells. *Sci. Rep.* 10:343. doi: 10.1038/s41598-019-57018-1

Lopez Sanchez, M. I., Mercer, T. R., Davies, S. M., Shearwood, A.-M. J., Nygård, K. K., Richman, T. R., et al. (2011). RNA processing in human mitochondria. *Cell Cycle* 10, 2904–2916. doi: 10.4161/cc.10.17.17060

Magalhães, P. J., Andreu, A. L., and Schon, E. A. (1998). Evidence for the presence of 5S rRNA in mammalian mitochondria. *Mol. Biol. Cell.* 9, 2375–2382. doi: 10.1091/mbc.9.9.2375

Mance, L. G., Mawla, I., Shell, S. M., and Cahoon, A. B. (2020). Mitochondrial mRNA fragments are circularized in a human HEK cell line. *Mitochondrion* 51, 1–6. doi: 10.1016/j.mito.2019.11.002

Marchese, F. P., Raimondi, I., and Huarte, M. (2017). The multidimensional mechanisms of long noncoding RNA function. *Genome Biol.* 18:206. doi: 10.1186/s13059-017-1348-2

McBride, H. M., Neuspiel, M., and Wasiak, S. (2006). Mitochondria: more than just a powerhouse. *Curr. Biol.* 16, R551–R560. doi: 10.1016/j.cub.2006.06.054

Mercer, T. R., Neph, S., Dinger, M. E., Crawford, J., Smith, M. A., Shearwood, A.-M. J., et al. (2011). The human mitochondrial transcriptome. *Cell* 146, 645–658. doi: 10.1016/j.cell.2011.06.051

Noh, J. H., Kim, K. M., Abdelmohsen, K., Yoon, J. H., Panda, A. C., Munk, R., et al. (2016). HuR and GRSF1 modulate the nuclear export and mitochondrial localization of the lncRNA RMRP. *Genes Dev.* 30, 1224–1239. doi: 10.1101/gad.276022.115

Ojala, D., Montoya, J., and Attardi, G. (1981). tRNA punctuation model of RNA processing in human mitochondria. *Nature* 290, 470–474. doi: 10.1038/290470a0

Puranam, R. S., and Attardi, G. (2001). The RNase P associated with HeLa cell mitochondria contains an essential RNA component identical in sequence to that of the nuclear RNase P. *Mol. Cell Biol.* 21, 548–561. doi: 10.1128/mcb.21.2.548-561.2001

Rackham, O., Shearwood, A. M., Mercer, T. R., Davies, S. M., Mattick, J. S., and Filipovska, A. (2011). Long noncoding RNAs are generated from the mitochondrial genome and regulated by nuclear-encoded proteins. *RNA* 17, 2085–2093. doi: 10.1261/rna.029405.111

Rashid, F., Shah, A., and Shan, G. (2016). Long non-coding RNAs in the cytoplasm. *Genomics Proteomics Bioinformatics* 14, 73–80. doi: 10.1016/j.gpb.2016.03.005

Ro, S., Ma, H. Y., Park, C., Ortogero, N., Song, R., Hennig, G. W., et al. (2013). The mitochondrial genome encodes abundant small noncoding RNAs. *Cell Res.* 23, 759–774. doi: 10.1038/cr.2013.37

Rubio, M. A., Rinehart, J. J., Krett, B., Duvezin-Caubet, S., Reichert, A. S., Söll, D., et al. (2008). Mammalian mitochondria have the innate ability to import tRNAs by a mechanism distinct from protein import. *Proc. Natl. Acad. Sci. U.S.A.* 105, 9186–9191. doi: 10.1073/pnas.0804283105

Scarpulla, R. C. (2008). Transcriptional paradigms in mammalian mitochondrial biogenesis and function. *Physiol. Rev.* 88, 611–638. doi: 10.1152/physrev.00025.2007

Sripada, L., Tomar, D., Prajapati, P., Singh, R., Singh, A. K., and Singh, R. (2012). Systematic analysis of small RNAs associated with human mitochondria by deep sequencing: detailed analysis of mitochondrial associated miRNA. *PLoS One* 7:e44873. doi: 10.1371/journal.pone.0044873

Taanman, J.-W. (1999). The mitochondrial genome: structure, transcription, translation and replication. *Biochim. Biophys. Acta.* 1410, 103–123. doi: 10.1016/s0005-2728(98)00161-3

Vendramin, R., Marine, J. C., and Leucci, E. (2017). Non-coding RNAs: the dark side of nuclear-mitochondrial communication. *EMBO J.* 36, 1123–1133. doi: 10.15252/embj.201695546

Vendramin, R., Verheyden, Y., Ishikawa, H., Goedert, L., Nicolas, E., Saraf, K., et al. (2018). SAMMSON fosters cancer cell fitness by concertedly enhancing mitochondrial and cytosolic translation. *Nat. Struct. Mol. Biol.* 25, 1035–1046. doi: 10.1038/s41594-018-0143-4

Villegas, J., Burzio, V., Villota, C., Landerer, E., Martinez, R., Santander, M., et al. (2007). Expression of a novel non-coding mitochondrial RNA in human proliferating cells. *Nucleic Acids Res.* 35, 7336–7347. doi: 10.1093/nar/gkm863

Wang, G., Chen, H. W., Oktay, Y., Zhang, J., Allen, E. L., Smith, G. M., et al. (2010). PNPASE regulates RNA import into mitochondria. *Cell* 142, 456–467. doi: 10.1016/j.cell.2010.06.035

Wiatrek, D. M., Candela, M. E., Sedmík, J., Oppelt, J., Keegan, L. P., and O'Connell, M. A. (2019). Activation of innate immunity by mitochondrial dsRNA in mouse cells lacking p53 protein. *RNA* 25, 713–726. doi: 10.1261/rna.069625.118

Wiedemann, N., and Pfanner, N. (2017). Mitochondrial machineries for protein import and assembly. *Annu. Rev. Biochem.* 86, 685–714. doi: 10.1146/annurev-biochem-060815-014352

Wu, Z., Sun, H., Wang, C., Liu, W., Liu, M., Zhu, Y., et al. (2020). Mitochondrial genome-derived circRNA mc-COX2 functions as an oncogene in chronic lymphocytic leukemia. *Mol. Ther. Nucleic Acids* 20, 801–811. doi: 10.1016/j.omtn.2020.04.017

Xu, X., Ji, H., Jin, X., Cheng, Z., Yao, X., Liu, Y., et al. (2019). Using Pan RNA-Seq Analysis to Reveal the Ubiquitous Existence of 5′ and 3′ End Small RNAs. *Front. Genet.* 10:105. doi: 10.3389/fgene.2019.00105

Yang, K. C., Yamada, K. A., Patel, A. Y., Topkara, V. K., George, I., Cheema, F. H., et al. (2014). Deep RNA sequencing reveals dynamic regulation of myocardial noncoding RNAs in failing human heart and remodeling with mechanical circulatory support. *Circulation* 129, 1009–1021. doi: 10.1161/CIRCULATIONAHA.113.003863

Yoshionari, S., Koike, T., Yokogawa, T., Nishikawa, K., Ueda, T., Miura, K., et al. (1994). Existence of nuclear-encoded 5S-rRNA in bovine mitochondria. *FEBS Lett.* 338, 137–142. doi: 10.1016/0014-5793(94)80351-x

Zelenka, J., Alán, L., Jabůrek, M., and Ježek, P. (2014). Import of desired nucleic acid sequences using addressing motif of mitochondrial ribosomal 5S-rRNA for fluorescent in vivo hybridization of mitochondrial DNA and RNA. *J. Bioenerg. Biomembr.* 46, 147–156. doi: 10.1007/s10863-014-9543-2

Zhang, J., Hou, L., Zuo, Z., Ji, P., Zhang, X., Xue, Y., et al. (2021). Comprehensive profiling of circular RNAs with nanopore sequencing and CIRI-long. *Nat. Biotechnol.* 39, 836–845. doi: 10.1038/s41587-021-00842-6

Zhang, X., Zuo, X., Yang, B., Li, Z., Xue, Y., Zhou, Y., et al. (2014). MicroRNA directly enhances mitochondrial translation during muscle differentiation. *Cell* 158, 607–619. doi: 10.1016/j.cell.2014.05.047

Zhao, Q., Liu, J., Deng, H., Ma, R., Liao, J. Y., Liang, H., et al. (2020). Targeting mitochondria-located circRNA SCAR alleviates NASH via reducing mROS output. *Cell* 183, 76–93. doi: 10.1016/j.cell.2020.08.009

Conflict of Interest: The authors declare that the research was conducted in the absence of any commercial or financial relationships that could be construed as a potential conflict of interest.

Publisher's Note: All claims expressed in this article are solely those of the authors and do not necessarily represent those of their affiliated organizations, or those of the publisher, the editors and the reviewers. Any product that may be evaluated in this article, or claim that may be made by its manufacturer, is not guaranteed or endorsed by the publisher.

frontiers in Cell and Developmental Biology

REVIEW
published: 03 August 2021
doi: 10.3389/fcell.2021.688523

Non-coding RNA Regulated Cross-Talk Between Mitochondria and Other Cellular Compartments

*Jinliang Huang[1], Sipeng Wu[2], Pengcheng Wang[2] and Geng Wang[2]**

[1] School of Life Sciences, Tsinghua University, Beijing, China, [2] State Key laboratory for Cellular Stress Biology, Innovation Center for Cell Signaling Network, School of Life Sciences, Xiamen University, Fujian, China

Mitochondria are the main hubs for cellular energy production. Metabolites produced in mitochondria not only feed many important biosynthesis pathways but also function as signaling molecules. Mitochondrial biosynthesis requires collaboration of both nuclear and mitochondrial gene expression systems. In addition, mitochondria have to quickly respond to changes inside and outside the cells and have their own functional states reported to the nucleus and other cellular compartments. The underlying molecular mechanisms of these complex regulations have not been well understood. Recent evidence indicates that in addition to small molecules, non-coding RNAs may contribute to the communication between mitochondria and other cellular compartments and may even serve as signals. In this review, we summarize the current knowledge about mitochondrial non-coding RNAs (including nucleus-encoded non-coding RNAs that are imported into mitochondria and mitochondrion-encoded non-coding RNAs that are exported), their trafficking and their functions in co-regulation of mitochondrial and other cellular processes.

Keywords: mitochondria, retrograde signaling, nucleus, non-coding RNAs, trafficking, PNPASE

OPEN ACCESS

Edited by:
Veronica Andrea Burzio, Andres Bello University, Chile

Reviewed by:
Johannes M. Herrmann, University of Kaiserslautern, Germany
Carlos Palmeira, University of Coimbra, Portugal

****Correspondence:***
Geng Wang
wangengfuan@xmu.edu.cn

Specialty section:
This article was submitted to Mitochondrial Research, a section of the journal Frontiers in Cell and Developmental Biology

Received: *31 March 2021*
Accepted: *12 July 2021*
Published: *03 August 2021*

Citation:
Huang J, Wu S, Wang P and Wang G (2021) Non-coding RNA Regulated Cross-Talk Between Mitochondria and Other Cellular Compartments. Front. Cell Dev. Biol. 9:688523. doi: 10.3389/fcell.2021.688523

INTRODUCTION

Mitochondria are organelles originated from ancient proteobacteria through endosymbiosis. Over time, the majority of their endosymbiont genome has been transferred to the host cell nucleus (Calvo et al., 2016). Mitochondria, however, maintain a small compact genome (Anderson et al., 1981). Mitochondrial biosynthesis thus requires collaboration of both nuclear and mitochondrial gene expression systems. Maintaining a small mitochondrial genome thereby provides mitochondria and the host cells a new layer of regulation and control by coordinating mitochondrial functional states with nuclear and other intracellular, and even extracellular events.

Through evolution, some other bacterial characteristics of mitochondria have also been preserved. Mitochondria still retain their own transcriptional and translational machineries, and the mitochondrial ribosomes resemble bacterial ribosomes in many ways (Brown et al., 2014; Greber et al., 2015; Rorbach et al., 2016). In addition, the fission of mitochondria and bacterial division share certain similarities, even though mitochondria have two membranes: the outer membrane and the inner membrane (Friedman and Nunnari, 2014). In a sense, some materials within mitochondria are still treated as foreign objects by the host cells. For example, mitochondrial DNA (mtDNA) could trigger the host cell immune responses when leaked into the cytosol, activating the cGAS-STING pathway (Oka et al., 2012).

Mitochondrial genome is circular, and in humans encodes 22 tRNAs, 2 rRNAs, and 13 OXPHOS proteins (Anderson et al., 1981). mtDNA is transcribed into poly-cistronic preRNAs. Processing and modification of the nascent RNAs yields functional mitochondrial mRNAs, rRNAs, tRNAs, and some other non-coding RNAs (Masters et al., 1987). Biosynthesis of mitochondria, nevertheless, depends largely on the nuclear genome, and the majority of mitochondrial proteins are synthesized in the cytosol or on the outer membrane of mitochondria, imported and then assembled into functional proteins and complexes (Schmidt et al., 2010; Richter-Dennerlein et al., 2015). Increasing evidence shows that various types of nucleus-originated RNA species can also translocate to mitochondria from the cytosol (Leucci et al., 2016; Kim et al., 2017; Vendramin et al., 2018; Gusic and Prokisch, 2020; Sang et al., 2021).

Recent studies have also shown that translocation of RNAs across mitochondrial membranes appears to be bidirectional: the imported RNAs or mitochondrion-transcribed RNAs can also be exported to the cytosol to regulate important cellular processes (Eduardo et al., 2011; Cheng et al., 2018; Dhir et al., 2018; Zheng et al., 2019).

Although more and more nuclear gene-encoded RNAs have been found in mitochondria, most of their functions remain unclear, and their translocation molecular mechanisms are still to be further uncovered. The first component of the RNA import machinery, polynucleotide phosphorylase (PNPASE) was identified in 2010 (Wang et al., 2010). Some progress has since been made on understanding the molecular mechanisms of mitochondrial RNA translocation and the functions of some of these mitochondrial non-coding RNAs, which we have summarized in this review.

MITOCHONDRIAL RNA IMPORT

Mitochondrial RNA import has been reported in many species, and the importomes seem to vary between species. Most of the studied species, however, seem to import one or more tRNAs. Trypanosomatids (Crausaz Esseiva et al., 2004) and apicomplexans (Esseiva et al., 2004) of parasitic protozoa completely lack tRNA genes in their mtDNAs. Therefore, all the tRNAs within their mitochondria are imported from the cytosol. The mtDNAs of some land plants and protists lack one or several tRNA genes, so tRNA import into mitochondria from the cytosol is also essential for mitochondrial translation (Akashi et al., 1998). Although yeast and mammalian mitochondria encode a full set of tRNAs, a few cytosolic tRNAs have been found within their mitochondria. In yeast, two cytosolic tRNAs, $tRNA^{Lys}_{CUU}$ (Tarassov et al., 1995b) and $tRNA^{Gln}$ (Rinehart et al., 2005), are imported into mitochondria, which may play a role in stress response. In mammals, mitochondrial localization of nucleus-encoded $tRNA^{Gln}_{CUG}$ and $tRNA^{Gln}_{UUG}$ has been reported (Rubio et al., 2008).

In addition to tRNAs, some nuclear or cytosolic non-coding RNAs have also been found in mammalian mitochondria, such as *5S* rRNA, *H1* RNA, *RMRP*, *SAMMSON*, *TERC*, *GAS5*, siRNA (Gao et al., 2021), pre-miRNAs (Barrey et al., 2011), and miRNAs (**Table 1**). Their individual regulations and functions have been expertly summarized in previous reviews (Vendramin et al., 2017; Jeandard et al., 2019). In this review, we focus mainly on their translocation mechanisms and their functions in communication between mitochondria and other cellular compartments.

Based on the existing data on RNA import into mitochondria, the mechanisms seem to be quite diverse, with different RNAs require different specific factors.

TABLE 1 | Mammalian mitochondrial RNA importome.

RNA	Function outside mitochondria	Proposed function in mitochondria	References
5S rRNA	Component of the cytosolic ribosome; assisting rhodanese import	Related to mitochondrial translation?	Magalhães et al., 1998; Smirnov et al., 2010; Smirnov et al., 2011; Wang et al., 2010; Yoshionari et al., 1994
H1 RNA	Component of the nuclear RNase P required for pre-tRNA processing	Pre-tRNA processing?	Ellis and Brown, 2009; Kikovska et al., 2007; Puranam and Attardi, 2001; Rossmanith et al., 1995; Turk et al., 2013; Wang et al., 2010
RMRP	*5.8S* rRNA processing	Involved in mitochondrial RNA metabolism?	Chang and Clayton, 1987b; Chang and Clayton, 1987a; Lu et al., 2010; Noh et al., 2016; Wang et al., 2010
SAMMSON	Facilitating p32 targeting to the mitochondria in melanoma cells; regulating rRNA maturation and protein synthesis	Unknown	Leucci et al., 2016; Vendramin et al., 2018
TERC	RNA component of telomerase	Mitochondrion-cytosol communication	Cheng et al., 2018; Zheng et al., 2019
GAS5	Regulating *INSR* gene transcription; functioning as an RNA sponge	Modulating mitochondrial tricarboxylic acid flux	Mourtada-Maarabouni et al., 2010; Sang et al., 2021
Various miRNAs (including miR-1, miR-181c, miR-378) pre-miRNAs, and siRNAs	Repressing mRNA translation	Repressing or activating mRNA translation; repressing transcription	Barrey et al., 2011; Gan et al., 2019; Gao et al., 2021; Jeandard et al., 2019; Vendramin et al., 2017; Zhang et al., 2014
28S rRNA	Component of the cytosolic ribosome	None (degraded in the mitochondrial IMS)	Huang et al., 2018

The mitochondrial RNA import process can be roughly divided into three steps:

The Step(s) Before Cross-Membrane Translocation

Cytosolic factors appear to be required for mitochondrial import of some non-coding RNAs but not all. In *Trypanosoma brucei*, the tRNA T-stem nucleotide pair and its cytosolic binding partner elongation factor 1a (EF1a) determine the specificity of tRNA import into mitochondria (Bouzaidi-Tiali et al., 2007). On the other hand, isolated mitochondria from *Leishmania tarentolae* can import *in vitro*-transcribed tRNAs without any added cytosolic factors (Rubio et al., 2000). Potato (*Solanum tuberosum*) mitochondria can also import cytosolic $tRNA^{Ala}$ of *Arabidopsis thaliana* in the absence of additional cytosolic protein fraction (Delage et al., 2003).

In *Saccharomyces cerevisiae*, one of the two cytoplasmic lysine-tRNA isoacceptors, $tRNA^{Lys}_{CUU}$ (*tRK1*), is selectively imported into mitochondria. Mitochondrial outer membrane-attached glycolytic enzyme enolase binds the aminoacylated $tRNA^{Lys}_{CUU}$ and acts as an RNA chaperone, possibly with the assistance of additional unidentified cytosolic factors. The interaction causes a conformational change that increases the affinity of $tRNA^{Lys}_{CUU}$ to another protein factor pre-mitochondrial lysyl-tRNA synthetase (preMsk1p) (Tarassov et al., 1995b), allowing $tRNA^{Lys}_{CUU}$ to be co-imported into mitochondrial matrix (Brandina et al., 2006; Entelis et al., 2006; Baleva et al., 2017). Moreover, *in vitro* import assays have shown that mitochondria isolated from HepG2 cells can internalize yeast $tRNA^{Lys}_{CUU}$ (*tRK1*) in the presence of yeast cytosolic factors, suggesting that the mitochondrial RNA import machinery might be conserved in yeast and humans (Kolesnikova et al., 2000). In contrast, yeast mitochondrial import of $tRNA^{Gln}$ does not seem to require any cytosolic factor (Rinehart et al., 2005), and neither does import of $tRNA^{Gln}$ into mammalian mitochondria (Rubio et al., 2008).

Cytosolic protein factors have also been shown to regulate the mitochondrial import of *5S* rRNA in mammals. Newly translated mitochondrial ribosomal protein L18 may bind and reshape the conformation of cytosolic *5S* rRNA (Smirnov et al., 2011). This conformational change allows *5S* rRNA to interact with newly synthesized rhodanese, and subsequently the RNA-protein complex is imported into mitochondrial matrix (Smirnov et al., 2010). *In vitro* import of *5S* rRNA into purified mitochondria, however, does not require any of these protein partners (Wang et al., 2010), suggesting that these protein factors are dispensable for mitochondrial import of *5S* rRNA.

In addition to co-importing with cytosolic factors, bringing non-coding RNAs to the close proximity of mitochondrial outer membrane seems to be another way of assisting their import. Most of the nucleus-encoded mitochondrial inner membrane proteins are translated by the ribosomes on the outer surface of mitochondrial outer membrane, and are imported co-translationally (Holt and Bullock, 2009; Williams et al., 2014). A mitochondrial RNA degradation machinery consisting of RNASET2 as the ribonuclease and PNPASE as an RNA transportation regulator has recently been identified in the mitochondrial IMS (Liu et al., 2017). It has been shown that mitochondrion-associated *28S* rRNA can be targeted for degradation by this RNA degradation machinery (Huang et al., 2018). How the *28S* rRNA is selected for degradation and how it is extracted from the ribosomes and imported into mitochondrial IMS remains to be elucidated.

Translocation Across the Mitochondrial Outer Membrane

Two classes of channels in the mitochondrial outer membrane, the translocase of the outer membrane (TOM) complex and the voltage-dependent anion channel (VDAC) have been postulated as the channels for mitochondrial RNA import.

In yeast *S. cerevisiae*, mitochondrial uptake of $tRNA^{Lys}_{CUU}$ is inhibited by treatment of mitochondria with proteases, suggesting that certain outer membrane receptors may have a role in $tRNA^{Lys}_{CUU}$ import (Tarassov et al., 1995a). Furthermore, the mitochondrial cross-membrane translocation of $tRNA^{Lys}_{CUU}$ is dependent on energy and an intact transmembrane potential, similar to mitochondrial protein import (Entelis et al., 2001). Mitochondria from yeast cells carrying mutant *mom19* or *mim44* alleles show significant defects in $tRNA^{Lys}_{CUU}$ import, indicating that yeast mitochondrial outer membrane translocase MOM19 and inner membrane translocase MIM44 are important for the import process (Tarassov et al., 1995a).

In plants, cytosolic $tRNA^{Ala}$ of *A. thaliana* has been shown to interact with *S. tuberosum* VDAC, and its import into isolated mitochondria is inhibited by mitochondrial respiration blockers, such as valinomycin, oligomycin, KCN, and FCCP (Delage et al., 2003). The import can also be inhibited by anti-VDAC antibodies and Ruthenium red, indicating the involvement of VDAC in translocation of tRNAs (Salinas et al., 2006). Moreover, the import is inhibited by trypsin treatment (Delage et al., 2003) and subsequent studies show that TOM20 and TOM40 may have additional roles in regulating tRNA import (Salinas et al., 2006). It should be noted that all these data only show that these proteins are somehow involved, but do not tell whether the involvement is direct or indirect.

Translocation Across the Mitochondrial Inner Membrane

Some mitochondrial non-coding RNAs may hitchhike the mitochondrial protein import pathway, especially those RNAs that have been shown to be co-imported with mitochondrial proteins such as tRNAs and *5S* rRNA. As mentioned above, in yeast, mitochondrial inner membrane translocase MIM44 has been implicated in $tRNA^{Lys}_{CUU}$ import (Tarassov et al., 1995a). Even though the inner membrane protein translocons have channels that can accommodate the size of an RNA molecule, they do not seem to be compatible with the predominantly negative charge of the molecule if the RNA is imported in a naked state. However, co-importing with mitochondria-targeted precursor proteins may overcome this incompatibility.

The dependence on membrane potential for RNA import varies between organisms. The membrane potential is required for the import of tRNAs into plant mitochondria and the import

of $tRNA^{Lys}_{CUU}$ into yeast mitochondria (Kolesnikova et al., 2000; Delage et al., 2003). However, tRNA import into protozoa *L. tarentolae* and mammalian mitochondria does not need a membrane potential (Rubio et al., 2000, 2008).

In *Leishmania tropica*, tRNA import across the mitochondrial inner membrane involves a 600-kDa RNA-import complex (RIC), and some of the subunits are members of the respiratory complex (Salinas et al., 2008). Whether this inner membrane protein complex exists in other species remains to be clarified.

In mammals, translocation of lncRNAs across the mitochondrial outer and inner membrane is facilitated by mitochondrial IMS protein PNPASE. Mammalian PNPASE localizes on the outer surface of mitochondrial inner membrane (Chen et al., 2006), forming a trimer or a dimer of trimers (Wang et al., 2010). It is unlike most peripheral membrane proteins, as the association with the inner membrane is much stronger. PNPASE is a 3′–5′ exoribonuclease in bacteria. PNPASE purified from mammalian mitochondria, however, has no ribonuclease activity (Liu et al., 2017). In fact, neither mitochondrial matrix, nor mitochondrial total membrane that harbors mammalian PNPASE contains any obvious ribonuclease activity (Liu et al., 2017). PNPASE has been shown to not only mediate the import of most lncRNAs and one miRNA *miRNA-378* into mitochondrial matrix, but also the export of mitochondrial RNAs from the matrix to the IMS to be degraded (Wang et al., 2010; Liu et al., 2017; Shepherd et al., 2017). In addition, import of cytosolic *28S* rRNA into mitochondrial IMS for degradation (Huang et al., 2018) and export of *TERC-53* are also mediated by PNPASE (Cheng et al., 2018).

Identifying the RNA channel in the mitochondrial inner membrane remains one of the biggest hurdles of the field. Research done on mtDNA import and export may provide some clues. DNA import into plant mitochondria has been shown to be inhibited by the adenine nucleotide translocase (ANT) inhibitor atractyloside, suggesting the involvement of ANT in DNA import (Koulintchenko et al., 2003). ANT proteins are the main components of the mitochondrial permeability transition pore (mPTP). The effectors of mPTP, however, have opposite effects on DNA import (Koulintchenko et al., 2003), suggesting that ANT itself but not mPTP is involved in DNA import into plant mitochondria. It should be noted that these are all indirect proofs.

Mitochondrial permeability transition pores, however, have been shown to be involved in the release of mtDNA into the cytosol under stress conditions (Oka et al., 2012; Jeonghan et al., 2019). Whether ANTs or mPTPs directly function in mitochondrial RNA translocation across the inner membrane remains to be investigated.

The mitochondrial translocation mechanisms of other mammalian non-coding RNAs, such as *SAMMSON*, *GAS5*, and mecciRNAs, remain largely unclear.

MITOCHONDRIAL RNA EXPORT

Studies have shown that mitochondria also export non-codings RNAs and mtDNA (**Table 2**). Under stress, mitochondria release mtDNA into the cytosol, which can trigger the immune response by activating the cGAS-STING pathway (Oka et al., 2012; Jeonghan et al., 2019). The mPTP and the outer membrane pore formed by VDAC oligomerization have been shown to be involved in the release of mtDNA (Oka et al., 2012; Jeonghan et al., 2019). Recent studies have shown that mitochondria also release double-stranded RNAs (dsRNAs) into the cytosol in a PNPASE-dependent manner (Dhir et al., 2018). It was proposed that PNPASE was the ribonuclease that degrades mitochondrial RNAs in the mitochondrial IMS but not in the matrix, and that defects in mitochondrial RNA degradation led to accumulation of mitochondrial dsRNAs in the cytosol (Chen et al., 2006). PNPASE localizes mainly in the mitochondrial IMS, and so do most mitochondrial nuclease activities such as RNASET2, REXO2 and Endonuclease G (Cote and Ruiz-Carrillo, 1993; Francesco et al., 2013; Huang et al., 2018). It should be noted that mammalian PNPASE has no ribonuclease activity, and neither does mitochondrial total membrane that harbors PNPASE (Liu et al., 2017). Therefore, it is more logical to conclude that PNPASE is involved in the substrate delivering step of mtRNA degradation.

In addition to dsRNAs, other mtDNA-encoded non-coding RNAs have been detected outside of mitochondria. One example is *SncmtRNA*, a 2374-nucleotide chimeric transcript composed of mitochondrial *16S* rRNA covalently linked to an 815-nucleotide 5′-leader fragment derived from the complementary strand (Birgit et al., 2007). *SncmtRNA* is polyadenylated and forms an 820 bp double-stranded structure

TABLE 2 | Mammalian mitochondrial RNA exportome.

Name	Mitochondrial function	Proposed function outside mitochondria	References
mtDNA	Mitochondrial genome	Initiating immune response	Jeonghan et al., 2019; Oka et al., 2012
SncmtRNA	Unknown	Related to cell proliferation and cell cycle?	Birgit et al., 2007; Burzio et al., 2009; Dietrich et al., 2015; Vidaurre et al., 2014
ASncmtRNA-1/2	Unknown	Functioning as tumor suppressors?	Birgit et al., 2007; Burzio et al., 2009; Dietrich et al., 2015; Vidaurre et al., 2014
LIPCAR	Unknown	Biomarker of cardiac remodeling?	Dietrich et al., 2015; Kai-Chien et al., 2018; Kumarswamy et al., 2014
mecciRNA	Unknown	Functioning as mitochondrial protein folding chaperones, facilitating mitochondrial protein import	Liu et al., 2020
TERC-53	Unknown	Initiating mitochondrial stress response?	Cheng et al., 2018; Zheng et al., 2019

with a 40-nucleotide loop (Dietrich et al., 2015). *SncmtRNA* is preferentially expressed in highly proliferating normal and cancer cells (Birgit et al., 2007). Two antisense lncRNAs of *SncmtRNA* (*ASncmtRNA-1* and *ASncmtRNA-2*) have also been identified in normal proliferating cells (Burzio et al., 2009). All three RNAs are present both in mitochondria and in the nucleus (Eduardo et al., 2011), suggesting a mitochondrial export process. *ASncmtRNAs* are downregulated in tumor cells, and a role as tumor suppressors has been postulated (Vidaurre et al., 2014).

Another mitochondrion-encoded lncRNA *LIPCAR* is also a chimeric transcript, formed between the 5′-end of *COX2* and 3′-end of *CYTB*. It was identified in the plasmas from patients with chronic heart failure (Kumarswamy et al., 2014; Kai-Chien et al., 2018). The function of *LIPCAR* remains unclear.

In addition to lncRNAs, mitochondrial genome also produces a set of miRNAs. These miRNAs, however, appear to remain within mitochondria (Ro et al., 2013). Recently, RNA-sequencing has identified hundreds of circular RNAs (mecciRNAs) that are also encoded by the mitochondrial genome (Liu et al., 2020). Unlike mitochondrial genome-encoded miRNA, mecciRNAs have been shown to shuttle in and out of mitochondria (Liu et al., 2020). While in the cytosol, mecciRNAs function as chaperones in the folding of mitochondrial proteins, facilitating their import (Liu et al., 2020).

Finally, one of the imported RNAs *TERC* has been shown to be processed within mitochondria, and the processing product *TERC-53* is exported to the cytosol, where it functions as a downstream indicator of mitochondrial stress (Cheng et al., 2018). Cytosolic *TERC-53* has been shown to be involved in cellular senescence and organismal aging (Zheng et al., 2019).

THE FUNCTIONS OF MITOCHONDRIAL NON-CODING RNAS IN COMMUNICATION BETWEEN MITOCHONDRIA AND OTHER CELLULAR COMPARTMENTS

The known functions of mitochondrial non-coding RNAs in communication between cellular compartments can be roughly categorized into following groups (**Figure 1**):

Rescuing Mitochondrial Defects Under Stress

Yeast $tRNA^{Lys}_{CUU}$ (*tRK1*) is one of the tRNAs that has been shown to be imported into mitochondria (Martin et al., 1979). Yeast mitochondrial genome already encodes a functional $tRNA^{Lys}$ (*tRK3*). The wobble uridine of the *tRK3* anticodon has a 2-thio modification, which cannot be formed efficiently at 37°C. Consequently, codon recognition by *tRK3* is compromised under heat-shock conditions, and the normally dispensable *tRK1* becomes essential for the translation of *AAG* codon (Martin et al., 1979).

Assisting Import of Mitochondrial Proteins

For a long time, it was believed that the imported *5S* rRNA was incorporated into mitochondrial ribosomes. However, recent cryo-EM studies show that mammalian mitochondrial ribosomes do not stably integrate *5S* rRNA, but contain a mitochondrion-encoded tRNA instead (Brown et al., 2014; Greber et al., 2015; Rorbach et al., 2016). The function of mitochondrial *5S* rRNA may lie in the import itself. It has been shown that *5S* rRNA is co-imported with rhodanese, acting as a molecular chaperone by interacting with newly-translated rhodanese and maintaining it in an enzymatically inactive state (Smirnov et al., 2010). The interaction facilitates the mitochondrial import of both *5S* rRNA and rhodanese (Smirnov et al., 2010).

Another example of non-coding RNA assisting mitochondrial protein import is *SAMMSON*. *SAMMSON* is predominantly expressed in aggressive melanomas (Leucci et al., 2016). Mitochondrial association of *SAMMSON* has been confirmed with multiplex RNA FISH. Whether *SAMMSON* is imported into mitochondria, however, remains to be confirmed. One of the *SAMMSON*-interacting protein is p32 (Leucci et al., 2016; Vendramin et al., 2018), a well-established regulator of mitochondrial ribosome assembly and mitochondrial protein synthesis (Fogal et al., 2010). Knockdown of *SAMMSON* in melanoma cells impairs mitochondrial targeting of p32, leading to mitochondrial translation defects and subsequently triggering apoptotic cell death (Leucci et al., 2016).

mecciRNAs are the last known group of mitochondrial RNAs that fall into this category (Liu et al., 2020). These circular RNAs can be imported into mitochondria by themselves (Liu et al., 2020). Linearization abolishes their import. mecciRNAs show certain degrees of specificity with the proteins that they assist. The import of the target proteins is most efficient when the RNAs are added co-translationally (Liu et al., 2020). Interaction of the RNAs with known components of mitochondrial protein and RNA import pathways such as TOM40 and PNPASE has also been observed (Liu et al., 2020). One of the mecciRNAs that have been further studied is *mecciDN1*. It has been shown to facilitate the mitochondrial import of RPA32 and RPA70, both of which are components of mtDNA replication and repair machineries (Liu et al., 2020). Under stress conditions such as UV and hydrogen peroxide treatments, *mecciDN1* levels are upregulated and mitochondrial RPA32 and RPA70 levels increase even though the total protein levels remain the same (Yue et al., 2006; Liu et al., 2020). Upregulation of *mecciDN1* levels was also observed in tumor samples.

Co-regulating Cytosolic and Mitochondrial Translation Programs

Mitochondrial biosynthesis requires coordination of nuclear and mitochondrial genomes. The subunits of OXPHOS complexes are encoded in both genomes, and synchronization of the cytosolic translation and mitochondrial translation programs has been shown to be critical for the assembly of these complexes and their functions (Couvillion et al., 2016). *SAMMSON*-interacting protein p32 in cancer cells is a well-established regulator of

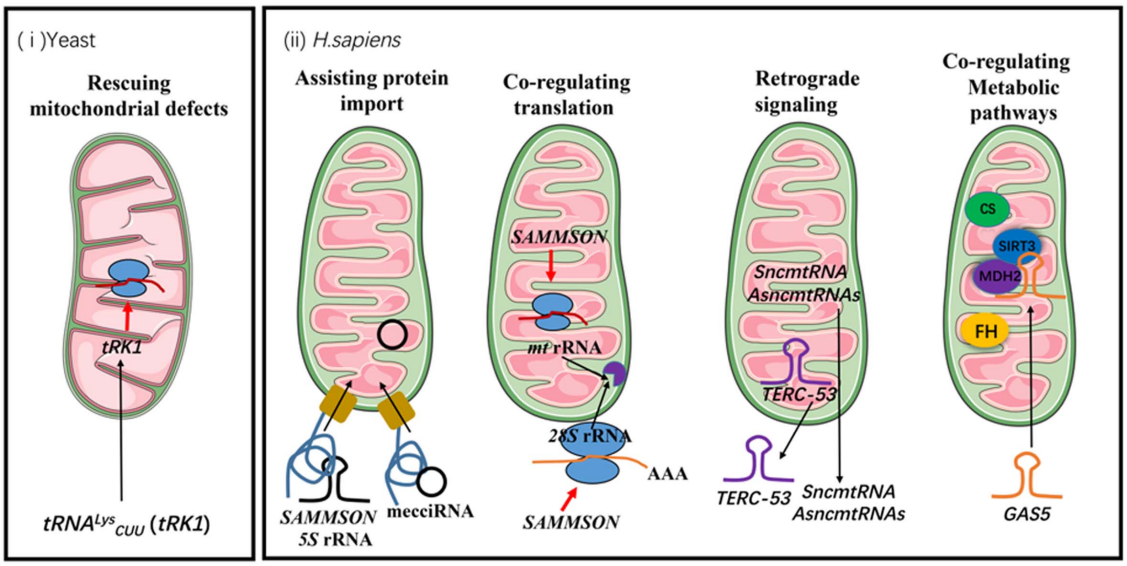

FIGURE 1 | The functions of mitochondrial non-coding RNAs in communication between mitochondria and other cellular compartments. The black arrows indicate the directions of trafficking. The red arrows indicate positive regulations of cellular processes. FH stands for fumarate hydratase and CS stands for citrate synthase.

mitochondrial ribosome assembly and mitochondrial protein synthesis (Fogal et al., 2010). Knockdown of *SAMMSON* in melanoma cells decreases mitochondrial p32 levels and induces mitochondrial protein synthesis defects (Leucci et al., 2016). Recent studies have shown that *SAMMSON* also regulates rRNA maturation and protein synthesis in the cytosol by interacting with CARF (Vendramin et al., 2018). CARF is normally a nucleoplasm protein that interacts with XRN2 (5′–3′ exoribonuclease 2) (Shigeko et al., 2015). XRN2 has a crucial role in maturation of virtually all RNAs and in nuclear RNA turnover. In the nucleoli, it is vital for maturation of *5.8S* rRNA and *28S* rRNA (Shigeko et al., 2015). Interaction of CARF with XRN2 in the nucleoplasm thus limits entry of XRN2 into the nucleoli. *SAMMSON* promotes p32 binding to CARF in the cytosol, which limits CARF localization in the nucleoplasm, interferes with its binding to XRN2, and favors localization of XRN2 to the nucleoli (Vendramin et al., 2018). Therefore, *SAMMSON* stimulates protein synthesis both in the cytosol and mitochondria, hence conferring a growth advantage to the cancer cells.

A recently discovered RNA degradation machinery in the mitochondrial IMS consisting of RNASET2 as the ribonuclease and PNPASE as an RNA transportation regulator has also been shown to co-regulate cytosolic translation and mitochondrial translation, but in a different fashion (Liu et al., 2017; Huang et al., 2018). Most of the nucleus-encoded mitochondrial inner membrane proteins have been shown to be translated by mitochondrion-associated ribosomes at the outer surface of mitochondrial outer membrane (Holt and Bullock, 2009; Williams et al., 2014). The IMS RNA degradation machinery not only functions in degradation of mitochondrial rRNAs and mRNAs, but also selectively degrades *28S* rRNA from the ribosomes on the outer surface of mitochondrial outer membrane (Liu et al., 2017; Huang et al., 2018). The ribonuclease activity responds sensitively to a series of cellular conditions, such as pH, ATP and divalent metal ions (Liu et al., 2017; Huang et al., 2018), providing an elegant mechanism for co-regulating translation programs in and out of mitochondria, as well as coordinating mitochondrial biosynthesis to these cellular conditions. Moreover, the ribonuclease activity regulates both nuclear rRNA transcription and mitochondrial rRNA transcription through a yet uncharacterized compensatory feedback signaling pathway (Liu et al., 2017; Huang et al., 2018). How the rRNAs are delivered across mitochondrial inner membrane and outer membrane also remains to be investigated.

What we have described are two cases where general translation programs are regulated by mitochondrial non-coding RNAs. There are also mitochondrial non-coding RNAs that regulate expression of individual proteins both inside and outside mitochondria. One example is *miR-1*, a microRNA specially induced during myogenesis (Zhang et al., 2014). *miR-1* is imported into mitochondria, where it recruits *ND1* and *COX1* mRNAs to mitochondrial ribosomes in an AGO2-dependent manner (Zhang et al., 2014). Instead of acting as a suppressor of protein expression, *miR-1* activates expression of ND1 and COX1 in the mitochondria during muscle differentiation (Zhang et al., 2014). *miR-1* has also been shown to target *IGF1* and *CCND1* mRNAs in the cytosol, where it functions as an inhibitor of the expression of these two proteins (Gan et al., 2019). CCND1 is an important cell cycle regulator and IGF1 has functions in many aspects of cell metabolism and proliferation (Montalto and Amicis, 2020). By inhibiting their expression, *miR-1* thus has a negative impact on G1/S phase transition, proliferation and viability of cardiomyocytes. By coordination its functions in and out of mitochondria, *miR-1* thereby fine-tunes the switch of cell types and metabolism programs.

Functioning as Retrograde Signals

Mitochondria have to change their functional states in response to cellular needs and environmental cues. One of the vital steps is reporting their functional states to the nucleus and other cellular compartments, so mitochondrial biosynthesis, and mitochondrial repair or recycling programs such as mitochondrial unfolded protein responses can be upregulated or inhibited (Li et al., 2021). Mitochondrial non-coding RNAs have also been shown to function in mitochondrial retrograde signaling. One example is the dsRNAs exported from mitochondria. In the cytosol, these RNAs engage a MDA5-driven immune signaling pathway that activates a type I interferon response (Dhir et al., 2018). The mitochondrial IMS degradation machinery that restricts the release of mitochondrial dsRNAs could therefore play a vital role in restricting this auto immune response (Liu et al., 2017; Huang et al., 2018; Maciej et al., 2020). Whether it is also involved in defense against the invasion of RNA viruses remains to be investigated.

Another example of mitochondrial RNAs initiating downstream signals outside of mitochondria is *TERC-53*. *TERC-53* is a cleavage product of telomerase RNA *TERC* by the above-mentioned ribonuclease RNASET2 in the mitochondrial IMS (Cheng et al., 2018; Zheng et al., 2019). After its processing, *TERC-53* is exported and localizes mainly in the cytosol. The cytosolic *TERC-53* engages different downstream effectors in different cell types (Cheng et al., 2018; Zheng et al., 2019). We have shown that in cancer cells and in neuronal cells, cytosolic *TERC-53* has very different binding partners (Unpublished data) (Cheng et al., 2018; Zheng et al., 2019). *TERC-53* levels respond to mitochondrial functional states and one of the downstream events is reprogramming the expression of a subset of genes that are involved in stress responses, which eventually manifests in cellular senescence and organismal aging (Cheng et al., 2018; Zheng et al., 2019).

SncmtRNA and its antisense lncRNAs (*ASncmtRNA-1* and *ASncmtRNA-2*) have been found both in mitochondria and in the nucleus (Birgit et al., 2007; Burzio et al., 2009; Vidaurre et al., 2014; Dietrich et al., 2015; **Figure 1**). Both *ASncmtRNAs* are downregulated in cancer cells, and further knockdown of *ASncmtRNAs* in cancer cells induces cell death by apoptosis. In endothelial cells, *ASncmtRNA-2* is upregulated in aging and replicative senescence (Bianchessi et al., 2015). Even though their exact functions remain unknown, their localization in the nucleus suggests a role in mitochondrial retrograde signaling.

Co-regulating Metabolic Pathways in Mitochondria and the Cytosol

Most of the functions summarized so far may eventually lead to co-regulation of the cytosolic and the mitochondrial metabolic programs, but some mitochondrial non-coding RNAs appear to directly regulate the activities of the components of these metabolic pathways. *GAS5* is a lncRNA that contains a 5′-terminal oligo pyrimidine (TOP) stretch (Mourtada-Maarabouni et al., 2010). The 5′-TOP sequence is normally found in mRNAs under the control of mTOR (Kahan and Meyuhas, 2015). Recent studies have shown that *GAS5* is translocated to mitochondria under nutrient stress, where it disrupts metabolic enzyme tandem association of fumarate hydratase, malate dehydrogenase, and citrate synthase (Sang et al., 2021). Downregulation of the interaction between *GAS5* and these enzymes has been observed in cancer cells (Sang et al., 2021). Even though the mechanistic details linking *GAS5* and mTOR are still to be elucidated, given the importance of mTOR in nutrient sensing and metabolism, these data suggest a co-regulation of the metabolic pathways in and out of mitochondria by *GAS5*.

DISCUSSION

There have been some doubts about the validity of the mitochondrial RNA import field, partially due to the technical challenge of truly separating isolated mitochondria and cytosolic contaminants. Other concerns came from the findings that some of the imported RNAs do not share the same functions as their cytosolic counterparts. Opposing evidence has been expertly summarized by Gammage et al. (2018). Most of the arguments have been focused on three non-coding RNAs: *RMRP*, *H1* RNA and *5S* rRNA.

Mitochondrial RNA processing ribonuclease (RNase MRP) was originally identified as a site-specific endoribonuclease that generates primer RNA for mtDNA replication (Chang and Clayton, 1987b). It contains an RNA subunit, *RMRP* (Chang and Clayton, 1987a; Lu et al., 2010). Mitochondrial G-rich RNA sequence-binding factor 1 (GRSF1) has been shown to bind *RMRP* and thus enhance its retention in the mitochondrial matrix (Noh et al., 2016). However, it has also been shown that after micrococcal nuclease treatment of Percoll gradient-purified HeLa mitochondria, the amount of full-length *RMRP* associated with the mitochondria is about 1 RNA molecule per 100 mitochondria (Kiss and Filipowicz, 1992), suggesting that the detected mitochondrial *RMRP* might come from outer membrane-associated contaminants. On the other hand, Topper and colleagues argued that the very low level of *RMRP* should be sufficient for its function (Topper et al., 1992). In addition, *in situ* hybridization and biochemical analysis has also supported mitochondrial localization of *RMRP* in mouse cardiomyocytes (Li et al., 1994). More recently, the necessity of *RMRP* in mitochondria was again brought into question, as it has been reported that the primer RNA required for mtDNA synthesis can be formed by transcription termination stimulated by the G-quadruplex structure of nascent RNA (Wanrooij et al., 2010), independent of RNase MRP. It, however, should be noted that the imported *RMRP* is cleaved and processed (Chang and Clayton, 1987a; Noh et al., 2016), so the quantification of the levels of the RNA within mitochondria might not be accurate and the function is most likely different from its nuclear counterpart.

The controversy on mitochondrial import of *H1* RNA is mostly based on two findings that could easily coexit. Nuclear *H1* RNA is the RNA subunit of RNase P. It forms the catalytic core of the enzyme, and can mediate the cleavage of tRNA precursors at the 5′ end in the absence of protein subunits (Kikovska et al., 2007). The secondary structures of bacterial, archaeal and eukaryotic nuclear *H1* RNAs are

conserved (Ellis and Brown, 2009). In yeast mitochondria, *H1* RNA is encoded by mitochondrial gene *RPM1* (Turk et al., 2013), but in mammalian mitochondria, a nucleus-encoded RNA has been shown to be a part of the RNase P activity. The RNA sequence of mitochondrial *H1* RNA appears to be identical with its nuclear counterpart (Puranam and Attardi, 2001), even though the substrate specificities are different (Rossmanith et al., 1995). The controversy arose when a protein-only RNase P complex, comprising of MRPP1, MRPP2, and MRPP3, has been identified in human mitochondria. *In vitro* assays showed that the complex reconstituted with the proteins purified from bacteria is capable of processing single tRNA procursors (Holzmann et al., 2008). Again, it should be noted that some mitochondrial tRNA genes are grouped together and lack an intervening presequence. Removing the RNA component of mitochondrial RNase P activities results in inefficient processing of these tRNA precursors (Wang et al., 2010), suggesting that the two mitochondrial RNase P complexes may coexist and have different substrate specificities.

The debate on *5S* rRNA import into mitochondria mainly stems from a lack of clear mitochondrial function. Even though mammalian mitochondrial genomes encode two ribosomal RNAs (*16S* and *12S* rRNA), nucleus-encoded *5S* rRNA has also been detected in highly purified mammalian mitochondria (Yoshionari et al., 1994; Magalhães et al., 1998). *5S* rRNA is an integral component of ribosomes in nearly all organisms. In plant, *5S* rRNA is encoded by the mitochondrial genome and is a component of plant mitochondrial ribosomes (Waltz et al., 2020). Therefore, it was naturally assumed to be a subunit of the mammalian mitochondrial ribosome. Unexpectedly, *5S* rRNA is absent in the structures of mammalian mitoribosomes. The putative position of *5S* rRNA is occupied by a L-shaped mitochondrial tRNA (Brown et al., 2014; Greber and Ban, 2016). Therefore, the molecular function of mitochondrial *5S* rRNA remains to be identified. Non-coding RNAs having different functions in different locations, however, has been proven to be more of a common theme than an exception (Noh et al., 2016; Zheng et al., 2019).

A few concepts also need to be clarified. Mitochondrion-association means colocalization of these RNAs with mitochondria. These RNAs could be on the outer surface of mitochondrial outer membrane or within the outer membrane. FISH assay is a good approach to verify the association but does not distinguish the two possibilities. Biochemical assays such as ribonuclease treatment and mitoplasting (striping mitochondria of their outer membrane) are usually required to determine whether an RNA is indeed imported into mitochondria. However, nuclease treatment and mitoplasting only enriches those RNAs that are imported into mitochondrial matrix. Biochemically, mitochondrial IMS localization of a certain RNA can only be confirmed if the RNA levels are higher in the mitochondrial IMS than in all the other cellular compartments such as ER, lysosomes and the mitochondrial matrix. Otherwise, it is very hard to prove that it is not from contamination. The same argument goes against the matrix localization of a very small fraction of PNPASE as claimed (Borowski et al., 2013). Combined FISH cryo-EM is the only technique with high enough resolution to directly examine mitochondrial IMS localization of an RNA. However, this technique also works best when the RNA levels are relatively high.

Therefore, the current mitochondrial RNA importome encompasses mostly RNAs imported into mitochondrial matrix. The real mitochondrial RNA importome is likely much bigger. As mentioned above, the trafficking appears to be bi-directional and there are at least three destinations. Some cytosolic RNAs are transported into the matrix, while some mitochondrial RNAs are exported to the cytosol. And some RNAs are imported to mitochondrial IMS. It has been shown that neither the mitochondrial matrix nor the mitochondrial total membrane contains any ribonuclease or nuclease activity under normal conditions (Liu et al., 2017). Mitochondrial IMS is where all the ribonucleases and nucleases reside (Liu et al., 2017; Huang et al., 2018). Therefore, most of the RNAs targeted into mitochondrial IMS are quickly degraded and their transportation has to be examined with indirect approaches.

Mitochondrion-associated *28S* rRNA and some other non-coding RNAs are selectively degraded by the RNASET2 in the mitochondrial IMS (Huang et al., 2018), suggesting the import of these RNAs into the mitochondrial IMS. Degradation of these RNAs responses to conditions such as pH, ATP and divalent metal ions both *in vitro* with purified ribonuclease and *in organello* (Huang et al., 2018), which should be a criterion for deducing whether an enzyme directly functions in a mitochondrial process. Most of the enzymes that have been postulated to directly function in mitochondrial RNA degradation do not meet this criterion and are most likely indirectly involved. Interestingly, this machinery seems to share some similarities with a newly discovered proteolytic pathway that degrades cytosolic protein aggregates (Jin et al., 2017).

In addition, we have performed the import assay of RNAs into isolated mitochondria and mitoplasts. Some RNAs are imported into mitochondria with higher efficiency than into mitoplasts, while some prefer mitoplasts to mitochondria, suggesting that the former group of RNAs may be mostly imported into mitochondrial IMS (unpublished data). Moreover, most of these imported RNAs are cleaved (unpublished data) (Chang and Clayton, 1987a; Noh et al., 2016; Cheng et al., 2018). Therefore, they are unlikely to perform similar functions in mitochondria as their full-length counterparts.

Up until now, few attempts have been made at understanding the RNA export processes, except that PNPASE has been shown to be involved in the export of mitochondrial dsRNAs (Dhir et al., 2018). Most of the studies have been conducted on the import processes. Based on the limited knowledge, import and export pathways may share most of their components. One of the biggest questions is about substrate selection. Because of the complete lack of evidence, we can only speculate that maybe interaction with other proteins might determine which RNAs remain in the matrix.

CONCLUSION

Nucleic acid translocation in and out of mitochondria has become an exciting field with lots of challenges. There are

still many important questions to be answered. How are these RNAs selected for import and export? Why are some destined for degradation in the mitochondrial IMS but not the other? How do RNAs cross mitochondrial inner membrane? What are the functions of these RNAs? With the recent development of sequencing and imaging technology, more mitochondrial non-coding RNAs are sure to be identified. Caution, however, should be taken when interpreting the results. It is important not to have pre-assumptions. Most of the time, we tend to look for similar functions for a biological molecule in a different location. No similar function found should never be a direct argument against the localization. Given the fact that most of the imported lncRNAs are processed, their functions in mitochondria are most likely different from those of the full-length cytosolic counterparts. On the other hand, a simple correlation study should not be used as the full proof of a direct function.

It has also become increasingly clear that most of these import and export events happen under specific conditions such as nutrient stress and only in certain cell types. Non-coding RNAs normally are involved in fine-tuning of cellular processes. The study on functions sometimes proves to be difficult given the lack of strong phenotypes. Finding the right conditions and right model systems is essential. Finally, it is always important to keep an open mind. It used to be believed by most that mitochondrial RNA degradation could only happen in the matrix, but with more evidence emerging, mitochondrial RNA degradation in the IMS has become more widely accepted even though the identity of the ribonuclease is still under debate.

AUTHOR CONTRIBUTIONS

JH and GW contributed in writing and revision of the manuscript. SW and PW contributed in preparing the tables and figure.

FUNDING

This review paper was supported by the Priority Research Program of the Ministry of Science and Technology of the People's Republic of China (2017YFA0504600) and National Natural Science Foundation of the People's Republic of China (grants 91649103 and 32091159).

REFERENCES

Akashi, K., Takenaka, M., Yamaoka, S., Suyama, Y., Fukuzawa, H., and Ohyama, K. (1998). Coexistence of nuclear DNA-encoded tRNAVal(AAC) and mitochondrial DNA-encoded tRNAVal(UAC) in mitochondria of a liverwort *Marchantia polymorpha*. *Nucleic Acids Res.* 26, 2168–2172. doi: 10.1093/nar/26.9.2168

Anderson, S., Bankier, A. T., Barrell, B. G., Bruijn, M., Coulson, A. R., Eperon, I. C., et al. (1981). Sequence and organization of the human mitochondrial genome. *Nature* 290, 457–465.

Baleva, M. V., Meyer, M., Entelis, N., Tarassov, I., Kamenski, P., and Masquida, B. (2017). Factors beyond enolase 2 and mitochondrial lysyl-tRNA synthetase precursor are required for tRNA import into yeast mitochondria. *Biochemistry* 82, 1324–1335. doi: 10.1134/s0006297917110104

Barrey, E., Saint-Auret, G., Bonnamy, B., Damas, D., Boyer, O., and Gidrol, X. (2011). Pre-microRNA and mature microRNA in human mitochondria. *PloS One* 6:e20220. doi: 10.1371/journal.pone.0020220

Bianchessi, V., Badi, I., Bertolotti, M., Nigro, P., and Lauri, A. (2015). The mitochondrial lncRNA ASncmtRNA-2 is induced in aging and replicative senescence in Endothelial Cells. *J. Mol. Cell. Cardiol.* 81, 62–70. doi: 10.1016/j.yjmcc.2015.01.012

Birgit, L., Anja, Z., Madej, M. J., Markus, S., Sandra, T., Stephanie, R., et al. (2007). Identification of small non-coding RNAs from mitochondria and chloroplasts. *Nucleic Acids Res.* 34, 3842–3852. doi: 10.1093/nar/gkl448

Borowski, L. S., Dziembowski, A., Hejnowicz, M. S., Stepien, P. P., and Szczesny, R. J. (2013). Human mitochondrial RNA decay mediated by PNPase-hSuv3 complex takes place in distinct foci. Nucleic Acids Res. 41, 1223–1240. doi: 10.1093/nar/gks1130

Bouzaidi-Tiali, N., Aeby, E., Charrière, F., Pusnik, M., and Schneider, A. (2007). Elongation factor 1a mediates the specificity of mitochondrial tRNA import in T. brucei. *EMBO J.* 26, 4302–4312. doi: 10.1038/sj.emboj.7601857

Brandina, I., Graham, J., Lemaitre-Guillier, C., Entelis, N., Krasheninnikov, I., Sweetlove, L., et al. (2006). Enolase takes part in a macromolecular complex associated to mitochondria in yeast. *Biochim. Biophys. Acta Bioenerg.* 1757, 1217–1228. doi: 10.1016/j.bbabio.2006.07.001

Brown, A., Amunts, A., Bai, X. C., Sugimoto, Y., Edwards, P. C., Murshudov, G., et al. (2014). Structure of the large ribosomal subunit from human mitochondria. *Science* 346, 718–722.

Burzio, V. A., Villota, C., Villegas, J., Landerer, E., Boccardo, E., Villa, L. L., et al. (2009). Expression of a family of noncoding mitochondrial RNAs distinguishes normal from cancer cells. *Proc. Natl. Acad. Sci. U.S.A.* 106, 9430–9434. doi: 10.1073/pnas.0903086106

Calvo, S. E., Clauser, K. R., and Mootha, V. K. (2016). MitoCarta2. 0: an updated inventory of mammalian mitochondrial proteins. *Nucleic Acids Res.* 44, D1251–D1257.

Chang, D. D., and Clayton, D. A. (1987a). A mammalian mitochondrial RNA processing activity contains nucleus-encoded RNA. *Science* 235, 1178–1184. doi: 10.1126/science.2434997

Chang, D. D., and Clayton, D. A. (1987b). A novel endoribonuclease cleaves at a priming site of mouse mitochondrial DNA replication. *EMBO J.* 6, 409–417. doi: 10.1002/j.1460-2075.1987.tb04770.x

Chen, H. W., Rainey, R. N., Balatoni, C. E., Dawson, D. W., Troke, J. J., Wasiak, S., et al. (2006). Mammalian polynucleotide phosphorylase is an intermembrane space RNase that maintains mitochondrial homeostasis. *Mol. Cell. Biol.* 26, 8475–8487. doi: 10.1128/mcb.01002-06

Cheng, Y., Liu, P., Zheng, Q., Gao, G., Yuan, J., Wang, P., et al. (2018). Mitochondrial trafficking and processing of telomerase RNA TERC. *Cell Rep.* 24, 2589–2595. doi: 10.1016/j.celrep.2018.08.003

Cote, J., and Ruiz-Carrillo, A. (1993). Primers for mitochondrial DNA replication generated by endonuclease G. *Science* 261, 765–769. doi: 10.1126/science.7688144

Couvillion, M. T., Soto, I. C., Shipkovenska, G., and Churchman, L. S. (2016). Synchronized mitochondrial and cytosolic translation programs. *Nature* 533, 499–503. doi: 10.1038/nature18015

Crausaz Esseiva, A., Marechal-Drouard, L., Cosset, A., and Schneider, A. (2004). The T-stem determines the cytosolic or mitochondrial localization of trypanosomal tRNAsMet. *Mol. Biol. Cell* 15, 2750–2757. doi: 10.1091/mbc.e03-11-0821

Delage, L., Dietrich, A., Cosset, A., and Maréchal-Drouard, L. (2003). In vitro import of a nuclearly encoded tRNA into mitochondria of *Solanum tuberosum*. *Mol. Cell. Biol.* 23, 4000–4012. doi: 10.1128/mcb.23.11.4000-4012.2003

Dhir, A., Dhir, S., Borowski, L. S., Jimenez, L., Teitell, M., Rotig, A., et al. (2018). Mitochondrial double-stranded RNA triggers antiviral signalling in humans. *Nature* 560, 238–242. doi: 10.1038/s41586-018-0363-0

Dietrich, A., Wallet, C., Iqbal, R. K., Gualberto, J. M., and Lotfi, F. (2015). Organellar non-coding RNAs: emerging regulation mechanisms sciencedirect. *Biochimie* 117, 48–62. doi: 10.1016/j.biochi.2015.06.027

Eduardo, L., Jaime, V., Veronica, A., Burzio, L., and Oliveira, C. (2011). Nuclear localization of the mitochondrial ncRNAs in normal and cancer cells. *Cell. Oncol.* 34, 297–305. doi: 10.1007/s13402-011-0018-8

Ellis, J. C., and Brown, J. W. (2009). The RNase P family. *RNA Biol.* 6, 362–369. doi: 10.4161/rna.6.4.9241

Entelis, N., Brandina, I., Kamenski, P., Krasheninnikov, I. A., Martin, R. P., and Tarassov, I. (2006). A glycolytic enzyme, enolase, is recruited as a cofactor of tRNA targeting toward mitochondria in *Saccharomyces cerevisiae*. *Genes Dev.* 20, 1609–1620. doi: 10.1101/gad.385706

Entelis, N. S., Kolesnikova, O. A., Martin, R. P., and Tarassov, I. A. (2001). RNA delivery into mitochondria. *Adv. Drug Deliv. Rev.* 49, 199–215.

Esseiva, A. C., Naguleswaran, A., Hemphill, A., and Schneider, A. (2004). Mitochondrial tRNA import in *Toxoplasma gondii*. *J. Biol. Chem.* 279, 42363–42368. doi: 10.1074/jbc.m404519200

Fogal, V., Richardson, A. D., Karmali, P. P., Scheffler, I. E., Smith, J. W., and Ruoslahti, E. (2010). Mitochondrial p32 protein is a critical regulator of tumor metabolism via maintenance of oxidative phosphorylation. *Mol. Cell. Biol.* 30:1303. doi: 10.1128/mcb.01101-09

Francesco, B., Pasqua, G., Oliveira, J., Lightowlers, R. N., Chrzanowska-Lightowlers, Z., and Cobine, P. A. (2013). REXO2 is an oligoribonuclease active in human mitochondria. *PloS One* 8:e64670. doi: 10.1371/journal.pone.0064670

Friedman, J. R., and Nunnari, J. (2014). Mitochondrial form and function. *Nature* 505, 335–343. doi: 10.1038/nature12985

Gammage, P. A., Moraes, C. T., and Minczuk, M. (2018). Mitochondrial genome engineering: the revolution may not be CRISPR-Ized. *Trends Genet.* 34, 101–110. doi: 10.1016/j.tig.2017.11.001

Gan, J., Tang, F. M. K., Su, X., Lu, G., Xu, J., Lee, H. S. S., et al. (2019). microRNA-1 inhibits cardiomyocyte proliferation in mouse neonatal hearts by repressing CCND1 expression. *Ann. Transl. Med.* 7, 455–455. doi: 10.21037/atm.2019.08.68

Gao, K., Cheng, M., Zuo, X., Lin, J., Hoogewijs, K., Murphy, M. P., et al. (2021). Active RNA interference in mitochondria. *Cell Res.* 31, 219–228. doi: 10.1038/s41422-020-00394-5

Greber, B. J., and Ban, N. (2016). Structure and function of the mitochondrial ribosome. Annu. Rev. Biochem. 85, 103–132.

Greber, B. J., Bieri, P., Leibundgut, M., Leitner, A., Aebersold, R., Boehringer, D., et al. (2015). The complete structure of the 55S mammalian mitochondrial ribosome. *Science* 348, 303–308. doi: 10.1126/science.aaa3872

Gusic, M., and Prokisch, H. (2020). ncRNAs: new players in mitochondrial health and disease? *Front. Genet.* 11:95. doi: 10.3389/fgene.2020.00095

Holt, C. E., and Bullock, S. L. (2009). Subcellular mRNA localization in animal cells and why it matters. *Science* 326, 1212–1216. doi: 10.1126/science.1176488

Holzmann, J., Frank, P., Loffler, E., Bennett, K. L., Gerner, C., and Rossmanith, W. (2008). RNase P without RNA: identification and functional reconstitution of the human mitochondrial tRNA processing enzyme. *Cell* 135, 462–474. doi: 10.1016/j.cell.2008.09.013

Huang, J., Liu, P., and Wang, G. (2018). Regulation of mitochondrion-associated cytosolic ribosomes by mammalian mitochondrial ribonuclease T2 (RNASET2). *J. Biol. Chem.* 293, 19633–19644. doi: 10.1074/jbc.ra118.005433

Jeandard, D., Smirnova, A., Tarassov, I., Barrey, E., Smirnov, A., and Entelis, N. (2019). Import of non-coding RNAs into human mitochondria: a critical review and emerging approaches. *Cells* 8:286. doi: 10.3390/cells8030286

Jeonghan, K., Rajeev, G., Blanco, L. P., Shutong, Y., Anna, S. K., Kening, W., et al. (2019). VDAC oligomers form mitochondrial pores to release mtDNA fragments and promote lupus-like disease. *Science* 366:1531. doi: 10.1126/science.aav4011

Jin, E., Zhang, Y., Florens, L., Ruan, L., and Zhou, C. (2017). Cytosolic proteostasis through importing of misfolded proteins into mitochondria. Nature 543, 443–446. doi: 10.1038/nature21695

Kahan, T., and Meyuhas, O. (2015). The race to decipher the top secrets of TOP mRNAs. *Biochim. Biophys. Acta* 1849, 801–811. doi: 10.1016/j.bbagrm.2014.08.015

Kai-Chien, Y., Yamada, K. A., Patel, A. Y., Topkara, V. K., Isaac, G., Cheema, F. H., et al. (2018). Deep RNA sequencing reveals dynamic regulation of myocardial noncoding RNAs in failing human heart and remodeling with mechanical circulatory support. *Circulation* 129, 1009–1021. doi: 10.1161/circulationaha.113.003863

Kikovska, E., Svard, S. G., and Kirsebom, L. A. (2007). Eukaryotic RNase P RNA mediates cleavage in the absence of protein. *Proc. Natl. Acad. Sci. U.S.A.* 104, 2062–2067. doi: 10.1073/pnas.0607326104

Kim, K. M., Noh, J. H., Abdelmohsen, K., and Gorospe, M. (2017). Mitochondrial noncoding RNA transport. *BMB Rep.* 50, 164–174. doi: 10.5483/bmbrep.2017.50.4.013

Kiss, T., and Filipowicz, W. (1992). Evidence against a mitochondrial location of the 7-2/MRP RNA in mammalian cells. *Cell* 70, 11–16. doi: 10.1016/0092-8674(92)90528-k

Kolesnikova, O. A., Entelis, N. S., Mireau, H., Fox, T. D., Martin, R. P., and Tarassov, I. A. (2000). Suppression of mutations in mitochondrial DNA by tRNAs imported from the cytoplasm. *Science* 289, 1931–1933. doi: 10.1126/science.289.5486.1931

Koulintchenko, M., Konstantinov, Y., and Dietrich, A. (2003). Plant mitochondria actively import DNA via the permeability transition pore complex. *EMBO J.* 22, 1245–1254. doi: 10.1093/emboj/cdg128

Kumarswamy, R., Bauters, C., Volkmann, I., Maury, F., Fetisch, J., Holzmann, A., et al. (2014). Circulating long noncoding RNA, LIPCAR, predicts survival in patients with heart failure. *Circ. Res.* 114, 1569–1575. doi: 10.1161/circresaha.114.303915

Leucci, E., Vendramin, R., Spinazzi, M., Laurette, P., Fiers, M., Wouters, J., et al. (2016). Melanoma addiction to the long non-coding RNA. *Nature* 531, 518–522.

Li, K., Smagula, C. S., Parsons, W. J., Richardson, J. A., Gonzalez, M., Hagler, H. K., et al. (1994). Subcellular partitioning of MRP RNA assessed by ultrastructural and biochemical analysis. *J. Cell Biol.* 124, 871–882. doi: 10.1083/jcb.124.6.871

Li, Z. A., Qz, A., Lu, H. B., and Lc, A. (2021). Mitochondrial unfolded protein response: an emerging pathway in human diseases. *Free Radic. Biol. Med.* 163, 125–134. doi: 10.1016/j.freeradbiomed.2020.12.013

Liu, P., Huang, J., Zheng, Q., Xie, L., Lu, X., Jin, J., et al. (2017). Mammalian mitochondrial RNAs are degraded in the mitochondrial intermembrane space by RNASET2. *Protein Cell* 8, 735–749. doi: 10.1007/s13238-017-0448-9

Liu, X., Wang, X., Li, J., Hu, S., Deng, Y., Yin, H., et al. (2020). Identification of mecciRNAs and their roles in the mitochondrial entry of proteins. *Sci. China Life Sci.* 63, 1429–1449. doi: 10.1007/s11427-020-1631-9

Lu, Q., Wierzbicki, S., Krasilnikov, A. S., and Schmitt, M. E. (2010). Comparison of mitochondrial and nucleolar RNase MRP reveals identical RNA components with distinct enzymatic activities and protein components. *RNA* 16, 529–537. doi: 10.1261/rna.1893710

Maciej, S., Deepshikha, M., Borowski, L. S., Sylwiad, C., Kotrys, A. V., Kamila, K. K., et al. (2020). Human REXO2 controls short mitochondrial RNAs generated by mtRNA processing and decay machinery to prevent accumulation of double-stranded RNA. *Nucleic Acids Res.* 48, 5572–5590. doi: 10.1093/nar/gkaa302

Magalhães, P. J., Andreu, A. L., and Schon, E. A. (1998). Evidence for the presence of 5S rRNA in mammalian mitochondria. Mol. Biol. Cell 9, 2375–2382. doi: 10.1091/mbc.9.9.2375

Martin, R. P., Schneller, J. M., Stahl, A., and Dirheimer, G. (1979). Import of nuclear deoxyribonucleic acid coded lysine-accepting transfer ribonucleic acid (anticodon C-U-U) into yeast mitochondria. *Biochemistry* 18, 4600–4605. doi: 10.1021/bi00588a021

Masters, B. S., Stohl, L. L., and Clayton, D. A. (1987). Yeast mitochondrial RNA polymerase is homologous to those encoded by bacteriophages T3 and T7. *Cell* 51, 89–99. doi: 10.1016/0092-8674(87)90013-4

Montalto, F. I., and Amicis, F. D. (2020). Cyclin D1 in cancer: a molecular connection for cell cycle control, adhesion and invasion in tumor and stroma. *Cells* 9:2648. doi: 10.3390/cells9122648

Mourtada-Maarabouni, M., Hasan, A. M., Farzaneh, F., and Williams, G. T. (2010). Inhibition of human T-cell proliferation by mammalian target of rapamycin (mTOR) antagonists requires noncoding RNA growth-arrest-specific transcript 5 (GAS5). *Mol. Pharmacol.* 78:19. doi: 10.1124/mol.110.064055

Noh, J. H., Kim, K. M., Abdelmohsen, K., Yoon, J. H., Panda, A. C., Munk, R., et al. (2016). HuR and GRSF1 modulate the nuclear export and mitochondrial localization of the lncRNA RMRP. *Genes Dev.* 30, 1224–1239.

Oka, T., Hikoso, S., Yamaguchi, O., Taneike, M., Takeda, T., Tamai, T., et al. (2012). Mitochondrial DNA that escapes from autophagy causes inflammation and heart failure. *Nature* 490:292. doi: 10.1038/nature11515

Puranam, R. S., and Attardi, G. (2001). The RNase P associated with heLa cell mitochondria contains an essential RNA component identical in sequence to

that of the nuclear RNase P. *Mol. Cell. Biol.* 21:548. doi: 10.1128/mcb.21.2.548-561.2001

Richter-Dennerlein, R., Dennerlein, S., and Rehling, P. (2015). Integrating mitochondrial translation into the cellular context. *Nat. Rev. Mol. Cell Biol.* 16, 586–592. doi: 10.1038/nrm4051

Rinehart, J., Krett, B., Rubio, M. A., Alfonzo, J. D., and Soll, D. (2005). Saccharomyces cerevisiae imports the cytosolic pathway for Gln-tRNA synthesis into the mitochondrion. *Genes Dev.* 19, 583–592. doi: 10.1101/gad.1269305

Ro, S., Ma, H. Y., Park, C., Ortogero, N., Song, R., Hennig, G. W., et al. (2013). The mitochondrial genome encodes abundant small noncoding RNAs. *Cell Res.* 23, 759–774. doi: 10.1038/cr.2013.37

Rorbach, J., Fei, G., Powell, C. A., D'Souza, A., and Chrzanowska-Lightowlers, Z. M. (2016). Human mitochondrial ribosomes can switch their structural RNA composition. *Proc. Natl. Acad. Sci. U.S.A.* 113, 12198–12201. doi: 10.1073/pnas.1609338113

Rossmanith, W., Tullo, A., Potuschak, T., Karwan, R., and Sbisà, E. (1995). Human mitochondrial tRNA processing. *J. Biol. Chem.* 270, 12885–12891.

Rubio, M. A., Liu, X., Yuzawa, H., Alfonzo, J. D., and Simpson, L. (2000). Selective importation of RNA into isolated mitochondria from *Leishmania tarentolae*. *RNA* 6, 988–1003. doi: 10.1017/s1355838200991519

Rubio, M. A., Rinehart, J. J., Krett, B., Duvezin-Caubet, S., Reichert, A. S., Soll, D., et al. (2008). Mammalian mitochondria have the innate ability to import tRNAs by a mechanism distinct from protein import. *Proc. Natl. Acad. Sci. U.S.A.* 105, 9186–9191. doi: 10.1073/pnas.0804283105

Salinas, T., Duchene, A. M., Delage, L., Nilsson, S., Glaser, E., Zaepfel, M., et al. (2006). The voltage-dependent anion channel, a major component of the tRNA import machinery in plant mitochondria. *Proc. Natl. Acad. Sci. U.S.A.* 103, 18362–18367. doi: 10.1073/pnas.0606449103

Salinas, T., Duchene, A. M., and Marechal-Drouard, L. (2008). Recent advances in tRNA mitochondrial import. *Trends Biochem. Sci.* 33, 320–329. doi: 10.1016/j.tibs.2008.04.010

Sang, L., Ju, H. Q., Yang, Z., Ge, Q., Zhang, Z., Liu, F., et al. (2021). Mitochondrial long non-coding RNA GAS5 tunes TCA metabolism in response to nutrient stress. *Nat. Metab.* 3, 90–106. doi: 10.1038/s42255-020-00325-z

Schmidt, O., Pfanner, N., and Meisinger, C. (2010). Mitochondrial protein import: from proteomics to functional mechanisms. *Nat. Rev. Mol. Cell Biol.* 11, 655–667. doi: 10.1038/nrm2959

Shepherd, D. L., Hathaway, Q. A., Pinti, M. V., Nichols, C. E., Durr, A. J., Sreekumar, S., et al. (2017). Exploring the mitochondrial microRNA import pathway through polynucleotide phosphorylase (PNPase). *J. Mol. Cell. Cardiol.* 110, 15–25. doi: 10.1016/j.yjmcc.2017.06.012

Shigeko, S., Hideaki, I., Harunori, Y., Keiichi, I., Simpson, R. J., and Nobuhiro, T. (2015). Collaborator of alternative reading frame protein (CARF) regulates early processing of pre-ribosomal RNA by retaining XRN2 (5′-3′ exoribonuclease) in the nucleoplasm. *Nucleic Acids Res.* 43, 10397–10410.

Smirnov, A., Comte, C., Mager-Heckel, A. M., Addis, V., Krasheninnikov, I. A., Martin, R. P., et al. (2010). Mitochondrial enzyme rhodanese is essential for 5S ribosomal RNA import into human mitochondria. *J. Biol. Chem.* 285, 30792–30803. doi: 10.1074/jbc.m110.151183

Smirnov, A., Entelis, N., Martin, R. P., and Tarassov, I. (2011). Biological significance of 5S rRNA import into human mitochondria: role of ribosomal protein MRP-L18. *Genes Dev.*25, 1289–1305. doi: 10.1101/gad.624711

Tarassov, I., Entelis, N., and Martin, R. P. (1995a). An intact protein translocating machinery is required for mitochondrial import of a yeast cytoplasmic tRNA. *J. Mol. Biol.* 245, 315–323. doi: 10.1006/jmbi.1994.0026

Tarassov, I., Entelis, N., and Martin, R. P. (1995b). Mitochondrial import of a cytoplasmic lysine-tRNA in yeast is mediated by cooperation of cytoplasmic and mitochondrial lysyl-tRNA synthetases. *EMBO J.* 14, 3461–3471. doi: 10.1002/j.1460-2075.1995.tb07352.x

Topper, J. N., Bennett, J. L., and Clayton, D. A. (1992). A role for RNAase MRP in mitochondrial RNA processing. *Cell* 70, 16–20. doi: 10.1016/0092-8674(92)90529-l

Turk, E. M., Das, V., Seibert, R. D., and Andrulis, E. D. (2013). The mitochondrial RNA landscape of *Saccharomyces cerevisiae*. *PloS One.* 8:e78105. doi: 10.1371/journal.pone.0078105

Vendramin, R., Marine, J., and Leu, E. (2017). Non−coding RNAs: the dark side of nuclear–mitochondrial communication. *EMBO J.* 36, 1123–1133. doi: 10.15252/embj.201695546

Vendramin, R., Verheyden, Y., Ishikawa, H., Goedert, L., Nicolas, E., Saraf, K., et al. (2018). SAMMSON fosters cancer cell fitness by concertedly enhancing mitochondrial and cytosolic translation. *Nat. Struct. Mol. Biol.* 25, 1035–1046. doi: 10.1038/s41594-018-0143-4

Vidaurre, S., Fitzpatrick, C., Burzio, V. A., Briones, M., Villota, C., Villegas, J., et al. (2014). Down-regulation of the antisense mitochondrial non-coding RNAs (ncRNAs) is a unique vulnerability of cancer cells and a potential target for cancer therapy. *J.Biol. Chem.* 289, 27182–27198. doi: 10.1074/jbc.m114.558841

Waltz, F., Soufari, H., Bochler, A., Giegé, P., and Hashem, Y. (2020). Cryo-EM structure of the RNA-rich plant mitochondrial ribosome. Nat. Plants 6, 377–383. doi: 10.1038/s41477-020-0631-5

Wang, G., Chen, H. W., Oktay, Y., Jin, Z., Allen, E. L., Smith, G. M., et al. (2010). PNPASE regulates RNA import into mitochondria. *Cell* 142, 456–467. doi: 10.1016/j.cell.2010.06.035

Wanrooij, P. H., Uhler, J. P., Simonsson, T., Falkenberg, M., and Gustafsson, C. M. (2010). G-quadruplex structures in RNA stimulate mitochondrial transcription termination and primer formation. *Proc. Natl. Acad. Sci. U.S.A.* 107, 16072–16077. doi: 10.1073/pnas.1006026107

Williams, C. C., Jan, C. H., and Weissman, J. S. (2014). Targeting and plasticity of mitochondrial proteins revealed by proximity-specific ribosome profiling. *Science* 346, 748–751. doi: 10.1126/science.1257522

Yoshionari, S., Koike, T., Yokogawa, T., Nishikawa, K., Ueda, T., Miura, K., et al. (1994). Existence of nuclear-encoded 5S-rRNA in bovine mitochondria. *FEBS Lett.* 338, 137–142. doi: 10.1016/0014-5793(94)80351-x

Yue, Z., Liu, Y., Wu, X., and Shell, S. M. (2006). Functions of human replication protein A (RPA): from DNA replication to DNA damage and stress responses. *J. Cell. Physiol.* 208, 267–273. doi: 10.1002/jcp.20622

Zhang, X., Zuo, X., Yang, B., Li, Z., Xue, Y., Zhou, Y., et al. (2014). MicroRNA directly enhances mitochondrial translation during muscle differentiation. *Cell* 158, 607–619. doi: 10.1016/j.cell.2014.05.047

Zheng, Q., Liu, P., Gao, G., Yuan, J., Wang, P., and Wang, G. (2019). Mitochondrion-processed TERC regulates senescence without affecting telomerase activities. *Protein Cell* 10, 631–648. doi: 10.1007/s13238-019-0612-5

Conflict of Interest: The authors declare that the research was conducted in the absence of any commercial or financial relationships that could be construed as a potential conflict of interest.

Publisher's Note: All claims expressed in this article are solely those of the authors and do not necessarily represent those of their affiliated organizations, or those of the publisher, the editors and the reviewers. Any product that may be evaluated in this article, or claim that may be made by its manufacturer, is not guaranteed or endorsed by the publisher.

frontiers in Physiology

MINI REVIEW
published: 03 September 2021
doi: 10.3389/fphys.2021.729452

Mitochondrial tRNA-Derived Fragments and Their Contribution to Gene Expression Regulation

Athanasios-Nasir Shaukat†, Eleni G. Kaliatsi†, Vassiliki Stamatopoulou and Constantinos Stathopoulos**

Department of Biochemistry, School of Medicine, University of Patras, Patras, Greece

Mutations in human mitochondrial tRNAs (mt-tRNAs) are responsible for several and sometimes severe clinical phenotypes, classified among mitochondrial diseases. In addition, post-transcriptional modifications of mt-tRNAs in correlation with several stress signals can affect their stability similarly to what has been described for their nuclear-encoded counterparts. Many of the perturbations related to either point mutations or aberrant modifications of mt-tRNAs can lead to specific cleavage and the production of mitochondrial tRNA-derived fragments (mt-tRFs). Although mt-tRFs have been detected in several studies, the exact biogenesis steps and biological role remain, to a great extent, unexplored. Several mt-tRFs are produced because of the excessive oxidative stress which predominantly affects mitochondrial DNA integrity. In addition, mt-tRFs have been detected in various diseases with possible detrimental consequences, but also their production may represent a response mechanism to external stimuli, including infections from pathogens. Finally, specific point mutations on mt-tRNAs have been reported to impact the pool of the produced mt-tRFs and there is growing evidence suggesting that mt-tRFs can be exported and act in the cytoplasm. In this review, we summarize current knowledge on mitochondrial tRNA-deriving fragments and their possible contribution to gene expression regulation.

Keywords: mitochondrial tRNA-derived fragments, mitochondrial tRNAs, tRNA-derived fragments, ncRNAs, mitochondria

OPEN ACCESS

Edited by:
Nina Entelis, Génomique et microbiologie (GMGM), France

Reviewed by:
Pooja Jadiya, Temple University, United States
Tarassov Ivan, Génomique et microbiologie (GMGM), France

****Correspondence:***
Constantinos Stathopoulos
cstath@med.upatras.gr
Vassiliki Stamatopoulou
v.stam@upatras.gr

†These authors share first authorship

Specialty section:
This article was submitted to Mitochondrial Research, a section of the journal Frontiers in Physiology

Received: *23 June 2021*
Accepted: *09 August 2021*
Published: *03 September 2021*

Citation:
Shaukat A-N, Kaliatsi EG, Stamatopoulou V and Stathopoulos C (2021) Mitochondrial tRNA-Derived Fragments and Their Contribution to Gene Expression Regulation. Front. Physiol. 12:729452. doi: 10.3389/fphys.2021.729452

INTRODUCTION

Mitochondria have evolved as the powerhouse of cells and the central nexus for major metabolic pathways that utilize oxygen for ATP production in eukaryotic cells. As such, they represent a major hub of the intracellular communication that define the cell's fate. Mitochondria-related networking and the bidirectional pathways that rule it have long been identified to have profound effects on cell's metabolism, bioenergetics, and homeostasis. However, several details regarding the molecular mechanisms and gene networks involved still remain unknown. Human mitochondrial DNA exists in multiple copies in each organelle and consists of 37 genes including 2 mt-rRNAs, 22 mutations in human mitochondrial tRNAs (mt-tRNAs), and 13 coding genes which are translated through specific decoding by mitochondrial ribosomes to the essential subunits of respiratory complexes (Anderson et al., 1981). The expression of the mitochondrial

genes provides, among others, energy supply and antioxidant defense depending also on several sets of devoted nuclear-encoded genes that act either in the mitochondrial milieu or at the mitochondrial membrane. Nuclear-encoded non-coding RNAs are also known to indirectly affect mitochondrial function either through regulating the expression and post-translational modifications of the approximately 1,500 proteins targeted to mitochondria or through their direct import and interaction with proteins and RNAs inside mitochondria (Gusic and Prokisch, 2020). Several miRNAs or long non-coding RNAs, like *SAMMSON*, modulate mitochondrial function by affecting the import of proteins (Leucci et al., 2016; Vendramin et al., 2017; Jeandard et al., 2019; Kaliatsi et al., 2020). It should be noted that in human, although RNA import mechanisms into mitochondria have been proposed and involve PNPase (polynucleotide phosphorylase) activity located in the intermembrane space (reviewed in Vendramin et al., 2017 and Jeandard et al., 2019), an export mechanism is still elusive.

Current knowledge suggests that several perturbations in the regulation of the mitochondrial gene expression can lead to dysfunction of mitochondria. In turn, defective mitochondria are characterized by impaired energy production and depending on the broadness of the mutations, can lead to disorders with severe clinical symptoms that mainly affect the highly energy-demanding tissues, like brain, heart, and muscles. More specifically, mitochondrial DNA mutations, especially on mt-tRNAs, have been linked initially to syndromes like MERRF (myoclonic epilepsy with ragged red fibers), MELAS (mitochondrial encephalomyopathy, lactic acidosis, and stroke-like episodes) and cardiomyopathies (Gorman et al., 2016), and nowadays to the emergence of specific types of cancer (Stewart et al., 2015). The fact that many of the known mitochondrial diseases have their molecular basis on mutations in mt-tRNA genes indicates the central role of mitochondrial translation in the pathophysiology of the cells and the tissues. Point mutations in mt-tRNAs can affect the efficiency of the 5' and 3' processing, the epigenetic changes deriving from specific post-transcriptional modifications, the accuracy of tRNA aminoacylation and decoding during translation, and overall the mt-tRNA stability, resulting in many cases in severe inherited mitochondrial diseases (Yan et al., 2006; Zifa et al., 2007; Xue et al., 2019; Chujo and Tomizawa, 2021; Ji et al., 2021; Karasik et al., 2021). It should be noted that several mitochondrial tRNAs appear truncated in their mature form when compared to their cytosolic counterparts and in the case of $tRNA^{Ser(AGY)}$, the D-stem and loop are missing. In addition, different point mutations in the same mt-tRNA molecule can result in different diseases, like in the case of mt-$tRNA^{Glu}$ where specific mutations have been linked with maternally inherited diabetes and deafness, while others in the same gene with infantile transient mitochondrial myopathy (Webb et al., 2020). Moreover, mutations in mt-tRNAs can co-exist with mutations in genes encoding mitochondrial enzymes, an observation that highlights the phenotypic diversity among mitochondrial mutations with possible clinical significance (Zifa et al., 2008). The accurate transcription and maturation of mt-tRNAs are essential to successfully decode several codon deviations from the conventional universal genetic code, like the UGA stop codon which encodes for tryptophan, the isoleucine AUA codon which encodes for methionine, and the two arginine codons AGA and AGG which in mitochondria designate termination (Kummer and Ban, 2021). As a result, defects that affect the mt-tRNA stability and utilization as substrate can impact not only the mitochondrial translation rate but also the pool of available molecules leading to specific tRNA fragmentation that could affect the mitochondrial gene expression and potentially the crosstalk with the cytoplasm and the nucleus.

Although fragments of tRNAs were sporadically observed many years ago, the recent advance of sequencing technologies and bioinformatics tools brought tRNA-derived fragments (tRFs) to the spotlight, categorizing them in groups depending on their site of origin on tRNA molecules (Kumar et al., 2016). More specifically, tRFs are classified as tRF-1 s, tRF-5 s, tRF-3 s, 5'-tRNA halves, 3' tRNA halves, or itRFs (internal tRFs) and are produced depending also on the external stimulus. More interestingly, each distinct class has been linked to specific biological function; global translation inhibition has been attributed mainly to 5' tRNA halves (but also to tRF-5 s), translation repression of specific mRNAs mainly to tRF-3 s, inhibition of specific gene transcription to tRF-5 s, inhibition of viral RNA translation to tRF-1 s, inhibition of apoptosis to 5' tRNA halves, and regulation of retrotransposon expression both to tRF-3 s and tRF-5 s (Schimmel, 2018; Su et al., 2020). In general, although tRFs production can be induced by stress, or the lack of specific post-transcriptional tRNA modifications, a certain number of tRFs has been proposed to act like miRNAs and to mediate gene silencing (Kumar et al., 2014; Skeparnias et al., 2020). Finally, although several known ribonucleases seem to contribute in the production of specific tRFs (see below), it is also likely that additional ribonucleolytic activities and/or biogenesis steps may mediate tRFs biogenesis (Su et al., 2020).

The advance of high throughput methodologies, such as next-generation sequencing and meta-analysis of existing data, has lately revealed the existence of mitochondrial tRNA-derived fragments (mt-tRFs) with possible correlation to pathological phenotypes. Strikingly, mt-tRFs appear as contributors to the synchronization of a series of essential cellular and mitochondrial biological processes, acting as "couriers" not only between nucleus and mitochondrion, but also between different cells of the same or different species (Saikia et al., 2014; Meseguer, 2021). Herein, the putative production pathways of mt-tRFs and their effect on gene expression regulation, along with the role of tRNA processing factors that may contribute to differential mt-tRF expression profiles in pathogenic phenotypes, are summarized.

CURRENT KNOWLEDGE ON mt-tRNA-DERIVED FRAGMENTS BIOGENESIS

Nowadays, the powerful methodological tools can provide an unprecedented opportunity to approach the nuclear-mitochondrial communication and the delicate coordination

of nuclear- and mitochondrial-encoded factors, enzymes, and cofactors aiming to delineate the mechanisms that drive to specific mitochondrial diseases. Although at the beginning, tRFs were first considered tRNA degradation byproducts, later studies showed they are abundant in all species and are generated following a specific endonucleolytic cleavage of precursor or mature tRNAs (Grafanaki et al., 2019; Su et al., 2020). Today, tRFs represent important modulators of various processes, including translation, apoptosis, anti-viral defense, and response to nutrient starvation or oxidative stress. Interestingly, with the accumulation of sequencing data and the development of highly specialized bioinformatic platforms, it becomes evident that not only nuclear-encoded tRNAs but also mt-tRNAs can produce tRFs (Kumar et al., 2015; Zheng et al., 2016; Pliatsika et al., 2018; Looney et al., 2020). Of note, differential expression of mt-tRFs has been observed in cancer, as a result of mtDNA mutations and as a response to external stimuli, including infections from pathogens (Meseguer et al., 2019; Nätt et al., 2019; Karousi et al., 2020; Looney et al., 2020). Subsequently, mt-tRFs appear to actively participate in the intracellular communication and the mitochondrial pathophysiology, affecting also the cytoplasmic translation machinery (Loher et al., 2017; Meseguer et al., 2019; Looney et al., 2020). Finally, there is growing interest regarding the possible transportation of mt-tRFs across the mitochondrial membrane which raises further questions on which and how many ribonucleases and modifiers could be implicated to mt-tRF biogenesis.

So far, specific endoribonucleases have been identified that participate in tRF production. The first endoribonucleases identified were RNase Z^L/ELAC2 and Angiogenin (ANG). RNase Z^L/ELAC2 is responsible for the maturation of the 3' end of tRNAs through pre-tRNA cleavage downstream of the discriminator base and the only activity which is localized both in the nucleus and mitochondria. ANG, on the other hand, cleaves predominantly in the anticodon loop and is mainly responsible for stress-induced tRFs production (Lee et al., 2009; Yamasaki et al., 2009; Siira et al., 2018). Additional enzymes that have been identified to participate in the generation of tRFs include SLFN11 (Schlafen 11), SLFN13, and RNase L (Li et al., 2012, 2018; Donovan et al., 2017; Yang et al., 2018), but interestingly, none of these activities have been detected in mitochondria. Although, the cleavage site of SLFN11 is unknown, SLFN13 cleaves in the junction of the T and anticodon stems of tRNAs, while RNase L cleaves at the anticodon loop (Donovan et al., 2017; Li et al., 2018; Yang et al., 2018). Dicer is also implicated to the generation of tRFs but only in specific cases (Hasler et al., 2016; Kuscu et al., 2018). For example, precursor tRNAs that escape the La-dependent maturation pathway are folded into structures that are recognized by exportin 5 (Xpo5) as miRNA precursors and exported in the cytoplasm, where they are cleaved by DICER producing tRFs, which are then loaded to AGO proteins (Hasler et al., 2016). Aside from La that protects tRNAs from being cleaved, it was found recently that SLFN2 binds mature tRNAs upon T-cell activation and inhibits oxidative stress-induced tRF biogenesis by ANG, thus preventing global translation inhibition (Yue et al., 2021). However, in most cases, the mechanism for producing tRNA halves, tRF-5 s, tRF-3 s, and itRFs is still elusive and the question whether specific tRNA-halves production is tightly regulated remains open (Su et al., 2019, 2020). Given the current knowledge regarding the activities that mediate tRFs production from nuclear-encoded tRNAs, the respective activities that are responsible for mt-tRFs production are still unknown (**Figure 1A**). It should also be noted that it remains debatable whether and which mt-tRNAs are processed either in the mitochondrion or the cytoplasm to generate mt-tRFs. Enzymes that are targeted into mitochondria could affect mt-tRF biogenesis, like RNase Z^L/ELAC2, which has been identified as a hotspot for mutations linked with mitochondrial diseases, such as hypertrophic cardiomyopathy but also with prostate cancer (Siira et al., 2018; Saoura et al., 2019). Although most of these mutations impair the efficient maturation of the 3' end of both the nuclear and mitochondrial tRNAs, the effect in mitochondria is more intense. For example, the R781H substitution in RNase Z^L/ELAC2, which has been linked with prostate cancer and hypertrophic cardiomyopathy, mainly affects mt-tRNA processing while has no major differences on the nuclear pre-tRNA processing (Minagawa et al., 2005; Saoura et al., 2019). This effect could potentially lead to production of differential mt-tRFs levels and a broader effect in gene expression regulation, both inside and outside mitochondria. Another candidate involved in the mt-tRF generation is LACTB2 (Lactamase B2), a mitochondrially targeted ribonuclease that is able to cleave single-stranded RNAs *in vitro* (Levy et al., 2016). Although LACTB2 is mainly involved in mt-mRNA turnover, *in vitro* cleavage assays demonstrated that in the presence of a hairpin-structured RNA substrate, LACTB2 cleaves only in the loop region and may also target the T, D, or anticodon loops of mt-tRNAs, generating mt-tRFs. Given the putative existence that a mechanism that actively shuffles mitochondrial RNAs across the mitochondrial membrane to be processed in the cytoplasm by known endoribonucleases, the possibility of mt-tRFs production by cytoplasmic enzymes cannot be excluded (Bruni et al., 2017; Jády et al., 2018; **Figure 1A**). Interestingly, it was shown recently that silencing of either *DICER* or *AGO2* downregulated the expression of mt-itRF$^{Glu(UUC)}$, mt-5'tRF$^{Leu(UUA)}$ carrying the A3243G mutation and mt-3'tRF$^{Val(UAC)}$ (Meseguer et al., 2019). This observation suggests that DICER could potentially cleave mt-tRNAs as well, however, whether this occurs in the cytoplasm or inside mitochondria is unclear (**Figure 1A**; Meseguer, 2021). The reason why *AGO2* silencing leads to decreased expression of mt-tRFs is also not clear. Considering the possibility that AGO2-bound mt-tRFs exhibit increased half-lives, the absence of AGO2 could increase the susceptibility of mt-tRFs to degradation. Although the defined mitochondrial export mechanism is still elusive, it is apparent that apoptosis and autophagic turnover of mitochondria cause mt-tRNAs to translocate in the cytoplasm (Marnef et al., 2016; Jády et al., 2018). Under these conditions, several RNA-binding proteins, including AGO2, Y-box-binding proteins (YBX1 and YBX3), mRNA-binding proteins (SRSF1, SRSF2, SRSF3, hnRNP A1, and hnRNP H), and polypyrimidine-binding proteins, have been found to interact with a subset of mt-tRNAs in

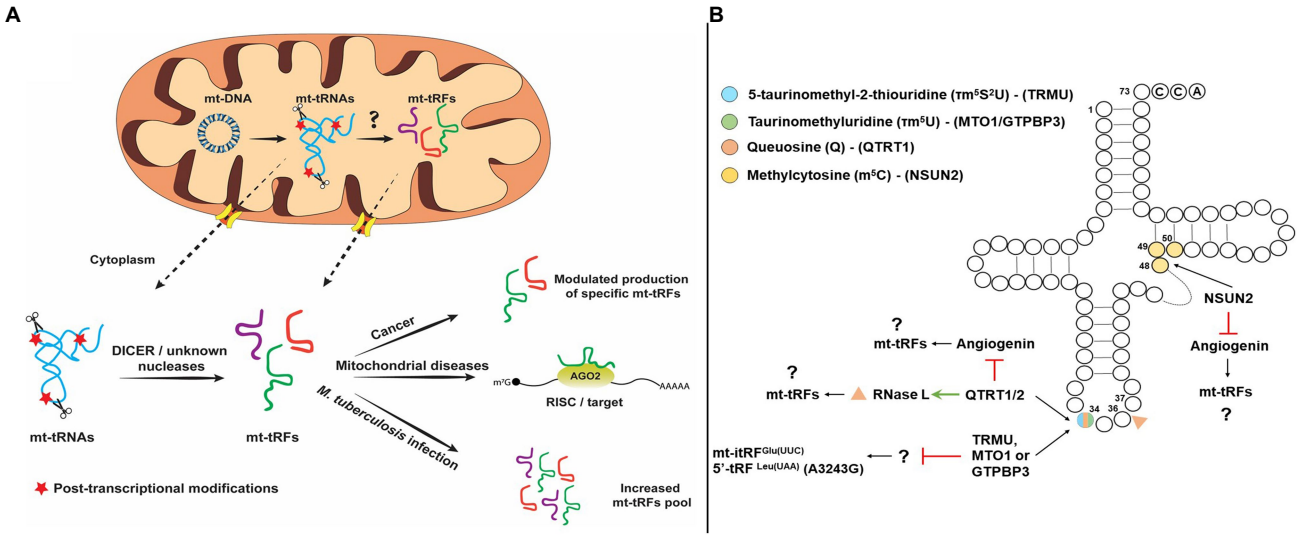

FIGURE 1 | (A) Schematic representation of putative pathways of mitochondrial tRNA-derived fragments (mt-tRFs) biogenesis and biological function and **(B)** Hypothetic model of mt-tRNA cleavage regulation by post-transcriptional modifications.

the cytoplasm. This interaction may indicate a possible mechanism *via* which, specific mt-tRNAs are processed by cytoplasmic ribonucleases, like ANG and DICER to produce mt-tRFs (Maniataki and Mourelatos, 2005; Marnef et al., 2016; Jády et al., 2018). However, as discussed above, additional ribonucleases may also be involved in cytosolic mt-tRF biogenesis.

Apart from the previously mentioned mechanisms, specific modification patterns on mt-tRNAs are key factors and not only contribute to structural stability and recognition by enzymes and proteins, but also act protectively against aberrant cleavage and fragmentation. More interestingly, lack of specific modifications has been linked with the production of specific tRFs under different conditions. Queuosine (Q) is an important modification of G34 of GUN anticodons and responsible for the efficient decoding of NAY codons in the cytosol and mitochondria (where N corresponds to any base and Y to pyrimidine) and lack of this modification affects the cleavage of both RNase L and ANG (Suzuki, 2021). More specifically, RNase L cleaves the *in vitro*-transcribed $tRNA^{His}$ in three different sites; however, isolation of endogenous and modified with Q34 $tRNA^{His}$ is only cleaved at position 36 (Donovan et al., 2017). On the other hand, Q34 inhibits ANG cleavage altogether (Wang et al., 2018). Thus, considering that Q34 modification status besides the decoding fidelity and efficiency affects also the cleavage specificity of mt-tRNAs and it may modulate mt-tRF production. Interestingly, the absence of an identified biosynthetic pathway for the micronutrient queuine in human, which is required for queuosine formation, suggests that the microbiome is mainly responsible for the existence of this modification (Müller et al., 2019). This observation provides a possible link between the role of the microbiome in tRF biogenesis. In the same line, a recent report that analyzed in detail the human tRNA modification landscape underlined the fact that several modifications occur near sites that are susceptible to potential pathogenic mutations. The presence of non-canonical nucleotides near modification sites could affect the binding affinity of modifying enzymes and/or affect their enzymatic efficiency, resulting in hypomodified and unstable mt-tRNAs, which are unable to participate efficiently in mitochondrial translation and are prone to cleavage (Suzuki et al., 2020). Fruit flies and mice lacking NSUN2 (NOP2/Sun methyltransferase 2) or DNMT2 (DNA methyltransferase 2), the methyltransferases that modify cytosines at position 5 (m^5C), were found to bear increased levels of stress-induced tRFs that are produced by ANG (**Figure 1B**). The correlation of NSUN2 with other modification enzymes that modify mt-tRNAs regulates their stability and functional properties (Suzuki, 2021). NSUN2 has recently been detected in mitochondria and is responsible for introduction of m^5 at C48, C49, or C50 of mt-tRNAs (Shinoda et al., 2019; Van Haute et al., 2019). Taking into account that *NSUN2* expression is dynamically modulated in various physiological conditions, such as cancer, neurodegenerative diseases, and during differentiation, it is possible that differential methyltransferase activity in mitochondria may also drives the production of specific mt-tRFs (Blanco et al., 2014; Chellamuthu and Gray, 2020). Of note, queuosine hypomodification has been reported in several cancers and in multiple sclerosis *via* reduced activity of tRNA guanine transglycosylase (TRT) or *via* promoter methylation of the genes coding for the TRT subunits (*QTRT1* and *QTRT2*) (Baranowski et al., 1994; Pathak et al., 2005; Varghese et al., 2017; Hayes et al., 2020).

Several tRNA modifications that are mitochondria specific-like 5-taurinomethyluridine (τm^5U), 5-taurinomethyl-2-thiouridine (τm^5S^2U), and 5-formylcytidine (f5C) that could play an important role in the regulation of mt-tRNA cleavage. Silencing of either *TRMU*, *GTPBP3,* or *MTO1* genes that code for enzymes that modify U34 of mt-tRNAs led to increased

expression of mt-itRF$^{Glu(UUC)}$, indicating that the modification state of mt-tRNAs can modulate mt-tRF biogenesis (**Figure 1B**; Schaefer et al., 2010; Tuorto et al., 2012; Meseguer et al., 2019). Also, the mt-tRNA$^{Leu(UUR)}$ harboring the MELAS mutation A3243G which is known to prevent the τm^5 modification of U34, also leads to the upregulation of a mt-tRF-5 derived from mt-tRNA$^{Leu(UUR)}$. Based on these observations, it has been proposed that lack of $\tau m^5 U34$ could drive the generation of specific mt-tRFs (Meseguer et al., 2019). Finally, $\tau m^5 U$ frequency in cultured cell lines and in animal models is highly affected by dietary uptake of taurine (Asano et al., 2018). Upon taurine starvation in cultured cells and animal tissues, $\tau m^5 U$ is replaced by $cmnm^5 U$ (5-carboxymethylaminomethyluridine), which could potentially alter the cleavage patterns of mt-tRNAs by specific ribonucleases, leading to the production of differential mt-tRF profiles.

MITOCHONDRIAL tRNA-DERIVED FRAGMENTS IN PATHOPHYSIOLOGY

The role of tRFs in gene expression regulation has gradually drawn the interest, with specific tRFs deriving from nuclear-encoded tRNA species to be considered as novel diagnostic and prognostic biomarkers of several types of disorders, such as cancer, as well as possible druggable targets for cancer treatment (Srinivasan et al., 2019; Zhu et al., 2019). Although, the biological function of mt-tRFs has not been clearly defined, they could bear similar value (**Table 1**). A previous extensive analysis of sRNA-seq data from mitoplasts derived from 143B osteosarcoma cells revealed the existence of several sRNA (small RNA) species that map to mitochondrial tRNAs (Mercer et al., 2011). Interestingly, most of the mt-tRFs detected in that study correspond to 5' mt-tRFs but also to the region downstream of tRNA 3' cleavage side, which correspond to tRF-1 s (Mercer et al., 2011). Moreover, the 5' mt-tRFs harbored several sequencing mismatches at positions known for being modified, indicating their origin from mature mt-tRNAs. Several studies have attempted to correlate the differential mt-tRFs patterns with various pathophysiological conditions. A reported correlation between differential abundance and length distribution of mt-tRFs between datasets from breast invasive carcinoma (BRCA; derived from The Cancer Genome Atlas project) and patient-derived lymphoblastoid cell lines (LCL) highlighted the importance of mt-tRFs patterns as biomarkers (Telonis et al., 2015). It is likely that specific mt-tRNAs produce only a specific type of mt-tRF (i.e., either 5'-tRF or 3'-tRF or i-tRF) while others can be fragmented to all types. Moreover, LCL and BRCA datasets contained not only different mt-tRF pools, but also different types of mt-tRFs generated from the same type of mt-tRNA, suggesting that the type of mt-tRF produced by each individual mt-tRNA is cancer type specific. A recent report interconnected the low overall survival of patients suffering from chronic lymphocytic leukemia (CLL) with the presence of an internal mt-tRF (Karousi et al., 2020). In this study, non-coding RNAs were quantified *via* bioinformatic analysis in CLL patients. Interestingly, a novel mt-tRF was identified derived from the mt-tRNA^{Phe} bearing the anticodon GAA and termed i-tRF$^{Phe(GAA)}$. Specifically, i-tRF$^{Phe(GAA)}$ could serve as a potential prognostic biomarker in CLL, since its high expression level was linked with poor outcome of the disease (Karousi et al., 2020). Although these observations await experimental validation and more in-depth investigation to attribute its biological significance, they illustrate the dynamic nature of mt-tRF biogenesis, which may reflect to their distinct biological functions under different conditions or pathophysiologies. Moreover, apart from the apparent correlation of mt-tRFs with several cancer types, their role has been also emerged in infections from pathogens. Although most studies have focused on viral infections, it was recently reported that infection with *Listeria monocytogenes* and *Mycobacterium tuberculosis* affected the tRF production in macrophages and more importantly, infection by *M. tuberculosis* significantly affected the abundance of the mt-tRFs pool (Looney et al., 2020). The study suggested that this effect could be driven by the hypoxic conditions that usually accompany *M. tuberculosis* infections which, in turn, alter the mitochondrial physiology and subsequently the mt-tRF production.

Very recently, the role of diet as factor that induces mt-tRFs production was described in relation to human sperm motility. Human sperm responds rapidly to changes in a sugar-rich diet exhibiting increased motility and upregulation of specific nuclear and mt-tRFs. Strikingly, although both nuclear and mt-tRFs production are sugar sensitive, the high percentage of mt-tRFs could correlate to the improved sperm motility (Nätt et al., 2019). In addition, considering that the modification state of

TABLE 1 | Examples of mitochondrial tRNA fragments affected under various conditions.

mt-tRF	Physiological State	Observation	Biological function	Reference
i-tRF$^{Phe(GAA)}$	Chronic lymphocytic leukemia (CLL)	Increased levels in PBMCs correlated with lower survival	Unknown	Karousi et al., 2020
Various mt-tRFs	Infection with intracellular pathogens, mainly *Mycobacterium tuberculosis*	Deregulation of expression	Unknown	Looney et al., 2020
i-tRF$^{His(GTG)}$, 5' and i-tRF$^{Ser(TGA)}$, 3'-half/3'-tRF/i-tRF$^{Thr(TGT)}$, 5' and 3'-tRF$^{Val(TAC)}$	Sugar-rich diet	Increased abundance in spermatozoa and increased motility	Unknown	Nätt et al., 2019
itRF$^{Glu(UUC)}$	MELAS	Upregulation in MELAS cybrid cells	Targets *MPC1* mRNA	Meseguer et al., 2019
5'-tRF$^{Leu(UAA)}$ (A3243G), 3'-tRF$^{Val(UAC)}$	MELAS	Upregulation in MELAS cybrid cells	Unknown	Meseguer et al., 2019
5'-tRF$^{Leu(UAA)}$	MELAS	Downregulation in MELAS cybrid cells	Unknown	Meseguer et al., 2019

tRNAs can affect the tRFs biogenesis, it seems that the mt-tRNA epitranscriptome can also give rise to the mt-tRFome (Martínez-Zamora et al., 2015). For example, the prevalent mutation A3243G, which leads to the MELAS disease, can cause differential expression of several mt-tRFs. This mutation resides inside the mt-tRNA$^{Leu(UUR)}$ and prevents the writing of the τm^5U34 modification that stabilizes the U-G wobble pair and makes the mutated mt-tRNA unable to decode the UUG codon efficiently (Kirino et al., 2004). Notably, a 5' mt-tRF derived from the mutated mt-tRNA$^{Leu(UUR)}$ was upregulated in MELAS cybrid cells, indicating that the loss of τm^5 modification at U34 favors the production of this mt-tRF. Finally, specific mt-tRFs and particularly, mt-itRF$^{Glu(UUC)}$, mt-5'tRF$^{Leu(UUA)}$ carrying the A3243G mutation and another mt-5'tRF$^{Leu(UAA)}$, apart from being accumulated inside the mitochondria, have been detected also in the cytosol.

Similar to their cytoplasmic counterparts, mt-tRFs presumably can act like miRNAs to induce gene silencing and, in some cases, may share common mRNA targets (Meseguer et al., 2019; Skeparnias et al., 2020). Interestingly, the differential expressed mt-tRFs in MELAS cybrid cells are predicted to target several mRNAs involved in the regulation of striated and cardiac muscle contraction but also in the development of these tissues (Meseguer et al., 2019). Since myopathy and muscle spasms are common symptoms in MELAS, these mt-tRFs may facilitate disease progression by affecting muscle tissue function, on top of the mitochondrial dysfunction that results from reduced mitochondrial translation. In this context, a mt-itRF derived from mt-tRNA$^{Glu(UUC)}$ was found upregulated in MELAS cybrid cells. This specific tRF directly interacts to and downregulates *MPC1* mRNA which encodes for the mitochondrial pyruvate carrier protein, leading to extracellular accumulation of lactate. Finally, mt-tRNA$^{Ser(UCN)}$ is a hotspot for mutations (T7510C, T7511C, and A7445G) that can lead to non-syndromic hearing loss, meaning that hearing impairment is the main, and usually the only symptom. It is known that inner-ear cells have structurally unique mitochondria which may be why this is usually the main symptom in individuals carrying this mtDNA mutation (Lesus et al., 2019). The pathogenesis of these mutations has been attributed to the reduced steady state levels of mt-tRNA$^{Ser(UCN)}$ because RNase Z^L/ELAC2 cannot process these transcripts efficiently (Yan et al., 2006). One possibility that should be further explored is whether these mutations could result in the production of specific mt-tRFs deriving from mt-tRNA$^{Ser(UCN)}$ and whether can be related to the progression of non-syndromic hearing loss.

Collectively, current knowledge suggests that among the main factors that lead to detection of differential levels of mt-tRFs in cancer includes, among others, rewiring of mitochondrial metabolism through translation deregulation. The latter indicates that several types of mitochondrial dysfunction, such as loss of mitochondrial membrane potential and mitochondrial calcium overload, can affect mt-tRF production, *via* their impact on mtDNA transcription and translation and possibly *via* impaired efficiency of non-coding RNAs and proteins import. Aberrant translation could increase the availability of mt-tRNAs for cleavage thus leading to production of mt-tRFs. On the other hand, reduced mtDNA transcription could lead to a reduction of the mt-tRNA pool and subsequently to overall availability for mt-tRFs production. Moreover, alterations during import of important proteins that are targeted into mitochondria can also potentially lead to differential mt-tRFs levels and the modulation of the genes that are potential targets.

CONCLUDING REMARKS

Mitochondria, although rather simple organelles, facilitate essential metabolic cascades and sense environmental cues to regulate energy production, manage oxidative stress, and serve an overall normal cellular function. Due to the dynamic crosstalk with other subcellular compartments and their profound effects on pathophysiology, mitochondria represent a unique field for studying several regulatory circuits that affect gene expression. During recent years, tRFs have been established as a novel class of small non-coding RNAs that predominantly have protective effect but can also play role in the deregulation of translation. Based on the central role of mitochondrial tRNAs during mitochondrial translation, the corresponding mt-tRFs could modulate gene expression regulation in a similar way to achieve fine-tuning of the communication with the nucleus.

It must be underlined that almost half the mutations in mtDNA occur on tRNA genes with various effects on mt-tRNA biogenesis, aminoacylation efficiency, and mRNA decoding (Zifa et al., 2007; Yarham et al., 2010; Suzuki, 2021). The increased instability of such mutated mt-tRNAs as well as of mt-tRNAs bearing aberrant modifications could be the leading cause for the differential mt-tRF production related to disease onset or progression. In addition to known point mutations on mt-tRNA genes or to deficiencies of ribonucleases and modifiers, external stimuli spanning from bacterial infections to specific nutrients can affect the homeostasis of mitochondria and therefore can directly affect mt-tRFs production. For instance, taurine administration has been shown to ameliorate stroke episodes in MELAS patients and is now used as a treatment regimen in Japan (Rikimaru et al., 2012; Ohsawa et al., 2019; Suzuki, 2021). Therefore, it is worth studying the effect of taurine intake on mt-tRF production in afflicted tissues of MELAS patients. It is evident that exploring the mt-tRF biogenesis and post-transcriptional modifications of both nuclear and mitochondrial tRNAs consist a critical step to unlock new RNA-mediated nuclear-mitochondrial circuits implicated in the cell metabolism and pathological conditions.

Apart from the undisputed existence of mt-tRFs and their correlation to specific human disorders, several questions regarding their biogenesis and role remain open. It is important to decipher how and which mt-tRNAs or mt-tRFs are exported from mitochondria but also in which subcellular compartment production of the majority of mt-tRF occurs. Import and export through the mitochondrial membrane currently remain a mystery. For this reason, experimental tools, such as specific RNA-aptamers, antisense oligonucleotides, or even delivery of free RNA, could be developed to carefully and reliably determine mt-tRFs spatiotemporal localization (Dovydenko et al., 2021). The putative mechanisms which control import and export of mt-tRNAs and

mt-tRFs could be targeted to treat mitochondrial diseases or to ameliorate secondary effects. The identification of specific enzymatic activities that are involved in mt-tRF production will provide valuable knowledge and will allow the better understanding of the possible role of mt-tRFs during intracellular communication. Given that the majority of mt-tRFs is accumulated inside mitochondria, it should be delineated which ribonucleases get involved, whether they are transported inside mitochondria and which is the cleavage pattern of their mt-tRNA substrates. Finally, considering that mitochondria originated from endosymbiotic events with prokaryotes, and regarding the similarities between mitochondria and bacteria, ranging from genome organization, membrane structure, and protein synthesis to overall structure, elucidation of the mechanism of mt-tRF biogenesis could provide new knowledge on the potential roles and biogenesis pathways of bacterial tRFs and *vice versa*.

AUTHOR CONTRIBUTIONS

A-NS, EK, VS, and CS contributed to the manuscript writing and the figure design and approved the review for publication. All authors contributed to the article and approved the submitted version.

FUNDING

This research was funded by the "INSPIRED-The National Research Infrastructures on Integrated Structural Biology, Drug Screening Efforts and Drug target functional characterization" (MIS 5002550), which is implemented under the action "Reinforcement of the Research and Innovation Infrastructure," funded by the Operational Program "Competitiveness, Entrepreneurship and Innovation" (NSRF 2014–2020) and co-financed by Greece and the European Union (European Regional Development Fund). A-NS is recipient of a fellowship from the "RIBOMAP" grant implemented under the Operational Program: Human Resources Development, Education and Lifelong Learning which is co-financed by the European Social Fund (ESF) and National Resources (MIS 5047175 to CS). EK is a recipient of a fellowship from the State Scholarships Foundation (IKY).

REFERENCES

Anderson, S., Bankier, A. T., Barrell, B. G., de Bruijn, M. H. L., Coulson, A. R., Drouin, J., et al. (1981). Sequence and organization of the human mitochondrial genome. *Nature* 290, 457–465. doi: 10.1038/290457a0

Asano, K., Suzuki, T., Saito, A., Wei, F., Ikeuchi, Y., Numata, T., et al. (2018). Metabolic and chemical regulation of tRNA modification associated with taurine deficiency and human disease. *Nucleic Acids Res.* 46, 1565–1583. doi: 10.1093/nar/gky068

Baranowski, W., Dirheimer, G., Jakowicki, J. A., and Keith, G. (1994). Deficiency of queuine, a highly modified purine base, in transfer RNAs from primary and metastatic ovarian malignant tumors in women. *Cancer Res*. 54, 4468–4471.

Blanco, S., Dietmann, S., Flores, J. V., Hussain, S., Kutter, C., Humphreys, P., et al. (2014). Aberrant methylation of t RNA s links cellular stress to neuro-developmental disorders. *EMBO J.* 33, 2020–2039. doi: 10.15252/embj.201489282

Bruni, F., Lightowlers, R. N., and Chrzanowska-Lightowlers, Z. M. (2017). Human mitochondrial nucleases. *FEBS J.* 284, 1767–1777. doi: 10.1111/febs.13981

Chellamuthu, A., and Gray, S. G. (2020). The RNA Methyltransferase NSUN2 and its potential roles in cancer. *Cell* 9:1758. doi: 10.3390/cells9081758

Chujo, T., and Tomizawa, K. (2021). Human transfer RNA modopathies: diseases caused by aberrations in transfer RNA modifications. *FEBS J.* 1–27. doi: 10.1111/febs.15736 [Epub ahead of print]

Donovan, J., Rath, S., Kolet-Mandrikov, D., and Korennykh, A. (2017). Rapid RNase L–driven arrest of protein synthesis in the dsRNA response without degradation of translation machinery. *RNA* 23, 1660–1671. doi: 10.1261/rna.062000.117

Dovydenko, I., Meschaninova, M., Heckel, A. M., Tarassov, I., Venyaminova, A., and Entelis, N. (2021). Lipophilic conjugates for carrier-free delivery of RNA importable into human mitochondria. *Methods Mol. Biol.* 2277, 49–67. doi: 10.1007/978-1-0716-1270-5_4

Gorman, G. S., Chinnery, P. F., DiMauro, S., Hirano, M., Koga, Y., McFarland, R., et al. (2016). Mitochondrial diseases. *Nat. Rev. Dis. Prim.* 2:16080. doi: 10.1038/nrdp.2016.80

Grafanaki, K., Anastasakis, D., Kyriakopoulos, G., Skeparnias, I., Georgiou, S., and Stathopoulos, C. (2019). Translation regulation in skin cancer from a tRNA point of view. *Epigenomics* 11, 215–245. doi: 10.2217/epi-2018-0176

Gusic, M., and Prokisch, H. (2020). ncRNAs: new players in mitochondrial health and disease? *Front. Genet.* 11:95. doi: 10.3389/fgene.2020.00095

Hasler, D., Lehmann, G., Murakawa, Y., Klironomos, F., Jakob, L., Grässer, F. A., et al. (2016). The lupus autoantigen La prevents Mis-channeling of tRNA fragments into the human MicroRNA pathway. *Mol. Cell* 63, 110–124. doi: 10.1016/j.molcel.2016.05.026

Hayes, P., Fergus, C., Ghanim, M., Cirzi, C., Burtnyak, L., McGrenaghan, C. J., et al. (2020). Queuine micronutrient deficiency promotes Warburg metabolism and reversal of the mitochondrial ATP synthase in hela cells. *Nutrients* 12, 1–18. doi: 10.3390/nu12030871

Jády, B. E., Ketele, A., and Kiss, T. (2018). Dynamic association of human mRNP proteins with mitochondrial tRNAs in the cytosol. *RNA* 24, 1706–1720. doi: 10.1261/rna.066738.118

Jeandard, D., Smirnova, A., Tarassov, I., Barrey, E., Smirnov, A., and Entelis, N. (2019). Import of non-coding RNAs into human mitochondria: a critical review and emerging approaches. *Cell* 8:286. doi: 10.3390/cells8030286

Ji, Y., Nie, Z., Meng, F., Hu, C., Chen, H., Jin, L., et al. (2021). Mechanistic insights into mitochondrial tRNAAla 3'-end metabolism deficiency. *J. Biol. Chem.* 297:100816. doi: 10.1016/j.jbc.2021.100816

Kaliatsi, E. G., Giarimoglou, N., Stathopoulos, C., and Stamatopoulou, V. (2020). Non-coding RNA-driven regulation of rRNA biogenesis. *Int. J. Mol. Sci.* 21:9738. doi: 10.3390/ijms21249738

Karasik, A., Wilhelm, C. A., Fierke, C. A., and Koutmos, M. (2021). Disease-associated mutations in mitochondrial precursor tRNAs affect binding, m1R9 methylation, and tRNA processing by mtRNase P. *RNA* 27, 420–432. doi: 10.1261/rna.077198.120

Karousi, P., Adamopoulos, P. G., Papageorgiou, S. G., Pappa, V., Scorilas, A., and Kontos, C. K. (2020). A novel, mitochondrial, internal tRNA-derived RNA fragment possesses clinical utility as a molecular prognostic biomarker in chronic lymphocytic leukemia. *Clin. Biochem.* 85, 20–26. doi: 10.1016/j.clinbiochem.2020.07.005

Kirino, Y., Yasukawa, T., Ohta, S., Akira, S., Ishihara, K., Watanabe, K., et al. (2004). Codon-specific translational defect caused by a wobble modification deficiency in mutant tRNA from a human mitochondrial disease. *Proc. Natl. Acad. Sci.* 101, 15070–15075. doi: 10.1073/pnas.0405173101

Kumar, P., Anaya, J., Mudunuri, S. B., and Dutta, A. (2014). Meta-analysis of tRNA derived RNA fragments reveals that they are evolutionarily conserved

and associate with AGO proteins to recognize specific RNA targets. *BMC Biol.* 12:78. doi: 10.1186/s12915-014-0078-0

Kumar, P., Kuscu, C., and Dutta, A. (2016). Biogenesis and function of transfer RNA-related fragments (tRFs). *Trends Biochem. Sci.* 41, 679–689. doi: 10.1016/j.tibs.2016.05.004

Kumar, P., Mudunuri, S. B., Anaya, J., and Dutta, A. (2015). tRFdb: a database for transfer RNA fragments. *Nucleic Acids Res.* 43, D141–D145. doi: 10.1093/nar/gku1138

Kummer, E., and Ban, N. (2021). Mechanisms and regulation of protein synthesis in mitochondria. *Nat. Rev. Mol. Cell Biol.* 22, 307–325. doi: 10.1038/s41580-021-00332-2

Kuscu, C., Kumar, P., Kiran, M., Su, Z., Malik, A., and Dutta, A. (2018). tRNA fragments (tRFs) guide ago to regulate gene expression post-transcriptionally in a Dicer-independent manner. *RNA* 24, 1093–1105. doi: 10.1261/rna.066126.118

Lee, Y. S., Shibata, Y., Malhotra, A., and Dutta, A. (2009). A novel class of small RNAs: tRNA-derived RNA fragments (tRFs). *Genes Dev.* 23, 2639–2649. doi: 10.1101/gad.1837609

Lesus, J., Arias, K., Kulaga, J., Sobkiv, S., Patel, A., Babu, V., et al. (2019). Why study inner ear hair cell mitochondria? *HNO* 67, 429–433. doi: 10.1007/s00106-019-0662-2

Leucci, E., Vendramin, R., Spinazzi, M., Laurette, P., Fiers, M., Wouters, J., et al. (2016). Melanoma addiction to the long non-coding RNA SAMMSON. *Nature* 531, 518–522. doi: 10.1038/nature17161

Levy, S., Allerston, C. K., Liveanu, V., Habib, M. R., Gileadi, O., and Schuster, G. (2016). Identification of LACTB2, a metallo-β-lactamase protein, as a human mitochondrial endoribonuclease. *Nucleic Acids Res.* 44, 1813–1832. doi: 10.1093/nar/gkw050

Li, M., Kao, E., Gao, X., Sandig, H., Limmer, K., Pavon-Eternod, M., et al. (2012). Codon-usage-based inhibition of HIV protein synthesis by human schlafen 11. *Nature* 491, 125–128. doi: 10.1038/nature11433

Li, M., Kao, E., Malone, D., Gao, X., Wang, J. Y. J., and David, M. (2018). DNA damage-induced cell death relies on SLFN11-dependent cleavage of distinct type II tRNAs. *Nat. Struct. Mol. Biol.* 25, 1047–1058. doi: 10.1038/s41594-018-0142-5

Loher, P., Telonis, A. G., and Rigoutsos, I. (2017). MINTmap: fast and exhaustive profiling of nuclear and mitochondrial tRNA fragments from short RNA-seq data. *Sci. Rep.* 7:41184. doi: 10.1038/srep41184

Looney, M. M., Lu, Y., Karakousis, P. C., and Halushka, M. K. (2020). Mycobacterium tuberculosis infection drives mitochondria-biased dysregulation of host transfer RNA–derived fragments. *J. Infect. Dis.* 223, 1796–1805. doi: 10.1093/infdis/jiaa596

Maniataki, E., and Mourelatos, Z. (2005). Human mitochondrial tRNAMet is exported to the cytoplasm and associates with the Argonaute 2 protein. *RNA* 11, 849–852. doi: 10.1261/rna.2210805

Marnef, A., Jády, B. E., and Kiss, T. (2016). Human polypyrimidine tract-binding protein interacts with mitochondrial tRNA(Thr) in the cytosol. *Nucleic Acids Res.* 44, 1342–1353. doi: 10.1093/nar/gkv1355

Martínez-Zamora, A., Meseguer, S., Esteve, J. M., Villarroya, M., Aguado, C., Enríquez, J. A., et al. (2015). Defective expression of the mitochondrial-tRNA modifying enzyme GTPBP3 triggers AMPK-mediated adaptive responses involving complex I assembly factors, uncoupling protein 2, and the mitochondrial pyruvate carrier. *PLoS One* 10:e0144273. doi:10.1371/journal.pone.0144273, PMID: 26642043.

Mercer, T. R., Neph, S., Dinger, M. E., Crawford, J., Smith, M. A., Shearwood, A. M. J., et al. (2011). The human mitochondrial transcriptome. *Cell* 146, 645–658. doi: 10.1016/j.cell.2011.06.051

Meseguer, S. (2021). MicroRNAs and tRNA-derived small fragments: key messengers in nuclear–mitochondrial communication. *Front. Mol. Biosci.* 8:643575. doi: 10.3389/fmolb.2021.643575

Meseguer, S., Navarro-González, C., Panadero, J., Villarroya, M., Boutoual, R., Sánchez-Alcázar, J. A., et al. (2019). The MELAS mutation m.3243A>G alters the expression of mitochondrial tRNA fragments. *Biochim. Biophys. Acta, Mol. Cell Res.* 1866, 1433–1449. doi: 10.1016/j.bbamcr.2019.06.004

Minagawa, A., Takaku, H., Takagi, M., and Nashimoto, M. (2005). The missense mutations in the candidate prostate cancer gene ELAC2 do not alter enzymatic properties of its product. *Cancer Lett.* 222, 211–215. doi: 10.1016/j.canlet.2004.09.013

Müller, M., Legrand, C., Tuorto, F., Kelly, V. P., Atlasi, Y., Lyko, F., et al. (2019). Queuine links translational control in eukaryotes to a micronutrient from bacteria. *Nucleic Acids Res.* 47, 3711–3727. doi: 10.1093/nar/gkz063

Nätt, D., Kugelberg, U., Casas, E., Nedstrand, E., Zalavary, S., Henriksson, P., et al. (2019). Human sperm displays rapid responses to diet. *PLoS Biol.* 17:e3000559. doi: 10.1371/journal.pbio.3000559

Ohsawa, Y., Hagiwara, H., Nishimatsu, S., Hirakawa, A., Kamimura, N., Ohtsubo, H., et al. (2019). Taurine supplementation for prevention of stroke-like episodes in MELAS: a multicentre, open-label, 52-week phase III trial. *J. Neurol. Neurosurg. Psychiatry* 90, 529–536. doi: 10.1136/jnnp-2018-317964

Pathak, C., Jaiswal, Y. K., and Vinayak, M. (2005). Hypomodification of transfer RNA in cancer with respect to queuosine. *RNA Biol.* 2, 143–148. doi: 10.4161/rna.2.4.2417

Pliatsika, V., Loher, P., Magee, R., Telonis, A. G., Londin, E., Shigematsu, M., et al. (2018). MINTbase v2.0: a comprehensive database for tRNA-derived fragments that includes nuclear and mitochondrial fragments from all the cancer genome atlas projects. *Nucleic Acids Res.* 46, D152–D159. doi: 10.1093/nar/gkx1075

Rikimaru, M., Ohsawa, Y., Wolf, A. M., Nishimaki, K., Ichimiya, H., Kamimura, N., et al. (2012). Taurine ameliorates impaired the mitochondrial function and prevents stroke-like episodes in patients with MELAS. *Intern. Med.* 51, 3351–3357. doi: 10.2169/internalmedicine.51.7529

Saikia, M., Jobava, R., Parisien, M., Putnam, A., Krokowski, D., Gao, X.-H., et al. (2014). Angiogenin-cleaved tRNA halves interact with cytochrome c, protecting cells from apoptosis during osmotic stress. *Mol. Cell. Biol.* 34, 2450–2463. doi: 10.1128/MCB.00136-14

Saoura, M., Powell, C. A., Kopajtich, R., Alahmad, A., Al-Balool, H. H., Albash, B., et al. (2019). Mutations in ELAC2 associated with hypertrophic cardiomyopathy impair mitochondrial tRNA 3'-end processing. *Hum. Mutat.* 40, 1731–1748. doi: 10.1002/humu.23777

Schaefer, M., Pollex, T., Hanna, K., Tuorto, F., Meusburger, M., Helm, M., et al. (2010). RNA methylation by Dnmt2 protects transfer RNAs against stress-induced cleavage. *Genes Dev.* 24, 1590–1595. doi: 10.1101/gad.586710

Schimmel, P. (2018). The emerging complexity of the tRNA world: mammalian tRNAs beyond protein synthesis. *Nat. Rev. Mol. Cell Biol.* 19, 45–58. doi: 10.1038/nrm.2017.77

Shinoda, S., Kitagawa, S., Nakagawa, S., Wei, F.-Y., Tomizawa, K., Araki, K., et al. (2019). Mammalian NSUN2 introduces 5-methylcytidines into mitochondrial tRNAs. *Nucleic Acids Res.* 47, 8734–8745. doi: 10.1093/nar/gkz575

Siira, S. J., Rossetti, G., Richman, T. R., Perks, K., Ermer, J. A., Kuznetsova, I., et al. (2018). Concerted regulation of mitochondrial and nuclear non-coding RNAs by a dual-targeted RNase Z. *EMBO Rep.* 19:e46198. doi: 10.15252/embr.201846198

Skeparnias, I., Anastasakis, D., Grafanaki, K., Kyriakopoulos, G., Alexopoulos, P., Dougenis, D., et al. (2020). Contribution of miRNAs, tRNAs and tRFs to aberrant Signaling and translation deregulation in lung cancer. *Cancers* 12:3056. doi: 10.3390/cancers12103056

Srinivasan, S., Yeri, A., Cheah, P. S., Chung, A., Danielson, K., De Hoff, P., et al. (2019). Small RNA sequencing across diverse biofluids identifies optimal methods for exRNA isolation. *Cell* 177, 446–462. doi: 10.1016/j.cell.2019.03.024

Stewart, J. B., Alaei-Mahabadi, B., Sabarinathan, R., Samuelsson, T., Gorodkin, J., Gustafsson, C. M., et al. (2015). Simultaneous DNA and RNA mapping of somatic mitochondrial mutations across diverse human cancers. *PLoS Genet.* 11:e1005333. doi: 10.1371/journal.pgen.1005333

Su, Z., Kuscu, C., Malik, A., Shibata, E., and Dutta, A. (2019). Angiogenin generates specific stress-induced tRNA halves and is not involved in tRF-3–mediated gene silencing. *J. Biol. Chem.* 294, 16930–16941. doi: 10.1074/jbc.RA119.009272

Su, Z., Wilson, B., Kumar, P., and Dutta, A. (2020). Noncanonical roles of tRNAs: tRNA fragments and Beyond. *Annu. Rev. Genet.* 54, 47–69. doi: 10.1146/annurev-genet-022620-101840

Suzuki, T. (2021). The expanding world of tRNA modifications and their disease relevance. *Nat. Rev. Mol. Cell Biol.* 11, 375–392. doi: 10.1038/s41580-021-00342-0

Suzuki, T., Yashiro, Y., Kikuchi, I., Ishigami, Y., Saito, H., Matsuzawa, I., et al. (2020). Complete chemical structures of human mitochondrial tRNAs. *Nat. Commun.* 11:4269. doi: 10.1038/s41467-020-18068-6

Telonis, A. G., Loher, P., Honda, S., Jing, Y., Palazzo, J., Kirino, Y., et al. (2015). Dissecting tRNA-derived fragment complexities using personalized transcriptomes reveals novel fragment classes and unexpected dependencies. *Oncotarget* 6, 24797–24822. doi: 10.18632/oncotarget.4695

Tuorto, F., Liebers, R., Musch, T., Schaefer, M., Hofmann, S., Kellner, S., et al. (2012). RNA cytosine methylation by Dnmt2 and NSun2 promotes tRNA stability and protein synthesis. *Nat. Struct. Mol. Biol.* 19, 900–905. doi: 10.1038/nsmb.2357

Van Haute, L., Lee, S.-Y., McCann, B. J., Powell, C. A., Bansal, D., Vasiliauskaitė, L., et al. (2019). NSUN2 introduces 5-methylcytosines in mammalian mitochondrial tRNAs. *Nucleic Acids Res.* 47, 8720–8733. doi: 10.1093/nar/gkz559

Varghese, S., Cotter, M., Chevot, F., Fergus, C., Cunningham, C., Mills, K. H., et al. (2017). In vivo modification of tRNA with an artificial nucleobase leads to full disease remission in an animal model of multiple sclerosis. *Nucleic Acids Res.* 45, 2029–2039. doi: 10.1093/nar/gkw847

Vendramin, R., Marine, J., and Leucci, E. (2017). Non-coding RNA s: the dark side of nuclear–mitochondrial communication. *EMBO J.* 36, 1123–1133. doi: 10.15252/embj.201695546

Wang, X., Matuszek, Z., Huang, Y., Parisien, M., Dai, Q., Clark, W., et al. (2018). Queuosine modification protects cognate tRNAs against ribonuclease cleavage. *RNA* 24, 1305–1313. doi: 10.1261/rna.067033.118

Webb, B. D., Diaz, G. A., and Prasun, P. (2020). Mitochondrial translation defects and human disease. *J. Transl. Genet. Genomics* 4, 71–80. doi: 10.20517/jtgg.2020.11

Xue, L., Chen, Y., Tang, X., Yao, J., Huang, H., Wang, M., et al. (2019). A deafness-associated mitochondrial DNA mutation altered the tRNASer(UCN) metabolism and mitochondrial function. *Mitochondrion* 46, 370–379. doi: 10.1016/j.mito.2018.10.001

Yamasaki, S., Ivanov, P., Hu, G., and Anderson, P. (2009). Angiogenin cleaves tRNA and promotes stress-induced translational repression. *J. Cell Biol.* 185, 35–42. doi: 10.1083/jcb.200811106

Yan, H., Zareen, N., and Levinger, L. (2006). Naturally occurring mutations in human mitochondrial pre-tRNASer(UCN) can affect the transfer ribonuclease Z cleavage site, processing kinetics, and substrate secondary structure. *J. Biol. Chem.* 281, 3926–3935. doi: 10.1074/jbc.M509822200

Yang, J.-Y., Deng, X.-Y., Li, Y.-S., Ma, X.-C., Feng, J.-X., Yu, B., et al. (2018). Structure of Schlafen13 reveals a new class of tRNA/rRNA- targeting RNase engaged in translational control. *Nat. Commun.* 9:1165. doi: 10.1038/s41467-018-03544-x

Yarham, J. W., Elson, J. L., Blakely, E. L., Mcfarland, R., and Taylor, R. W. (2010). Mitochondrial tRNA mutations and disease. *Wiley Interdiscip. Rev. RNA* 1, 304–324. doi: 10.1002/wrna.27

Yue, T., Zhan, X., Zhang, D., Jain, R., Wang, K., Choi, J. H., et al. (2021). SLFN2 protection of tRNAs from stress-induced cleavage is essential for T cell–mediated immunity. *Science* 80:eaba4220. doi: 10.1126/science.aba4220

Zheng, L.-L., Xu, W.-L., Liu, S., Sun, W.-J., Li, J.-H., Wu, J., et al. (2016). tRF2Cancer: A web server to detect tRNA-derived small RNA fragments (tRFs) and their expression in multiple cancers. *Nucleic Acids Res.* 44, W185–W193. doi: 10.1093/nar/gkw414

Zhu, L., Li, J., Gong, Y., Wu, Q., Tan, S., Sun, D., et al. (2019). Exosomal tRNA-derived small RNA as a promising biomarker for cancer diagnosis. *Mol. Cancer* 18:74. doi: 10.1186/s12943-019-1000-8

Zifa, E., Giannouli, S., Theotokis, P., Stamatis, C., Mamuris, Z., and Stathopoulos, C. (2007). Mitochondrial tRNA mutations: clinical and functional perturbations. *RNA Biol.* 4, 38–66. doi: 10.4161/rna.4.1.4548

Zifa, E., Theotokis, P., Kaminari, A., Maridaki, H., Leze, H., Petsiava, E., et al. (2008). A novel G3337A mitochondrial ND1 mutation related to cardiomyopathy co-segregates with tRNALeu(CUN) A12308G and tRNAThr C15946T mutations. *Mitochondrion* 8, 229–236. doi: 10.1016/j.mito.2008.04.001

Conflict of Interest: The authors declare that the research was conducted in the absence of any commercial or financial relationships that could be construed as a potential conflict of interest.

Publisher's Note: All claims expressed in this article are solely those of the authors and do not necessarily represent those of their affiliated organizations, or those of the publisher, the editors and the reviewers. Any product that may be evaluated in this article, or claim that may be made by its manufacturer, is not guaranteed or endorsed by the publisher.

frontiers in Physiology

REVIEW
published: 09 September 2021
doi: 10.3389/fphys.2021.734976

MicroRNAs as Factors in Bidirectional Crosstalk Between Mitochondria and the Nucleus During Cellular Senescence

Chiara Giordani[1†], Andrea Silvestrini[1†], Angelica Giuliani[1], Fabiola Olivieri[1,2] and Maria Rita Rippo[1]*

[1]Department of Clinical and Molecular Sciences, DISCLIMO, Università Politecnica delle Marche, Ancona, Italy, [2]Center of Clinical Pathology and Innovative Therapy, IRCCS INRCA, Ancona, Italy

OPEN ACCESS

Edited by:
Eleonora Leucci,
KU Leuven, Belgium

Reviewed by:
Anna Blumental-Perry,
University at Buffalo, United States
Carlos Palmeira,
University of Coimbra, Portugal

****Correspondence:***
Angelica Giuliani
angelica.giuliani@staff.univpm.it

[†]These authors have contributed equally to this work

Specialty section:
This article was submitted to Mitochondrial Research, a section of the journal Frontiers in Physiology

Received: *01 July 2021*
Accepted: *12 August 2021*
Published: *09 September 2021*

Citation:
Giordani C, Silvestrini A, Giuliani A, Olivieri F and Rippo MR (2021) MicroRNAs as Factors in Bidirectional Crosstalk Between Mitochondria and the Nucleus During Cellular Senescence. Front. Physiol. 12:734976. doi: 10.3389/fphys.2021.734976

Mitochondria are essential organelles that generate most of the chemical energy to power the cell through ATP production, thus regulating cell homeostasis. Although mitochondria have their own independent genome, most of the mitochondrial proteins are encoded by nuclear genes. An extensive bidirectional communication network between mitochondria and the nucleus has been discovered, thus making them semi-autonomous organelles. The nucleus-to-mitochondria signaling pathway, called Anterograde Signaling Pathway can be deduced, since the majority of mitochondrial proteins are encoded in the nucleus, less is known about the opposite pathway, the so-called mitochondria-to-nucleus retrograde signaling pathway. Several studies have demonstrated that non-coding RNAs are essential "messengers" of this communication between the nucleus and the mitochondria and that they might have a central role in the coordination of important mitochondrial biological processes. In particular, the finding of numerous miRNAs in mitochondria, also known as mitomiRs, enabled insights into their role in mitochondrial gene transcription. MitomiRs could act as important mediators of this complex crosstalk between the nucleus and the mitochondria. Mitochondrial homeostasis is critical for the physiological processes of the cell. Disruption at any stage in their metabolism, dynamics and bioenergetics could lead to the production of considerable amounts of reactive oxygen species and increased mitochondrial permeability, which are among the hallmarks of cellular senescence. Extensive changes in mitomiR expression and distribution have been demonstrated in senescent cells, those could possibly lead to an alteration in mitochondrial homeostasis. Here, we discuss the emerging putative roles of mitomiRs in the bidirectional communication pathways between mitochondria and the nucleus, with a focus on the senescence-associated mitomiRs.

Keywords: microRNA, senescence, mitochondria, mitonuclear communication, mitomiRs

INTRODUCTION

The aging process is considered a universal and inevitable process of physiological decline associated with a greater vulnerability to disease and death. This vulnerability is linked to the complexity of the organism, which comes from the myriad of interactions and feedback controls that operate between its different structural units. These mechanisms allow cells, tissues, and entire organisms the ability to respond and adapt to stressful environmental conditions. However, several studies suggest that this complexity diminishes with age due to the progressive loss of functions of cells, tissues, and organs and importantly of their ability to communicate, determining an increase of structural disorder; therefore, the complexity decrease is closely related to the increase in entropy, both determining the reduction of the functional reserve of older people (López-Otín et al., 2013). In this context, the Lorenz's Butterfly metaphor makes the concept of "instability of the aging system" easier: even the slightest change can cause consequences that are not proportionate to the initial event; a small accident can induce fatal effects in the elderly or biologically old individual just as "a flapping of the wings of a butterfly in Brazil can trigger a hurricane in Texas" (Lorenz, 1972). During organismal aging, senescent cells accumulate in tissues, where they alter microenvironment homeostasis. Many theories of the origin of cellular senescence have started from the observation of microscopic changes in aging cells. López-Otín et al. (2013) tried to identify and categorize common cellular and molecular hallmarks of aging: stem cell exhaustion, genomic instability, telomere attrition, epigenetic alterations, loss of proteostasis, deregulated nutrient sensing pathways and mitochondrial dysfunction. Senescent cells exhibit several functional, phenotypic, and molecular changes including a stable arrest of proliferation. The metabolic alterations and changes in gene expression allow these cells to remain viable and resist to apoptosis for a long time but are also the cause of the acquisition of a common secretory phenotype. Cell cycle arrest in senescence is largely mediated *via* the activation of either one or both p16/pRB and p53/p21 tumor suppressor pathways. Prolonged overexpression of these four components is sufficient to induce senescence: pRB and p53 are key transcriptional regulators whereas p16 and p21 are cyclin-dependent kinase inhibitors which negatively regulate cell cycle progression. p53 and its downstream effector p21, are activated by DNA damage caused by oncogenic or oxidative stress and telomere attrition; however, epigenetically induced senescence mostly acts by inducing p16 expression that prevents phosphorylation of RB and thus the transcription of genes required for cell cycle progression (Kumari and Jat, 2021).

The secretory phenotype, called Senescence Associated Secretory Phenotype (SASP), and the altered intercellular communication are both important aspects of aging cells because they cause a low grade systemic, chronic inflammation called inflammaging (Franceschi et al., 2000). This condition plays a key role in the pathophysiology of inflammatory age-related diseases (ARDs), i.e., cancer, diabetes, cardiovascular and neurodegenerative diseases. Judith Campisi and her group first coined the term SASP and demonstrated that genotoxic stress-induced senescent cells secrete a myriad of factors associated with inflammation and oncogenesis (Coppé et al., 2008). Since then, scientific data on the characterization and the pathogenetic role of the SASP has increased enormously, but from our understanding, SASP is represented by the release of different soluble factors, regardless of the type of senescence, i.e., induced or replicative, pro-inflammatory cytokines, chemokines, and non-coding RNAs (ncRNAs), including small (microRNAs), long (lncRNA) and circular RNA (Terlecki-Zaniewicz et al., 2018; Mensà et al., 2020). The SASP can propagate signals (proteins, lipoproteins, DNA and RNA) at systemic levels, which contributes to the communication between different types of cells and tissues (Fafián-Labora and O'Loghlen, 2020). Consolidated data have revealed that NF-κB signaling is the major signaling pathway which stimulates the appearance of the SASP and the production of pro-inflammatory mediators (Salminen et al., 2012).

MicroRNAs (miRNAs or miRs) are small non-coding RNAs (sncRNAs), about 18–25 nucleotides long, which can modulate various physiological and pathophysiological processes at a post-transcriptional level by binding the 3'-untranslated region of the target mRNA in the cytoplasm, inhibiting its expression. Their biogenesis, which has been elegantly described by other authors (Bartel, 2004; Ha and Kim, 2014; Wang et al., 2017a; Treiber et al., 2019) occurs in multiple steps, both in the nucleus and the cytoplasm. After pri-miRNAs are transcribed, they are subsequently cleaved to the more stable form pre-miRNAs by Drosha. Then they translocate in the cytoplasm where they associate with Ago2, after Dicer processing. It is only at this stage that the RNA-inducing silencing complex (RISC) takes shape, thus the binding with the target mRNA. MicroRNAs are potentially involved in all cellular functions, including development, proliferation, differentiation, apoptosis, and aging. A multitude of genome wide expression profile experiments have shown a differential modulation of non-coding RNA, including miRNAs, between proliferating and senescent cells (Faraonio et al., 2012; Giuliani et al., 2020). Most of ncRNAs and miRNAs play a pivotal role in inducing cellular senescence and related organismal dysfunction. MiRNAs can be actively released by living cells, shuttled by proteins and/or extracellular vesicles (EVs) and internalized by target cells, which spreads specific signals at paracrine and systemic levels. Senescent cells *via* the release of EVs containing a number of senescence-associated (SA)-miRNAs can spread the senescent

Abbreviations: ARDs, Age-related diseases; AMPK, AMP-activated protein kinase; DDR, DNA damage response; EVs, extracellular vesicles; Drp1, dynamin-related protein 1; ETC, electron transport chain; FOXO, forkhead box O; GPS2, G-Protein Pathway Suppressor 2; lncRNA, long non-coding RNA; miRNA, miR, microRNA; MDPs, mitochondrial-derived peptides; mtDNA, mitochondrial DNA; mitosRNA, mitochondrial genome-encoded small RNA; NF-κB, nuclear factor kappa-light-chain-enhancer of activated B cells; ncRNA, non-coding RNA; NRF-1, nuclear-respiratory factor 1; ORF, open reading frame; OXPHOS, oxidative phosphorylation; PARK2, Parkin; piRNA, Piwi-interacting RNA; PPAR, peroxisome proliferator-activated receptor; PGC1α, PPARγ co-activator 1α; PINK1, PTEN induced kinase 1; pRB, retinoblastoma protein; RTG, retrograde; RISC, RNA-inducing silencing complex; ROS, reactive oxygen species; SA, senescent-associated; SASP, Senescence Associated Secretory Phenotype; SncmtRNA, sense mitochondrial ncRNA; ASncmtRNA, antisense mitochondrial ncRNA; SIRT1, sirtuin 1; sncRNA, small non-coding RNA; Tfam, mitochondrial transcription factor A; p53, tumor protein P53; UTR, untranslated region.

phenotype (Mariani et al., 2020; Mensà et al., 2020; Olivieri et al., 2021; Prattichizzo et al., 2021).

Several SA-miRNAs were shown to affect mitochondrial dynamics and bioenergetics. All known SA-miRNAs are coded by the nuclear genome and some of these have been found overexpressed within mitochondria of replicative senescent cells compared to younger, impacting on resident proteins and functions. The implications of nuclear-coded miRNAs targeting mitochondrial functions on the acquisition of the senescent phenotype (anterograde signals) and the onset of ARDs will be explored in this review. Furthermore, recent studies regarding retrograde signals (RTG) from mitochondria to the nucleus in the senescent cells will be discussed. The study of these relationships could be useful to figure out effective interventions in slowing aging and preventing ARDs.

MITOCHONDRIA AND SENESCENCE

Mitochondria are involved in many processes besides energy metabolism such as cell cycle regulation, apoptosis and inflammation (Nunnari and Suomalainen, 2012). This suggests a close relationship between the proper performance of these organelles and cellular senescence. Mitochondrial dysfunction is in fact associated with the aging process and with the pathogenesis of ARDs. Some features of aged mitochondria, such as accumulation of mutation in mitochondrial DNA (mtDNA), altered mitochondria dynamics and increased reactive oxygen species (ROS) generation accompanied by progressive decrease in energy production, will be discussed below.

The mtDNA is circular and extremely small (16,569 nucleotides, 37 genes): it contains 13 mRNAs coding for some of the protein subunits of the oxidative phosphorylation (OXPHOS) machinery, two ribosomal RNAs (12S and 16S rRNAs) and 22 transfer RNAs (tRNAs; Carelli and Chan, 2014). However, about 3,000 genes are needed to make a mitochondrion and therefore their resulting proteins must be transported from the nucleus to the developing organelle. Only about 3% of the genes needed to make a mitochondrion are for ATP production. The remaining genes are involved in other functions related to the specialised tasks of the differentiated cells in which they reside. The integrity of mtDNA plays a key role in maintaining cellular homeostasis. Several studies carried out both on *in vitro* and *ex vivo* cellular models have demonstrated a close positive correlation between mtDNA mutations and the activation of mechanisms that lead to cellular dysfunction and, more generally, to the aging process (Trifunovic, 2006). We understand that mtDNA undergoes a higher mutation rate compared to nuclear DNA. In a neuronal stem cells model, for example, the accumulation of mtDNA damage led to a greater predisposition to differentiation towards an astrocytic lineage to a detrimental neurogenesis (Wang et al., 2011).

Mitochondrial dynamics, which vary through the life cycle of the cell depending on energy demands and cell division state, are critical to maintain mitochondrial integrity. During their life, which is about 10 days, mitochondria are faced with fission and fusion (Hales, 2010). The former is required to remove depolarized, damaged, and dysfunctional mitochondria *via* autophagy (mitophagy). The second mechanism allows viable mitochondria maintenance since repolarized organelles can be recovered and restored by fusion with healthy elements of the mitochondrial network. During fusion events some functional components can be irregularly redistributed between mitochondria; as a consequence, dissimilar mitochondria can be generated by the next fission event (Westermann, 2010).

Several mitochondrial alterations, i.e., mtDNA mutation, ROS overproduction, depolarization, and misfolded protein lead to the accumulation of PTEN induced kinase 1 (PINK1) on outer mitochondrial membrane, which phosphorylates Parkin (PARK2). Parkin 2 in turn promotes the ubiquitination of proteins that are then recognised by the autophagic machinery. The autophagosome containing the dysfunctional mitochondria is then transported and fused to a lysosome where it is then degraded (Kazlauskaite and Muqit, 2015). However, during aging dysfunctional mitochondria accumulate, mainly for two reasons: autophagy declines (Wang and Klionsky, 2011), and fission overcomes fusion (Amartuvshin et al., 2020; Spurlock et al., 2020). Indeed, in senescent cells, the transcription factor p53 interacts with Parkin by inhibiting its accumulation on the outer membrane and consequently blocking the process of mitophagy (Hoshino et al., 2013; Badr et al., 2014; Correia-Melo et al., 2017; Manzella et al., 2018). Therefore, the number of mitochondria is greater in senescent cells than in young cells, but their functionality is severely compromised (Kim et al., 2018; Chapman et al., 2019).

We thoroughly explored the phenotype of mitochondria in human endothelial cells undergoing replicative senescence and observed elongated/branched morphology concomitantly with autophagic vacuole accumulation (Giuliani et al., 2018). Accordingly, Mai and co-workers suggest an hyper-fused state of the mitochondria due to downregulation of the fission regulating proteins, i.e., fission1 and dynamin-related protein 1 (Drp1; Mai et al., 2010). Similar mitochondrial morphology was observed in primary dermal fibroblasts induced to senescence with doxorubicin or hydrogen peroxide. These data show that mitochondrial hyperfusion can be associated with aging; this may appear contradictory with respect to the concept that mitochondrial fusion is an adaptive and protective response during stress. In this respect it has been suggested that in certain cell types an apparently compensatory mitochondria hyperfusion may have long-term negative consequences and accelerate aging.

This severe impairment of mitochondria function in senescent cells is also characterized by a higher basal oxygen consumption rate, which leads both to an increase in energy production and to a greater release of ROS (Hutter et al., 2004). Excessive ROS production provokes telomere shortening which culminates in the DNA-damage response, thus speeding up the senescence process (Passos et al., 2007; Rai et al., 2009; Hewitt et al., 2012).

Therefore, it has been postulated that mitochondrial morphology transitions might regulate mitochondrial function by RTG signaling (Picard et al., 2013; Walczak et al., 2017).

MITONUCLEAR COMMUNICATION

Mitochondria biogenesis is controlled by two physically separated genomes: the mtDNA and the nuclear genome. Therefore, an intense communication with the nucleus is required in order to provide mitochondria with nuclear-encoded proteins, which are necessary for mitochondrial homeostasis and function.

The coordination between the nucleus and the mitochondrion is mediated by a sophisticated communication system, named mitonuclear communication, which occurs in a bi-directional way, known as anterograde signaling (nucleus-to-mitochondrion) and retrograde signaling (mitochondrion-to-nucleus). The former mechanism reflects the accepted outlook of the nucleus as a regulatory factor, which coordinates the function of subcellular organelles, allowing mitochondria to adapt to the cellular milieu in response to endogenous alterations or extracellular stimuli. The retrograde (RTG) signaling is meant to be a feedback system of the mitochondrial functional state to the nucleus to initiate adaptive responses (Quirós et al., 2016; Bhatti et al., 2017). It might be considered as a quality control mechanism, which compensates for the loss of mitochondrial quality that naturally occurs with age.

Anterograde Signaling

The anterograde signals are induced by extracellular stimuli, like physical exercise, cold exposure and dietary restrictions, through the activation of several genes including transcription factors, such as nuclear-respiratory factor 1 (NRF-1) and GA-binding protein-α (known as "NRF2"), peroxisome proliferator-activated receptors (PPARs); mitochondrial transcription factor A, uncoupling proteins, oestrogen-related receptors and PPARγ co-activator 1α (PGC1α; Hock and Kralli, 2009; Whelan and Zuckerbraun, 2013; Quirós et al., 2016). For example, during exercise or caloric restriction, there is an overall increase of AMP/ATP ratio, which in turn triggers AMP-activated protein kinase, along with an increment of NAD^+ levels. This event leads to the activation of sirtuin 1 (SIRT1), a positive regulator of PGC1α, which is known to stimulate mitochondria metabolism and proliferation.

In the last few decades, there is growing evidence to underpin the involvement of ncRNAs in the regulation of mitochondrial homeostasis. Several research groups have examined their possible localization within mitochondria. In 2006, from an RNA sequencing experiment on rat's liver mitochondria, a few miRNAs were identified inside the organelle, the so-called mitomiRs. Although initially thought as cytosolic contamination, just a few years later, several independent studies involving microarray profiling confirmed the initial findings (Lung et al., 2006; Kren et al., 2009; Bandiera et al., 2013).

Extensive miRNA mapping analysis revealed that most of them are nuclear encoded, strengthening the assumption of a nuclear involvement in mitochondria homeostasis, which ultimately implies a miRNA import mechanism inside mitochondria. Only recently, we have started to discover mechanisms of RNA export and import into mitochondria, but none of which are miRNAs' specific (**Figure 1**; Zeng et al., 2008; Wang et al., 2010; Jannot et al., 2016).

Since Ago2, an essential protein for RISC functioning, and some of its targets, such as some tRNA genes, have been localized into mitochondria (Bandiera et al., 2011), Bandiera and colleagues proposed an Ago2 involvement in the transport of miRNAs into mitochondria, as a protein import system similar to those involved in RNA trafficking. It has been demonstrated that phosphorylation of Ago2 induces miRNA:Ago2 complex intake into cytoplasmic processing bodies (P-bodies), which are known to interact with mitochondria (Zeng et al., 2008; Huang et al., 2011).

An important role is also played by GW-bodies in the formation of structures where the protein GW182 holds the association miRNA:Ago2 in a cap-like structure to make a stable RISC. A subsequent deletion of the cap and of the poly(A) tail, or the detachment of GW182 alone, presumably induced by cellular stresses, leaves miRNA:Ago2 complex free to head towards mitochondria (Gibbings et al., 2009). The proposed mechanism of miRNA:Ago2 entry involves gates such as SAM50, TOM20 and TIM (Jusic and Devaux, 2020).

Another import mechanism might involve the polynucleotide phosphorylase PNPASE, a 3'→5' exoribonuclease and poly-A polymerase located in the mitochondrial intermembrane space, that regulates mitochondrial homeostasis and adenine nucleotide levels (Wang et al., 2010). Wang and co-worker showed how PNPASE imports RNA from the cytosol into the mitochondrial matrix by binding to specific stem-loop motifs in the RNA sequence, making assumption on its potential involvement in mitochondrial miRNA trafficking (Wang et al., 2012).

Finally, porins, highly conserved proteins located in the outer membrane of mitochondria, could participate in miRNA translocation from cytosol to mitochondria, as proposed by Bandiera et al. (2013).

Notably, there is increasing body of evidence to suggest that mitochondria or mtDNA are exposed to intracellular or intercellular transfer *via* exosome and tunnelling nanotubes (Spees et al., 2006; Borralho et al., 2014).

It is widely accepted that housekeeping mitochondrial nuclear-encoded ncRNAs regulate mitochondrial function and homeostasis (Gusic and Prokisch, 2020), but less is known about their deregulation and possible correlation with mitochondrial-related diseases. Several nuclear-encoded lncRNAs have been localized in mitochondria and it has been hypothesized that they could regulate mitochondrial functions (Vendramin et al., 2017). It has been demonstrated that SAMMSON, a nuclear-encoded lncRNA acts as an oncogene in several malignancies (Leucci et al., 2016; Zheng et al., 2020), as well as MALAT1, which is known to be associated with cancer and metastasis (Sun and Ma, 2019). However, it is still an uncovered field, since not much data are available and mitochondria import mechanisms have still to be elucidated; therefore, the presence and the function of these transcripts in mitochondria, especially during cellular senescence, need further investigation. As mentioned above, different nuclear-encoded ncRNAs, such as miRNAs, are involved in mitochondrial

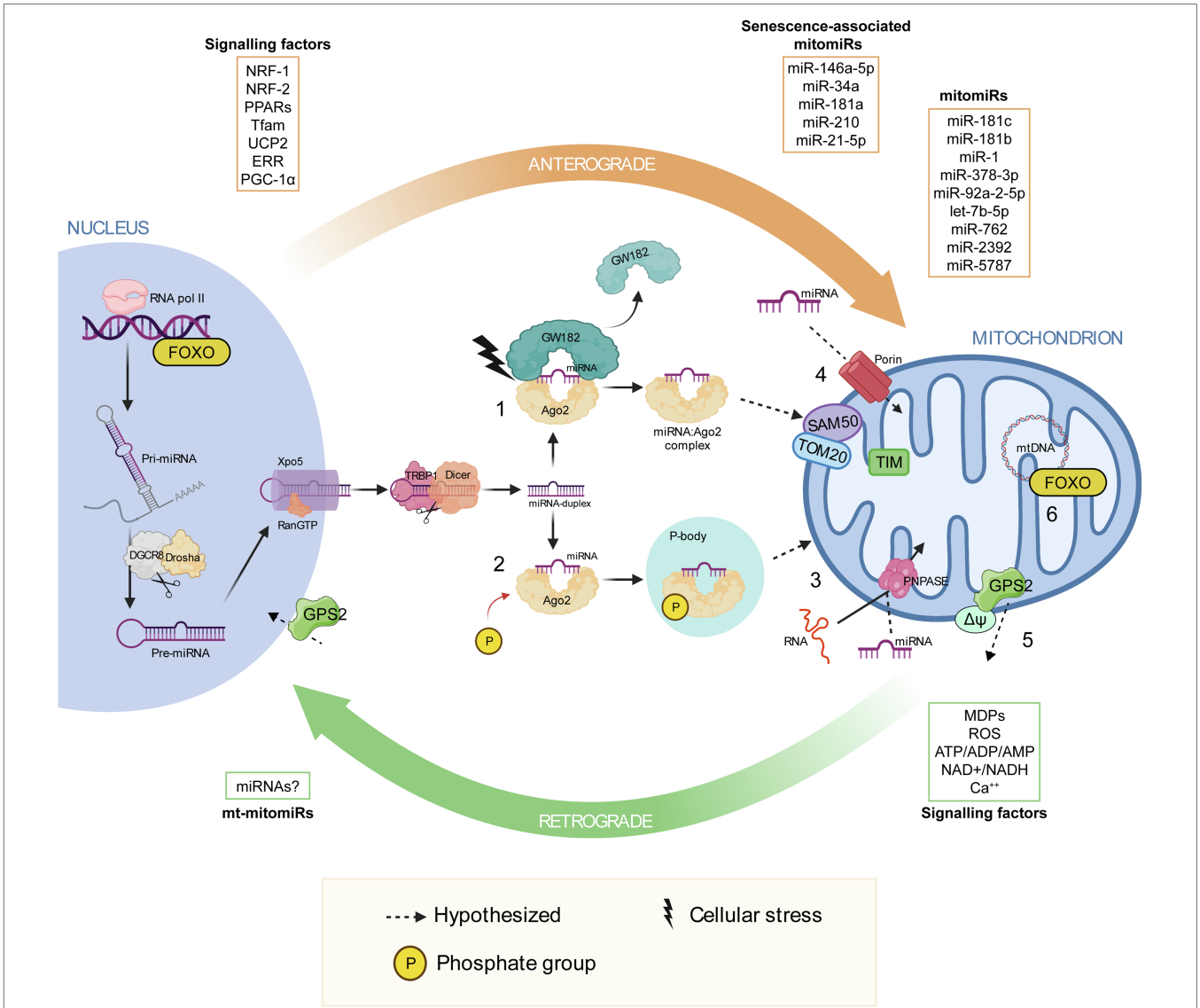

FIGURE 1 | Mitonuclear communication with a focus on the proposed mechanisms of miRNA import into mitochondria. Mitonuclear communication plays a key role in mitochondrial homeostasis. The nucleus coordinates a number of mitochondrial functions through the so-called anterograde signaling, which involve various signaling factors, including nuclear-respiratory factor 1, nuclear-respiratory factor 2, peroxisome proliferator-activated receptors, mitochondrial transcription factor A, uncoupling proteins, ERR and PPARγ co-activator 1α. MicroRNAs have been observed in this communication network, some are transported into the mitochondria (mitomiRs) and a few of which are associated with cellular senescence associated-mitomiRs. At the same time, mitochondria communicate their functional and oxidative state to the nucleus *via* the retrograde response, which involve mitochondria-derived peptides and metabolites, such as ROS, ATP/ADP/AMP, NAD^+/NADH and Ca^{2+}. After their biogenesis in the nucleus and their translocation in the cytosol, miRNA duplexes are unwound, they bind to the Argonaute protein 2 (Ago2) and are loaded into the RNA-inducing silencing complex. (1) Due to cellular stress GW182 dislocates from RISC, leaving the miRNA:Ago2 complex free in the cytosol. It has been proposed that miRNA:Ago2 might be imported into mitochondria through the SAM50 and TOM20 pores in the outer membrane and TIM in the inner mitochondrial membrane (Jusic and Devaux, 2020). (2) Phosphorylation of Ago2 induces miRNA:Ago2 intake into a P-body, which is known to interact with mitochondria. (3) Translocation of miRNA:Ago2 complex into mitochondria may be supported by polynucleotide phosphorylase. Polynucleotide phosphorylase facilitates mRNA import into mitochondria, by binding to stem loop motifs in the RNA sequence. (4) Porins participate in miRNA translocation into mitochondria, as proposed by Bandiera et al. (2013). (5) After mitochondrial depolarization, GSP2 translocates into the nucleus, triggering the expression of genes involved in mitochondrial homeostasis. (6) Upon sensing stress stimuli in the mitochondrion, Forkhead box O can induce specific sets of nuclear genes, including autophagy effectors and antioxidant activators. Parts of the figure were realized using BioRender (http://biorender.com).

homeostasis and are deregulated during senescence. The section "Anterograde signaling *via* nuclear-encoded mitomiRs in ARDs" will deeply describe nuclear-encoded miRNAs and their impact in mitochondria function and dysregulation.

Retrograde Signaling

The retrograde signaling pathway is activated when dysfunctional mitochondria try to communicate their oxidative, metabolic and respiratory stressful conditions to the nuclear compartment,

thus inducing a wide range of cellular adaptations (Passos et al., 2007; Quirós et al., 2016).

The most well studied retrograde signals are pleiotropic and include ROS, pro-apoptotic molecules such as ATP/ADP/AMP and metabolites such as NAD^+/NADH and Ca^{2+} (Picard et al., 2013), which, however, lack specificity as signaling molecules. Thus, the exact mechanism underlying the retrograde signaling by which mitochondria regulate cellular processes has not been completely unravelled yet.

Recently, mitochondrial-derived peptides (MDPs) encoded by a short open reading frame into mtDNA have been identified. Three types of MDPs have been discovered so far, including Humanin, MOTS-c and SHLP1-6. Their role is associated with cell survival, metabolism, inflammation and response to stressors with the final aim of maintaining mitochondrial function under stress conditions (Yang et al., 2019; Conte et al., 2021).

Recent reports highlight that the mammalian mitochondrial genome, in addition to the 37 known mitochondrial genes, encodes several classes of sncRNAs, "mitochondrial genome-encoded small RNAs" (mitosRNA), whose deregulation have been correlated with dysfunctional mitochondria and ultimately with a variety of diseases (Ro et al., 2013). To examine mitosRNA biogenesis, the presence of a mitochondrial RNAi machinery was investigated by Ro and colleagues, but neither Dicer nor AGO2 expression was detected. Therefore, mitosRNAs do not derive from RNA turnover, but they must be products of unknown mitochondrial ribonucleases (Ro et al., 2013).

NGS analyses performed by Larriba et al. (2018), who classified mitosRNAs into several groups of sncRNAs, emphasized the predominance of Piwi-interacting RNAs compared to other sncRNA categories, with regulatory functions in mitochondria and important for gametes and zygotic cells development, showing cell-type specific expression.

Despite mitosRNAs exact biogenesis and cellular trafficking are still uncertain (Vendramin et al., 2017), many studies about their possible function were carried out. Of note, mito-ncR-805 has been shown to have a protective effect to cigarette smoke in alveolar epithelial cells, as well as an increased expression of nuclear-encoded genes important for mitochondrial function, supporting the idea that mitosRNAs regulation and function might be cell-type specific (Blumental-Perry et al., 2020).

How mitosRNAs are exported from mitochondria and imported into the nucleus is still not known (Gammage et al., 2018), however studies about the expression of sense mitochondrial ncRNAs (SncmtRNAs) and antisense mitochondrial ncRNAs (ASncmtRNAs) between normal and cancer cells, demonstrated a cytoplasmic and nuclear localization of these mitochondrial transcripts, reinforcing the concept that they are exported from mitochondria (Villegas et al., 2007; Landerer et al., 2011; Borgna et al., 2020).

A direct mitonuclear communication strategy for mammals, similar to those found in yeasts and worms (Jazwinski and Kriete, 2012; Nargund et al., 2012, 2015), has been proposed by Cardamone et al., who characterized the G-Protein Pathway Suppressor 2 (GPS2; Cardamone et al., 2017), which also regulates insulin signaling, lipid metabolism and inflammation (Jakobsson et al., 2009). Cardamone and colleagues demonstrated that upon mitochondrial depolarization, GPS2 translocates into the nucleus, triggering the expression of genes involved in mitochondrial homeostasis. Other transcription factors involved in retrograde signaling have been identified, such as Forkhead box O (FOXO), which is known to help in the transcription of mitochondrial antioxidant enzymes, inducing mitophagy (Kim and Koh, 2017).

However, to our knowledge, since the details of this complex pathway are still unexplored, not much is known about other RNA export mechanisms from mitochondria, and if these also involve mitosRNAs.

New data support the idea of a mitonuclear communication involvement in aging. Since Ca^{2+} is the most important signaling molecule in the retrograde signaling pathway and studies in senescent human MRC5 fibroblasts correlated with increased mitochondrial biogenesis and Ca^{2+} alterations, it has been proposed that dysfunctional mitochondria might communicate with the nucleus *via* calcium signaling (Passos et al., 2007). Moreover, several studies reported that during induced or replicative senescence, mitochondria produce a higher amount of MDPs (humanin and MOTS-c), which can regulate mitochondrial energy metabolism, playing a cytoprotective role in ARDs. For example, humanin has a crucial role in reducing oxidative stress, while MOTS-c in glycolipids metabolism protects endothelial cells from atherosclerosis (Kim et al., 2018). Additional researchers have outlined that the increased production of ROS by defective mitochondria induces cytoplasmic chromatin fragments formation, which is JNK kinase-mediated, which is a trigger of SASP (Vizioli et al., 2020).

As far as we know, only a few studies have outlined the possibility of a relationship between mitosRNAs and ARDs. For example, SncmtRNA-1, SncmtRNA-2, ASncmtRNA-1 and ASncmtRNA-2 have been associated with cancer (Burzio et al., 2009; Vidaurre et al., 2014; Villota et al., 2019), whereas mt-lncRNA has been correlated with cardiovascular diseases (Yang et al., 2014). An interesting work by Shinde and colleagues (Shinde and Bhadra, 2015), demonstrates the expression of six novel mitochondrial genome-encoded miRNAs (mt-mitomiRs; Giuliani et al., 2019) in mitochondria and that the MT-RNR2 gene could be a potential target of two of them, hsa-miR-mit-3 and hsa-miR-mit-4. Curiously, MT-RNR2 gene also encodes for the humanin peptide, which has been correlated with Alzheimer's disease (Tajima et al., 2002), indicating a potential involvement of them in the development of the disease. MitosRNA association with ARDs makes them promising biomarkers of the diseases, therefore future studies will be required for a potential application in clinical practice.

ANTEROGRADE SIGNALING *VIA* NUCLEAR-ENCODED mitomiRs IN ARDs

One of the first piece of evidence that nuclear-encoded miRNA can regulate the expression of mitochondrial genome was provided by Das and colleagues. The authors showed that after its maturation in the cytoplasm, miR-181c translocated in the

mitochondrial compartment, where its principal target is the mt-COX-1 gene. Since mitochondrial DNA is sequentially transcribed as a polycistronic unit, miR-181c affects multiple proteins, including mt-COX2 and mt-COX3, resulting in complex IV remodelling (Das et al., 2012). Being the last complex of the respiratory chain, complex IV plays an important role in the transfer of electrons from cytochrome c oxidase to oxygen. Mutations or deregulation of complex IV lead to higher levels of ROS and mitochondrial dysfunction and are associated with a negative impact on lifespan and tissue integrity (Reichart et al., 2019). Cardiac myocytes are the cells with the highest volume density of mitochondria in the body and rely their extraordinary demand for continuous energy production on oxidative metabolism. As a result, these cells have been used to unravel mitomiR role in mitochondrial homeostasis. Das and co-workers confirmed their results *in vivo* using a lipid-based cationic nanoparticles miR-181c delivery system, which demonstrated that chronic overexpression of miR-181c is involved in heart failure (Das et al., 2014). Besides miR-181c, other miR-181 family members – i.e. miR-181a -181b, -181d – are found in mitochondria and have implications in heart mitochondrial health (Das et al., 2017). Interestingly, miR-181a and miR-181b have been shown to exert divergent roles in myocardial function. At the early stages of heart failure, miR-181a and -181b are consistently upregulated in cardiomyocyte mitochondria whereas, at the later stages, only miR-181b levels tend to remain stable, in association with a downregulation of miR-181a (Wang et al., 2017b). In this framework, mitomiRs acquire a critical role in cardiac function. Another miRNA widely studied in cardiac and skeletal muscle tissues is miR-1, which is actively involved in myogenesis and muscle proliferation (Chen et al., 2006). Increased expression of miR-1 was found in aging hearts, suggesting that this miRNA participates in additional cellular or pathophysiological functions other than myogenesis (Yang et al., 2007). MiR-1 has several cytosolic targets; however, during muscle differentiation it translocates to the mitochondria where it, surprisingly, enhances translation of mt-COX-1 and mt-ND1, resulting in boosted ATP generation. Zhang and colleagues showed that overexpression of miR-1 could have a negative impact on mitochondrial morphology and physiology in cancer stem cells, by targeting nuclear-encoded proteins required for mitochondria organization (Zhang et al., 2019). The non-canonical role as a translational activator of miR-1 seems to be linked to the lack of miRNA-mediated gene silencing GW182 inside the mitochondria, suggesting that the miRNA machinery is rearranged in this organelle (Zhang et al., 2014).

MitomiRs are also emerging players in the pathogenetic processes of diabetic heart diseases. Diabetes is associated with cardiac functional deficits, which may result from a decreased mitochondrial ATP output. Jagannathan et al. analyzed mitomiR distribution in the two spatially distinct mitochondrial subpopulations, i.e., subsarcolemmal and interfibrillar mitochondria, following diabetic insult. Of particular interest is mitomiR-378-3p, which originates from the first intron of peroxisome proliferator-activated receptor gamma, coactivator 1 beta gene that encodes PGC1β. This miRNA has been implicated in lipid metabolism, mitochondrial function, and shift towards the glycolytic pathway (Carrer et al., 2012; Krist et al., 2015). MitomiR-378 binds the ATP synthase F0 subunit 6 (ATP6), leading to a drop of ATP production following diabetes insult in interfibrillar mitochondria of mice (Jagannathan et al., 2015). In a condition of diabetic cardiomyopathy, mitomiR-92a-2-5p and let-7b-5p enter into the mitochondria to counteract cytochrome-b downregulation. Overexpression of miR-92a-2-5p enhances mitochondrial translation and reduces ROS production and lipid deposition, rescuing cardiac diastolic dysfunction in the db/db mouse model (Li et al., 2019). Also, miR-762 translocates to mitochondria upon ischemia/reperfusion model and downregulates ND2 leading to inhibition of ATP production and the enzyme activity of complex I, induction of ROS generation and apoptotic cell death in cardiomyocytes (Yan et al., 2019).

Metabolic reprogramming is a feature of cancer cells. Two interesting papers showed how mitomiRs can promote chemotherapy resistance by inducing glycolysis in cancer cells. Nuclear-encoded mitomiR-2,392 and -5,787 are involved in reprogramming metabolism *via* increase of glycolysis and inhibition of OXPHOS, resulting in enhanced chemoresistance in tongue squamous cell carcinoma cells (Chen et al., 2019; Fan et al., 2019).

The mitomiR-mediated switch of energy sources during cellular differentiation suggests a pivotal role of mitomiRs in all processes requiring metabolic reprogramming, including cellular senescence (Sabbatinelli et al., 2019). Indeed, during senescence mitochondrial function declines, which creates an energy deficit. Retrograde signaling tries to overcome this energy deficit by increasing mitochondrial biogenesis as well as glycolysis, as a compensatory measure. However, this compensation is partial and accompanied by an increase in ROS production, thus creating a cycle of further damage to the mitochondria itself and to the cell.

Overall, we can conclude that mitomiRs can interact with mitochondrial genome in multiple ways: (i) as prompt compensators after a negative insult — e.g., miR-92a-2-5p and let-7b-5p, (ii) as effectors of mitochondrial dysfunction — e.g., miR-738-3p, (iii) as mediators of physiological cellular processes — e.g., miR-1.

SENESCENCE-ASSOCIATED miRNAs IMPACT ON MITOCHONDRIAL FUNCTION

Senescence associated-mitomiRs have been demonstrated to affect all aspects of mitochondrial homeostasis. While the role of SA-mitomiRs on the expression of mitochondrial genes has yet to be elucidated, multiple pieces of evidence support their ability in modulating several processes linked to mitochondrial function.

Through an *in silico* analysis we have suggested that SA-mitomiRs may affect endothelial cell sensitivity to apoptosis through Bcl2 family member regulation (Rippo et al., 2014).

Furthermore, we have recently demonstrated that miR-146a-5p, miR-34a and miR-181a levels are increased during replicative senescence of endothelial cells and enriched in senescent mitochondria. Their overexpression induces permeability transition pore opening, ROS production, caspase-1 and -3 activation and autophagic vacuole accumulation at least due to Bcl-2 downregulation (Giuliani et al., 2018).

MiR-146a is one of the most extensively studied miRNAs in the field of senescence and inflammation (Olivieri et al., 2013a,b) The synthesis of miR-146a is intimately linked to inflammatory processes and its effects on cellular processes are highly stimulus- and context-dependent. Indeed, miR-146a, which is particularly enriched in the mitochondrial fraction of cardiomyocytes, exerts a cardioprotective role by inhibiting the mitochondria-dependent apoptotic pathway and attenuating the loss of mitochondrial membrane potential. Evidence from cardiomyocyte-specific knockout and overexpression experiments supported the hypothesis that adequate miR-146a levels are required to reduce the extent of myocardial infarction and cardiac dysfunction following ischemia/reperfusion damage (Su et al., 2021). Notably, acute cellular damage can affect the trafficking of miRNAs between the mitochondrial and cytosolic compartments. Following a severe traumatic brain injury (TBI), miR-146a-5p levels decrease in the hippocampal mitochondrial fraction, in association with an increase of its cytosolic expression. This compartmental shift was shown to be triggered by decreased mitochondrial bioenergetics following TBI.

MiR-146a cytosolic enrichment avoids uncontrolled activation of the NF-kB pathway by targeting its upstream members TRAF6 and IRAK1. Mitochondria can act as first-line responders to cellular stressors by triggering pathways leading to altered nuclear gene expression, also by affecting miRNA intracellular localization (Wang et al., 2015, 2021). Interestingly, miR-146a-5p also impacts mitochondrial dynamics by targeting PARK2, one of proteins involved in mitophagy. Decreased amounts of PARK2 lead to the accumulation of damaged and dysfunctional mitochondria, which exacerbates the ROS-induced neuronal damage (Jauhari et al., 2020). Parkin 2 is a component of a multiprotein E3 ubiquitin ligase complex that mediates the targeting of substrates, including mitochondrial proteins, for proteasomal degradation and mitophagy. Interestingly, PARK2 mutations have been associated with early onset Parkinson's disease (Kitada et al., 1998). Besides its neuroprotective and cardioprotective function, a role in liver homeostasis has been demonstrated for miR-146a. Its hepatocyte expression is needed to promote the mitochondrial oxidation of fatty acids and improve insulin sensitivity, which prevents the detrimental lipid accumulation in the liver. These effects are achieved by promoting both mitochondrial biogenesis and synthesis of electron transport chain complex subunits through targeting of MED1, a component of the mammalian mediator complex involved in adipogenesis and mitochondrial gene expression (Li et al., 2020). Moreover, bioinformatic analysis identified multiple miR-146a potential targets in mitochondrial genome, suggesting there is still much to uncover about the crosstalk between miR-146a and bioenergetic pathways (Dasgupta et al., 2015; Giuliani et al., 2017).

MiR-34a-5p has been implicated in the pathogenesis of ARDs accompanied by mitochondrial dysfunction and impairment of the autophagic flux, such as neurodegenerative disorders. MiR-34a-5p targets PINK1, a stress sensor that localizes to the outer mitochondrial membrane following the loss of mitochondrial potential. This triggers mitochondrial clearance. Similarly to PARK2, also PINK1 mutations have been involved in the pathogenesis of early onset Parkinson's disease. In this framework, overexpression of miR-34a-5p attenuates mitochondrial protein ubiquitination and prevents the recruitment of PARK2, thus delaying mitophagy (Tai et al., 2021). One of the main targets of miR-34a with a well-established role in aging is SIRT1. The rescue of SIRT1 levels following miR-34a inhibition reduced age-related hearing loss in C57BL/6 mice. Although the full signaling pathway responsible for this effect has still to be elucidated, the miR-34a/SIRT1 axis was hypothesized to affect the balance between mitophagy and mitochondrial biogenesis and to protect cochlear cells against oxidative stress-mediated apoptosis (Xiong et al., 2019). MiR-34a was also shown to accelerate renal aging by affecting the mitochondrial function of mesangial cells. MiR-34a targets the mRNA of thioredoxin reductase 2, a protein involved in the scavenging and detoxification of mitochondrial ROS. The levels of miR-34a were particularly high in senescent mesangial cells and, at the same time, miR-34a overexpression induced premature senescence in these cells due to the accumulation of dysfunctional mitochondria (Bai et al., 2011).

The link between mitochondrial function and miR-181a has been elucidated in multiple cellular models (Mancini et al., 2012; Indrieri et al., 2020). Interestingly, miR-181a is among the most characterized miRNAs in lymphoid tissue, with a well-documented role in T cell aging and immune senescence (Ye et al., 2018; Kim et al., 2021). The age-related decline in miR-181a expression in naive and memory T cells may account for some of the age-associated defects in T cell function. To this regard, restoration of miR-181a intracellular levels provided a feasible strategy to boost T cell response in the elderly (Li et al., 2012; Ye et al., 2018, 2021). Recently, it also has been shown a decline of miR-181a-5p in NK cells from the aged mice, impairing the production of IFN-γ (Lu et al., 2021). Moreover, miR-181a shows an age-dependent decline in peripheral blood mononuclear cells from donors of different ages (Xu et al., 2020). Similarly to miR-34a, miR-181a is a regulator of mitochondrial dynamics through the action on several proteins implied in the mitophagy process. Restoration of the expression of miR-181a in the skeletal muscle of old mice improved mitochondrial quality (Goljanek-Whysall et al., 2020). The prominent role of miR-181a-5p in age muscle homeostasis was elegantly reviewed by Borja-Gonzalez and colleagues (Borja-Gonzalez et al., 2020). MiR-181a is closely associated to inflammation and apoptosis in neuronal cells, where it targets mitochondria-related proteins, i.e., heat shock protein 70, glucose regulated protein 78, anti-apoptotic Bcl-2, and myeloid cell leukemia-1 (Ouyang et al., 2012; Hutchison et al., 2013).

MiR-210 is considered the master hypoxia-related miR, because of its prompt upregulation under hypoxia in most

TABLE 1 | Shows senescence-associated mitomiR targets.

SA-mitomiRs	Cytosolic target	Effect on senescence-related pathways	Mt-DNA target	Effect on mitochondrial functions
miR-21-5p	-NFIB and CDC25A (Dellago et al., 2013) -TLR8 (ligand; Zhang et al., 2018) -A20 (Xue et al., 2019) -PTEN (Buscaglia and Li, 2011; Ma et al., 2013) -PDCD4 (Matsuhashi et al., 2019)	-Cell proliferation arrest-Pro-inflammatory cytokine production-Activation of NF- κB pathway and NLRP3 inflammasome	-mt-Cyb (Li et al., 2016)	-enhanced mitochondrial translation
miR-146a-5p	-TLR4 (Xiao et al., 2019) -TRAF6 (Taganov et al., 2006) -IRAK1 (Taganov et al., 2006) -BCL2 (Giuliani et al., 2018)	-Pro-inflammatory cytokine production-Apoptosis sensitivity alteration-Activation of NF-κB pathway	-mt-ND1, mt-ND2, mt-ND4, mt-ND5, mt-ND6; -mt-ATP8 (PREDICTED; Dasgupta et al., 2015)	
miR-181a-5p	-SIRT1 (Di Val Cervo et al., 2012) -BCL2 (Giuliani et al., 2018) -PARK2 and p62/SQSTM1 (Goljanek-Whysall et al., 2020)	-Cell proliferation arrest-Apoptosis sensitivity alteration-Impaired autophagy		
miR-210	-NDUFA4 and SDHD (Puisségur et al., 2011) -ISCU1/2 (Chan et al., 2009)-RAD52 (Crosby et al., 2009) -E2F3 (Biswas et al., 2010)	-Mitochondrial dysfunction-DNA repair loss - Cell proliferation arrest		
miR-34a	-SIRT1/P53 axis-BCL2 (Giuliani et al., 2018) -Txnrd2 (Bai et al., 2011)	-Apoptosis sensitivity alteration-Cell proliferation arrest-Pro-inflammatory cytokine production-Increased oxidative stress		

Tumor necrosis factor, alpha-induced protein 3(A20); B-cell lymphoma 2 (Bcl-2); Cell division cycle 25 A(CDC25A); E2F transcription factor 3 (E2F3); Interleukin 1 Receptor Associated Kinase 1 (IRAK1); Iron–sulfur cluster assembly enzyme (ISCU); mtDNA-encoded cytochrome b (mt-Cytb); Nuclear factor 1 B-type (NFIB); Phosphatase and tensin homolog (PTEN); succinate dehydrogenase complex subunit D (SDHD); Sirtuin 1 (SIRT1); Sequestosome-1 (SQSTM1); Toll like receptor (TLR); TNF Receptor Associated Factor 6 (TRAF6); Thioredoxin Reductase 2 (Txnrd2).

cell types. MiR-210 is upregulated in senescent cells where it is involved in double-strand DNA breaks and ROS accumulation (Faraonio et al., 2012) *via* the inhibition of the electron transport chain (ETC) protein translation (Karshovska et al., 2019). MiR-210 directly targets NDUFA4 and SDHD — subunits of the ETC complex I and II, respectively — and induces mitochondrial dysfunction (Puisségur et al., 2011). Future studies are warranted to unravel its specific activity in mitochondrial function.

MiR-21, initially classified as an 'onco-miR' due to its modulation in different types of cancer, has an extensively established role in inflammatory and senescence processes (Olivieri et al., 2021). Increased expression of miR-21-5p was found in replicative and stress-induced models of senescence (Dellago et al., 2013; Mensà et al., 2020).

A particular myocardial enrichment of miR-21-5p has been observed in several models of cardiovascular disease, cardiac dysfunction, and heart failure, where it has been reported to prevent cardiomyocyte apoptosis by targeting the PDCD4 mRNA (Qin et al., 2012). *In vivo* silencing of miR-21, using a specific antagomir, has been found to attenuate cardiac fibrosis and cardiac dysfunction in pressure-overloaded hearts (Thum et al., 2008). Overexpression of miR-21 decreases mitochondrial fatty acid oxidation and concomitant mitochondrial respiration in rat cardiomyocytes, suggesting that miR-21 coordinates the shifting of cellular metabolism towards the glycolytic pathway (Nasci et al., 2019). This hypothesis was later confirmed by the evidence that miR-21 is able to translocate into the mitochondria and target mt-Cyb to enhance its translation in a spontaneous hypertensive rat model (Li et al., 2016). Moreover, miR-21-5p affects mitochondrial dynamics in a model of oxidized LDL-induced endothelial cell senescence by targeting Drp1 protein (Zhang et al., 2017).

Although miR-21 is also involved in several mitochondrial functions, the precise role of miR-21 in senescent mitochondria is far from being elucidated. **Table 1** summarizes the mitomiR targets with a well-recognized role on senescence. The involved pathways are functional to the acquisition of the senescent phenotype, including cell cycle arrest, mitochondrial dysfunction, and production of pro-inflammatory cytokines, that is, SASP.

CONCLUSION

The central role of mitochondria in cellular senescence is now a dogma recognized by all gerontologists in the world. Many biochemical and morphological changes to which these organelles meet are common to both stress-induced or replicative senescence: branching and elongation, ROS production, mtDNA mutations and membrane depolarization. Several of these phenomena are due to the sophisticated communication system (anterograde and retrograde signaling) between the nucleus and the mitochondrion. While an increasing number of research reports are shedding light on the anterograde signaling routes, retrograde signaling mechanisms are almost completely unknown although there is the certainty that they play important roles. Nuclear-encoded miRNAs shuttle within mitochondria, and at the epigenetic level, regulate both mt-DNA encoded proteins and those encoded by nuclear genes that are functional in mitochondria.

Since the mitochondrial alterations observed in the senescent cells represent etiopathogenetic factors in age-associated diseases, the deepening of the communication routes between nucleus

and mitochondria may lead to devise new preventive and therapeutic strategies.

AUTHOR CONTRIBUTIONS

CG, AS, and AG performed literature search, drafted the manuscript and prepared the figure. MR conceived the idea and participated in manuscript drafting. FO reviewed the manuscript. All authors approved the final version of the manuscript.

FUNDING

The present work has been supported by grants from Università Politecnica delle Marche, Italy to MR.

REFERENCES

Amartuvshin, O., Lin, C. H., Hsu, S. C., Kao, S. H., Chen, A., Tang, W. C., et al. (2020). Aging shifts mitochondrial dynamics toward fission to promote germline stem cell loss. *Aging Cell* 19:e13191. doi: 10.1111/acel.13191

Badr, H., Carmaack, C. L., Kashy, D. A., and Cristofanilli, M. (2014). 基因的改变NIH public access. *Bone* 23, 1–7.

Bai, X. Y., Ma, Y., Ding, R., Fu, B., Shi, S., and Chen, X. M. (2011). miR-335 and miR-34a promote renal senescence by suppressing mitochondrial antioxidative enzymes. *J. Am. Soc. Nephrol.* 22, 1252–1261. doi: 10.1681/ASN.2010040367

Bandiera, S., Matégot, R., Girard, M., Demongeot, J., and Henrion-Caude, A. (2013). MitomiRs delineating the intracellular localization of microRNAs at mitochondria. *Free Radic. Biol. Med.* 64, 12–19. doi: 10.1016/j.freeradbiomed.2013.06.013

Bandiera, S., Rüberg, S., Girard, M., Cagnard, N., Hanein, S., Chrétien, D., et al. (2011). Nuclear outsourcing of RNA interference components to human mitochondria. *PLoS One* 6:e20746. doi: 10.1371/journal.pone.0020746

Bartel, D. P. (2004). MicroRNAs: genomics, biogenesis, mechanism, and function. *Cell* 116, 281–297. doi: 10.1016/S0092-8674(04)00045-5

Bhatti, J. S., Bhatti, G. K., and Reddy, P. H. (2017). Mitochondrial dysfunction and oxidative stress in metabolic disorders — A step towards mitochondria based therapeutic strategies. *Biochim. Biophys. Acta Mol. basis Dis.* 1863, 1066–1077. doi: 10.1016/j.bbadis.2016.11.010

Biswas, S., Roy, S., Banerjee, J., Hussain, S. R. A., Khanna, S., Meenakshisundaram, G., et al. (2010). Hypoxia inducible microRNA 210 attenuates keratinocyte proliferation and impairs closure in a murine model of ischemic wounds. *Proc. Natl. Acad. Sci. U. S. A.* 107, 6976–6981. doi: 10.1073/pnas.1001653107

Blumental-Perry, A., Jobava, R., Bederman, I., Degar, A. J., Kenche, H., Guan, B. J., et al. (2020). Retrograde signaling by a mtDNA-encoded non-coding RNA preserves mitochondrial bioenergetics. *Commun. Biol.* 3:626. doi: 10.1038/s42003-020-01322-4

Borgna, V., Lobos-González, L., Guevara, F., Landerer, E., Bendek, M., Ávila, R., et al. (2020). Targeting antisense mitochondrial noncoding RNAs induces bladder cancer cell death and inhibition of tumor growth through reduction of survival and invasion factors. *J. Cancer* 11, 1780–1791. doi: 10.7150/jca.38880

Borja-Gonzalez, M., Casas-Martinez, J. C., McDonagh, B., and Goljanek-Whysall, K. (2020). Aging science talks: the role of miR-181a in age-related loss of muscle mass and function. *Transl. Med. Aging* 4, 81–85. doi: 10.1016/j.tma.2020.07.001

Borralho, P. M., Rodrigues, C. M. P., and Steer, C. J. (2014). Mitochondrial MicroRNAs and their potential role in cell function. *Curr. Pathobiol. Rep.* 2, 123–132. doi: 10.1007/s40139-014-0047-x

Burzio, V. A., Villota, C., Villegas, J., Landerer, E., Boccardo, E., Villa, L. L., et al. (2009). Expression of a family of noncoding mitochondrial RNAs distinguishes normal from cancer cells. *Proc. Natl. Acad. Sci. U. S. A.* 106, 9430–9434. doi: 10.1073/pnas.0903086106

Buscaglia, L. E. B., and Li, Y. (2011). Apoptosis and the target genes of microRNA-21. *Chin. J. Cancer* 30, 371–380. doi: 10.5732/cjc.30.0371

Cardamone, M. D., Tanasa, B., Cederquist, C., and Huang, J. (2017). Mitochondrial Retrograde Signaling in Mammals Is Mediated by the Transcriptional Cofactor GPS2 via Direct Mitochondria-to-Nucleus Translocation. *Mol. Cell* 69, 757–772.e7. doi: 10.1016/j.molcel.2018.01.037

Carelli, V., and Chan, D. C. (2014). Mitochondrial DNA: impacting central and peripheral nervous systems. *Urology* 84, 1126–1142. doi: 10.1016/j.neuron.2014.11.022

Carrer, M., Liu, N., Grueter, C. E., Williams, A. H., Frisard, M. I., Hulver, M. W., et al. (2012). Control of mitochondrial metabolism and systemic energy homeostasis by microRNAs 378 and 378*. *Proc. Natl. Acad. Sci. U. S. A.* 109, 15330–15335. doi: 10.1073/pnas.1207605109

Chan, S. Y., Zhang, Y. Y., Hemann, C., Mahoney, C. E., Zweier, J. L., and Loscalzo, J. (2009). MicroRNA-210 controls mitochondrial metabolism during hypoxia by repressing the iron-sulfur cluster assembly proteins ISCU1/2. *Cell Metab.* 10, 273–284. doi: 10.1016/j.cmet.2009.08.015

Chapman, J., Fielder, E., and Passos, J. F. (2019). Mitochondrial dysfunction and cell senescence: deciphering a complex relationship. *FEBS Lett.* 593, 1566–1579. doi: 10.1002/1873-3468.13498

Chen, J. F., Mandel, E. M., Thomson, J. M., Wu, Q., Callis, T. E., Hammond, S. M., et al. (2006). The role of microRNA-1 and microRNA-133 in skeletal muscle proliferation and differentiation. *Nat. Genet.* 38, 228–233. doi: 10.1038/ng1725

Chen, W., Wang, P., Lu, Y., Jin, T., Lei, X., Liu, M., et al. (2019). Decreased expression of mitochondrial mir-5787 contributes to chemoresistance by reprogramming glucose metabolism and inhibiting MT-CO3 translation. *Theranostics* 9, 5739–5754. doi: 10.7150/thno.37556

Conte, M., Sabbatinelli, J., Chiariello, A., Martucci, M., Santoro, A., Monti, D., et al. (2021). Disease-specific plasma levels of mitokines FGF21, GDF15, and Humanin in type II diabetes and Alzheimer's disease in comparison with healthy aging. *GeroScience* 43, 985–1001. doi: 10.1007/s11357-020-00287-w

Coppé, J. P., Patil, C. K., Rodier, F., Sun, Y., Muñoz, D. P., Goldstein, J., et al. (2008). Senescence-associated secretory phenotypes reveal cell-nonautonomous functions of oncogenic RAS and the p53 tumor suppressor. *PLoS Biol.* 6, 2853–2868. doi: 10.1371/journal.pbio.0060301

Correia-Melo, C., Ichim, G., Tait, S. W. G., and Passos, J. F. (2017). Depletion of mitochondria in mammalian cells through enforced mitophagy. *Nat. Protoc.* 12, 183–194. doi: 10.1038/nprot.2016.159

Crosby, M. E., Kulshreshtha, R., Ivan, M., and Glazer, P. M. (2009). MicroRNA regulation of DNA repair gene expression in hypoxic stress. *Cancer Res.* 69, 1221–1229. doi: 10.1158/0008-5472.CAN-08-2516

Das, S., Bedja, D., Campbell, N., Dunkerly, B., Chenna, V., Maitra, A., et al. (2014). miR-181c regulates the mitochondrial genome, bioenergetics, and propensity for heart failure in vivo. *PLoS One* 9:e96820. doi: 10.1371/journal.pone.0096820

Das, S., Ferlito, M., Kent, O. A., Fox-Talbot, K., Wang, R., Liu, D., et al. (2012). Nuclear miRNA regulates the mitochondrial genome in the heart. *Circ. Res.* 110, 1596–1603. doi: 10.1161/CIRCRESAHA.112.267732

Das, S., Kohr, M., Dunkerly-Eyring, B., Lee, D. I., Bedja, D., Kent, O. A., et al. (2017). Divergent effects of miR-181 family members on myocardial function through protective cytosolic and detrimental mitochondrial microRNA targets. *J. Am. Heart Assoc.* 6:e004694. doi: 10.1161/JAHA.116.004694

Dasgupta, N., Peng, Y., Tan, Z., Ciraolo, G., Wang, D., and Li, R. (2015). miRNAs in mtDNA-less cell mitochondria. *Cell Death Dis.* 1:150024. doi: 10.1038/cddiscovery.2015.4

Dellago, H., Preschitz-Kammerhofer, B., Terlecki-Zaniewicz, L., Schreiner, C., Fortschegger, K., Chang, M. W. F., et al. (2013). High levels of oncomiR-21 contribute to the senescence-induced growth arrest in normal human cells and its knock-down increases the replicative lifespan. *Aging Cell* 12, 446–458. doi: 10.1111/acel.12069

Di Val Cervo, P. R., Lena, A. M., Nicoloso, M., Rossi, S., Mancini, M., Zhou, H., et al. (2012). p63-microRNA feedback in keratinocyte senescence. *Proc. Natl. Acad. Sci. U. S. A.* 109, 1133–1138. doi: 10.1073/pnas.1112257109

Fafián-Labora, J. A., and O'Loghlen, A. (2020). Classical and nonclassical intercellular communication in senescence and ageing. *Trends Cell Biol.* 30, 628–639. doi: 10.1016/j.tcb.2020.05.003

Fan, S., Tian, T., Chen, W., Lv, X., Lei, X., Zhang, H., et al. (2019). Mitochondrial miRNA determines chemoresistance by reprogramming metabolism and regulating mitochondrial transcription. *Cancer Res.* 79, 1069–1084. doi: 10.1158/0008-5472.CAN-18-2505

Faraonio, R., Salerno, P., Passaro, F., Sedia, C., Iaccio, A., Bellelli, R., et al. (2012). A set of miRNAs participates in the cellular senescence program in human diploid fibroblasts. *Cell Death Differ.* 19, 713–721. doi: 10.1038/cdd.2011.143

Franceschi, C., Bonafè, M., Valensin, S., Olivieri, F., De Luca, M., Ottaviani, E., et al. (2000). Inflamm-aging:An evolutionary perspective on immunosenescence. *Ann. N. Y. Acad. Sci.* 908, 244–254. doi: 10.1111/j.1749-6632.2000.tb06651.x

Gammage, P. A., Moraes, C. T., and Minczuk, M. (2018). Mitochondrial genome engineering: the revolution may not be CRISPR-Ized. *Trends Genet.* 34, 101–110. doi: 10.1016/j.tig.2017.11.001

Gibbings, D. J., Ciaudo, C., Erhardt, M., and Voinnet, O. (2009). Multivesicular bodies associate with components of miRNA effector complexes and modulate miRNA activity. *Nat. Cell Biol.* 11, 1143–1149. doi: 10.1038/ncb1929

Giuliani, A., Cirilli, I., Prattichizzo, F., Mensà, E., Fulgenzi, G., Sabbatinelli, J., et al. (2018). The mitomiR/Bcl-2 axis affects mitochondrial function and autophagic vacuole formation in senescent endothelial cells. *Aging* 10, 2855–2873. doi: 10.18632/aging.101591

Giuliani, A., Londin, E., Ferracin, M., Mensà, E., Prattichizzo, F., Ramini, D., et al. (2020). Long-term exposure of human endothelial cells to metformin modulates miRNAs and isomiRs. *Sci. Rep.* 10:21782. doi: 10.1038/s41598-020-78871-5

Giuliani, A., Micolucci, L., Olivieri, F., Procopio, A. D., and Rippo, M. R. (2019). "MitomiRs in Human Inflamm-Aging," in *Handbook of Immunosenescence*. eds. T. Fulop, C. Franceschi, K. Hirokawa and G. Pawelec (Springer: Cham), 1681–1708.

Giuliani, A., Prattichizzo, F., Micolucci, L., Ceriello, A., Procopio, A. D., and Rippo, M. R. (2017). Mitochondrial (Dys) function in Inflammaging: do MitomiRs influence the energetic, oxidative, and inflammatory status of senescent cells? *Mediat. Inflamm.* 2017:2309034. doi: 10.1155/2017/2309034

Goljanek-Whysall, K., Soriano-Arroquia, A., McCormick, R., Chinda, C., and McDonagh, B. (2020). miR-181a regulates p62/SQSTM1, parkin, and protein DJ-1 promoting mitochondrial dynamics in skeletal muscle aging. *Aging Cell* 19:e13140. doi: 10.1111/acel.13140

Gusic, M., and Prokisch, H. (2020). ncRNAs: new players in mitochondrial health and disease? *Front. Genet.* 11:95. doi: 10.3389/fgene.2020.00095

Ha, M., and Kim, V. N. (2014). Regulation of microRNA biogenesis. *Nat. Rev. Mol. Cell Biol.* 15, 509–524. doi: 10.1038/nrm3838

Hales, K. G. (2010). Iron testes: sperm mitochondria as a context for dissecting iron metabolism. *BMC Biol.* 8:79. doi: 10.1186/1741-7007-8-79

Hewitt, G., Jurk, D., Marques, F. D. M., Correia-Melo, C., Hardy, T., Gackowska, A., et al. (2012). Telomeres are favoured targets of a persistent DNA damage response in ageing and stress-induced senescence. *Nat. Commun.* 3:708. doi: 10.1038/ncomms1708

Hock, M. B., and Kralli, A. (2009). Transcriptional control of mitochondrial biogenesis and function. *Annu. Rev. Physiol.* 71, 177–203. doi: 10.1146/annurev.physiol.010908.163119

Hoshino, A., Mita, Y., Okawa, Y., Ariyoshi, M., Iwai-Kanai, E., Ueyama, T., et al. (2013). Cytosolic p53 inhibits Parkin-mediated mitophagy and promotes mitochondrial dysfunction in the mouse heart. *Nat. Commun.* 4:2308. doi: 10.1038/ncomms3308

Huang, L., Mollet, S., Souquere, S., Le Roy, F., Ernoult-Lange, M., Pierron, G., et al. (2011). Mitochondria associate with P-bodies and modulate microRNA-mediated RNA interference. *J. Biol. Chem.* 286, 24219–24220. doi: 10.1074/jbc.M111.240259

Hutchison, E. R., Kawamoto, E. M., Taub, D. D., Lal, A., Abdelmohsen, K., Zhang, Y., et al. (2013). Evidence for miR-181 involvement in neuroinflammatory responses of astrocytes. *Glia* 61, 1018–1028. doi: 10.1002/glia.22483

Hutter, E., Renner, K., Pfister, G., Stöckl, P., Jansen-Dürr, P., and Gnaiger, E. (2004). Senescence-associated changes in respiration and oxidative phosphorylation in primary human fibroblasts. *Biochem. J.* 380, 919–928. doi: 10.1042/bj20040095

Indrieri, A., Carrella, S., Carotenuto, P., Banfi, S., and Franco, B. (2020). The pervasive role of the MiR-181 family in development, neurodegeneration, and cancer. *Int. J. Mol. Sci.* 21:2092. doi: 10.3390/ijms21062092

Jagannathan, R., Thapa, D., Nichols, C. E., Shepherd, D. L., Stricker, J. C., Croston, T. L., et al. (2015). Translational regulation of the mitochondrial genome following redistribution of mitochondrial MicroRNA in the diabetic heart. *Circ. Cardiovasc. Genet.* 8, 785–802. doi: 10.1161/CIRCGENETICS.115.001067

Jakobsson, T., Venteclef, N., Toresson, G., Damdimopoulos, A. E., Ehrlund, A., Lou, X., et al. (2009). GPS2 is required for cholesterol efflux by triggering histone demethylation, LXR recruitment, and Coregulator assembly at the ABCG1 locus. *Mol. Cell* 34, 510–518. doi: 10.1016/j.molcel.2009.05.006

Jannot, G., Michaud, P., Quévillon Huberdeau, M., Morel-Berryman, L., Brackbill, J. A., Piquet, S., et al. (2016). GW182-free microRNA silencing complex controls post-transcriptional gene expression during Caenorhabditis elegans embryogenesis. *PLoS Genet.* 12:e1006484. doi: 10.1371/journal.pgen.1006484

Jauhari, A., Singh, T., Mishra, S., Shankar, J., and Yadav, S. (2020). Coordinated action of miR-146a and parkin gene regulate rotenone-induced neurodegeneration. *Toxicol. Sci.* 176, 433–445. doi: 10.1093/toxsci/kfaa066

Jazwinski, S. M., and Kriete, A. (2012). The yeast retrograde response as a model of intracellular signaling of mitochondrial dysfunction. *Front. Physiol.* 3:139. doi: 10.3389/fphys.2012.00139

Jusic, A., and Devaux, Y. (2020). Mitochondrial noncoding RNA-regulatory network in cardiovascular disease. *Basic Res. Cardiol.* 115:23. doi: 10.1007/s00395-020-0783-5

Karshovska, E., Wei, Y., Subramanian, P., Mohibullah, R., Geißler, C., Baatsch, I., et al. (2019). HIF-1α (hypoxia-inducible factor-1α) promotes macrophage necroptosis by regulating miR-210 and miR-383. *Arterioscler. Thromb. Vasc. Biol.* 40, 583–596. doi: 10.1161/ATVBAHA.119.313290

Kazlauskaite, A., and Muqit, M. M. K. (2015). PINK1 and Parkin - mitochondrial interplay between phosphorylation and ubiquitylation in Parkinson's disease. *FEBS J.* 282, 215–223. doi: 10.1111/febs.13127

Kim, S., and Koh, H. (2017). Role of FOXO transcription factors in crosstalk between mitochondria and the nucleus. *J. Bioenerg. Biomembr.* 49, 335–341. doi: 10.1007/s10863-017-9705-0

Kim, S. J., Mehta, H. H., Wan, J., Kuehnemann, C., Chen, J., Fan, J., et al. (2018). Mitochondrial peptides modulate mitochondrial function during cellular senescence. *Aging* 10, 1239–1256. doi: 10.18632/aging.101463

Kim, C., Ye, Z., Weyand, C. M., and Goronzy, J. J. (2021). miR-181a-regulated pathways in T-cell differentiation and aging. *Immun. Ageing* 18:28. doi: 10.1186/s12979-021-00240-1

Kitada, T., Asakawa, S., Hattori, N., Matsumine, H., Yamamura, Y., Minoshima, S., et al. (1998). Mutations in the parkin gene cause autosomal recessive juvenile parkinsonism. *Nature* 392, 605–608. doi: 10.1038/33416

Kren, B. T., Wong, P. Y. P., Sarver, A., Zhang, X., Zeng, Y., and Steer, C. J. (2009). microRNAs identified in highly purified liver-derived mitochondria may play a role in apoptosis. *RNA Biol.* 6, 65–72. doi: 10.4161/rna.6.1.7534

Krist, B., Florczyk, U., Pietraszek-Gremplewicz, K., Józkowicz, A., and Dulak, J. (2015). The role of miR-378a in metabolism, angiogenesis, and muscle biology. *Int. J. Endocrinol.* 2015:281756. doi: 10.1155/2015/281756

Kumari, R., and Jat, P. (2021). Mechanisms of cellular senescence: cell cycle arrest and senescence associated secretory phenotype. *Front. Cell Dev. Biol.* 9:645593. doi: 10.3389/fcell.2021.645593

Landerer, E., Villegas, J., Burzio, V. A., Oliveira, L., Villota, C., Lopez, C., et al. (2011). Nuclear localization of the mitochondrial ncRNAs in normal and cancer cells. *Cell. Oncol.* 34, 297–305. doi: 10.1007/s13402-011-0018-8

Larriba, E., Rial, E., and del Mazo, J. (2018). The landscape of mitochondrial small non-coding RNAs in the PGCs of male mice, spermatogonia, gametes and in zygotes. *BMC Genomics* 19:634. doi: 10.1186/s12864-018-5020-3

Leucci, E., Vendramin, R., Spinazzi, M., Laurette, P., Fiers, M., Wouters, J., et al. (2016). Melanoma addiction to the long non-coding RNA SAMMSON. *Nature* 531, 518–522. doi: 10.1038/nature17161

Li, H., Dai, B., Fan, J., Chen, C., Nie, X., Yin, Z., et al. (2019). The different roles of miRNA-92a-2-5p and let-7b-5p in mitochondrial translation in db/db mice. *Mol. Ther. Nucleic Acids* 17, 424–435. doi: 10.1016/j.omtn.2019.06.013

Li, G., Yu, M., Lee, W. W., Tsang, M., Krishnan, E., Weyand, C. M., et al. (2012). Decline in miR-181a expression with age impairs T cell receptor sensitivity by increasing DUSP6 activity. *Nat. Med.* 18, 1518–1524. doi: 10.1038/nm.2963

Li, H., Zhang, X., Wang, F., Zhou, L., Yin, Z., Fan, J., et al. (2016). MicroRNA-21 lowers blood pressure in spontaneous hypertensive rats by upregulating mitochondrial translation. *Circulation* 134, 734–751. doi: 10.1161/CIRCULATIONAHA.116.023926

Li, K., Zhao, B., Wei, D., Wang, W., Cui, Y., Qian, L., et al. (2020). MiR-146a improves hepatic lipid and glucose metabolism by targeting MED1. *Int. J. Mol. Med.* 45, 543–555. doi: 10.3892/ijmm.2019.4443

López-Otín, C., Blasco, M. A., Partridge, L., Serrano, M., and Kroemer, G. (2013). The hallmarks of aging. *Cell* 153, 1194–1217. doi: 10.1016/j.cell.2013.05.039

Lorenz, E. N. (1972). The central program of the 1972 AAAS annual meeting. *Science* 178, 886–914. doi: 10.1126/science.178.4063.886

Lu, J., Li, S., Li, X., Zhao, W., Duan, X., Gu, X., et al. (2021). Declined miR-181a-5p expression is associated with impaired natural killer cell development and function with aging. *Aging Cell* 20:e13353. doi: 10.1111/acel.13353

Lung, B., Zemann, A., Madej, M. J., Schuelke, M., Techritz, S., Ruf, S., et al. (2006). Identification of small non-coding RNAs from mitochondria and chloroplasts. *Nucleic Acids Res.* 34, 3842–3852. doi: 10.1093/nar/gkl448

Ma, X., Choudhury, S. N., Hua, X., Dai, Z., and Li, Y. (2013). Interaction of the oncogenic miR-21 microRNA and the p53 tumor suppressor pathway. *Carcinogenesis* 34, 1216–1223. doi: 10.1093/carcin/bgt044

Mai, S., Klinkenberg, M., Auburger, G., Bereiter-Hahn, J., and Jendrach, M. (2010). Decreased expression of Drp1 and Fis1 mediates mitochondrial elongation in senescent cells and enhances resistance to oxidative stress through PINK1. *J. Cell Sci.* 123, 917–926. doi: 10.1242/jcs.059246

Mancini, M., Saintigny, G., Mahé, C., Annicchiarico-Petruzzelli, M., Melino, G., and Candi, E. (2012). MicroRNA-152 and -181a participate in human dermal fibroblasts senescence acting on cell adhesion and remodeling of the extracellular matrix. *Aging* 4, 843–853. doi: 10.18632/aging.100508

Manzella, N., Santin, Y., Maggiorani, D., Martini, H., Douin-Echinard, V., Passos, J. F., et al. (2018). Monoamine oxidase-A is a novel driver of stress-induced premature senescence through inhibition of parkin-mediated mitophagy. *Aging Cell* 17:e12811. doi: 10.1111/acel.12811

Mariani, M., Mattiucci, D., Rossi, E., Mari, V., Masala, E., Giuliani, A., et al. (2020). Serum Inflamma-miR signature: a biomarker of myelodysplastic syndrome? *Front. Oncol.* 10:595838. doi: 10.3389/fonc.2020.595838

Matsuhashi, S., Manirujjaman, M., Hamajima, H., and Ozaki, I. (2019). Control mechanisms of the tumor suppressor PDCD4: expression and functions. *Int. J. Mol. Sci.* 20:2304. doi: 10.3390/ijms20092304

Mensà, E., Guescini, M., Giuliani, A., Bacalini, M. G., Ramini, D., Corleone, G., et al. (2020). Small extracellular vesicles deliver miR-21 and miR-217 as pro-senescence effectors to endothelial cells. *J. Extracell. Vesicles* 9:1725285. doi: 10.1080/20013078.2020.1725285

Nargund, A. M., Fiorese, C. J., Pellegrino, M. W., Deng, P., and Haynes, C. M. (2015). Mitochondrial and nuclear accumulation of the transcription factor ATFS-1 promotes OXPHOS recovery during the UPRmt. *Mol. Cell* 58, 123–133. doi: 10.1016/j.molcel.2015.02.008

Nargund, A., Pellegrino, M. W., Fiorese, C. J., Baker, B. M., and Haynes, C. M. (2012). Mitochondrial import efficiency of ATFS-1 regulates mitochondrial UPR activation. *Science* 337, 587–590. doi: 10.1126/science.1223560

Nasci, V. L., Chuppa, S., Griswold, L., Goodreau, K. A., Dash, R. K., and Kriegel, A. J. (2019). Mir-21-5p regulates mitochondrial respiration and lipid content in h9c2 cells. *Am. J. Physiol. Heart Circ. Physiol.* 316, H710–H721. doi: 10.1152/ajpheart.00538.2017

Nunnari, J., and Suomalainen, A. (2012). Mitochondria: In sickness and in health. *Cell* 148, 1145–1159. doi: 10.1016/j.cell.2012.02.035

Olivieri, F., Lazzarini, R., Babini, L., Prattichizzo, F., Rippo, M. R., Tiano, L., et al. (2013a). Anti-inflammatory effect of ubiquinol-10 on young and senescent endothelial cells via miR-146a modulation. *Free Radic. Biol. Med.* 63, 410–420. doi: 10.1016/j.freeradbiomed.2013.05.033

Olivieri, F., Lazzarini, R., Recchioni, R., Marcheselli, F., Rippo, M. R., Di Nuzzo, S., et al. (2013b). MiR-146a as marker of senescence-associated pro-inflammatory status in cells involved in vascular remodelling. *Age* 35, 1157–1172. doi: 10.1007/s11357-012-9440-8

Olivieri, F., Prattichizzo, F., Giuliani, A., Matacchione, G., Rippo, M. R., Sabbatinelli, J., et al. (2021). miR-21 and miR-146a: the microRNAs of inflammaging and age-related diseases. *Ageing Res. Rev.* 70:101374. doi: 10.1016/j.arr.2021.101374

Ouyang, Y. B., Lu, Y., Yue, S., Xu, L. J., Xiong, X. X., White, R. E., et al. (2012). MiR-181 regulates GRP78 and influences outcome from cerebral ischemia in vitro and in vivo. *Neurobiol. Dis.* 45, 555–563. doi: 10.1016/j.nbd.2011.09.012

Passos, J. F., Saretzki, G., Ahmed, S., Nelson, G., Richter, T., Peters, H., et al. (2007). Mitochondrial dysfunction accounts for the stochastic heterogeneity in telomere-dependent senescence. *PLoS Biol.* 5:e110. doi: 10.1371/journal.pbio.0050110

Picard, M., Shirihai, O. S., Gentil, B. J., and Burelle, Y. (2013). Mitochondrial morphology transitions and functions: implications for retrograde signaling? *Am. J. Phys. Regul. Integr. Comp. Phys.* 304, R393–R406. doi: 10.1152/ajpregu.00584.2012

Prattichizzo, F., De Nigris, V., Sabbatinelli, J., Giuliani, A., Castaño, C., Párrizas, M., et al. (2021). CD31+ extracellular vesicles From patients With type 2 diabetes shuttle a miRNA signature associated With cardiovascular complications. *Diabetes* 70, 240–254. doi: 10.2337/db20-0199

Puisségur, M. P., Mazure, N. M., Bertero, T., Pradelli, L., Grosso, S., Robbe-Sermesant, K., et al. (2011). MiR-210 is overexpressed in late stages of lung cancer and mediates mitochondrial alterations associated with modulation of HIF-1 activity. *Cell Death Differ.* 18, 465–478. doi: 10.1038/cdd.2010.119

Qin, Y., Yu, Y., Dong, H., Bian, X., Guo, X., and Dong, S. (2012). MicroRNA 21 inhibits left ventricular remodeling in the early phase of rat model with ischemia-reperfusion injury by suppressing cell apoptosis. *Int. J. Med. Sci.* 9, 413–423. doi: 10.7150/ijms.4514

Quirós, P. M., Mottis, A., and Auwerx, J. (2016). Mitonuclear communication in homeostasis and stress. *Nat. Rev. Mol. Cell Biol.* 17, 213–226. doi: 10.1038/nrm.2016.23

Rai, P., Onder, T. T., Young, J. J., McFaline, J. L., Pang, B., Dedon, P. C., et al. (2009). Continuous elimination of oxidized nucleotides is necessary to prevent rapid onset of cellular senescence. *Proc. Natl. Acad. Sci. U. S. A.* 106, 169–174. doi: 10.1073/pnas.0809834106

Reichart, G., Mayer, J., Zehm, C., Kirschstein, T., Tokay, T., Lange, F., et al. (2019). Mitochondrial complex IV mutation increases reactive oxygen species production and reduces lifespan in aged mice. *Acta Physiol.* 225:e13214. doi: 10.1111/apha.13214

Rippo, M. R., Olivieri, F., Monsurrò, V., Prattichizzo, F., Albertini, M. C., and Procopio, A. D. (2014). MitomiRs in human inflamm-aging: a hypothesis involving miR-181a, miR-34a and miR-146a. *Exp. Gerontol.* 56, 154–163. doi: 10.1016/j.exger.2014.03.002

Ro, S., Ma, H. Y., Park, C., Ortogero, N., Song, R., Hennig, G. W., et al. (2013). The mitochondrial genome encodes abundant small noncoding RNAs. *Cell Res.* 23, 759–774. doi: 10.1038/cr.2013.37

Sabbatinelli, J., Prattichizzo, F., Olivieri, F., Procopio, A. D., Rippo, M. R., and Giuliani, A. (2019). Where metabolism meets senescence: focus on endothelial cells. *Front. Physiol.* 10, 1–17. doi: 10.3389/fphys.2019.01523

Salminen, A., Kauppinen, A., and Kaarniranta, K. (2012). Emerging role of NF-κB signaling in the induction of senescence-associated secretory phenotype (SASP). *Cell. Signal.* 24, 835–845. doi: 10.1016/j.cellsig.2011.12.006

Shinde, S., and Bhadra, U. (2015). A complex genome-MicroRNA interplay in human mitochondria. *Biomed. Res. Int.* 2015:206382. doi: 10.1155/2015/206382

Spees, J. L., Olson, S. D., Whitney, M. J., and Prockop, D. J. (2006). Mitochondrial transfer between cells can rescue aerobic respiration. *Proc. Natl. Acad. Sci. U. S. A.* 103, 1283–1288. doi: 10.1073/pnas.0510511103

Spurlock, B., Tullet, J. M. A., Hartman, J. L., and Mitra, K. (2020). Interplay of mitochondrial fission-fusion with cell cycle regulation: possible impacts on stem cell and organismal aging. *Exp. Gerontol.* 135:110919. doi: 10.1016/j.exger.2020.110919

Su, Q., Xu, Y., Cai, R., Dai, R., Yang, X., Liu, Y., et al. (2021). miR-146a inhibits mitochondrial dysfunction and myocardial infarction by targeting cyclophilin D. *Mol. Ther. Nucleic Acids* 23, 1258–1271. doi: 10.1016/j.omtn.2021.01.034

Sun, Y., and Ma, L. (2019). New insights into long non-coding rna malat1 in cancer and metastasis. *Cancers* 11:216. doi: 10.3390/cancers11020216

Taganov, K. D., Boldin, M. P., Chang, K. J., and Baltimore, D. (2006). NF-κB-dependent induction of microRNA miR-146, an inhibitor targeted to signaling proteins of innate immune responses. *Proc. Natl. Acad. Sci. U. S. A.* 103, 12481–12486. doi: 10.1073/pnas.0605298103

Tai, Y., Pu, M., Yuan, L., Guo, H., Qiao, J., Lu, H., et al. (2021). miR-34a-5p regulates PINK1-mediated mitophagy via multiple modes. *Life Sci.* 276:119415. doi: 10.1016/j.lfs.2021.119415

Tajima, H., Niikura, T., Hashimoto, Y., Ito, Y., Kita, Y., Terashita, K., et al. (2002). Evidence for in vivo production of Humanin peptide, a neuroprotective factor against Alzheimer's disease-related insults. *Neurosci. Lett.* 324, 227–231. doi: 10.1016/S0304-3940(02)00199-4

Terlecki-Zaniewicz, L., Lämmermann, I., Latreille, J., Bobbili, M. R., Pils, V., Schosserer, M., et al. (2018). Small extracellular vesicles and their miRNA cargo are anti-apoptotic members of the senescence-associated secretory phenotype. *Aging* 10, 1103–1132. doi: 10.18632/aging.101452

Thum, T., Gross, C., Fiedler, J., Fischer, T., Kissler, S., Bussen, M., et al. (2008). MicroRNA-21 contributes to myocardial disease by stimulating MAP kinase signaling in fibroblasts. *Nature* 456, 980–984. doi: 10.1038/nature07511

Treiber, T., Treiber, N., and Meister, G. (2019). Regulation of microRNA biogenesis and its crosstalk with other cellular pathways. *Nat. Rev. Mol. Cell Biol.* 20, 5–20. doi: 10.1038/s41580-018-0059-1

Trifunovic, A. (2006). Mitochondrial DNA and ageing. *Biochim. Biophys. Acta Bioenerg.* 1757, 611–617. doi: 10.1016/j.bbabio.2006.03.003

Vendramin, R., Marine, J., and Leucci, E. (2017). Non-coding RNA s: the dark side of nuclear–mitochondrial communication. *EMBO J.* 36, 1123–1133. doi: 10.15252/embj.201695546

Vidaurre, S., Fitzpatrick, C., Burzio, V. A., Briones, M., Villota, C., Villegas, J., et al. (2014). Down-regulation of the antisense mitochondrial non-coding RNAs (ncRNAs) is a unique vulnerability of cancer cells and a potential target for cancer therapy. *J. Biol. Chem.* 289, 27182–27198. doi: 10.1074/jbc.M114.558841

Villegas, J., Burzio, V., Villota, C., Landerer, E., Martinez, R., Santander, M., et al. (2007). Expression of a novel non-coding mitochondrial RNA in human proliferating cells. *Nucleic Acids Res.* 35, 7336–7347. doi: 10.1093/nar/gkm863

Villota, C., Varas-Godoy, M., Jeldes, E., Campos, A., Villegas, J., Borgna, V., et al. (2019). HPV-18 E2 protein downregulates antisense noncoding mitochondrial RNA-2, delaying replicative senescence of human keratinocytes. *Aging* 11, 33–47. doi: 10.18632/aging.101711

Vizioli, M. G., Liu, T., Miller, K. N., Robertson, N. A., Gilroy, K., Lagnado, A. B., et al. (2020). Mitochondria-to-nucleus retrograde signaling drives formation of cytoplasmic chromatin and inflammation in senescence. *Genes Dev.* 34, 428–445. doi: 10.1101/gad.331272.119

Walczak, J., Partyka, M., Duszyński, J., and Szczepanowska, J. (2017). Implications of mitochondrial network organization in mitochondrial stress signaling in NARP cybrid and Rho0 cells. *Sci. Rep.* 7:14864. doi: 10.1038/s41598-017-14964-y

Wang, G., Chen, H. W., Oktay, Y., Zhang, J., Allen, E. L., Smith, G. M., et al. (2010). PNPASE regulates RNA import into mitochondria. *Cell* 142, 456–467. doi: 10.1016/j.cell.2010.06.035

Wang, W., Esbensen, Y., Kunke, D., Suganthan, R., Rachek, L., Bjørås, M., et al. (2011). Mitochondrial DNA damage level determines neural stem cell differentiation fate. *J. Neurosci.* 31, 9746–9751. doi: 10.1523/JNEUROSCI.0852-11.2011

Wang, K., and Klionsky, D. J. (2011). Mitochondria removal by autophagy. *Autophagy* 7, 297–300. doi: 10.4161/auto.7.3.14502

Wang, W. X., Prajapati, P., Vekaria, H., Spry, M., Cloud, A., Sullivan, P., et al. (2021). Temporal changes in inflammatory mitochondria-enriched microRNAs following traumatic brain injury and effects of miR-146a nanoparticle delivery. *Neural Regen. Res.* 16, 514–522. doi: 10.4103/1673-5374.293149

Wang, G., Shimada, E., Koehler, C. M., and Teitell, M. A. (2012). PNPASE and RNA trafficking into mitochondria. *Biochim. Biophys. Acta. Gene Regul. Mech.* 1819, 998–1007. doi: 10.1016/j.bbagrm.2011.10.001

Wang, X., Song, C., Zhou, X., Han, X., Li, J., Wang, Z., et al. (2017b). Mitochondria associated MicroRNA expression profiling of heart failure. *Biomed. Res. Int.* 2017:4042509. doi: 10.1155/2017/4042509

Wang, W. X., Visavadiya, N. P., Pandya, J. D., Nelson, P. T., Sullivan, P. G., and Springer, J. E. (2015). Mitochondria-associated microRNAs in rat hippocampus following traumatic brain injury. *Exp. Neurol.* 265, 84–93. doi: 10.1016/j.expneurol.2014.12.018

Wang, H., Wang, H., Duan, X., Liu, C., and Li, Z. (2017a). Digital quantitative analysis of microRNA in single cell based on ligation-depended polymerase colony (Polony). *Biosens. Bioelectron.* 95, 146–151. doi: 10.1016/j.bios.2017.04.001

Westermann, B. (2010). Mitochondrial fusion and fission in cell life and death. *Nat. Rev. Mol. Cell Biol.* 11, 872–884. doi: 10.1038/nrm3013

Whelan, S. P., and Zuckerbraun, B. S. (2013). Mitochondrial signaling: forwards, backwards, and in between. *Oxidative Med. Cell. Longev.* 2013:351613. doi: 10.1155/2013/351613

Xiao, Q., Zhu, X., Yang, S., Wang, J., Yin, R., Song, J., et al. (2019). LPS induces CXCL16 expression in HUVECs through the miR-146a-mediated TLR4 pathway. *Int. Immunopharmacol.* 69, 143–149. doi: 10.1016/j.intimp.2019.01.011

Xiong, H., Chen, S., Lai, L., Yang, H., Xu, Y., Pang, J., et al. (2019). Modulation of miR-34a/SIRT1 signaling protects cochlear hair cells against oxidative stress and delays age-related hearing loss through coordinated regulation of mitophagy and mitochondrial biogenesis. *Neurobiol. Aging* 79, 30–42. doi: 10.1016/j.neurobiolaging.2019.03.013

Xu, Y., Xu, L., Chen, C., Zhang, Y., Zeng, C., Jin, Z., et al. (2020). Age-related immune profile of the T cell receptor repertoire, thymic recent output function, and miRNAs. *Biomed. Res. Int.* 2020:5910823. doi: 10.1155/2020/5910823

Xue, Z., Xi, Q., Liu, H., Guo, X., Zhang, J., Zhang, Z., et al. (2019). miR-21 promotes NLRP3 inflammasome activation to mediate pyroptosis and endotoxic shock. *Cell Death Dis.* 10:461. doi: 10.1038/s41419-019-1713-z

Yan, K., An, T., Zhai, M., Huang, Y., Wang, Q., Wang, Y., et al. (2019). Mitochondrial miR-762 regulates apoptosis and myocardial infarction by impairing ND2. *Cell Death Dis.* 10:500. doi: 10.1038/s41419-019-1734-7

Yang, Y., Gao, H., Zhou, H., Liu, Q., Qi, Z., Zhang, Y., et al. (2019). The role of mitochondria-derived peptides in cardiovascular disease: recent updates. *Biomed. Pharmacother.* 117:109075. doi: 10.1016/j.biopha.2019.109075

Yang, B., Lin, H., Xiao, J., Lu, Y., Luo, X., Li, B., et al. (2007). The muscle-specific microRNA miR-1 regulates cardiac arrhythmogenic potential by targeting GJA1 and KCNJ2. *Nat. Med.* 13, 486–491. doi: 10.1038/nm1569

Yang, K. C., Yamada, K. A., Patel, A. Y., Topkara, V. K., George, I., Cheema, F. H., et al. (2014). Deep RNA sequencing reveals dynamic regulation of myocardial noncoding RNAs in failing human heart and remodeling with mechanical circulatory support. *Circulation* 129, 1009–1021. doi: 10.1161/CIRCULATIONAHA.113.003863

Ye, Z., Gould, T. M., Zhang, H., Jin, J., Weyand, C. M., and Goronzy, J. J. (2021). The GSK3β-β-catenin-TCF1 pathway improves naive T cell activation in old adults by upregulating miR-181a. *NPJ Aging Mech. Dis.* 7:4. doi: 10.1038/s41514-021-00056-9

Ye, Z., Li, G., Kim, C., Hu, B., Jadhav, R. R., Weyand, C. M., et al. (2018). Regulation of miR-181a expression in T cell aging. *Nat. Commun.* 9:3060. doi: 10.1038/s41467-018-05552-3

Zeng, Y., Sankala, H., Zhang, X., and Graves, P. R. (2008). Phosphorylation of Argonaute 2 at serine-387 facilitates its localization to processing bodies. *Biochem. J.* 413, 429–436. doi: 10.1042/BJ20080599

Zhang, Z. J., Guo, J. S., Li, S. S., Wu, X. B., Cao, D. L., Jiang, B. C., et al. (2018). TLR8 and its endogenous ligand miR-21 contribute to neuropathic pain in murine DRG. *J. Exp. Med.* 215, 3019–3037. doi: 10.1084/jem.20180800

Zhang, J. J., Liu, W. Q., Peng, J. J., Ma, Q. L., Peng, J., and Luo, X. J. (2017). miR-21-5p/203a-3p promote ox-LDL-induced endothelial cell senescence through down-regulation of mitochondrial fission protein Drp1. *Mech. Ageing Dev.* 164, 8–19. doi: 10.1016/j.mad.2017.03.009

Zhang, S., Liu, C., and Zhang, X. (2019). Mitochondrial damage mediated by miR-1 overexpression in cancer stem cells. *Mol. Ther. Nucleic Acids* 18, 938–953. doi: 10.1016/j.omtn.2019.10.016

Zhang, X., Zuo, X., Yang, B., Li, Z., Xue, Y., Zhou, Y., et al. (2014). MicroRNA directly enhances mitochondrial translation during muscle differentiation. *Cell* 158, 607–619. doi: 10.1016/j.cell.2014.05.047

Zheng, X., Tian, X., Zhang, Q., Shi, P., and Li, S. (2020). Long non-coding RNA SAMMSON as a novel potential diagnostic and prognostic biomarker for oral squamous cell carcinoma. *J. Dent. Sci.* 15, 329–335. doi: 10.1016/j.jds.2019.11.008

Conflict of Interest: The authors declare that the research was conducted in the absence of any commercial or financial relationships that could be construed as a potential conflict of interest.

Publisher's Note: All claims expressed in this article are solely those of the authors and do not necessarily represent those of their affiliated organizations, or those of the publisher, the editors and the reviewers. Any product that may be evaluated in this article, or claim that may be made by its manufacturer, is not guaranteed or endorsed by the publisher.

frontiers in Physiology

HYPOTHESIS AND THEORY
published: 03 November 2021
doi: 10.3389/fphys.2021.738140

Mitochondrial MicroRNAs Contribute to Macrophage Immune Functions Including Differentiation, Polarization, and Activation

Isabelle Duroux-Richard[1], Florence Apparailly[1,2] and Maroun Khoury[3,4,5]**

[1] IRMB, INSERM, Université de Montpellier, CHU Montpellier, Montpellier, France, [2] Clinical Department for Osteoarticular Diseases, University Hospital of Montpellier, Montpellier, France, [3] Laboratory of Nano-Regenerative Medicine, Faculty of Medicine, Universidad de Los Andes, Santiago, Chile, [4] Cells for Cells and REGENERO, The Chilean Consortium for Regenerative Medicine, Santiago, Chile, [5] IMPACT, Center of Interventional Medicine for Precision and Advanced Cellular Therapy, Santiago, Chile

OPEN ACCESS

Edited by:
Eric Barrey, INRA UMR 1313 Genetique Animale et Biologie Integrative, France

Reviewed by:
Javier Traba, Autonomous University of Madrid, Spain
Arnon Henn, Technion Israel Institute of Technology, Israel

***Correspondence:**
Florence Apparailly
Florence.apparailly@inserm.fr
Maroun Khoury
mkhoury@uandes.cl

Specialty section:
This article was submitted to Mitochondrial Research, a section of the journal Frontiers in Physiology

Received: *08 July 2021*
Accepted: *22 September 2021*
Published: *03 November 2021*

Citation:
Duroux-Richard I, Apparailly F and Khoury M (2021) Mitochondrial MicroRNAs Contribute to Macrophage Immune Functions Including Differentiation, Polarization, and Activation. Front. Physiol. 12:738140. doi: 10.3389/fphys.2021.738140

A subset of microRNA (miRNA) has been shown to play an important role in mitochondrial (mt) functions and are named MitomiR. They are present within or associated with mitochondria. Most of the mitochondrial miRNAs originate from the nucleus, while a very limited number is encoded by mtDNA. Moreover, the miRNA machinery including the Dicer and Argonaute has also been detected within mitochondria. Recent, literature has established a close relationship between miRNAs and inflammation. Indeed, specific miRNA signatures are associated with macrophage differentiation, polarization and functions. Nevertheless, the regulation of macrophage inflammatory pathways governed specifically by MitomiR and their implication in immune-mediated inflammatory disorders remain poorly studied. Here, we propose a hypothesis in which MitomiR play a key role in triggering macrophage differentiation and modulating their downstream activation and immune functions. We sustain this proposition by bioinformatic data obtained from either the human monocytic THP1 cell line or the purified mitochondrial fraction of PMA-induced human macrophages. Interestingly, 22% of the 754 assayed miRNAs were detected in the mitochondrial fraction and are either exclusively or highly enriched cellular miRNA. Furthermore, the *in silico* analysis performed in this study, identified a specific MitomiR signature associated with macrophage differentiation that was correlated with gene targets within the mitochondria genome or with mitochondrial pathways. Overall, our hypothesis and data suggest a previously unrecognized link between MitomiR and macrophage function and fate. We also suggest that the MitomiR-dependent control could be further enhanced through the transfer of mitochondria from donor to target cells, as a new strategy for MitomiR delivery.

Keywords: miRNA, mitochondria, macrophage, inflammmation, mitochondria transfer, microRNA, MitomiR

MITOCHONDRIA AS KEY ORGANELLES IN MACROPHAGE FUNCTIONS

Mitochondria are crucial cellular organelles that act as metabolic hubs and signaling platforms. Beyond the fateful endosymbiosis theory (Gray et al., 1999; Roger et al., 2017), mitochondria are multitasking, highly dynamic organelles that continually adjust their morphology, function, number and even their cellular host, in response to metabolic needs and environmental changes (Caicedo et al., 2017). Hence, their functions go beyond cellular ATP production and energy metabolism. In fact, they have indispensable roles in the immune system, especially in regulating macrophage polarization and responses to infection, tissue damage and inflammation.

MITOCHONDRIA TRIGGERING MACROPHAGE POLARIZATION

During pro-inflammatory activation of macrophages (so-called M1 polarization), aerobic glycolysis is activated (Van den Bossche et al., 2016; Liu Y. et al., 2021). This metabolic switch involves increased glucose uptake and pyruvate conversion to lactic acid, providing macrophages with the sufficient energy necessary for their anti-bactericidal activity (He et al., 2021). Moreover, the M1-type activation of macrophages inhibits mitochondrial OXPHOS and promotes mitochondrial nitric oxide (NO) production, thus preventing repolarization toward the anti-inflammatory M2 phenotype (Van den Bossche et al., 2016).

M2 macrophages have a complete tricarboxylic acid (TCA) cycle involving IL-4-mediated fatty acid oxidation (FAO) and mitochondrial energy metabolism as opposed to M1 macrophages (Jha et al., 2015). IL-4 induces ATP citrate lyase activation and oxidative phosphorylation (OXPHOS). In addition, it increases acetyl coenzyme A (acetyl-CoA) synthesis for histone acetylation, which is a key epigenetic regulator of the expression of several M2 marker genes. M2 macrophages maintain anti-inflammatory responses by obtaining most of their energy from FAO and oxidative metabolism (Qing et al., 2020).

IL-25 increases the mitochondrial respiratory capacity and oxygen consumption rate of macrophages and the production of NAD/NADH and ATP (Feng et al., 2017). This leads to the secretion of a large number of anti-inflammatory factors by macrophages for M2 polarization. Furthermore, the inhibition of NO production improves mitochondrial function and reprogramming into M2 macrophages (Mehla and Singh, 2019).

Mitophagy, a mechanism that selectively removes damaged mitochondria from cells, has also been related to macrophage polarization. During M1 polarization, mitophagy inhibition increases mitochondrial mass and decreases the expression of glycolysis-related genes and proinflammatory cytokines (Meng et al., 2021).

Although mitochondria are expected to act as a main target in macrophage regulation, the exact molecular mechanisms by which they regulate macrophage polarization is still not completely elucidated.

MITOCHONDRIA ROLE IN THE INTERPLAY BETWEEN MACROPHAGE METABOLISM AND HOST DEFENSE MECHANISM

Mitochondria are implicated in the tight interplay between host metabolic modifications and immune responses during bacterial infection (Ramond et al., 2019). Recently, it has been demonstrated that intracellular bacterial pathogens are able to modulate mitochondrial functions to maintain their replicative niche. Infection induces mitochondrial changes in infected macrophages, triggering modifications of the host metabolism that lead to important immunological reprogramming (Ramond et al., 2019). Indeed, stimulation by the bacterial toxin nigericin, or LPS, induced the NOD-like receptor family pyrin domain-containing 3 (NLRP3) to interacts with mitochondria via the mitochondria-associated adaptor protein MAVS, leading to ASC (Apoptosis-associated speck like protein) polymerization and downstream activation of caspase 1 and cytokine production (Subramanian et al., 2013). Assembly of the NLRP3 complex leads to the autocatalytic activation of caspase-1 and then the pro-inflammatory cytokines IL-1β and IL-18 (Kelley et al., 2019).

The uncoupling proteins (UCP), a subfamily of mitochondrial proteins, also plays a pivotal role in reprogramming macrophages during infection (Pecqueur et al., 2009). Upon LPS activation, macrophages downregulate UCP2 transcription, leading to a control of the mitochondria-derived reactive oxygen species (Emre and Nübel, 2010). Moreover, UCP2-(–/–) macrophages are more prompt to clear *S. typhimurium* intracellular infection (Arsenijevic et al., 2000).

INVOLVEMENT OF MicroRNAs IN THE REGULATION OF MITOCHONDRIAL PROCESSES

MicroRNA (miRNA) are evolutionarily conserved small non-coding RNAs, which regulate gene expression post-transcriptionally through mRNA degradation or translational inhibition (Bartel, 2004). Several studies demonstrate the presence of miRNAs in various organelles, including the nucleus, endoplasmic reticulum and the mitochondria. Mitochondria-associated endoplasmic reticulum membranes (MAM) are sites of contact where the endoplasmic reticulum domains interact with the mitochondria, facilitating communication between these two organelles (Gao P. et al., 2020). Recently, these sites have shown to contain a substantial number of miRNAs, which may be re-distributed in response to cellular stress and metabolic demands (Wang et al., 2020).

There are three main types of miRNAs enriched in the mitochondrial fractions (MitomiR): (1) They can originate from the nuclear genome and mature in the cytoplasm to target cellular genes that modulate mitochondrial functions (nuc-MiR), (2) they can translocate into the mitochondria to target mitochondrial genes and functions (nuc-MitomiR), or (3) they can be transcribed from the mitochondrial genome and target

mitochondrial genes and functions (mt-MitomiR) (Bandiera et al., 2011; **Figure 1**).

The subclass of MitomiRs that originate from the nuclear genome that mature and regulate the expression of genes associated with mitochondrial pathways in the cytoplasm compartment is the most abundant. Numerous studies report and demonstrate their involvement in mitochondrial functions and activity, such as in apoptosis. Mitochondria play an important role in apoptosis progression, through the mitochondrial fission/fusion dynamics and the release of pro-apoptotic factors (Sheridan and Martin, 2010). For example, miR-200a-3p, miR-125b, miR-30 family, miR-485-5p, miR-195, and miR-140 regulate mitochondrial fission/fusion dynamics by targeting mitochondrial factors such as the mitochondrial fission factor (MFF) (Lee et al., 2017), the mitochondrial 18 kDa protein (MTP18) (Duroux-Richard et al., 2016), the dynamin-1-like protein (DRP1) (Li et al., 2010), the mitofusin (MFN) 1 and 2 (Li et al., 2014; Zhao et al., 2017; Purohit et al., 2019). As the heart is the organ with a perpetual high energy requirement, mitochondria occupy a large portion of cardiomyocytes, and are located between the myofibrils and just below the sarcolemma (Gustafsson and Gottlieb, 2008). Hence, strategic positioning and abundance of mitochondria ensure a highly efficient localized ATP delivery system to support contraction, metabolism, and ion homeostasis (Andrienko et al., 2003). The involvement of miRNAs in the energy control of mitochondria is therefore crucial in those cells. Indeed, in cardiomyocytes, upon apoptotic stimulation, miR-140 negatively regulates MFN1 and controls the release of endonuclease G, which participates in causing DNA fragmentation, and leads to apoptosis (Li et al., 2014). Following the anti-tumor drug Doxorubicin (DOX) treatment, miR-532-3p directly targets the caspase recruitment domain (ARC) and participates in DOX-induced mitochondrial fission and apoptosis. MiR-499-5p attenuates mitochondrial fission and DOX cardiotoxicity through p21 targeting (Wan et al., 2019).

MitomiR AND CELLULAR FUNCTIONS

Apoptosis is also related to the pathogenesis of many diseases such as tumors, cardiovascular disorders and inflammatory responses, and miRNAs participate in the regulation of mitochondria-mediated apoptosis and metabolism. The miR-30 family regulates apoptosis through the targeting of the mitochondrial fission machinery leading to a suppression in the expression of p53 and its downstream target DRP1 (Li et al., 2010).

In human monocytes upon inflammatory signal, miR-125b attenuates mitochondrial respiration and promotes mitochondrial hyper-fusion through the silencing of both the BH3-only proapoptotic protein BIK and the pro-fission protein MTP18, leading to macrophage apoptosis (Duroux-Richard et al., 2016). In renal tubular cells, under hypoxia, MTP18 is silenced by miR-668, preserving mitochondria from fragmentation and

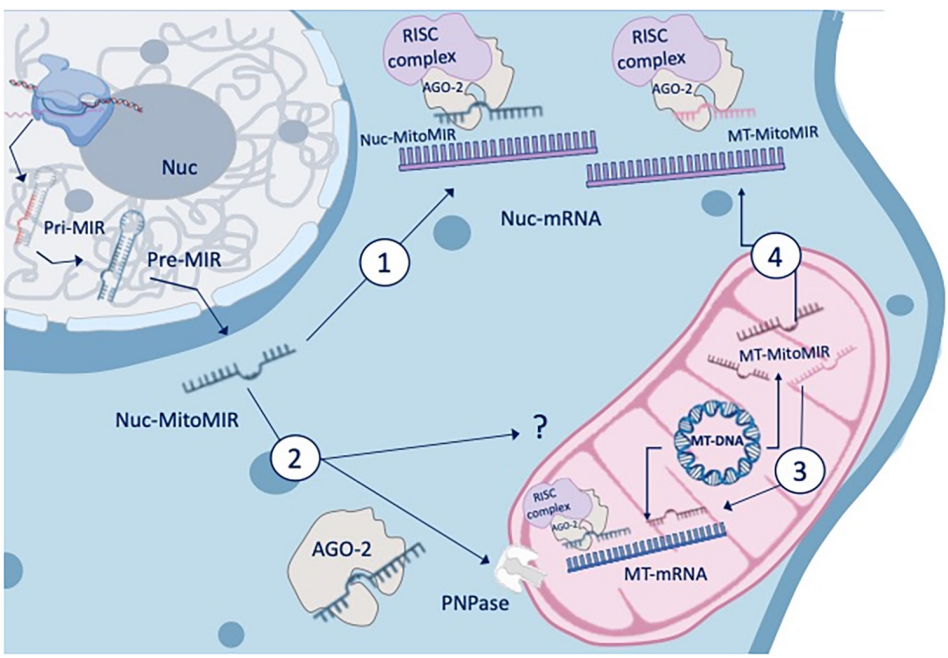

FIGURE 1 | MitomiR and gene regulation. The three main types of miRNAs that are enriched in the mitochondrial fractions can either originate from the nuclear genome and mature in the cytoplasm to target cellular genes that modulate mitochondrial functions (nuc-MiR) or translocate into the mitochondria to target mitochondrial genes and functions (nuc-MitomiR), or be transcribed from the mitochondrial genome and target mitochondrial genes and functions (MT-MitomiR). The AGO2 protein, an endonuclease, has been reported to colocalize with mitochondria, and to be associated with small mtRNA. RNA and MitomiR import into mitochondria is facilitated by multi-subunit RNA import complex (RIC), through a pathway independent of protein import and recently, through AGO2 and the protein PNPase (poly nucleotide phosphorylase).

cell death (Wei et al., 2018). In addition, it has been shown that miR-338 targets cytochrome c oxidase IV, a key nuclear-encoded protein within the electron transfer chain in mitochondria, which is involved in ATP production (Aschrafi et al., 2008).

The first evidence that miRNAs can be imported into mitochondria and regulate mtRNA expression was demonstrated in the mtDNA-lacking 206 ρ°cell line. Several nuc-MitomiR, such as miR-181c-5p and miR-146a-5p were identified in mitochondria and target mitochondrial RNAs and mitochondria-associated mRNAs encoded by nuclear genes (Dasgupta et al., 2015). In 2014, Das et al. (2014) demonstrated that miR-181c encoded in the nucleus but matured in the cytosol, translocates into the mitochondria regulating the expression of mitochondrial genes such as *mt-COX1* (known as mitochondrially encoded cytochrome c oxidase I). Using an *in vivo* systemic miR-181c delivery to the heart, enforced expression of miR-181c leads to an alteration in oxygen consumption, ROS production, matrix calcium and mitochondrial membrane potential of mitochondria isolated from cardiac cells (Das et al., 2014). More recently it has been shown that all members of the miR-181 family can alter the myocardial response to oxidative stress, by either targeting *mt-COX1* (miR-181c) or tensin homolog gene *PTEN* (miR-181a and miR-181b) (Das et al., 2017).

IDENTIFICATION OF MITOCHONDRIAL-ENRICHED MicroRNAs

To identify mitochondrial-enriched miRNAs, miRNome studies of mitochondrial and cytosolic RNA fractions from the same cells were performed. nuc-MitomiR signatures, such as miR-494, miR-1275 and miR-1974, were enriched in mitochondrial fractions (Bandiera et al., 2011). Subcellular trafficking and cellular dynamics of intracellular miRNA translocation depends on AGO2 levels and its status of phosphorylation. The AGO2 protein, an endonuclease shared across multiple species necessary for RNAi, has been reported to colocalize with mitochondria and to be associated with small mtRNA (Maniataki, 2005; Bandiera et al., 2011). In addition, it has been shown that RNA import into mitochondria is facilitated by multi-subunit RNA import complex (RIC), such as pathways independent of protein import (Mukherjee et al., 2007), co-localization of AGO2 and AGO3 (Bandiera et al., 2011), and recently, AGO2 and the protein PNPase (poly nucleotide phosphorylase) (Shepherd et al., 2017).

The functional RNAs encoded by the mitochondrial genome are mainly ribosomal RNAs (rRNAs) and transfer RNAs (tRNAs). The AGO2 protein has been shown to be associated with mitochondrial tRNAs in the cytoplasm. In addition, new types of RNA of mitochondrial origin have recently been identified. These are double-stranded RNAs encoded in mitochondria that are capable of triggering antiviral signaling in humans (Dhir et al., 2018). Interestingly, Bandiera et al. (2011) profiled the expression of miRNAs in mitochondrial fractions purified from HeLa cells and interrogated their genomics to better understand the molecular basis underlying their mitochondrial localization. They showed that miR-1974, miR-1977, and miR-1978 have a perfect match in the mitochondrial genome with two mitochondrial tRNA genes, *TRNE* and *TRNN*, and with a stretch of the mitochondrial rRNA sequence *RNR1* (Bandiera et al., 2011).

Thus, the post-transcriptional regulation of miRNAs directly into the mitochondria, or next to the mitochondria, especially in MAMs, allows the rapid expression of mitochondrial genome to be adjusted according to the metabolic conditions and demands of the cell. The importance of metabolism in deciding the fate of immune populations is very clear. Under conditions of stress, macrophages adjust their metabolism to meet the energy demand, necessary for their activation and functions.

MitomiR PROFILING OF MITOCHONDRIA EXTRACTED FROM MONOCYTIC CELL LINE

MiRNAs play pivotal roles in regulating macrophage functions, including differentiation, polarization, recruitment, and activation of inflammation (Self-Fordham et al., 2017). The ability of the mitochondria to modify cellular metabolic profile, thereby allowing an appropriate response, is crucial for the correct establishment of immune responses. However, little is known about mitomiR involvement when taking into account macrophage functions, such as differentiation. Thus, in this review, to provide novel insight into macrophage differentiation-specific mitomiR signatures and associated mitochondrial pathways, we performed a global miRNA profiling on extracted mitochondria and total cell content of human macrophages. The THP-1 monocytic cell line was treated with phorbol-12-myristate-13-acetate (PMA) to induce differentiation into macrophages.

The mitochondrial fraction of the cells was enriched and purified using anti-TOM22 microbeads (Miltenyi Biotec). Briefly, 2×10^6 were required to allow purification of the total fraction while 40×10^6 cells were used for the isolation of the mitochondrial fraction. PMA-differentiated and undifferentiated THP-1 cells were centrifuged at 300 g at 4°C for 10 min, after homogenization in ice-cold lysis-buffer supplemented with antiprotease cocktail using 26G and 30G needles and 1 ml syringes (5 times round trips for each size). After checking that at least half of the effective lysis is achieved, the total cell fraction was obtained following centrifugation at 13,000 g for 5 min at 4°C. The obtained pellets were resuspended in 700 µl of Qiazol (Qiagen). In parallel, the mitochondrial cell fraction purification is carried out directly on the cell lysate by anti-TOM22 magnetic labeling (Miltenyi Biotec), according to the manufacturer's instructions. After mitochondrial fraction elution, samples were centrifugated at 13,000 g for 5 min at 4°C, and mitochondria pellets resuspended in 700 µl of Qiazol for RNA extraction, using the miRNeasy kit (Qiagen). We performed the global miRNA profiling by considering 754 human miRNAs on extracted mitochondria and compared with total cell content. Total 500 ng RNA per sample were reverse transcribed to cDNA with Megaplex

Human Pool A and B stem loop RT primers and TaqMan MicroRNA RT kit (Life Technology), and miRNA expression profiles were analyzed using the TaqMan® Array Human MicroRNA Card Set v3.0, according to the manufacturer's instructions.[1] To address differences, the distribution of miRNA expression was visualized using unsupervised hierarchical clustering (**Figure 2A**). Data showed that 78% of miRNAs were very poorly detected in the mitochondrial fraction. The supervised hierarchical clustering analysis showed that 22 miRNAs are increased or decreased during macrophage differentiation in the mitochondrial compartment (**Figure 2A**, miRNAs name in right top panel). A miRNA profiling between total cell content and purified endoplasmic reticulum was also performed and showed no enrichment of the identified MitomiR (data not show), suggesting that these miRNAs are specific for mitochondria. Using ingenuity pathway analysis (IPA) tool,[2] we examined which biological pathways were affected with the twenty-two identified MitomiRs and constructed mRNA-miRNA networks and miRNA-target gene interactions (**Figure 2B**). This analysis highlighted 9 (miR-331-5p, miR-18a-8p, miR-132, miR-29b-3p, miR-17-5p, miR-186-5p, miR-124-3p, miR-192-5p, and miR-23a-3p) and 4 (miR-494-3p, miR-214-3p, miR-16-5p, and miR-154-5p) MitomiRs were down- and up-expressed upon macrophage differentiation, respectively, and were potentially linked to key genes associated with regulation, permeabilization, morphology, depolarization, development, quantity, and transmembrane potential of mitochondria.

[1]https://www.ncbi.nlm.nih.gov/geo/query/acc.cgi?acc=GSE182255

[2]http://www.ingenuity.com

MitomiR AND MACROPHAGE FUNCTIONS

Interestingly, among these thirteen MitomiRs, miR-494 is probably one of the most described nuc-MitomiR. It is enriched in mitochondrial fractions and controls cell differentiation and mitochondrial functions in different cell types. It regulates mitochondrial biogenesis by silencing *mtTFA* and *Foxj3* during myocyte differentiation and skeletal muscle adaptation to physical exercise (Yamamoto et al., 2012). In ARPE-19 cells, a spontaneously arising retinal pigment epithelia (RPE) cell line, miR-494 is enriched in mitochondria and present in extracellular vesicles released by cells treated with rotenone to induce mitochondrial injury (Ahn et al., 2021). Thus, in addition to being the most frequently identified MitomiR (Geiger and Dalgaard, 2017), miR-494 is also involved in macrophage polarization and functions. Shao et al. (2020) showed that miR-494 enhances M1 macrophage polarization via *NRDP1* targeting in an

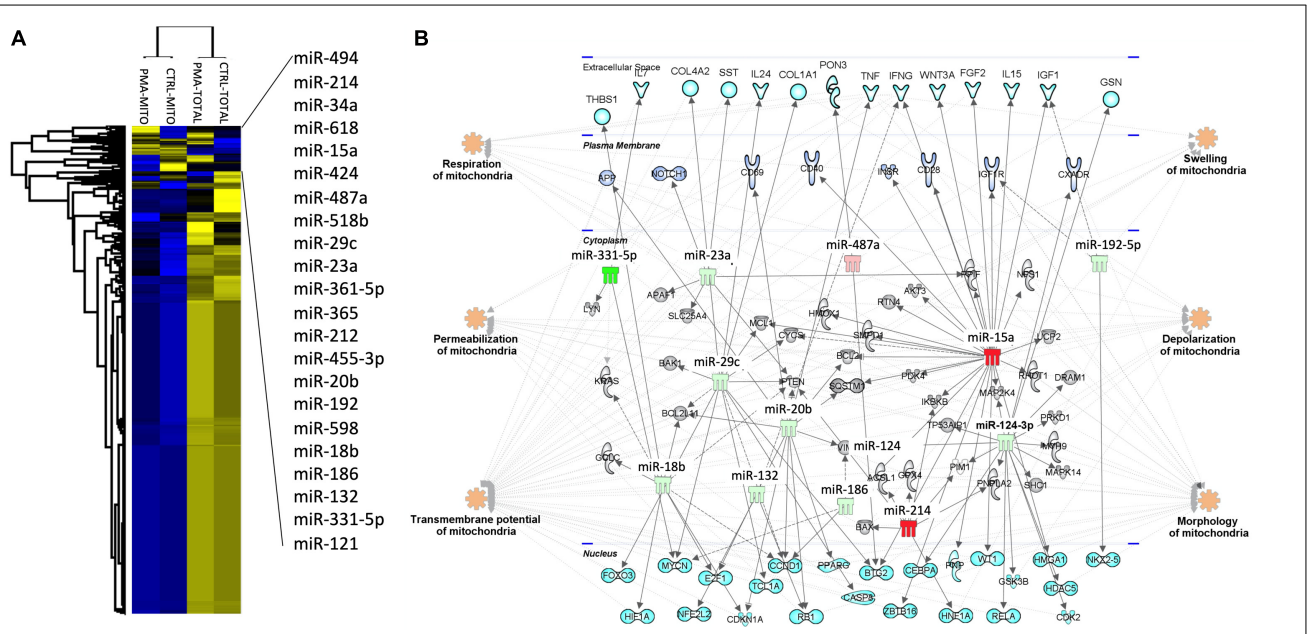

FIGURE 2 | Macrophage mitomiRs signature: The human monocytic cell line THP-1 cells was differentiated into THP-1 derived macrophages with 40 ng/mL phorbol 12-myristate 13-acetate (PMA) over-night in RPMI 1640 Medium GlutaMAX™ Supplement with 10% FBS at 37°C and 5% CO2. Total cellular and mitochondrial enrichment fractions were prepared at 4°C using a MACS Mitochondria kit (Miltenyi), and total RNA including miRNAs were extracted using miRNeasy kit (Qiagen). miRNA quantification was performed using the TaqMan® Array Human MicroRNA Card Set v3.0 (Applied Biosystems), according to the manufacturer's instructions. **(A)** Using Perseus software, a non-supervised hierarchical analysis of the distribution of total and mitochondria enrichment cell fractions based on relative log2 expression of 762 human miRNAs significantly modified by PMA compared to untreated controls. Yellow and blue represent the increase and decrease in expression, respectively. **(B)** miRNA-mRNA networks generated with Ingenuity Pathway Analysis (IPA) for the 22 macrophage-specific mitomiRs. IPA analysis was performed to investigate Mt-miRNA associated genes, filters were set to include experimentally observed or high-confidence-predicted miRNA-mRNA interaction partners, associated with mitochondria biological pathways. miRNAs were colored in red or green depending on whether they were upregulated or downregulated in mitochondria fractions following macrophage differentiation, respectively.

intracerebral hemorrhage mice model. miR-494 also regulates inflammatory responses by targeting the phosphatase and *PTEN* and suppresses LPS-induced nuclear factor (NF)-κB signaling, in LPS-induced inflammation in mouse macrophages (Zhang et al., 2019). Interestingly, *PTEN* expression is strongly regulated by several miRNAs, including miR-214, which we found enriched in the mitochondrial fraction too. Down-regulation of *PTEN* expression leads to LPS-induced *AKT1* activation and inflammation (Fang et al., 2018). Furthermore, Lu et al. (2014) showed that the effect of macrophage polarization associated with the anti-cancer drug Norcantharidin on anti-hepatocellular carcinoma was due to increased miR-214 expression, which resulted in the inhibition of β-catenin signaling pathway. Recently, three studies demonstrated the key role of miR-214, miR-487a, and miR-124 in M2 macrophage polarization. The long non-coding RNA *NEAT1* promotes M2 macrophage polarization by sponging miR-214, which silences *B7-H3* (alias CD276), thus accelerating multiple myeloma progression via the JAK2/STAT3 signaling pathway (Gao Y. et al., 2020). MiR-487a is enriched in M2 macrophage-derived exosomes, which promote gastric cancer proliferation and tumorigenesis (Yang et al., 2021). Finally, miR-124 contributes to M2-type polarization of monocytic cells in normal conditions and during allergic inflammation (Veremeyko et al., 2013).

To study the mitochondrial signaling pathways and to shed light on the implication of MitomiRs on the regulation of mitochondrial functions, we performed an *in silico* analysis with the two most described MitomiRs, miR-494 and miR-214, whose expressions are up- and down-expressed, respectively, during monocyte differentiation into macrophage. Using IPA, we constructed a *mt*-mRNA-miRNA networks and a miRNA-target *mt*-gene interactions using putative miR-214 and miR-494 direct and indirect targets (**Figure 3**). Interestingly, miR-214-3p and miR-494-3p putatively target two *mt*-genes: the cytochrome C oxidase subunit I (*mt-CO1*, alias *COX1*) and subunit III (*mt-CO3*, *COX3*), respectively. Human cytochrome c oxidase (COX) is composed of 13 subunits, including three catalytic subunits I-III (*mt-CO1*, *mt-CO2,* and *mt-CO3*) encoded by mitochondrial DNA and ten nuclear-coded subunits by nuclear DNA (Kadenbach and Hüttemann, 2015). Furthermore, COX phosphorylation is described as having a strong influence on mitochondrial respiration and controlling macrophage function during inflammatory stimuli.

For example, the osteopontin, a cell attachment protein, that trigger a number of signal transduction pathways controlling survival, proliferation and migration of macrophages (Gao et al., 2007), decreases its expression in the presence of *mt-CO1* and *mt-CO3* in RAW264, murine macrophages, through a CD44-dependent transcriptional regulatory mechanism of the mitochondrial H strand (Gao et al., 2003). In macrophages, endotoxin-stimulated NO production inhibits cellular respiration and mitochondrial electron transport by inhibiting cytochrome c oxidase activity, and inhibits *mt-CO1* expression at the mRNA and protein levels, determining the host inflammatory response (Wei et al., 2002).

Finally, a RNA sequencing study of human macrophage subpopulation isolated from bronchoalveolar lavage fluid, aiming at deciphering macrophage plasticity in the lung microenvironment, revealed that macrophages with reduced expression of the classical surface markers M1 and M2 exhibit pro-inflammatory gene signatures, and overexpress 15 mitochondrial genes including *mt-CO3*, *mt-CO1*, *mt-RN*R2,

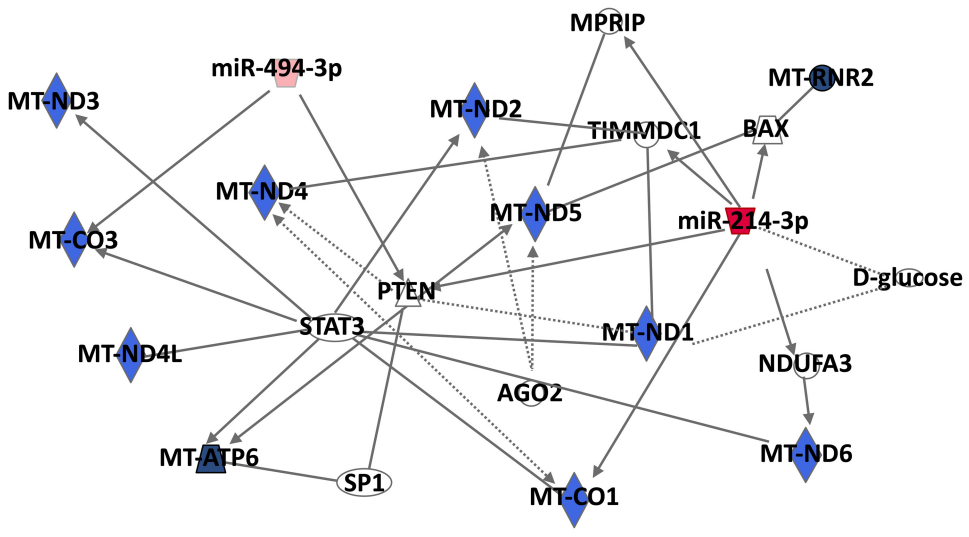

FIGURE 3 | Mt-mRNA-miRNA networks generated with Ingenuity Pathway Analysis (IPA) for the two most described MitomiRs, miR-494, and miR-214. IPA analysis was performed to investigate genes associated with Mt-mRNAs. Filters were set to include either putative, experimentally observed or high-confidence-predicted miRNA-mRNA interaction partners. MiRNAs were colored in red depending on whether they were upregulated in mitochondria fractions following macrophage differentiation. The red color intensity corresponds to the fold change in miRNA expression in the mitochondria-enriched fraction of PMA-differentiated THP-1 macrophages compared to untreated THP-.

mt-ATP6, *mt-ND1*, *mt-ND2,* and *mt-ND4L*, which may contribute to the pathogenesis and manifestations of inflammatory lung diseases such as chronic obstructive pulmonary disease (Takiguchi et al., 2021).

MitomiR TRANSFER TO MACROPHAGE, A NOVEL MODULATORY STRATEGY?

The clinical significance of this phenomenon was first assessed in a model of Lipopolysaccharide (LPS)-induced lung injury in which the intra-tracheal administration of mesenchymal stem/stromal cells (MSCs) to LPS treated mice was associated with the transfer of mitochondria to alveolar epithelium. MSCs triggered an increase in the concentration of ATP, metabolic activity, also an improvement in lung damage while reducing mortality in the diseased animals. Jackson et al. (2016) observed that mitochondria transferred from MSCs were able to increase the phagocytic capabilities of macrophages, increasing basal respiration and ATP turnover *in vitro* and *in vivo* in a murine model of acute respiratory distress syndrome (ARDS). The mechanism by which MSCs transferred mitochondria in this case was independent of *CNX43*, but related to the establishment of cellular highways (also known as tunneling nanotubules) between both cell types (Jackson et al., 2016). Interestingly, the artificial transfer of mitochondria from MSCs into macrophages, conveys the same metabolic and phagocytic improvement, evidencing a role for mitochondria in macrophage function (Liu D. et al., 2021). Recently, Yuan et al. (2021) showed in a diabetic nephropathy mice model, that mitochondrial transfer from MSCs to macrophages restricts inflammation and alleviates kidney injury via PGC-1α activation. These results represent strong evidence in favor of the hypothesis that the transfer of mitochondria from MSCs to immune active cells could play a role in the control of immune function mediated by MSCs (Court et al., 2020). However, mitochondrial transfer to macrophages is not specific for MSCs, Brestoff et al. (2021) demonstrated that adipocytes transfer their mitochondria to macrophages *in vivo*, mediated by heparan sulfates, which regulates white adipose tissue homeostasis, and plays a key role in obesity. In addition, recent studies showed that mitochondria from extracellular vesicles are involved in intercellular communication and immune regulation (She et al., 2021).

Also, mitochondria delivery can be applied following an artificial procedure, known mitoception (Caicedo et al., 2015), where extracted mitochondria from donor cells are transferred into recipient cells. Following this method, freshly isolated-mitochondria from MSCs could be transferred into immune cells including monocytes based on centrifugation and endocytosis. The "mitocepted" cells were able to increase their ATP production while shifting toward a glycolytic pathway. Thus, the process of mitoception allows a distinct analysis of the functional role of mitochondria, independently from the paracrine and cell-mediated effects from donor cells.

Mitochondrial transfer, whether mediated by cell-to-cell contact or through mitoception, presents a novel modulatory strategy through the delivery of mitomiR(s) to target cells, including macrophages (Jorgensen and Khoury, 2021).

HYPOTHESIS AND CONCLUSION

Our *in silico* analysis identified a specific MitomiR signature associated with macrophage functions including differentiation, polarization, recruitment and activation of the inflammatory response. This MitomiR profiling correlated with gene targets within the mitochondrial genome or mitochondrial pathways. Our emitted hypothesis and data suggest a previously unrecognized link between MitomiR and macrophage functions and fate leading to a modulation of the downstream immune responses.

DATA AVAILABILITY STATEMENT

The datasets presented in this study can be found in online repositories. The names of the repository/repositories and accession number(s) can be found below: NCBI GEO GSE182255.

AUTHOR CONTRIBUTIONS

ID-R, FA, and MK drafted the manuscript. ID-R performed *in silico* analyses. All authors were involved in reading and editing the manuscript and approved the final version.

FUNDING

This work was supported by grants from the Chilean National Agency for Investigation and Development: ANID (Agencia Nacional de Investigación y Desarrollo) (FONDECYT regular, 2021, #1211749). In addition to research funds from the INSERM (Institut National de la Santé et Recherche Médicale); the University of Montpellier; and the International research project INSERM France-Chile 2020.

ACKNOWLEDGMENTS

We thank Francesca Velarde from the University of Los Andes, Chile for the critical proofreading of the manuscript.

REFERENCES

Ahn, J. Y., Datta, S., Bandeira, E., Cano, M., Mallick, E., Rai, U., et al. (2021). Release of extracellular vesicle miR-494-3p by ARPE-19 cells with impaired mitochondria. *Biochim. Biophys. Acta Gen. Subj.* 1865:129598. doi: 10.1016/j.bbagen.2020.129598

Andrienko, T., Kuznetsov, A. V., Kaambre, T., Usson, Y., Orosco, A., Appaix, F., et al. (2003). Metabolic consequences of functional complexes of mitochondria,

myofibrils and sarcoplasmic reticulum in muscle cells. *J. Exp. Biol.* 206, 2059–2072. doi: 10.1242/JEB.00242

Arsenijevic, D., Onuma, H., Pecqueur, C., Raimbault, S., Manning, B. S., Miroux, B., et al. (2000). Disruption of the uncoupling protein-2 gene in mice reveals a role in immunity and reactive oxygen species production. *Nat. Genet.* 26, 435–439. doi: 10.1038/82565

Aschrafi, A., Schwechter, A. D., Mameza, M. G., Natera-Naranjo, O., Gioio, A. E., and Kaplan, B. B. (2008). MicroRNA-338 regulates local Cytochrome c Oxidase IV mRNA levels and Oxidative Phosphorylation in the axons of sympathetic neurons. *J. Neurosci.* 28, 12581–12590. doi: 10.1523/JNEUROSCI.3338-08.2008

Bandiera, S., Rüberg, S., Girard, M., Cagnard, N., Hanein, S., Chrétien, D., et al. (2011). Nuclear outsourcing of RNA interference components to human mitochondria. *PLoS One* 6:e20746. doi: 10.1371/journal.pone.0020746

Bartel, D. P. (2004). MicroRNAs: genomics, biogenesis, mechanism, and function. *Cell* 116, 281–297. doi: 10.1016/S0092-8674(04)00045-5

Brestoff, J. R., Wilen, C. B., Moley, J. R., Li, Y., Zou, W., Malvin, N. P., et al. (2021). Intercellular mitochondria transfer to macrophages regulates white adipose tissue homeostasis and is impaired in obesity. *Cell Metab.* 33, 270–282.e8. doi: 10.1016/j.cmet.2020.11.008

Caicedo, A., Aponte, P. M., Cabrera, F., Hidalgo, C., and Khoury, M. (2017). Artificial mitochondria transfer: current challenges, advances, and future applications. *Stem Cells Int.* 2017:7610414. doi: 10.1155/2017/7610414

Caicedo, A., Fritz, V., Brondello, J.-M., Ayala, M., Dennemont, I., Abdellaoui, N., et al. (2015). MitoCeption as a new tool to assess the effects of mesenchymal stem/stromal cell mitochondria on cancer cell metabolism and function. *Sci. Rep.* 5:9073. doi: 10.1038/srep09073

Court, A. C., Le-Gatt, A., Luz-Crawford, P., Parra, E., Aliaga-Tobar, V., Bátiz, L. F., et al. (2020). Mitochondrial transfer from MSCs to T cells induces Treg differentiation and restricts inflammatory response. *EMBO Rep.* 21:e48052. doi: 10.15252/embr.201948052

Das, S., Bedja, D., Campbell, N., Dunkerly, B., Chenna, V., Maitra, A., et al. (2014). miR-181c regulates the mitochondrial genome, bioenergetics, and propensity for heart failure in vivo. *PLoS One* 9:e96820. doi: 10.1371/journal.pone.0096820

Das, S., Kohr, M., Dunkerly-Eyring, B., Lee, D. I, Bedja, D., Kent, O. A., et al. (2017). Divergent effects of miR-181 family members on myocardial function through protective cytosolic and detrimental mitochondrial microRNA targets. *J. Am. Heart Assoc.* 6:e004694. doi: 10.1161/JAHA.116.004694

Dasgupta, N., Peng, Y., Tan, Z., Ciraolo, G., Wang, D., and Li, R. (2015). miRNAs in mtDNA-less cell mitochondria. *Cell Death Discov.* 1:15004. doi: 10.1038/cddiscovery.2015.4

Dhir, A., Dhir, S., Borowski, L. S., Jimenez, L., Teitell, M., Rötig, A., et al. (2018). Mitochondrial double-stranded RNA triggers antiviral signalling in humans. *Nature* 560, 238–242. doi: 10.1038/s41586-018-0363-0

Duroux-Richard, I., Roubert, C., Ammari, M., Présumey, J., Grün, J. R., Häupl, T., et al. (2016). miR-125b controls monocyte adaptation to inflammation through mitochondrial metabolism and dynamics. *Blood* 128, 3125–3136. doi: 10.1182/blood-2016-02-697003

Emre, Y., and Nübel, T. (2010). Uncoupling protein UCP2: when mitochondrial activity meets immunity. *FEBS Lett.* 584, 1437–1442. doi: 10.1016/J.FEBSLET.2010.03.014

Fang, Y., Qiu, J., Jiang, Z., Xu, S., Zhou, Z., and He, R. (2018). Increased serum levels of miR-214 in patients with PCa with bone metastasis may serve as a potential biomarker by targeting PTEN. *Oncol. Lett.* 17, 398–405. doi: 10.3892/ol.2018.9522

Feng, J., Li, L., Ou, Z., Li, Q., Gong, B., Zhao, Z., et al. (2017). IL-25 stimulates M2 macrophage polarization and thereby promotes mitochondrial respiratory capacity and lipolysis in adipose tissues against obesity. *Cell. Mol. Immunol.* 15, 493–505. doi: 10.1038/cmi.2016.71

Gao, C., Guo, H., Mi, Z., Grusby, M. J., and Kuo, P. C. (2007). Osteopontin induces ubiquitin-dependent degradation of STAT1 in RAW264.7 murine macrophages. *J. Immunol.* 178, 1870–1881. doi: 10.4049/JIMMUNOL.178.3.1870

Gao, C., Guo, H., Wei, J., and Kuo, P. C. (2003). Osteopontin inhibits expression of cytochrome c oxidase in RAW 264.7 murine macrophages. *Biochem. Biophys. Res. Commun.* 309, 120–125. doi: 10.1016/S0006-291X(03)01534-1

Gao, P., Yan, Z., and Zhu, Z. (2020). Mitochondria-associated endoplasmic reticulum membranes in cardiovascular diseases. *Front. Cell Dev. Biol.* 8:604240. doi: 10.3389/FCELL.2020.604240

Gao, Y., Fang, P., Li, W.-J., Zhang, J., Wang, G.-P., Jiang, D.-F., et al. (2020). LncRNA NEAT1 sponges miR-214 to regulate M2 macrophage polarization by regulation of B7-H3 in multiple myeloma. *Mol. Immunol.* 117, 20–28. doi: 10.1016/j.molimm.2019.10.026

Geiger, J., and Dalgaard, L. T. (2017). Interplay of mitochondrial metabolism and microRNAs. *Cell. Mol. Life Sci.* 74, 631–646. doi: 10.1007/s00018-016-2342-7

Gray, M. W., Burger, G., and Lang, B. F. (1999). Mitochondrial evolution. *Science* 283, 1476–1481. doi: 10.1126/SCIENCE.283.5407.1476

Gustafsson, ÅB., and Gottlieb, R. A. (2008). Heart mitochondria: gates of life and death. *Cardiovasc. Res.* 77, 334–343. doi: 10.1093/CVR/CVM005

He, W., Heinz, A., Jahn, D., and Hiller, K. (2021). Complexity of macrophage metabolism in infection. *Curr. Opin. Biotechnol.* 68, 231–239. doi: 10.1016/J.COPBIO.2021.01.020

Jackson, M. V., Morrison, T. J., Doherty, D. F., McAuley, D. F., Matthay, M. A., Kissenpfennig, A., et al. (2016). Mitochondrial transfer via tunneling nanotubes is an important mechanism by which mesenchymal stem cells enhance macrophage phagocytosis in the in vitro and in vivo models of ARDS. *Stem Cells* 34, 2210–2223. doi: 10.1002/stem.2372

Jha, A. K., Huang, S. C. C., Sergushichev, A., Lampropoulou, V., Ivanova, Y., Loginicheva, E., et al. (2015). Network integration of parallel metabolic and transcriptional data reveals metabolic modules that regulate macrophage polarization. *Immunity* 42, 419–430. doi: 10.1016/J.IMMUNI.2015.02.005

Jorgensen, C., and Khoury, M. (2021). Musculoskeletal Progenitor/Stromal Cell-Derived Mitochondria Modulate Cell Differentiation and Therapeutical Function. *Front. Immunol.* 12:606781. doi: 10.3389/FIMMU.2021.606781

Kadenbach, B., and Hüttemann, M. (2015). The subunit composition and function of mammalian cytochrome c oxidase. *Mitochondrion* 24, 64–76. doi: 10.1016/j.mito.2015.07.002

Kelley, N., Jeltema, D., Duan, Y., and He, Y. (2019). The NLRP3 Inflammasome: an overview of mechanisms of activation and regulation. *Int. J. Mol. Sci.* 20:3328. doi: 10.3390/IJMS20133328

Lee, H., Tak, H., Park, S. J., Jo, Y. K., Cho, D. H., and Lee, E. K. (2017). microRNA-200a-3p enhances mitochondrial elongation by targeting mitochondrial fission factor. *BMB Rep.* 50, 214–219. doi: 10.5483/BMBRep.2017.50.4.006

Li, J., Donath, S., Li, Y., Qin, D., Prabhakar, B. S., and Li, P. (2010). miR-30 Regulates Mitochondrial Fission through Targeting p53 and the Dynamin-Related Protein-1 Pathway. *PLoS Genet.* 6:e1000795. doi: 10.1371/journal.pgen.1000795

Li, J., Li, Y., Jiao, J., Wang, J., Li, Y., Qin, D., et al. (2014). Mitofusin 1 is negatively regulated by microrna 140 in Cardiomyocyte Apoptosis. *Mol. Cell. Biol.* 34, 1788–1799. doi: 10.1128/MCB.00774-13

Liu, D., Gao, Y., Liu, J., Huang, Y., Yin, J., Feng, Y., et al. (2021). Intercellular mitochondrial transfer as a means of tissue revitalization. *Signal Transduct. Target. Ther.* 6:65. doi: 10.1038/s41392-020-00440-z

Liu, Y., Xu, R., Gu, H., Zhang, E., Qu, J., Cao, W., et al. (2021). Metabolic reprogramming in macrophage responses. *Biomark. Res.* 9:1. doi: 10.1186/S40364-020-00251-Y

Lu, S., Gao, Y., Huang, X., and Wang, X. (2014). Cantharidin exerts Anti-Hepatocellular Carcinoma by Mir-214 modulating macrophage polarization. *Int. J. Biol. Sci.* 10, 415–425. doi: 10.7150/ijbs.8002

Maniataki, E. (2005). Human mitochondrial tRNAMet is exported to the cytoplasm and associates with the Argonaute 2 protein. *RNA* 11, 849–852. doi: 10.1261/rna.2210805

Mehla, K., and Singh, P. K. (2019). Metabolic Regulation of Macrophage Polarization in Cancer. *Trends Cancer* 5, 822–834. doi: 10.1016/J.TRECAN.2019.10.007

Meng, L., Lu, C., Wu, B., Lan, C., Mo, L., Chen, C., et al. (2021). Taurine Antagonizes Macrophages M1 Polarization by Mitophagy-Glycolysis Switch Blockage via Dragging SAM-PP2Ac Transmethylation. *Front. Immunol.* 12:648913. doi: 10.3389/FIMMU.2021.648913

Mukherjee, S., Basu, S., Home, P., Dhar, G., and Adhya, S. (2007). Necessary and sufficient factors for the import of transfer RNA into the kinetoplast mitochondrion. *EMBO Rep.* 8, 589–595. doi: 10.1038/sj.embor.7400979

Pecqueur, C., Alves-Guerra, C., Ricquier, D., and Bouillaud, F. (2009). UCP2, a metabolic sensor coupling glucose oxidation to mitochondrial metabolism? *IUBMB Life* 61, 762–767. doi: 10.1002/IUB.188

Purohit, P. K., Edwards, R., Tokatlidis, K., and Saini, N. (2019). MiR-195 regulates mitochondrial function by targeting mitofusin-2 in breast

cancer cells. *RNA Biol.* 16, 918–929. doi: 10.1080/15476286.2019.1600999

Qing, J., Zhang, Z., Novák, P., Zhao, G., and Yin, K. (2020). Mitochondrial metabolism in regulating macrophage polarization: an emerging regulator of metabolic inflammatory diseases. *Acta Biochim. Biophys. Sin. (Shanghai)* 52, 917–926. doi: 10.1093/abbs/gmaa081

Ramond, E., Jamet, A., Coureuil, M., and Charbit, A. (2019). Pivotal role of mitochondria in macrophage response to bacterial pathogens. *Front. Immunol.* 10:2461. doi: 10.3389/fimmu.2019.02461

Roger, A. J., Muñoz-Gómez, S. A., and Kamikawa, R. (2017). The origin and diversification of mitochondria. *Curr. Biol.* 27, R1177–R1192. doi: 10.1016/j.cub.2017.09.015

Self-Fordham, J. B., Naqvi, A. R., Uttamani, J. R., Kulkarni, V., and Nares, S. (2017). MicroRNA: dynamic regulators of macrophage polarization and plasticity. *Front. Immunol.* 8:1062. doi: 10.3389/fimmu.2017.01062

Shao, G., Zhou, C., Ma, K., Zhao, W., Xiong, Q., Yang, L., et al. (2020). MiRNA-494 enhances M1 macrophage polarization via Nrdp1 in ICH mice model. *J. Inflamm.* 17:17. doi: 10.1186/s12950-020-00247-3

She, Z., Xie, M., Hun, M., Abdirahman, A. S., Li, C., Wu, F., et al. (2021). Immunoregulatory effects of mitochondria transferred by extracellular vesicles. *Front. Immunol.* 11:628576. doi: 10.3389/fimmu.2020.628576

Shepherd, D. L., Hathaway, Q. A., Pinti, M. V., Nichols, C. E., Durr, A. J., Sreekumar, S., et al. (2017). Exploring the mitochondrial microRNA import pathway through Polynucleotide Phosphorylase (PNPase). *J. Mol. Cell. Cardiol.* 110, 15–25. doi: 10.1016/j.yjmcc.2017.06.012

Sheridan, C., and Martin, S. J. (2010). Mitochondrial fission/fusion dynamics and apoptosis. *Mitochondrion* 10, 640–648. doi: 10.1016/j.mito.2010.08.005

Subramanian, N., Natarajan, K., Clatworthy, M. R., Wang, Z., and Germain, R. N. (2013). The Adaptor MAVS Promotes NLRP3 mitochondrial localization and inflammasome activation. *Cell* 153, 348–361. doi: 10.1016/J.CELL.2013.02.054

Takiguchi, H., Yang, C. X., Yang, C. W. T., Sahin, B., Whalen, B. A., Milne, S., et al. (2021). Macrophages with reduced expressions of classical M1 and M2 surface markers in human bronchoalveolar lavage fluid exhibit pro-inflammatory gene signatures. *Sci. Rep.* 11:8282. doi: 10.1038/s41598-021-87720-y

Van den Bossche, J., Baardman, J., Otto, N. A., van der Velden, S., Neele, A. E., van den Berg, S. M., et al. (2016). Mitochondrial dysfunction prevents repolarization of inflammatory macrophages. *Cell Rep.* 17, 684–696. doi: 10.1016/J.CELREP.2016.09.008

Veremeyko, T., Siddiqui, S., Sotnikov, I., Yung, A., and Ponomarev, E. D. (2013). IL-4/IL-13-Dependent and Independent Expression of miR-124 and Its Contribution to M2 Phenotype of Monocytic Cells in Normal Conditions and during Allergic Inflammation. *PLoS One* 8:e81774. doi: 10.1371/journal.pone.0081774

Wan, Q., Xu, T., Ding, W., Zhang, X., Ji, X., Yu, T., et al. (2019). miR-499-5p Attenuates Mitochondrial Fission and Cell Apoptosis via p21 in Doxorubicin Cardiotoxicity. *Front. Genet.* 9:734. doi: 10.3389/fgene.2018.00734

Wang, W.-X., Prajapati, P., Nelson, P. T., and Springer, J. E. (2020). The mitochondria-associated ER membranes are novel subcellular locations enriched for inflammatory-responsive MicroRNAs. *Mol. Neurobiol.* 57, 2996–3013. doi: 10.1007/s12035-020-01937-y

Wei, J., Guo, H., and Kuo, P. C. (2002). Endotoxin-Stimulated Nitric Oxide Production Inhibits Expression of Cytochrome c Oxidase in ANA-1 Murine Macrophages. *J. Immunol.* 168, 4721–4727. doi: 10.4049/jimmunol.168.9.4721

Wei, Q., Sun, H., Song, S., Liu, Y., Liu, P., Livingston, M. J., et al. (2018). MicroRNA-668 represses MTP18 to preserve mitochondrial dynamics in ischemic acute kidney injury. *J. Clin. Invest.* 128, 5448–5464. doi: 10.1172/JCI121859

Yamamoto, H., Morino, K., Nishio, Y., Ugi, S., Yoshizaki, T., Kashiwagi, A., et al. (2012). MicroRNA-494 regulates mitochondrial biogenesis in skeletal muscle through mitochondrial transcription factor A and Forkhead box j3. *Am. J. Physiol. Metab.* 303, E1419–E1427. doi: 10.1152/ajpendo.00097.2012

Yang, X., Cai, S., Shu, Y., Deng, X., Zhang, Y., He, N., et al. (2021). Exosomal miR-487a derived from m2 macrophage promotes the progression of gastric cancer. *Cell Cycle* 20, 434–444. doi: 10.1080/15384101.2021.1878326

Yuan, Y., Yuan, L., Li, L., Liu, F., Liu, J., Chen, Y., et al. (2021). Mitochondrial transfer from mesenchymal stem cells to macrophages restricts inflammation and alleviates kidney injury in diabetic nephropathy mice via PGC-1α activation. *Stem Cells* 39, 913–928. doi: 10.1002/stem.3375

Zhang, S., He, K., Zhou, W., Cao, J., and Jin, Z. (2019). miR-494-3p regulates lipopolysaccharide-induced inflammatory responses in RAW264.7 cells by targeting PTEN. *Mol. Med. Rep.* 19, 4288–4296. doi: 10.3892/mmr.2019.10083

Zhao, Y., Ponnusamy, M., Liu, C., Tian, J., Dong, Y., Gao, J., et al. (2017). MiR-485-5p modulates mitochondrial fission through targeting mitochondrial anchored protein ligase in cardiac hypertrophy. *Biochim. Biophys. Acta Mol. Basis Dis.* 1863, 2871–2881. doi: 10.1016/j.bbadis.2017.07.034

Conflict of Interest: MK was the chief scientific officer of Cells for Cells and Regenero, the Chilean Consortium for Regenerative Medicine.

The remaining authors declare that the research was conducted in the absence of any commercial or financial relationships that could be construed as a potential conflict of interest.

Publisher's Note: All claims expressed in this article are solely those of the authors and do not necessarily represent those of their affiliated organizations, or those of the publisher, the editors and the reviewers. Any product that may be evaluated in this article, or claim that may be made by its manufacturer, is not guaranteed or endorsed by the publisher.

frontiers in Physiology

ORIGINAL RESEARCH
published: 29 November 2021
doi: 10.3389/fphys.2021.718982

Neurogenic Hypertension Mediated Mitochondrial Abnormality Leads to Cardiomyopathy: Contribution of UPR^{mt} and Norepinephrine-miR-18a-5p-HIF-1α Axis

Shyam S. Nandi[1], Kenichi Katsurada[1], Sushil K. Mahata[2,3] and Kaushik P. Patel[1]*

[1] *Department of Cellular and Integrative Physiology, University of Nebraska Medical Center, Omaha, NE, United States,* [2] *Metabolic Physiology and Ultrastructural Biology Laboratory, Department of Medicine, University of California, San Diego, San Diego, CA, United States,* [3] *VA San Diego Healthcare System, San Diego, CA, United States*

OPEN ACCESS

Edited by:
John Hollander, West Virginia University, United States

Reviewed by:
D. Brian Foster, John Hopkins University School of Medicine, United States
Dhanendra Tomar, Temple University, United States

***Correspondence:**
Shyam S. Nandi
shyam.nandi@unmc.edu

Specialty section:
This article was submitted to Mitochondrial Research, a section of the journal Frontiers in Physiology

Received: *01 June 2021*
Accepted: *15 September 2021*
Published: *29 November 2021*

Citation:
Nandi SS, Katsurada K, Mahata SK and Patel KP (2021) Neurogenic Hypertension Mediated Mitochondrial Abnormality Leads to Cardiomyopathy: Contribution of UPR^{mt} and Norepinephrine-miR-18a-5p-HIF-1α Axis. Front. Physiol. 12:718982. doi: 10.3389/fphys.2021.718982

Aims: Hypertension increases the risk of heart disease. Hallmark features of hypertensive heart disease is sympathoexcitation and cardiac mitochondrial abnormality. However, the molecular mechanisms for specifically neurally mediated mitochondrial abnormality and subsequent cardiac dysfunction are unclear. We hypothesized that enhanced sympatho-excitation to the heart elicits cardiac miR-18a-5p/HIF-1α and mitochondrial unfolded protein response (UPR^{mt}) signaling that lead to mitochondrial abnormalities and consequent pathological cardiac remodeling.

Methods and Results: Using a model of neurogenic hypertension (NG-HTN), induced by intracerebroventricular (ICV) infusion of Ang II (NG-HTN; 20 ng/min, 14 days, 0.5 μl/h, or Saline; Control, 0.9%) through osmotic mini-pumps in Sprague-Dawley rats (250–300 g), we attempted to identify a link between sympathoexcitation (norepinephrine; NE), miRNA and HIF-1α signaling and UPR^{mt} to produce mitochondrial abnormalities resulting in cardiomyopathy. Cardiac remodeling, mitochondrial abnormality, and miRNA/HIF-1α signaling were assessed using histology, immunocytochemistry, electron microscopy, Western blotting or RT-qPCR. NG-HTN demonstrated increased sympatho-excitation with concomitant reduction in UPR^{mt}, miRNA-18a-5p and increased level of HIF-1α in the heart. Our *in silico* analysis indicated that miR-18a-5p targets HIF-1α. Direct effects of NE on miRNA/HIF-1α signaling and mitochondrial abnormality examined using H9c2 rat cardiomyocytes showed NE reduces miR-18a-5p but increases HIF-1α. Electron microscopy revealed cardiac mitochondrial abnormality in NG-HTN, linked with hypertrophic cardiomyopathy and fibrosis. Mitochondrial unfolded protein response was decreased in NG-HTN indicating mitochondrial proteinopathy and proteotoxic stress, associated with increased mito-ROS and decreased mitochondrial membrane potential ($\Delta\Psi$m), and oxidative phosphorylation. Further, there was reduced cardiac mitochondrial biogenesis and fusion, but increased mitochondrial fission, coupled with mitochondrial impaired

TIM-TOM transport and UPR^{mt}. Direct effects of NE on H9c2 rat cardiomyocytes also showed cardiomyocyte hypertrophy, increased mitochondrial ROS generation, and UPR^{mt} corroborating the *in vivo* data.

Conclusion: In conclusion, enhanced sympatho-excitation suppress miR-18a-5p/HIF-1α signaling and increased mitochondrial stress proteotoxicity, decreased UPR^{mt} leading to decreased mitochondrial dynamics/OXPHOS/$\Delta\Psi$m and ROS generation. Taken together, these results suggest that ROS induced mitochondrial transition pore opening activates pro-hypertrophy/fibrosis/inflammatory factors that induce pathological cardiac hypertrophy and fibrosis commonly observed in NG-HTN.

Keywords: hypertension, mitochondrial damage, cardiac hypertrophy, cardiac fibrosis, HIF-1α, miR-18a-5p, UPR^{mt}

INTRODUCTION

Hypertension is an independent risk factor for heart failure, and is rapidly becoming a prominent threat, since it affects ∼80% of the elderly population (65 years and older) (Lionakis et al., 2012). Persistent sympatho-excitation and hypertension lead to cardiomyopathy and increases the risk of heart failure (Nadruz, 2015; Nandi et al., 2016). Hypertension causes heart failure in two ways; first, and most common, it induces left ventricular hypertrophy, fibrosis and stiffens the heart, which causes diastolic dysfunction (with preserved ejection fraction, HFpEF; Tam et al., 2017), and second, as a risk factor for myocardial infarction due to pressure overload (Volpe et al., 2016). Plasma levels of norepinephrine (NE) are known to be elevated during both hypertension and heart failure indicating an exaggerated sympatho-excitatory state (Patel et al., 2016). Blocking this exaggerated sympathetic drive with β-blockers has been useful to treat heart failure pathology. Further, attenuation of heart failure pathology with β-blockers has been attributed to relieving some of the mitochondrial dysfunction (Brown et al., 2017). Consistent with these observations, the β-blocker, carvedilol, has been clinically shown to be cardioprotective by improving mitochondrial metabolism and function (Igarashi et al., 2006). Metoprolol, another β-blocker, inhibits the defective accumulation of acyl-CoA and fatty acid uptake in the mitochondria (Nanki et al., 1987). However, the underlying molecular mechanisms linking sympatho-excitation and cardiac dysfunctions directly in hypertension remain unexplored (Eirin et al., 2018).

It has been reported that mitochondrial abnormalities are common feature in all types of cardiomyopathies (Shirakabe et al., 2016; Nandi et al., 2020a). However, the driving mechanisms underlying these mitochondrial abnormalities are largely unknown (Eirin et al., 2014). In all forms of heart disease, one common feature is abnormal mitochondrial structure due to either compromised mitochondrial metabolism/respiration, dynamics, quality control, reduced proteostasis, and altered import activities or impaired mitophagic clearance (Wrobel et al., 2015; Shirakabe et al., 2016). Newly discovered features of mitochondrial dysfunction associated with dynamics, proteostasis, and oxidative phosphorylation (OXPHOS) quality control factors in maintaining cardiac mitochondrial health are observed in clinical hypertension and cardiomyopathy. Furthermore, hypertrophic cardiomyopathy has been reported due to mitochondrial disease (Garcia-Diaz et al., 2013). Cardiomyopathy also has been reported in children and adults with mitochondrial disease (Holmgren et al., 2003; Sharp et al., 2014). Mitochondrial unfolded protein response (UPR^{mt}) is a feature of retrograde mitochondrial signaling that influences to ensure the maintenance of mitochondria quality control mechanisms to stabilize the functional integrity of the mitochondrial proteostasis (Shpilka and Haynes, 2018; Rolland et al., 2019). When misfolded/misprocessed mitochondrial pre-proteins or unassembled mitochondrial supercomplex proteins accumulate beyond their folding capacity, it leads to altered protein trafficking of mitochondria, and induces mitochondrial proteotoxic stress and dysfunction (Wrobel et al., 2015). Under normal conditions, the heart relies on adequate mitochondrial ATP production to match myocardial energy demand, mostly through OXPHOS.

The discovery and understanding of miRNAs in regulation of cellular events have opened new therapeutic approaches for cardiovascular diseases (Nandi et al., 2015, 2016, 2018; Nandi and Mishra, 2018). Cardiac microRNAs that are downregulated during cardiac pathology appear to have a link to cardiomyopathy progression (Nandi and Mishra, 2015; Seeger and Boon, 2016). Expression of microRNAs is dynamically changed during cardiomyocyte hypertrophy, fibrosis, and cardiac remodeling. The miR-18a-5p is known as an anti-hypertrophy/anti-fibrosis miRNA in the heart (van Almen et al., 2011). Interestingly, cardiac miR-18a-5p is reduced in spontaneously hypertensive rats (SHR) (Huang et al., 2017), known to have increased sympathetic activation (Kline et al., 1983), suggesting a possible nexus between symptho-excitation and miR-18a-5p. Furthermore, miR-18a-5p is reduced in aged hearts and is associated with a decline in cardiac function (van Almen et al., 2011). This is thought to occur by regulating cardiac fibrosis by targeting pro-fibrotic miR-18a-5p genes in the heart. Moreover, loss of miR-18a-5p in the heart severely impairs cardiac function during hypertension, and restoration of cardiac-specific miR-18a-5p expression in SHR alleviated the cardiac dysfunction (Huang et al., 2017). We have reported that the "miRNA mimic"

treatment mitigates cardiac fibrosis and hypertrophy in diabetic hearts (Nandi et al., 2016, 2018). Interestingly, previous studies have also demonstrated a role for miR-18a-5p in optimizing HIF-1α gene and protein expression during inflammation, cell survival, proliferation, and migration (Montoya et al., 2017). Further, HIF-1α mRNA levels have been shown to be regulated in an oxygen-independent manner by neurohumoral activators such as NE (Nikami et al., 2005), commonly elevated in hypertension (Zucker et al., 2001). However, the contribution of enhanced NE mediated changes in miR-18a-5p possibly *via* HIF-1α axis in the regulation of mitochondrial abnormalities within the hearts remains to be examined. Increased HIF-1α protein has been found in heart samples from patients with heart disease (Hölscher et al., 2012). The long-term stabilization and persistent activation of HIF-1α promote cardiac hypertrophy in hypertension and pressure overload heart disease (Krishnan et al., 2009; Hölscher et al., 2012; Fukai et al., 2015; Kumar et al., 2018). Furthermore, it has been shown that increased HIF-1α suppresses cardiac mitochondrial function (Kim et al., 2006; Papandreou et al., 2006; Kumar et al., 2018). Despite this information, the mechanisms of mitochondrial dysfunction and metabolic maladaptation are largely unknown in the heart during hypertension.

The aim of study is designed to explore the mechanistic link between exaggerated sympathetic drive, miRNA/HIF-1α signaling and cardiac mitochondrial abnormalities and associated development of pathological cardiac remodeling in a rat model of neurogenic hypertension (NG-HTN).

MATERIALS AND METHODS

Animals and Ethics

Male Sprague-Dawley rats (250–300 g) from the Jackson Laboratory were housed in the animal facility of the University of Nebraska Medical Center. Rats were kept in hygienic cages in a room maintained at 22–24°C temperature, 30–40% humidity, with a 12 h of dark-light cycle, and provided *ad libitum* food and water. All experimental protocols were approved by the Institutional Animal Care and Use Committee, University of Nebraska Medical Center and all protocols/methods were conducted in accordance with the relevant guidelines and regulations of our institutional, the American Physiological Society, and the National Institutes of Health Guide for the Care and Use of Laboratory Animals.

Neurogenic Hypertension Model

We used healthy male Sprague-Dawley rats aged 12 weeks, weighing 250–300 g and subjected them to intracerebroventricular (ICV) Ang II to develop the rat model of NG-HTN. Rats were randomly assigned to two groups, Saline ICV (Control) and Ang II ICV (NG-HTN). For ICV brain cannulation and mini-pump survival surgery, rats were anesthetized using a single i.p. injection of Ketamine (87 mg/kg) and Xylazine (10 mg/kg) mixture. A longitudinal skin incision was made on the head to expose the bregma and a small burr hole was made in the skull to access the dura. Rats were placed in a stereotaxic apparatus for infusion into the ICV space by stereotaxic implantation of an Alzet cannula of Brain Infusion Kit1 into the lateral ventricle. The tip of the cannula implanted was 1.5 mm lateral to the midline, 4.0 mm ventral to the dorsal surface and 0.8 mm caudal to bregma, as per Paxinos and Watson atlas (Paxinos and Watson, 2005). The cannula was connected to an osmotic minipump (Alzet, model 2002) for ICV infusion of Ang II (20 ng/min) or sterile isotonic saline as vehicle control for 14 days. Ang II infused rats that lacked dipsogenic response were considered not to have viable Ang II ICV infusion and therefore were excluded from the study.

In vivo Hemodynamic Measurements

At the end of 14 days of ICV treatment, hemodynamic parameters were recorded using a Mikro-Tip catheter (SPR-407), Millar Instruments; Houston, TX, United States) with a non-survival terminal procedure in an experimenter-blinded fashion. In brief, animals were anesthetized using a single injection of urethane (0.75 g/kg i.p.) and chloralose (60 mg/kg i.p.). The catheter was inserted into the LV chamber *via* the right carotid artery as described previously (Nandi et al., 2016). The mean arterial pressure (MAP), heart rate (HR), and hemodynamic parameters were simultaneously recorded on a PowerLab data acquisition system (8SP, ADInstruments, United States) and analyzed as reported previously (Nandi et al., 2016; Patel et al., 2016). The cardiac responsiveness (change in ±dP/dt) were measured with intravenous infusion of 0.5 μg/kg isoproterenol (a β-AR agonist). At the end of the experiment, rats were euthanized by Fatal Plus euthanasia solution (120 mg/kg pentobarbital, i.p.).

Assessment of Cardiac Function by M-Mode Echocardiography

Rats were lightly anesthetized with 1.5% isoflurane nose cone. M-mode echocardiography (using Vevo 3100 Imaging System, VisualSonics) was performed at 5 days of ICV post-surgery recovery (for baseline) and at the end of 14 days of ICV saline or Ang II mini-pump infusion. Left ventricular mitral filing parameters (E/A) was measured and compared with respective baseline for the assessment of diastolic dysfunction in NG-HTN rats.

Western Immunoblotting

The routine Western immunoblotting protocol was used for protein expression analysis. Cell or tissue protein lysates was estimated by protein assay (BCA Kit, cat# 23227, Pierce, United States). Boiled protein lysate (25 μg/lane) in 4× denaturing Laemmli Sample Buffer (cat# 161-0747, Bio-Rad Laboratories, United States) were loaded on SDS-PAGE. Next, gels were transferred onto a PVDF (Polyvinylidene fluoride) membrane. Transferred membranes were incubated with 5% milk (Bio-Rad, non-fat dried milk) in TBS for 60 min at room temperature and washed twice in TBS for 5 min each. Blots were then incubated overnight at 4°C with diluted primary antibodies in TBS (1:1000). The primary antibodies used were OXPHOS WB antibody cocktail assay (cat# ab110413), FIS1 (cat# ab71498), OPA1 (cat# ab157457), TIM17 (cat# ab192246), TOM20 (cat# ab186734), HIF-1α (cat# ab179483),

ATF5 (cat# ab184923), and VDAC1/Porin (cat# ab14734) was from Abcam, and HSP60 monoclonal antibody (cat# ADI-SPA-806-D, Enzo Life Science), YME1L1 (cat# 11510-1-AP, Proteintech), and Mn-SOD (cat# 06-984) was from Millipore Sigma. The β-actin antibody (cat# Sc-47778) was from Santa Cruz Biotechnology, United States. Respective secondary antibodies with HRP conjugates were diluted at 1:4000 in TBS and incubated at room temperature for 2 h. After washing in TBST (3 × 5 min) membranes were developed using SuperSignal® West Femto Stable peroxidase buffer (cat# 1859023, Thermo Scientific, United States) using a ChemiDoc™ XRS Molecular Imager (Bio-Rad Laboratories, United States). Restorer-restriping buffer (cat# 46430) was used for membrane stripping. The images were captured using the Image Lab software version 6 (Bio-Rad Laboratories, United States).

Isolation of Mitochondrial Proteins

Freshly isolated left-ventricle tissue of hearts were processed for the separation of cytosolic and mitochondrial fractions using pierce mitochondria isolation kit (cat# 89801) as per manufacturer's instructions. In brief, tissues were lysed and homogenized in series of extraction buffers and proceeds for mitochondrial and cytosolic protein isolation by centrifugations. CHAPS buffer (2% CHAPS in Tris buffered saline) was used to lyse the mitochondrial pellets at 4°C. Isolated proteins were quantified using standard BCA protein assay kit (cat# 23225) and processed for Western blot measurements.

Wheat Germ Agglutinin Staining

Wheat germ agglutinin (WGA) staining was performed on 5 μm transverse cryosections of the heart. Heart cryosections were prepared using a CryoStarNX50 (Thermo Fisher Scientific, United States) and fixed in 4% paraformaldehyde solution for 30 min. Sections were washed 2 × 5 min in TBS post-fixation and then incubated with WGA staining solution (5 mg/ml, cat# W834, Thermo Fisher Scientific, United States) for 15 min at RT. Next, sections were washed and mounted with coverslip, and images were captured using a fluorescence microscope (Olympus IX71 Imaging Systems) to measured mean cardiomyocyte diameter and numbers per unit area.

Masson's Trichrome Staining

To determine cardiac fibrosis, we performed Masson's trichrome staining, where the blue color staining represents collagen fibers. We used Masson's Trichrome kit (cat# 87019, Thermo Fisher Scientific, United States) to stain 5 μm paraffin transverse sections of the heart. We calculated perivascular (PV) and interstitial (INT) fibrosis by quantifying % blue pixel intensity/total pixel intensity of areas using color deconvolution tool of Fiji ImageJ software, NIH. We used the Tissue Core Facility of the University of Nebraska Medical Center for Masson's Trichrome staining procedure.

Picrosirius Red Staining

To corroborate Masson's trichrome staining results, we performed Picrosirius red staining. In brief, 10% formalin-fixed left ventricular paraffin sections (5 μm) were processed for picrosirius red staining. The reagents were Direct Red 80 (cat# 365548) and picric acid (cat# P6744-1GA) from Sigma Aldrich, United States, and glacial acetic acid (cat# A38-50) from Thermo Fisher Scientific, United States. We followed the standard kit protocol for this staining at the Tissue Core Facility of the University of Nebraska Medical Center.

Transmission Electron Microscopy

The left ventricular heart samples were processed for evaluation by transmission electron microscopy (TEM) as described previously (Nandi et al., 2020a). Briefly, 2 mm thin slices are immersion fixed with 2.5% glutaraldehyde and 2% paraformaldehyde in 0.15 M cacodylate buffer and post-fixed in 1% OsO4 in 0.1 M cacodylate buffer for 1 h on ice, followed by en bloc staining with 2–3% uranyl acetate for 1 h on ice. Next, the tissue slices are dehydrated using series of graded ethanol (20–100%) on ice followed by a single wash with 100% ethanol and subsequent two washes with acetone (15 min each) and finally embedded with Durcupan. Leica UCT ultramicrotome was used for ultrathin tissue sections (50–60 nm), which were adhered to Formvar and carbon-coated copper grids. Grids were stained with 2% uranyl acetate for 5 min and Sato's lead stain for 60 s. A JEOL JEM1400-plus Transmission Electron Microscope (JEOL, Peabody, MA, United States) was used to view the grids and a Gatan OneView digital camera with 4000 × 4000 resolution (Gatan, Pleasanton, CA, United States) was used to take the photographs. NIH ImageJ tool was used to calculate the area by manual tracing around the mitochondria and cristae. Mitochondrial area was calculated by dividing the total mitochondria area with the area of the cell and multiplied by 100. Likewise, cristae area was determined by dividing the total cristae area with the total area of mitochondria and multiplied by 100 as described previously, and the number of autophagosomes was also calculated as per our previous publication. All these quantifications were done with a blinded fashion.

Mito-SOX Staining of Heart Sections

Mitochondrial superoxide assay was performed using Mito-SOX Red (cat# M36008, Life Technologies, United States) staining, Mito-SOX is a fluorogenic dye that specifically stains mitochondrial superoxide in live cells. Oxidation of Mito-SOX produces red fluorescence upon binding to mitochondrial nucleic acid. H9c2 cells were incubated with 5 μM of Mito-SOX in incomplete medium and cells were incubated for 10 min at 37°C, followed by a quick wash with PBS, and images were captured immediately under a fluorescence microscope (Olympus IX71 Imaging Systems). The Mito-SOX intensity was quantified by ImageJ software (NIH, United States).

Immunohistology

Immunofluorescence (IF) histology was performed on 5 μm transverse cryosections. Standard protocol was used for these staining as per our previous publications (Nandi et al., 2016). The primary (1:100) and secondary antibodies (1:200) used were; HIF-1α (cat# ab179483), and Sarcomeric alpha-actinin (cat# ab9465) from Abcam, anti-mouse Alexa®Fluor 594 (cat# A21201) and anti-rabbit Alexa®Fluor 488 (cat# A21441) from Life Technologies, and anti-rabbit-HRP (cat# sc-2054) from Santa-Cruz Biotechnology. Images were captured using bright-field

microscope (Leica Microsystems, United States) and Olympus IX71 fluorescence Imaging Systems (Olympus, United States) respectively. Images were quantified using ImageJ software (NIH, United States).

Immunocytochemistry

Immunocytochemistry was performed on *in vitro* cultured rat H9c2 cardiomyocytes. In brief, cardiomyocytes were washed in PBS and fixed with 4% paraformaldehyde solution for 40 min. Cells were permeabilized with 0.025% Triton-X-100 (v/v) solution in PBS for 40 min and blocked in 1% sterile BSA solution for 60 min at RT. After blocking, cells were washed and incubated in 1:100 diluted primary antibody anti-ANP (cat# GTX109255, GeneTex, United States) in PBS at 4°C for overnight. On the next day, cells were washed in PBS and incubated with 1:200 dilution of anti-rabbit Alexa®Fluor 488 conjugated secondary antibody (cat# A11008, Life Technologies, United States). Cardiomyocyte nuclei were counterstained with 1 μg/ml DAPI in PBS (cat #A1001, AppliChem, United States) and Alexa®Fluor 594 Phalloidin (cat# A12381, Life Technologies, United States) was used to counterstain the F-actin filaments. Fluorescence images were captured by Olympus IX71 Imaging Systems (Olympus, United States) and quantified with ImageJ software (NIH, United States).

F-Actin Staining of Cardiomyocytes

Rat H9c2 cardiomyocytes were fixed with 4% paraformaldehyde for 40 min at RT, followed by permeabilization with 0.5% Triton-X-100 (v/v) in PBS for 40 min. After fixation, cells were incubated with Alexa Fluor®594 Phalloidin, 200 μM (cat# A12381, Life Technologies, United States) in PBS for 40 min and protected from direct light, and then washed with PBST. Images were captured by Olympus IX71 Imaging Systems (Olympus, United States) and the F-actin red intensity was quantified by ImageJ software (NIH, United States).

TMRE Assay

In order to evaluate mitochondrial membrane potential ($\Delta\Psi m$), cultured rat H9c2 cardiomyocytes are stained with TMRE dye (cat# T669, Life Technologies) as per the manufacturer's instruction. TMRE is a cell-permeant, cationic, red-orange fluorescent dye that is readily sequestered by active mitochondria. H9c2 cardiomyocytes are incubated with TMRE dye (50 nM) for 40 min at 37°C in incomplete DMEM medium following the manufacturer's instructions. Post-staining the TMRE-incubated medium is replaced with fresh incomplete DMEM medium, and fluorescent microscopic images are captured using a fluorescence microscope (Olympus IX71 Imaging Systems). TMRE intensity was quantified by ImageJ software (NIH, United States).

MiR-18a-5p Assay

Standard miRNA assay protocols were used for the quantification of miR-18a-5p levels (Nandi et al., 2016). We used total RNA extraction and TaqMan based primers for miRNA assays. In brief, the mirVana miRNA Isolation Kit (cat# AM1560) was used to extract total RNAs from heart and cultured cardiomyocytes. The highly pure quality of RNA (A260/A280 > 1.8–2.0) was quality checked by a NanoDrop 2000c (Thermo Fisher Scientific, United States). TaqMan miRNA reverse transcription kit (cat# 4366597, Life Technologies, United States) was used for the first strand synthesis, and then in the second step PCR reaction mixture was amplified using TaqMan based primers specific for miR-18a-5p (Assay ID:002422, Life Technologies, United States). TaqMan U6 SnRNA (assay ID: 001973, Life Technologies, United States) was used as an endogenous control for the miR-18a-5p. Bio-Rad CFX qPCR instrument (Bio-Rad Laboratories, United States) was used to run the PCR reaction mixtures and data were analyzed by a Bio-Rad CFX Manager software (Bio-Rad Laboratories, United States).

Luciferase Reporter Assay

We performed a miRNA target validation luciferase reporter assay using H9c2 cells. In brief, cells were transfected with lentiviruses either GFP-tagged miR-18a-5p (cat# RmiR6078) or scrambled miRNA (cat# CmiR0001), which were purchased from GeneCopoeia. We received custom-designed HIF-1α 3′ untranslated region (UTR) clones (WT 3′UTR: cat# RmiT050798; mutant 3′UTR: cat# CS-RmiT050798) from GeneCopoeia, Rockville, MD, United States. For luciferase reporter assay, we co-treated 1 μg of WT or mutant HIF-1α 3′UTR clones with either miR-18a-5p or GFP-scrambled overexpression for 48 h, and measured the relative firefly to Renilla luciferase activity using a Dual-Glow Luciferase Assay kit (cat# E2920, Promega Corp., Madison, WI, United States) and a GloMax-Multi + Detection System (Promega) following the manufacturer's manual.

MiRNA–mRNA Electrophoretic Mobility Shift Assay

We followed the published protocol for the miRNA–mRNA EMSA (Nandi and Mishra, 2017). For binding assay oligonucleotides were custom synthesized (IDT, United States). The sequences used are listed in **Table 2**. Probes were incubated in EMSA binding buffer (10 mM $MgCl_2$, 100 mM NaCl, 50 mM HEPES pH 7.2 and 5% glycerol) for 30 min at 37°C with corresponding WT or mutant 3′UTR oligonucleotides. Binding reactions were electrophoresed in a 12% PAGE (10 mM $MgCl_2$, 50 mM HEPES pH 7.2 and 5% glycerol) for 2 h at 190V at 4°C. EMSA was performed using fluorescence-based EMSA Kit (cat# E33075, Thermo Scientific Inc., United States) and labeling of the oligonucleotides was performed with SYBR green EMSA nucleic acid gel stain. The SYBR Green stained gel was scanned in a Chemidoc (ChemiDoc, Image Lab 4.1, Bio-Rad Laboratories, United States), using a SYBR Green filter with UV trans-illumination.

H9c2 Cardiomyoblast Culture, Differentiation and *in vitro* Treatment

The H9c2 rat myofibroblasts were cultured following the standard protocol ATCC®. Cells were cultured in DMEM high glucose (cat# D5796, Sigma) with 10% FBS (Sigma, F6178) and supplemented with 1% penicillin/streptomycin in a CO_2

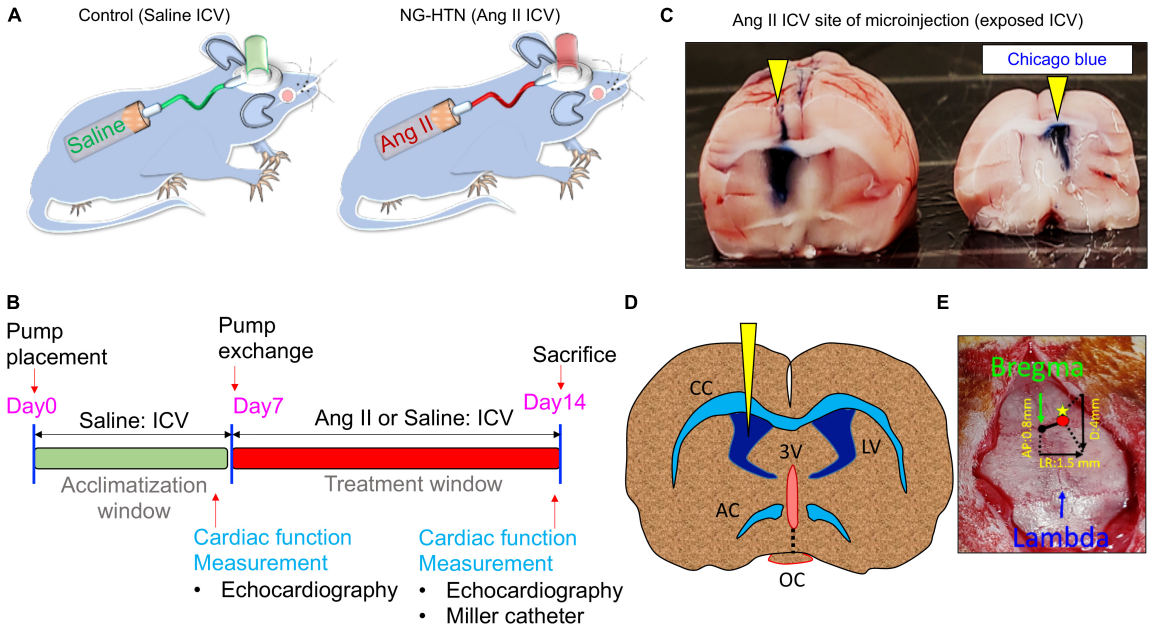

FIGURE 1 | Schematic showing chronic Ang II intracerebroventricular (ICV) infusion timeline and protocol to develop NG-HTN. **(A)** Schematic showing development of rat model of neurogenic hypertension *via* ICV Ang II brain minipump infusion. Sprague-Dawley rats (250–300 g) subjected to ICV Ang II brain minipump infusion (20 ng/min, 14 days, 0.5 μl/h) or vehicle (control, 0.9% sterile saline infusion) through osmotic mini-pumps. **(B)** Schematic timeline of treatment and cardiac function measurements. **(C)** Representative whole brain image showing exposed ICV cannulation site of Ang II or saline infusion confirmed by Chicago blue dye flushing through the cannulation tube at the time of sacrifice (yellow arrowheads). **(D)** Schematic coronal brain slice shown for ICV cannulation. **(E)** Stereotactic co-ordinate measurements of brain cannulation and ICV pump implantation, AP, LR, and D co-ordinate measurement are shown with a referenced from the bregma.

incubator (Thermoelectric Corporation, 800-WJ, United States) at 37°C with 5% CO_2. H9c2 myofibroblast were allowed to differentiate toward cardiomyocytes in presence of 1 μM retinoic acid (RA) and 1%FBS (cat# F2442, United States) for 7 days. Differentiated H9c2 were subjected to norepinephrine (2 μM) treatment for 48 h and post-treatment cell samples were trypsinized to isolate RNA and proteins using standard protocols. MiR-18a-5p mimic (cat# 4464066), inhibitor (cat# 4464084), and scrambled negative control (cat# 4464058) used for miRNA gain and loss of function assays were from Life Technologies. The pDsRed2-Mito Vector (cat# 632421) was from Clontech.

Statistical Analysis

Data are presented as mean ± SE. Means ± SE between two groups were compared with a Student's *t*-test. Differences between more than two groups were determined by one- or two-way ANOVA, followed by the Tukey's multiple comparisons test for *post hoc* analysis if there was a significant interaction using Prism7.0 GraphPad software. *P*-value < 0.05 is considered statistically significant.

RESULTS

Neurogenic Hypertension, Cardiac Hypertrophy, and Fibrosis

The consequence of ICV infusion of Ang II was an increase in MAP compared to the Saline (ICV) infused Control group (125 ± 8 mmHg; Ang II vs. 83 ± 4 mmHg; Saline) with a concomitant increase in cardiac sympathetic tone (95 ± 6 bpm; Ang II vs. 73 ± 6 bpm Saline) as well as basal renal sympathetic nerve activity (19.8 ± 2.0%, Ang II vs. 6.9 ± 1.9%; Saline of Max). In addition, the left ventricular end diastolic pressure (LVEDP) increased slightly in NG-HTN (3.6 ± 0.5 mmHg; NG-HTN vs. 2.0 ± 0.3 mmHg; Control) but not significantly. There was an increase in HW/BW(g) ratio (4.5 ± 0.4; NG-HTN vs. 2.8 ± 0.06; Control). Echocardiography measurements showed decreased mitral filing velocity (E/A ratio, NG-HTN: 1.2 ± 0.1 vs. 1.5 ± 0.2; Control), which confirmed that rats with NG-HTN developed diastolic heart failure. Furthermore, cardiac contractile responsiveness to isoproterenol (0.5 μg/kg ISO) was significantly lower for negative dP/dt in NG-HTN rats (NG-HTN: −8581 ± 661 vs. −11,765 ± 708; Control) which is indicative of abnormal diastole or relaxation in NG-HTN rats. Additional characteristics and experimental timeline details of Control and NG-HTN rats are provided in the **Figures 1A–E** and **Table 1**.

To characterize and identify features of cardiac remodeling in NG-HTN we measured morphometry, hypertrophy, and indices of fibrosis in the heart. First, to investigate whether NG-HTN cause a change in the gross cardiac shape and size we monitored heart morphometry along with the left ventricular anatomy (**Figure 2A**). The results showed that NG-HTN increased LV wall-thickness. Next, we analyzed heart weight to body weight ratio (HW:BW), which showed an increase in the

TABLE 1 | Characteristics of Control and NG-HTN rats used in the studies.

Parameters	Control (n = 6)	NG-HTN (n = 6)
Body weight; BW (g)	331.1 ± 11.2	235.3 ± 18.2*
Heart weight; HW (g)	0.94 ± 0.02	1.03 ± 0.03*
HW/BW × 1000	2.86 ± 0.06	4.54 ± 0.45*
Heart rate; HR (bpm)	372 ± 13	386 ± 11
+dP/dt (mmHg/s)	7258 ± 486	7778 ± 404
−dP/dt (mmHg/s)	7987 ± 860	8387 ± 561
MAP (mmHG)	83 ± 4	125 ± 8
LVEDP (mmHg)	2.0 ± 0.3	3.6 ± 0.5
E/A	1.5 ± 0.2	1.2 ± 0.1*
%EF	69 ± 5%	67 ± 2%
−dP/dt with ISO	−11,765 ± 708	−8581 ± 661*

*LVEDP, left ventricular end-diastolic pressure; MAP, mean arterial pressure; HR, heart rate; EF, ejection fraction; ISO, Isoproterenol. Data are represented as mean ± SE of six rats in each group. *P < 0.05 sham vs. NG-HTN. Student's t-test.*

NG-HTN group compared to Control group, suggesting cardiac hypertrophy in rats with NG-HTN (**Figure 2B**). To further validate cardiac hypertrophy, we performed H&E staining of the longitudinal whole heart sections in order to visualize the atrial and ventricular wall histology. Our results confirmed an increase in gross heart size and thickening of the left ventricular wall in NG-HTN rats (**Figure 2B**, top panel). WGA-Fluorescein (Wheat Germ Agglutinin-Fluorescein) staining of the left ventricular transverse sections (**Figure 2B**, bottom panel) determined the hypertrophic changes at the level of the cardiomyocyte. WGA is a lectin, which specifically stains the sialic acid and N-acetylglucosaminyl residues delineating cardiomyocyte boundaries allowing the quantification of cardiomyocyte number and diameter per unit area of left ventricular tissue. NG-HTN increased cardiomyocyte size and decreased the number of cardiomyocytes per unit area of left ventricular section (**Figure 2B**) suggesting pathological hypertrophic changes at the level of cardiomyocytes. Masson's trichrome staining on transverse and longitudinal cardiac sections (**Figure 2C**, top and middle panel) determined widespread cardiac fibrosis (blue). This was corroborated by similar increase in perivascular, and interstitial collagen deposition (red) in picrosirius red stained hearts NG-HTN group (**Figure 2C**, bottom panel). Our data demonstrate an increase in perivascular and interstitial collagen deposition in NG-HTN rats (**Figure 2C**), indicating an increase in cardiac fibrosis. Taken together, the cardiac pathology associated with our model of NG-HTN showed hypertrophic cardiomyopathy that is similar to cardiomyopathy complications commonly observed in patients with hypertension.

Neurogenic Hypertension and Cardiac Mitochondrial Dysfunction

Mitochondrial Abnormality

Alterations in mitochondrial ultrastructure, at the level of the cristae, were examined by electron microscopy (EM) on left ventricular tissues from Control and NG-HTN rats. NG-HTN resulted in marked decrease in mitochondrial area (by 36%) as well as decrease in cristae area in subsarcolemmal (SSM: by 42%) and inter/intra-myofibrillar mitochondria (IFM: by 38%) (**Figures 3A–H,M–O**), indicating a reduced in mitochondrial quality control mechanisms and function. While increased numbers of microautophagosomes (MiAPs) were detected in NG-HTN hearts compared to WT hearts, macroautophagosomes (MeAPs) were exclusively observed in the NG-HTN hearts (**Figures 3I–L,P,Q**) implicating profound changes caused by NG-HTN. Marked decrease in mitochondrial abundance coupled with significant decrease in cristae surface area indicate compromised heart function in NG-HTN group.

Mitochondrial ROS Generation, Depolarization, and Altered Oxidative Phosphorylation

Mitochondrial superoxide staining of cardiac tissue sections using mitochondrial superoxide-specific dye Mito-SOX red, was performed to evaluate altered mitochondrial reactive oxygen species in hearts from rats with NG-HTN. There was an increase in Mito-SOX red intensity in the hearts of NG-HTN compared to Control rats (**Figure 4A**). To address the mechanism of increased superoxide we measured Mn-SOD protein level in control and NG-HTN heart lysate (**Figure 4B**). Our results showed that Mn-SOD protein level is decreased in the heart of NG-HTN. These results suggest a downregulated antioxidant defense mechanism resulting in an increased mitochondrial ROS generation. The direct effect of NE on mitochondrial ROS and mitochondrial transmembrane potential ($\Delta\Psi m$) markers were evaluated by Mito-SOX staining assay in control and NE-treated H9c2 cardiomyocytes. NE caused an increase in Mito-SOX red intensity in isolated cardiomyocytes (**Figure 4C**), suggesting that depolarized $\Delta\Psi m$ induces mitochondrial superoxide production. Next, to assess mitochondrial depolarization, we performed TMRE (Tetramethylrhodamine, ethyl ester) assay in H9c2 cardiomyocytes. NE-treatment decreased mitochondrial $\Delta\Psi m$, as indicated by a decrease in the TMRE red intensity in cardiomyocytes treated with NE (**Figure 4D**) and associated with cardiomyocyte hypertrophic changes (**Figures 5A–E**). These results suggest that NE-drive increased ROS, but decreased $\Delta\Psi m$ in NG-HTN.

We further examined whether NG-HTN induces mitochondrial OXPHOS/respiratory dysfunction and altered expression of mitochondrial OXPHOS Complexes I, -II, -III, -IV, and -V, proteins. Although NG-HTN significantly increased Complex-I, II, IV, and V, Complex-III remained unchanged (**Figure 6A**). These results indicate an altered OXPHOS and a shifted mitochondrial metabolism in the hearts of rats with NG-HTN. This is possibly due to increased Complex-I expression that accepts reduced NADH carried energy to force protons into the mitochondrial intermembrane space for ATP synthesis *via* Complex-V. Our results demonstrate that OXPHOS supercomplex subunit abundance is increased in NG-HTN whole heart lysate, therefore we further compared the OXPHOS subunit level in cytosol vs. isolated mitochondria to distinguish a subunit assembly over an import defects. Our results confirmed that increased Complex-I and –IV, and

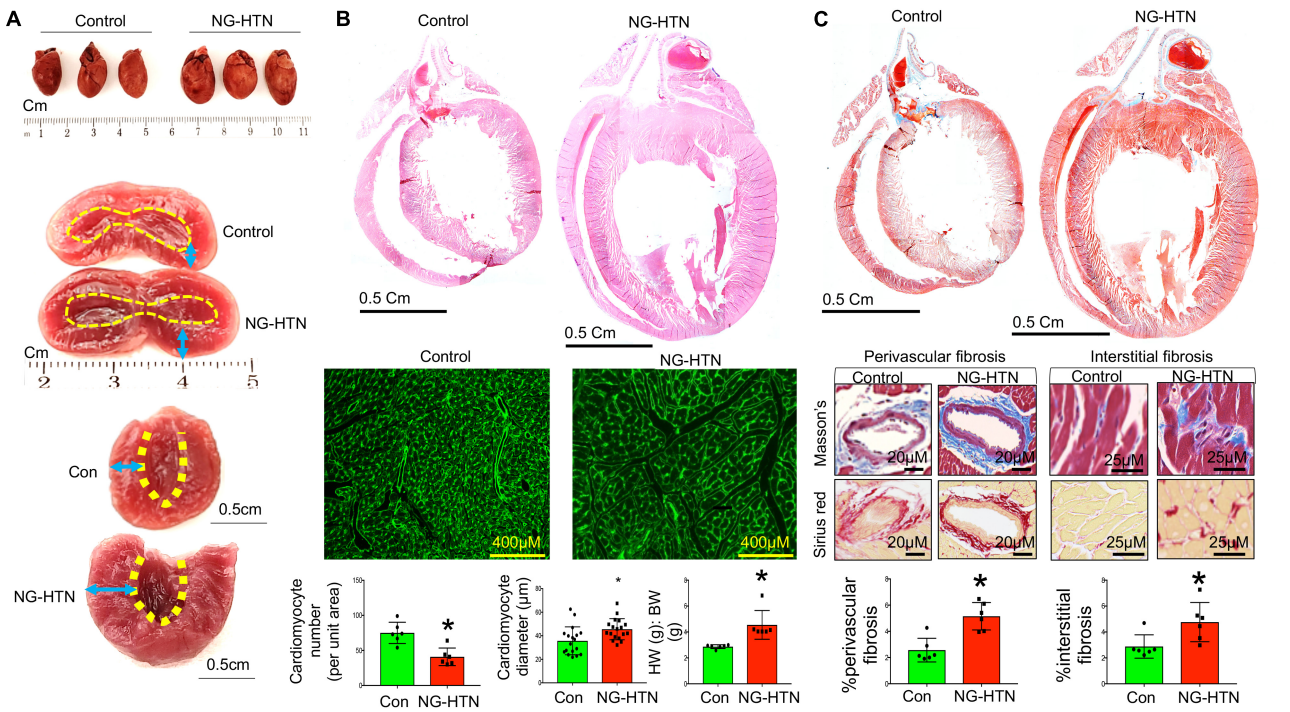

FIGURE 2 | Neurogenic hypertension induces cardiac hypertrophy and fibrosis. **(A)** Top, whole heart images of control and NG-HTN hearts, $n = 3$. Middle, representative image showing exposed hearts chambers. Bottom, endocardium outlined with dotted line, arrow space highlights wall thickness. **(B)** Top, HE stained images showing longitudinal whole heart sections of control and NG-HTN rats. Middle, WGA-488 staining of heart sections, green represents cardiomyocyte boundaries stained with WGA. Bottom, quantifications of cardiomyocyte numbers (each dot represent number of cardiomyocytes count per image, $n = 6$ rats) and cardiomyocyte diameter (μm, per unit area, each dot represent individual cardiomyocytes diameter per section from $n = 6$ rats), and heart weight (HW) to body weight (BW) ratio in control vs. NG-HTN rats, $n = 6$ rats. **(C)** Top, representative Masson's trichrome (MT) stained longitudinal whole heart sections, blue represents collagen staining. Middle, representative MT (blue), and Picrosirius (red) images of whole heart sections showing perivascular and interstitial fibrosis. Bottom, quantification for % fibrosis in control and NG-HTN rats, each dot represents Mansson's blue intensity per unit area. Values are presented as mean ± SEM, $n = 6$. $^*P < 0.05$ vs. Control, Student's *t*-test.

-V abundance in mitochondrial compartments of NG-HTN hearts compared to control hearts (**Figure 6B**), while their cytosolic levels were comparable. These results support an OXPHOS subunit assembly defect perhaps associated with misfolded peptide accumulation due to reduced mitochondrial proteases activation.

Mitochondrial Biogenesis and Fusion/Fission Dynamics

Mitochondrial biogenesis, was assessed by measuring relative mt-DNA content compared to the nuclear DNA content. In addition, mitochondrial fission was evaluated by measuring the level of FIS1 that facilitates the fission of mitochondria. Levels of OPA1 that facilitates fusion of mitochondria, in combination with mitochondrial fragmentation and mitophagy vacuoles were assessed by EM (**Figure 7C**). Mitochondrial relative DNA content was significantly lower in the NG-HTN group suggesting decreased mitochondrial biogenesis (**Figure 7A**). Furthermore, mitochondrial fission marker FIS1 and mitophagosome abundances were increased but mitochondrial fusion marker OPA1 was decreased in NG-HTN compared to Control hearts (**Figures 7B,C**). This was corroborated by, our *in vitro* data with H9c2 cardiomyocytes treated with NE showing a decrease in mitochondrial biogenesis (**Figure 7D**). Overall, these data support the general hypothesis that mitochondrial biogenesis, dynamics, and mitophagy are suppressed with enhanced neurogenic tone in NG-HTN hearts.

Mitochondrial Proteinopathies

To determine if NG-HTN causes changes in mitochondrial protein import, TIM and TOM translocase, key sub-units involved in mitochondrial protein import were measured. Levels of TOM20 are decreased in NG-HTN, while levels of TIM17 are increased (**Figures 7E,F**), which indicates an altered mitochondrial protein import efficiency and YME1L1 protease activation (Rainbolt et al., 2013; **Figures 8C,F**) and thus associated with the overall compromised mitochondrial proteostasis in the hearts of rats with NG-HTN.

Mitochondrial Proteotoxic Stress

To determine if NG-HTN causes mitochondrial proteotoxic stress and downregulates UPR^{mt} we measured levels of ATF5, a hallmark UPR^{mt} marker (**Figures 8C,D**). In the absence of mitochondrial stress, ATF5 is targeted to mitochondria and accumulates within mitochondria. However, during

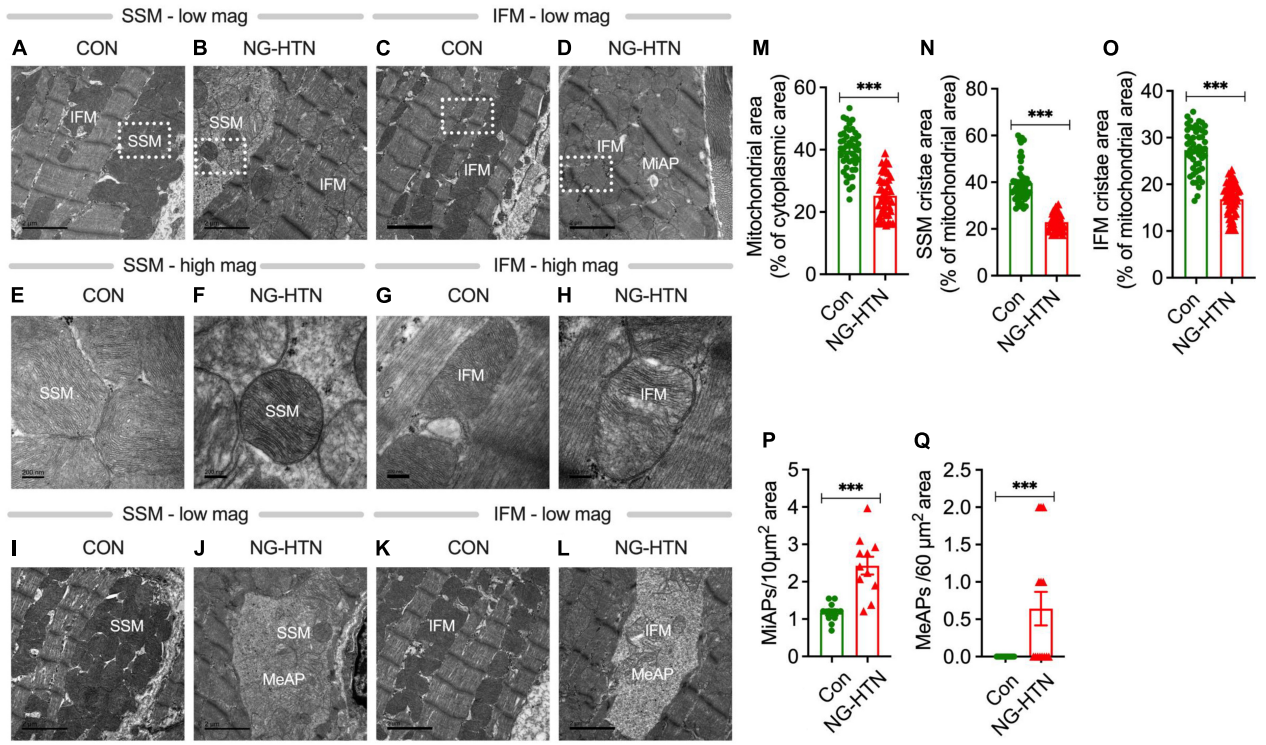

FIGURE 3 | Neurogenic hypertension and cardiac mitochondrial injury. **(A–D)** Low magnification EM micrographs showing mitochondrial population and microautophagosomes. **(E–H)** Higher magnification of a selected area in **(A–D)** showing the mitochondrial ultrastructure abnormalities. **(I–L)** Low magnification EM micrographs showing macroautophagosomes. Morphometric analyses: **(M)** mitochondrial area, **(N)** SSM cristae area, **(O)** IFM cristae area, **(P)**, microautophagosomes, and **(Q)** macroautophagosomes. Mitochondrial area was calculated from 15 micrographs per rat heart (dot represents 45 individual mitochondria counts), $n = 3$ rats. Cristae area was calculated from at least 15 micrographs from each rat (dot represents 50 individual mitochondria counts), $n = 3$ rats. Microautophagosomes were calculated from 11 micrographs representing $n = 3$ rats, dot represents numbers per unit area. Megaautophagosomes were calculated from 14 micrographs representing 3 rats, dot represents numbers/unit area. ***$P < 0.001$ vs. Control, Student's *t*-test. Scales bars: **(A–D)**, 2 nM; **(E–H)**, 200 nM; and **(I–L)**, 2 nM.

mitochondrial respiratory chain dysfunction, high levels of ROS, and during mitochondrial protein folding stress, ATF5 fails to import into mitochondria and a percentage of ATF5 accumulates in the cytosol and traffics to the nucleus where it activates the UPR^{mt} that promote cascade of gene activation for mitochondrial proteostasis and the recovery of depolarized/defective mitochondria. Our results suggest that ATF5 protein level is reduced in both, cytosol and in mitochondria of NG-HTN hearts compared to control hearts, suggesting an UPR^{mt} downregulation in NG-HTN (**Figures 8C,D**). Since ATF5 increased HSP60 therefore we measured and compared HSP60 protein level in cytosol, mitochondria, as well as in whole heart tissue lysates (**Figure 8A**). The heat shock protein 60 (HSP60, is another UPR^{mt} marker downstream of ATF5), which is a chaperon responsible for refolding and transportation of nuclear-encoded mitochondrial proteins from the cytoplasm into the mitochondrial matrix under stress conditions. There was increased UPR^{mt} activation marker HSP60, in the NG-HTN group whole heart tissue lysate indicating an altered mitochondrial proteotoxic stress in response to mitochondrial abnormality (**Figure 8A**). However, further analyses of HSP60 in cytosol to mitochondria showed that HSP60 protein level is decreased in cytosol but increased in mitochondrial compartments of NG-HTN (**Figures 8C,E**). Furthermore, our *in vitro* data using H9c2 cardiomyocytes treated with NE showed congruent result of increased HSP60 in whole cell lysate (**Figure 8B**). To understand a mechanistic link to these observations, we studied the mitochondrial AAA (ATPases associated) YME1L1 protease that involved in the quality control and processing of mitochondrial inner-membrane proteins. Reports suggests that YME1L1 (a mitochondrial AAA protease) controls the accumulation of respiratory chain supercomplex subunits and depletion of YME1L1 led to excessive accumulation of non-assembled respiratory chain subunits (Ndufb6, ND1, and Cox4) in the inner membrane (Stiburek et al., 2012; Rainbolt et al., 2013). Therefore, we investigated the activity of YME1L1 in the mitochondrial compartment of NG-HTN hearts and control hearts. Our results demonstrate the YME1L1 is highly suppressed in the mitochondria of NG-HTN (**Figures 8C,F**), supporting the hypothesis of non-assembled/misfolded mitochondrial inner membrane OXPHOS proteins accumulation (**Figure 6B**). All these results suggests that a decreased ATF5 import, and lack of UPR^{mt} activation increased OXHOS assembly defects in the mitochondria

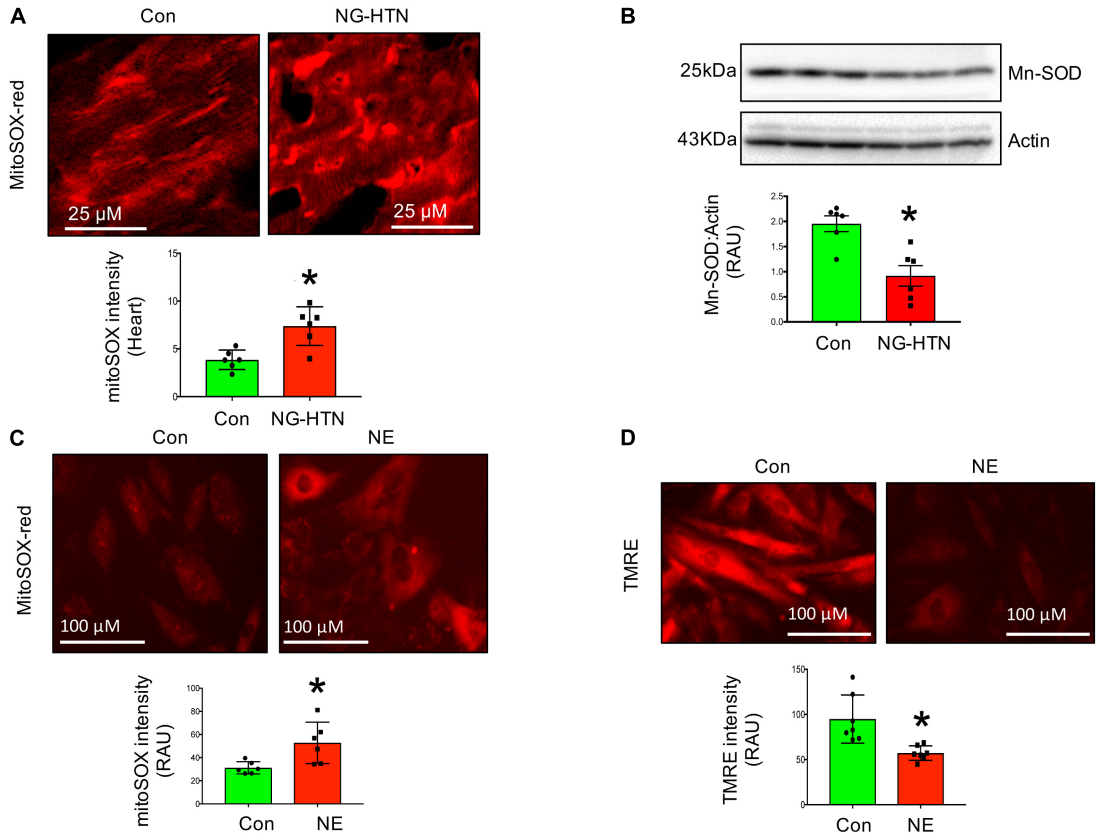

FIGURE 4 | Neurogenic hypertension and cardiac mitochondrial quality control events. **(A)** Top, Mito-SOX red (mitochondrial ROS marker) staining of control and NG-HTN heart sections. Bottom, quantification of Mito-SOX intensity. **(B)** Western blot to assess Mn-SOD protein level in control and NG-HTN whole hearts lysate, bottom, WB quantification of Mn-SOD. **(C)** Live cell Mito-SOX imaging and quantification showing Mito-SOX intensity in control and NE-treated H9c2 cardiomyocytes. **(D)** Live cell TMRE imaging and quantification showing mitochondrial membrane potential ($\Delta\Psi m$) in control and NE-treated H9c2 cardiomyocytes. Values are mean ± SEM, $n = 6$ rats, $^*P < 0.05$ vs. Control, Student's *t*-test.

of NG-HTN hearts. Overall, our data support the notion that an exaggerated neurogenic drive causes mitochondrial proteotoxic stress.

Neurogenic Hypertension Reduces MiR-18a-5p but Increases Cardiac HIF-1α

Levels of miR-18a-5p are significantly decreased in the hearts of rats with NG-HTN (**Figure 9A**). Further, our *in silico* data predicted that miR-18a-5p targets HIF-1α 3′UTR mRNA (**Figure 9C**). HIF-1α protein expression was evaluated using Western blotting of left ventricular cardiac tissues of Control and NG-HTN groups. HIF-1α protein levels are increased in the NG-HTN compared to Control rats (**Figure 9D**). Further, immunofluorescence of HIF-1α demonstrated a distinct increase in cellular and nuclear immunolabeling of HIF-1α in cardiomyocytes of rats with NG-HTN (**Figure 9E**). Consistent with these data, direct treatment of NE on H9c2 cardiomyocytes *in vitro,* demonstrated reduced miR-18a-5p level with a concomitant increase in the expression of HIF-1α as well as cardiomyocyte hypertrophy (**Figures 5A–E**, **9B,F**). To further examine the relationship between miR-18a-5p and HIF-1α we transfected H9c2 cardiomyocytes with miR-18a-5p or anti-miR-18a-5p mimic probes to elicit either miRNA gain or loss of function, respectively, and then examined HIF-1α protein levels after 24 h treatment. In addition, we transfected cardiomyocytes with scrambled (scm) miRNA as a negative "control mimic." Loss of miR-18a-5p significantly increased HIF-1α protein levels in cardiomyocytes (**Figure 10A**), which indicates that miR-18a-5p inhibits the expression of HIF-1α, however in normal or unstressed cells miR-18a-5p mimic forced overexpression maintains basal HIF-1α protein level by finetuning mRNA stability and protein translation. Notably, the gain of function by miR-18a-5p overexpression efficiently blunted NE-induced HIF-1α increase in H9c2 cardiomyocytes (**Figure 10B**).

To further investigate whether, increased HIF-1α contributes to a change in mitochondrial dynamics in cardiomyocytes we monitored the mitochondrial network using pDsRed2-Mito plasmid transfection in the cardiomyocytes, a mitochondria-reporter clone that visualizes mitochondria network with red fluorescence. The pDsRed2-Mito vector transfection visualized tubular shaped mitochondrial structures to identify fused mitochondria and globular shaped structures representing

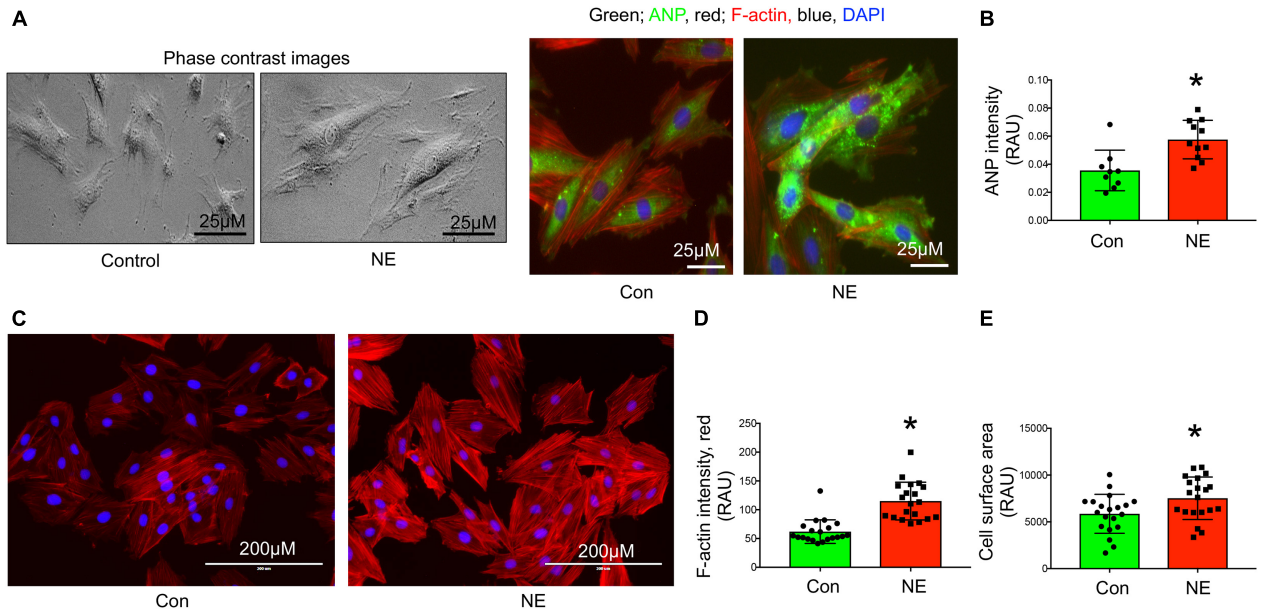

FIGURE 5 | Norepinephrine induced hypertrophy in H9c2 rat cardiomyocytes. **(A)** Representative phase contrast and immunocytochemistry images showing cardiomyocyte hypertrophy marker ANP localization in control and NE-treated H9c2 cardiomyocytes. **(B)** Bargraph showing quantification of ANP intensity (green), $n = 10$ cells per group, dot represent individual cell intensity from three independent experimental groups. **(C)** Representative images showing F-actin staining using Alexa®Fluor 594 Phalloidin conjugate dye of control and NE-treated H9c2 cardiomyocytes. Red, F-actin; blue, DAPI stained nucleus. **(D)** Bargraph showing quantification of F-actin intensity and **(E)** cell surface area measurement in control and NE-treated H9c2 cardiomyocytes, $n = 20$ cells per group, dot represent individual cells intensity or area from three independent experimental groups. Data are presented as mean ± SEM. *P-values < 0.05 considered as significant, Student's t-test.

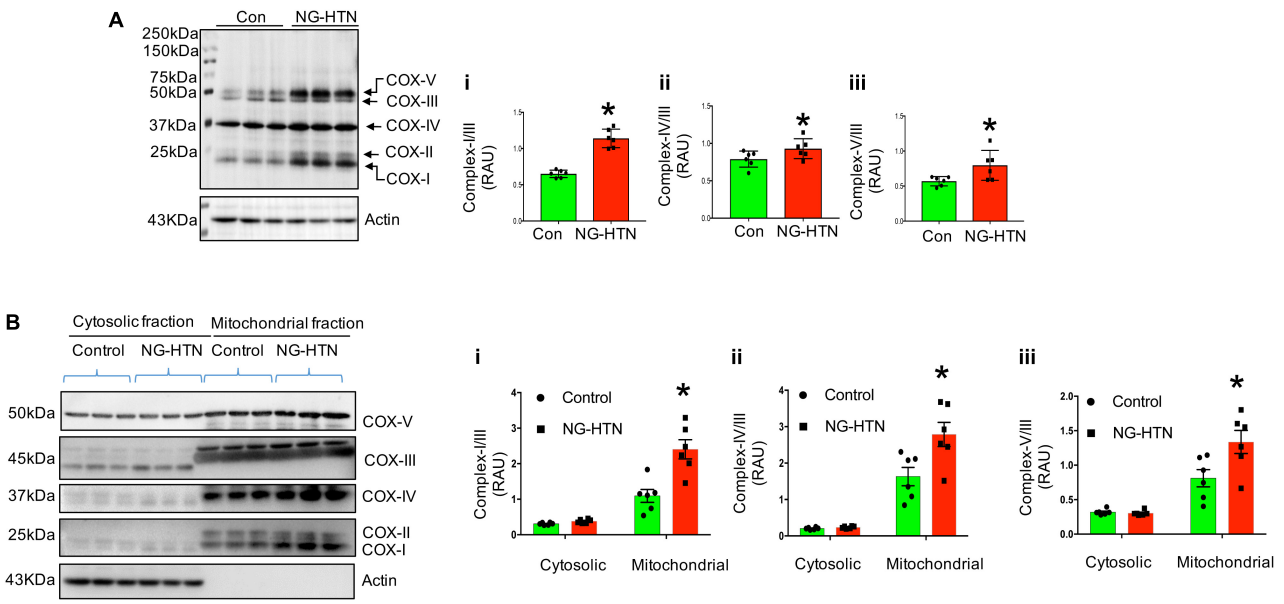

FIGURE 6 | Neurogenic hypertension and cardiac mitochondrial defective OXPHOS subunit assembly/import. **(A)** Left, Western blot showed mitochondrial OXPHOS complex protein level in control and NG-HTN whole hearts lysate (total OXPHOS WB antibody cocktail, cat# ab110413, Abcam). Right, (i–iii) WB quantification of mitochondrial Complex-I/III, Complex-IV/III, and Complex-V/III ratio, respectively. **(B)** Left, Western blots showed mitochondrial OXPHOS complex protein level in cytosol vs. mitochondria fraction in control and NG-HTN hearts. Right, (i–iii) Western blot quantification of mitochondrial Complex-I/III, Complex-IV/III, and Complex-V/III ratio, respectively. Values are mean ± SEM, dot represents $n = 6$ rats, *$P < 0.05$ vs. Control, **(A)**, Student's t-test, **(B)**; two-way ANOVA with Tukey's multiple comparison test.

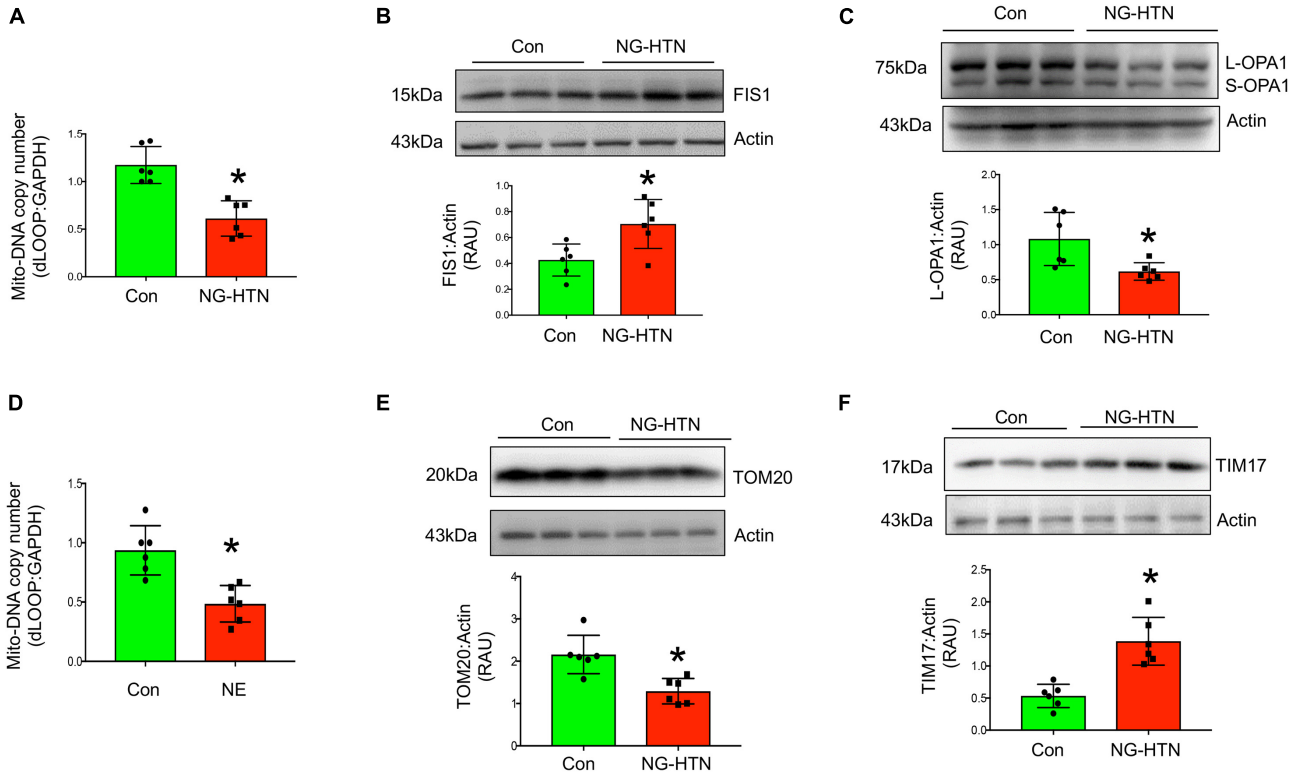

FIGURE 7 | Neurogenic hypertension induces shifts in cardiac mitochondrial dynamics and protein transport. **(A)** Measurement of relative d-LOOP/GAPDH DNA ratio by qPCR from control and NG-HTN hearts. **(B,C)** Western blot representative and quantification showing expression of FIS1 and OPA1 level, receptively, normalized to Actin in control and NG-HTN hearts. **(D)** Measurement of relative d-LOOP/GAPDH DNA ratio by qPCR in control and NE-treated H9c2. **(E,F)** Representative Western blot and quantification showing expression of TOM20 and TIM17 level, respectively, normalized to Actin. Values are mean ± SEM, dot represents $n = 6$ rats, $^*P < 0.05$ vs. Control, Student's *t*-test.

fragmented mitochondria. Our results demonstrated that anti-miR-18a-5p treatment increased fragmented or globular mitochondrial structures indicating increased mitochondrial fission (**Figure 10C**).

Link Between MiR-18a-5p and HIF-1α

In silico analysis indicates that HIF-1α is a potential target for miR-18a-5p (**Figure 9C**). To determine whether miR-18a-5p targets HIF-1α 3′ untranslated region (3′UTR), we performed luciferase reporter assay using WT 3′UTR and mutant 3′UTR clones of HIF-1α (**Figures 11A,B**). In Mut HIF-1α 3′UTR clone the miR-18a-5p binding seed sequence region on 3′UTR of HIF-1α was mutated. The H9c2 rat cardiomyocytes were transfected with either with WT HIF-1α 3′UTR or Mut HIF-1α 3′UTR luciferase assay clones, with miR-18a-5p or scrambled miRNAs overexpression and then the relative firefly to Renilla luciferase activities was assessed. MiR-18a-5p decreased relative firefly to Renilla luciferase activity in WT HIF-1α 3′UTR compared to scrambled, suggesting that miR-18a-5p targets WT HIF-1α 3′UTR. As anticipated, luciferase activity remained unchanged with miR-18a-5p mimic treatment to Mut HIF-1α 3′UTR (**Figure 11B**), which confirms that miR-18a-5p targets HIF-1α 3′UTR.

To further confirm that miR-18a-5p target HIF-1α 3′UTR seed sequence, we performed miRNA–mRNA electrophoretic mobility shift assay (miRNA–mRNA EMSA; Nandi and Mishra, 2017) using WT HIF-1α 3′UTR and Mutant HIF-1α 3′UTR EMSA oligonucleotide probes in the presence and absence of miR-18a-5p or anti-miR-18a-5p mimic probes (**Table 2**). In miRNA-EMSA, the miR-18a-5p and anti-miR-18a-5p display one band (**Figure 11C**, lanes 3 and 4). The incubation of miR-18a-5p with an equimolar (300 nM) concentration of anti-miR-18a-5p reduces the mobility of miR-18a-5p band due to the formation of miR-anti-miR dimer complex (**Figure 11C**, lane 5). Furthermore, the miR-18a-5p probe incubation with three different concentrations (1, 2, and 4 μM) of WT HIF-1α 3′UTR form a low mobility second band of miR-18a-WT HIF-1α 3′UTR complex (**Figure 11C**, lanes 9, 10, and 11). This second band represents the binding of the miR-18a-5p with WT HIF-1α 3′UTR seed binding sequence. Noticeably, there was an increased band intensity of this second band with increasing concentrations of WT HIF-1α EMSA probe (**Figures 11C,D**, lanes 9, 10, and 11). To further verify the specificity of miR-18a-5p-WT HIF-1α 3′UTR complex, we used respective concentrations (1, 2, and 4 μM) of Mut HIF-1α 3′UTR EMSA probes, which had mismatch mutations with the miR-18a-5p seed sequence binding region. As expected, we did not

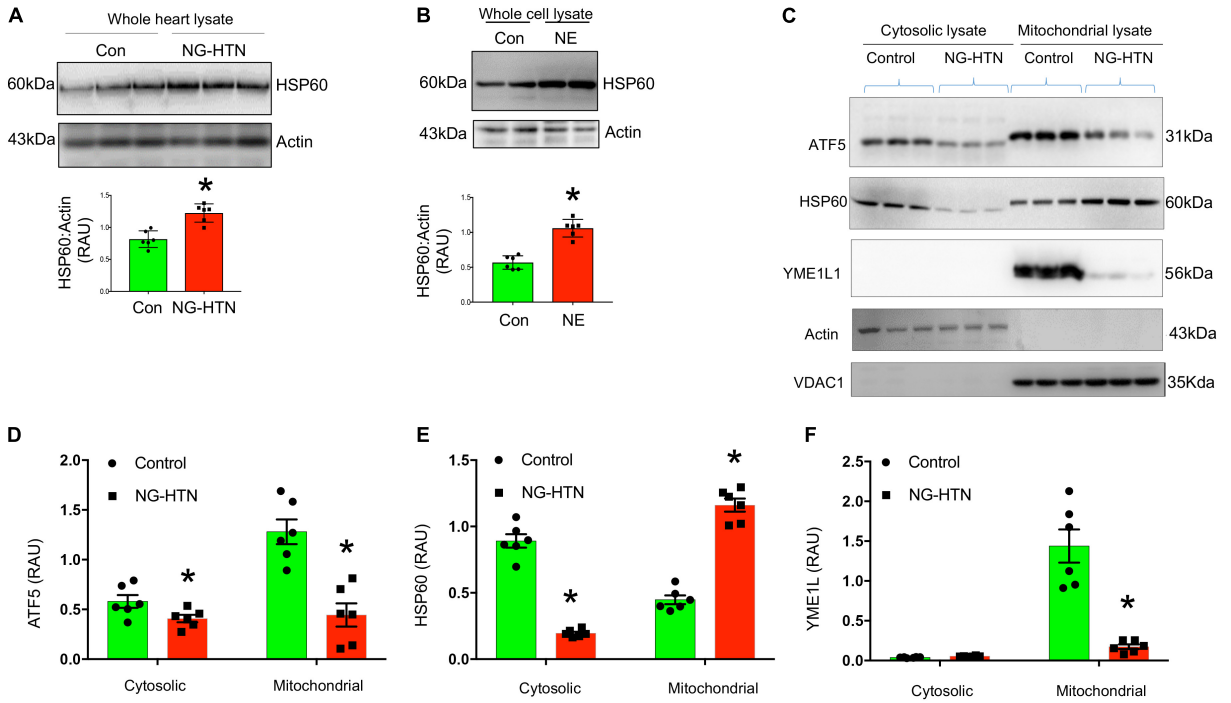

FIGURE 8 | Neurogenic hypertension (NG-HTN) downregulates mitochondrial UPR (UPR^{mt}). **(A)** Representative Western blots and quantification of cardiac HSP60 expression normalized to Actin in control and NG-HTN whole hearts lysate. **(B)** Representative Western blots and quantification of HSP60 expression normalized to Actin in NE-treated H9c2 whole cell lysate. **(C)** Representative Western blots and **(D–F)** quantifications of cytosol vs. mitochondrial ATF5, HSP60, and YME1L1 expression level normalized to loadings controls in NG-HTN and control hearts. Values are mean ± SEM, dot represents $n = 6$ rats, $^*P < 0.05$ vs. Control, **(A,B)**, Student's *t*-test, **(D–F)**; two-way ANOVA with Tukey's multiple comparison test.

observe a low mobility second band formation with Mut HIF-1α 3′UTR probes suggesting an absence of miR-18a-5p-Mut-HIF-1α 3′UTR complex formation (**Figure 11C**, lanes 6, 7, and 8). Altogether, our target validation data demonstrated the specificity of miR-18a-5p binding to WT HIF-1α 3′UTR, which confirms that miR-18a-5p targets HIF-1α and mitochondrial function (**Figures 11**, **12**).

DISCUSSION

There is a strong link between cardiac pathogenesis and changes in mitochondrial quality and function. However, mitochondrial changes in the progression of cardiac diseases is not yet fully understood, particularly little is known as to how mitochondrial dysfunction is initiated in cardiac disease to cause final cardiac pathology. The present study shows that central Ang II infusion causes enhanced sympatho-excitation that leads to hypertension in rats. In response to sympatho-excitation, these hypertensive rats demonstrate pathological cardiac hypertrophy and fibrosis, with concomitant abnormal mitochondrial function due to multiple events, such as altered mitochondrial ultrastructure, compromised OXPHOS, impaired structural dynamics and biogenesis, suppressed UPR^{mt} and protein quality control that is associated with reduced proteostasis, altered pre-protein transport activities, impaired mitophagosome clearance and increased ROS generation. At the same time there was decreased miR-18a-5p expression (a cardiac anti-hypertrophic, anti-fibrotic) and increased HIF-1α level (a glycolytic activator that suppress mitochondrial metabolism and function) in the hearts of rat with NG-HTN. Further, we observed an inverse relationship between miR-18a-5p expression and HIF-1α levels. Finally, we demonstrated that norepinephrine directly down-regulates miR-18a-5p expression. Taken together, these data demonstrates that enhanced sympathetic tone initiates a reduction in miR-18a-5p expression, a potential HIF-1α targeting miRNA which in turn allows for an increase in HIF-1α levels that leads to altered cardiac metabolic shift and increased ROS generation mediated mitochondrial dysfunction. These results are consistent with cardiac mitochondrial complications that are reported during hypertension, such as increased cellular/mitochondrial ROS, compromised mitochondrial OXPHOS, and mitochondrial abnormality (Eirin et al., 2014; Power et al., 2016). It is postulated that persistence cardio-neuronal norepinephrine overstimulation in the heart of rat with NG-HTN activates cytosolic and mitochondrial Ca_2^+ overload that results in increased Calcium–Calcineurin–NFAT, and enhanced noradrenergic tone induced desensitization of β-AR signaling *via* receptor internalization (Almela et al., 2020; Boyman et al., 2021). These changes need an adaptive shift in mitochondrial energy fueling and QC changes to accommodate the hypertensive cardiac contractility, requiring increased

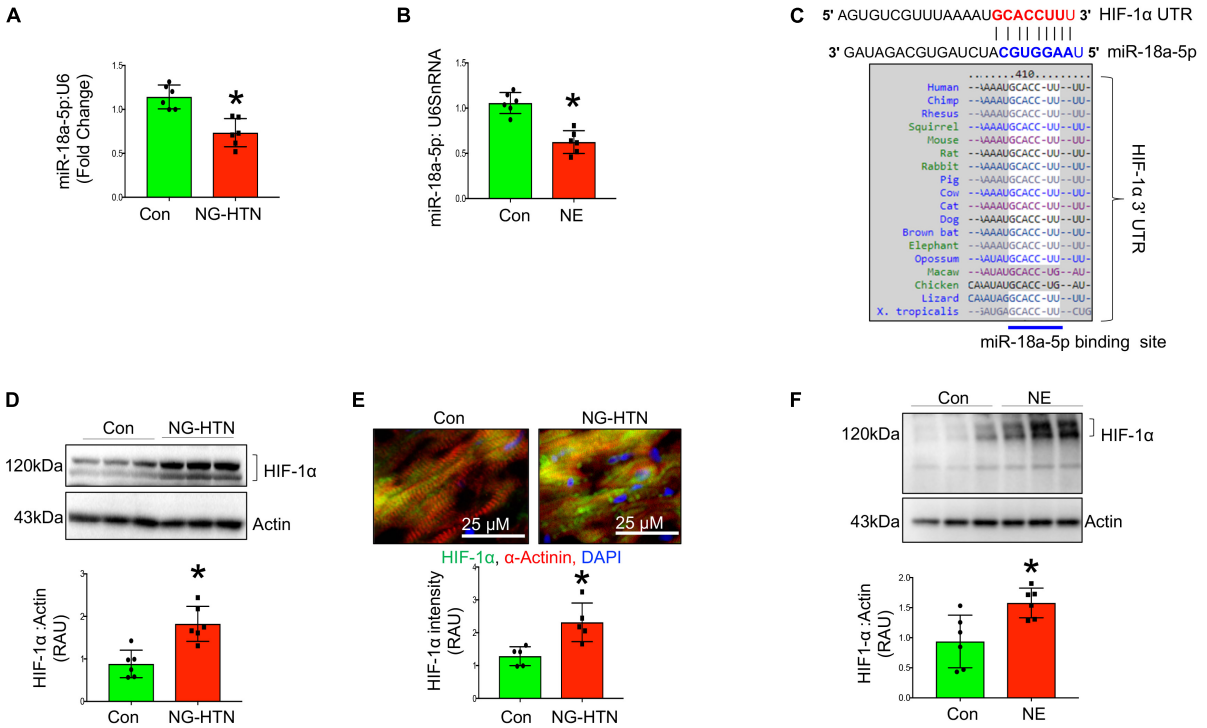

FIGURE 9 | Neurogenic hypertension (NG-HTN) and miR-18a-5p/HIF-1α axis. **(A)** Quantification of miR-18a-5p level in control and NG-HTN hearts normalized to U6SnRNA. **(B)** Quantification of miR-18a-5p level in control and NE-treated H9c2 cardiomyocytes normalized to U6SnRNA. **(C)** *In silico* prediction of miR-18a-5p binding on 3′UTR of HIF-1α and its species conserveness. **(D)** Western blot and quantification showing expression of HIF-1α in control and NG-HTN rats normalized to Actin. **(E)** Immunofluorescence assay and quantification showing HIF-1α localization in control and NG-HTN hearts (HIF-1α, green; α-actinin, red; and DAPI, blue). **(F)** Western blot and quantification showing expression of HIF-1α normalized to Actin in control and H9c2 cardiomyocytes treated with NE. Values are mean ± SEM, dot represents $n = 6$ rats, $^*P < 0.05$ vs. Control, Student's *t*-test.

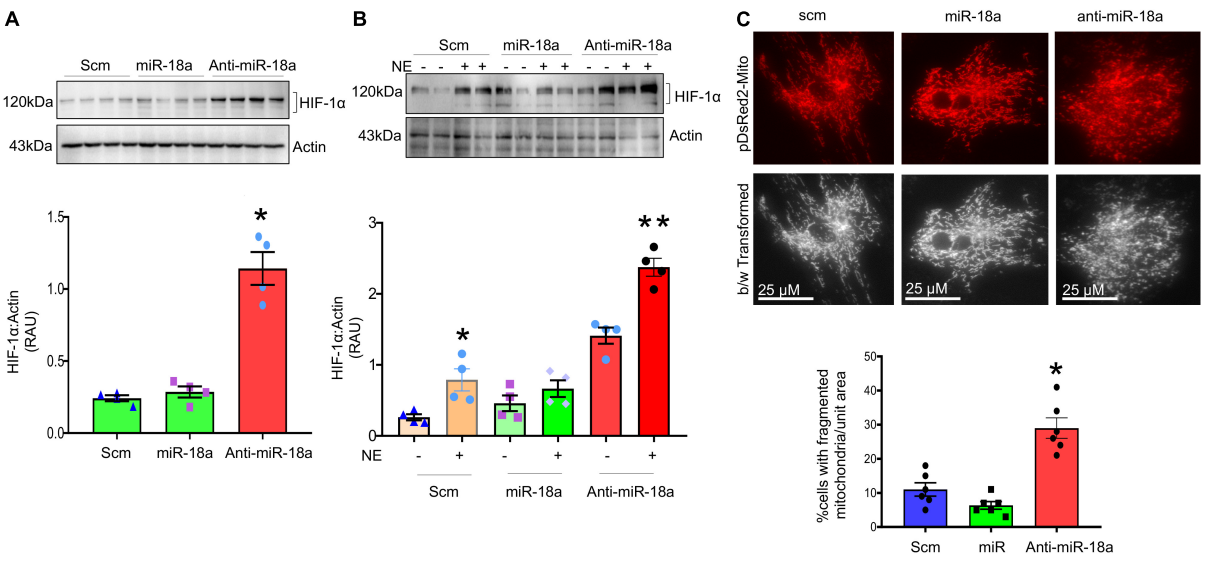

FIGURE 10 | MiR-18a-5p targets HIF-1α and mitochondrial fission. **(A)** Western blot and quantification showing expression of HIF-1α normalized to Actin in the H9c2 cardiomyocytes treated with scm, miR-18a-5p, and anti-miR-18a-5p. **(B)** Western blot and quantification showing expression of HIF-1α normalized to Actin in H9c2 cardiomyocytes treated by scm, miR-18a-5p, and anti-miR-18a-5p, with NE or no NE. Values are mean ± SEM, $^*P < 0.05$ vs. scm, $^{**}P < 0.05$ vs. miR-18a-5p. One-way ANOVA. **(C)** Top, live cell pDsRed2-Mito image of H9c2 cardiomyocytes treated with scm, miR-18a-5p, and anti-miR-18a-5p. Bottom, quantification of % number of cells with fragmented mitochondria (all globular) per unit areas in each group from six independent experiments.

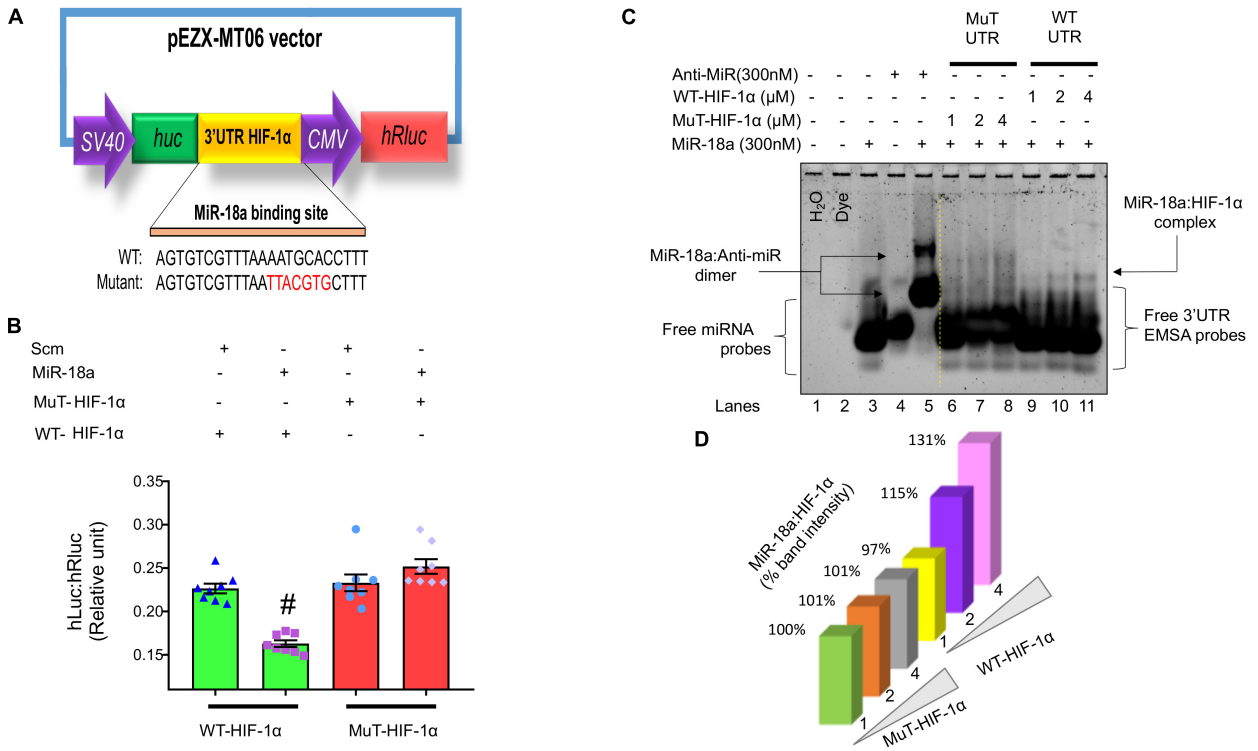

FIGURE 11 | MiR-18a-5p targets HIF-1α 3′UTR. **(A)** Dual-luciferase reporter assay construct showing WT and mutant miR-18a-5p binding sequences. **(B)** Luciferase reporter quantification showing relative expression of luciferase activity in miR-18a-5p, or scrambled miRNA-treated H9c2 cells co-transfected with either WT or mutant HIF-1α 3′UTR, dot represents individual values, $n = 8$ wells/group. $^{\#}P < 0.05$ vs. WT-HIF-1α 3′UTR, two-way ANOVA. **(C)** MiRNA–mRNA EMSA showing binding affinity of miR-18a-5p with WT or mutant HIF-1α 3′UTR (1, 2, or 4 μM). **(D)** Quantification of miR-18a-5p % band intensity shift with 1, 2, or 4 μM of WT or mutant HIF-1α 3′UTR promoter.

mitochondrial workload *via* alternate substrate utilization. This causes leaky mitochondrial respiration and increase mitochondrial ROS generation. The increased mitochondrial ROS generation opens mitochondrial transition pores (MPTP; Javadov et al., 2009) to release mitochondrial cytochromes into cytoplasm and to activate pro-hypertrophy/fibrosis/apoptotic and necrotic factors. Eventually this causes pathological cardiac hypertrophy, fibrosis and associated secondary inflammation from the circulation in the heart in response to sympatho-excitation commonly observed in NG-HTN that progress to heart failure over the time.

Some of the previous evidence for this were obtained while studying animal model of hypertension induced by subcutaneous delivery of Ang II, where the effects of Ang II is on the peripheral circulation including the heart to increase the blood pressure (Dai et al., 2011; Wei et al., 2017) and not specifically directed to the central nervous system. This model of hypertension initially promotes a compensatory cardiac hypertrophy due to peripheral vasoconstriction-mediated increased afterload, which later progresses to hypertension mediated heart failure (Dai et al., 2011; Power et al., 2016). However, whether these cardiac mitochondrial impairments are initiated by the enhanced sympathetic drive to the heart (*per se*) leading to NE programmed left ventricular remodeling in hypertension remains unclear (Zucker et al., 2001; Zhu et al., 2002). The hallmarks of hypertensive cardiomyopathy are hypertrophy, fibrosis, ECM expansion, apoptosis, inflammation, impaired autophagy/mitophagy, and vascular complications (Wang et al., 2010; Eirin et al., 2014). Our current model of hypertension is unique in that it purports to elicit a neurogenic cause for the cardiac excitation with concomitant elevated vascular resistance leading to the development of hypertension and consequent cardiomyopathy progression. Therefore, we studied the development of heart disease in this neurogenic model of hypertension. Our results confirmed that NG-HTN increased cardiac hypertrophy and fibrosis, and diastolic dysfunctions in the hearts of these rats, associated with increased general sympathetic activation.

The nuclear encoded mitochondrial protein quality controls are maintained by several signaling events both in the cytosol and mitochondria (Schmidt et al., 2010), which remain unstudied in the NG-HTN-induced cardiomyopathies. Mitochondrial dysfunction induces retrograde signaling of UPR^{mt} activation for mitochondrial proteostasis (Melber and Haynes, 2018). Activation of UPR^{mt} by mislocalized/misfolded mitochondrial precursor (pre) proteins indicates a compromised cytosol to mitochondrial protein import (Wrobel et al., 2015). Here, we determined the impact of elevated sympatho-excitation

TABLE 2 | Details of PCR primers and EMSA probes.

Probe name	Oligonucleotide sequences
D-Loop F	5′-CTACCATCCTCCGTGAAAC-3′
D-Loop R	5′-TGATTAGACCCGATACCATC-3′
gGAPDH F	5′-AAGCGGACTTACAGAGGTC-3′
gGAPDH R	5′-ACTACAGGAGCCATTTTGTG-3′
Wild type HIF-1α 3′UTR EMSA	5′-ATCATTTTAAAAAATGCACCTTT-3′
Mutant HIF-1α 3′UTR EMSA	5′-ATCATTTTAAAAAATTCAGCCTA-3′
MiR-18a-5p EMSA	5′-TAAGGTGCATCTAGTGCAGATAG-3′
Anti-miR-18a-5p EMSA	5′-CTATCTGCACTAGATGCACCTTA-3′

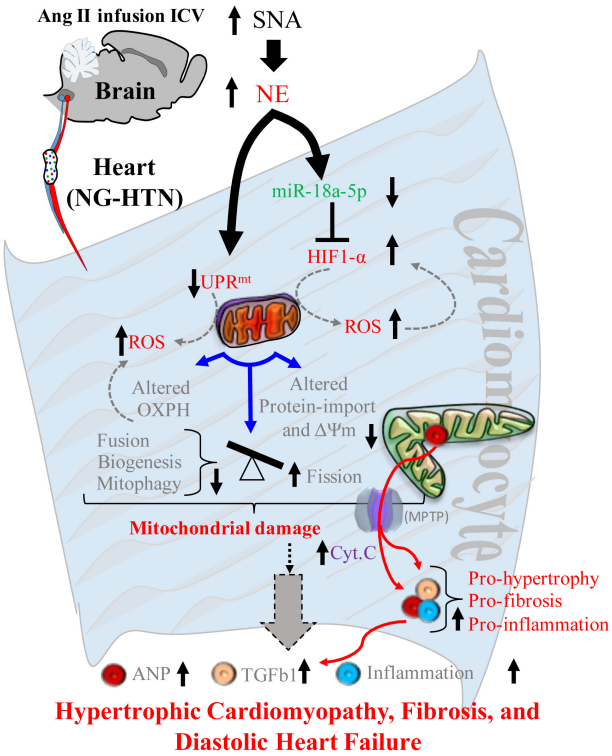

FIGURE 12 | Schematic showing mechanisms of mitochondrial dysfunction in central Ang II (ICV) infusion induced NG-HTN. Schematic model showing proposed molecular mechanisms causing mitochondrial abnormality in the heart of rat with neurogenic hypertension resulting in progression to hypertrophic cardiomyopathy. An increased sympathoexcitation (SNA) induces an increase in cardio-neuronal norepinephrine which causes either UPR^{mt} and/or miR-18a-5p/HIF-1α axis dysregulation that leads to increased mitochondrial ROS generation. Increased ROS alters mitochondrial OXPHOS, protein-import, and mitochondrial dynamics to tip the balance of Fusion/Fission to greater Fission, leading to overall mitochondrial abnormality. These underlies ROS induced release of mitochondrial cytochrome-c into cytoplasm *via* mitochondrial permeability transition pores (MPTP) opening eventually mitochondrial abnormality that progressively contributes to hypertrophic remodeling, fibrosis, inflammation and diastolic heart failure in the rats with NG-HTN.

on mitochondrial UPR^{mt} downregulation and increased mitochondrial proteotoxic stress signaling for the progression of NG-HTN-induced cardiomyopathy. We further identified a direct link between NE in mitochondrial UPR^{mt} and proteotoxic stress. Since mitochondrial dysfunction exhibits increased ROS generation and compromised OXPHOS, therefore, we focused our studies on measuring the effect of enhanced neurogenic sympathetic tone on mitochondrial ROS generation and OXPHOS event. Our data demonstrated that NG-HTN increased mitochondrial ROS levels and altered expression of mitochondrial respiratory complexes. Consistent with these observations, the direct application of NE *in vitro* on H9c2 cardiomyocytes showed increased mitochondrial ROS levels and decreased mitochondrial membrane potential suggesting that noradrenergic activation cascade initiated these changes in the mitochondria. In addition to this, our data uncovered an abundant amount of abnormal mitochondria in myocardial cells under EM, suggesting structurally impaired and functionally compromised mitochondria in the hearts of rats with NG-HTN, which is analogous to what is observed in clinical hypertension and related heart disease (Dikalov and Dikalova, 2016; Wei et al., 2017). Our results are also congruent with the previous reports which demonstrated that mitochondrial abnormalities are one common feature in all types of cardiomyopathies and increased mitochondrial ROS compromised mitochondrial respiration (Power et al., 2016). Based on these observations one may speculate that perhaps the neurogenic component may be the critical factor for these observed alterations in all forms of hypertension.

The mitochondrial network in cardiomyocytes undergoes biogenesis, fission/fusion, and mitophagy events to maintain a balance of healthy pool of mitochondria. Fragmented mitochondrial phenotypes, lack of fusion, and decreased biogenesis has been observed during diverse pathological cardiac remodeling and heart failure (Chen et al., 2009; Ong et al., 2010). However, the mechanisms which underly the changes in mitochondrial dynamics during hypertrophic growth of cardiomyocytes is not entirely clear. Our data demonstrate that mitochondrial biogenesis is decreased in the hearts of rats with NG-HTN, suggesting a dysfunction in mitochondrial biogenesis that does not manage to recover damaged mitochondrial loss *via* mitophagy. Our results further demonstrated that mitochondrial fission is increased and fusion is decreased in the heart of rat with NG-HTN, which are in accordance with the data presented with FIS1 and OPA1 that further corroborates with increased fission and decreased fusion events of the mitochondria in the heart of NG-HTN (Papanicolaou et al., 2011; Ikeda et al., 2015). Further, EM data demonstrated attenuated mitochondrial area coupled with decreased cristae area, implicating compromised mitochondrial function including OXPHOS. This is supported by the presence of meAPs as well as increased numbers of miAPs, indicating impairment of mitophagy events. However, whether mitophagy flux is decreased or increased in hypertensive heart disease remains to be determined definitively using mitophagy reporter animal models. Our findings are consistent with previous reports in hypertensive hearts showing an abundant amount of abnormal mitochondria in myocardial cells examined by EM, which support impaired mitophagy (Wei et al., 2017; Nandi et al., 2020a). Decreased mitochondrial biogenesis, fission-fusion dynamics, and mitophagy leading to mitochondrial

abnormality in NG-HTN was not explored prior to this study. In this regard, NE signaling has been purported to play a significant role in cardiac remodeling and hypertrophy, adaptations (Barki-Harrington et al., 2004). It is of interest to note that NE has been reported to increase mitochondrial fission and suppress mitochondrial function in the heart (Pennanen et al., 2014). Furthermore, cardiomyocyte hypertrophy has been associated with diminished mitochondrial metabolism in compensatory hypertrophied myocardium of hypertensive rats (Power et al., 2016). Other reports suggest that mitochondrial fusion events *via* OPA1 or MFN1/2 appear to decrease in heart failure (Javadov et al., 2011; Papanicolaou et al., 2011), as well. In accordance with these reports, our results demonstrated that treatment of cultured H9c2 rat cardiomyocytes with NE increased cardiomyocyte hypertrophy, decreased mitochondrial biogenesis, $\Delta\Psi m$, and increased mitochondrial fission and ROS generation and shifted OXPHOS. Therefore, these data strongly suggest an initiating role for enhanced neurogenic tone as a possible origin for the impaired mitochondrial dynamics. The overall assessments of norepinephrine effect on heart and cardiomyocytes showed changes in mitochondrial quality control parameters indicating reduced mitochondrial functional capacity. These data further suggest a potential role of NE→reduced UPR^{mt}→ROS and miR-18a-5p/HIF-1α→ROS induced decrease in mitochondrial fission-fusion dynamics and biogenesis in the development of sympatho-excitation-induced cardiac hypertrophic remodeling. Notably, these changes are accomplished *via* OXPHOS metabolic shifts toward glycolytic substrates utilization for cardiac hypertrophy (Dai et al., 2011; Chu et al., 2012). In this context, cardiomyocyte hypertrophy has been reported with diminished mitochondrial metabolism, and fragmentation of the mitochondrial network precedes metabolic alterations in response to norepinephrine (Pennanen et al., 2014). Furthermore, our results showed that lack of miR-18a-5p increased mitochondrial fragmentation in hypertrophic cardiomyocyte in response to norepinephrine. Related studies demonstrated that inhibiting mitochondrial fission protects the heart against ischemia/reperfusion injury (Ong et al., 2010) and mdivi-1, a pharmacological inhibitor for mitochondrial fission inducer Drp1, ameliorated pressure overload-induced heart failure in mice (Givvimani et al., 2012). In addition, a dominant negative Drp1, is reported to blunt hypertrophic growth, and prevent norepinephrine-induced reduced mitochondrial function (Pennanen et al., 2014). Moreover, a deficiency of mitochondrial fusion inducer Mfn2 further showed cardiac hypertrophy and reduced cardiac function (Papanicolaou et al., 2011). Taken together, all these reports support the notion that mitochondrial dynamics play a crucial role in the development of heart diseases in the downstream of sympathetic activation. Therefore, our results imply that targeting mitochondrial dynamics can be a potential therapeutic approach for preserving mitochondrial function for cardioprotection in NG-HTN.

In addition to UPR^{mt} marker ATF5 downregulations there was a concomitant decreased expression of mitochondrial outer membrane translocase proteins TOM20 but increased abundance of nuclear-encoded mitochondrial inner membrane protein TIM17A in NG-HTN hearts (Rainbolt et al., 2013). These results suggest that the nucleus to mitochondria communication for mitochondrial pre-protein import and proteostasis is reduced in the NG-HTN myocardium. Our results suggest a notion that in NG-HTN hearts several nuclear encoded mitochondrial pre-proteins transcription or translation are suppressed due to suppressed UPR^{mt} stress response signal inside the mitochondrial matrix. Our cytosol vs. mitochondrial western blot data demonstrated that in control hearts the key UPR^{mt} marker ATF5 is imported into mitochondria. However, due to mitochondrial proteotoxic stress in NG-HTN, ATF5 fails to be imported into mitochondria, and cytosolic ATF5 level is also reduced in NG-HTN, indicating UPR^{mt} downregulation. In addition, transcriptional factor ATF5, which regulates expression of key downstream UPR^{mt} genes like HSP60 showed its increased protein level of accumulation in the NG-HTN mitochondria, while HSP60 cytosolic level is reduced in NG-HTN. Furthermore, assessment of the mitochondrial quality-control protease YME1L1, a central to UPR^{mt} signal transduction for OXPHOS subunit assembly/import, was reduced in the mitochondrial matrix of NG-HTN. These changes suppressed UPR^{mt} and perhaps increases the OXPHOS subunits misfolded supercomplex accumulation, and increased HSP60 level in mitochondrial fraction with a decreased Mn-SOD antioxidant capacity as we noticed with our Western blots. The turnover of HSP60 stabilization in NG-HTN mitochondria may possibly increases to cope the newly synthesized mitochondrial genome encoded proteins folding overload and their subsequent assembly. We therefore concluded that ATF5 and HSP60 signal mechanisms are complex and perhaps regulated by different axes of the canonical or non-canonical UPR^{mt} in NG-HTN heart. Notably, UPR^{mt} activation eliminates severely defective or damaged mitochondria *via* mitophagy, however a suppressed UPR^{mt} in NG-HTN heart perhaps increased mega-autophagosome accumulation as we noticed with EM evaluations (Pellegrino et al., 2013). In addition, the decreased mtDNA content in NG-HTN indicates a reduced new mitochondrial biogenesis, which further supports a lack of UPR^{mt} activation in the heart of NG-HTN (Shpilka et al., 2021). Furthermore, our data suggested that a weaker ATF5 signal in NG-HTN hearts may allow a reduction signal for mitochondrial overall protein import capacity. However, the UPR^{mt} is highly complex and how the UPR^{mt} is regulated in mammal still remains unclear (Fiorese et al., 2016). Therefore, further study is necessary to understand the signaling communications from the cytosol to mitochondria, and nucleus to mitochondria for the mitochondrial proteostasis in NG-HTN heart and if mitochondrial matrix proteases preferentially regulates OXPHOS complexes to stablish an ETC or metabolic switch due to mitochondrial stress and reduced the pre-protein import that leading to the accumulation of unassembled subunits of ETC complexes or causing canonical or non-canonical UPR^{mt} axes are unclear at present (Nargund et al., 2012; Melber and Haynes, 2018; Rolland et al., 2019).

Several reports suggest that mitochondrial dysfunction presents a new horizon to predict the progression of

hypertension cardiomyopathy (Drazner, 2011; Nadruz, 2015; Eirin et al., 2018). Considering that one-third of the intracellular volume of a cardiomyocyte is mitochondria, our results support the general hypothesis that hypertension-induced mitochondrial abnormality in cardiomyocytes is a major contributor to NG-HTN-induced cardiac hypertrophy and fibrotic remodeling. Further, our *in vitro* data with direct action of NE on cultured cardiomyocytes corroborates the concept that enhanced sympathetic tone is the initiating factor for these mitochondrial injuries leading to hypertensive cardiomyopathy. In this regard, it has been well documented that mitochondrial abnormality is associated with hypertensive heart diseases (Eirin et al., 2014, 2018; Dikalov and Dikalova, 2016). However, the mitochondrial impairments that prevails in NE-induced programmed left ventricular remodeling associated with hypertension remained unclear until the current study.

Several miRNAs have been reported to be lower during hypertension (Lee et al., 2015; Seeger and Boon, 2016). The cause for this decrease is not entirely clear. The results from this study demonstrate that concomitant with the sympatho-excitatory state in NG-HTN there is decreased levels of miR-18a-5p. Furthermore, our *in vitro* data using cardiomyocyte cultures clearly demonstrated that direct application of NE causes a decrease in miR-18a-5p. Taken together these data provides a possible mechanistic link between sympatho-excitation and reduced levels of cardiac miR-18a-5p in NG-HTN (Huang et al., 2017; Nandi et al., 2020b).

Previously we reported that downregulation of anti-hypertrophic and anti-fibrosis miRNAs can induce cardiac fibrosis and hypertrophy (Nandi et al., 2016). MiRNAs have been reported to lower hypertension in SHR by upregulating mitochondrial translation (Li et al., 2016). MiR-18a-5p has been purported to be an anti-hypertrophy/anti-fibrosis miRNA in the heart (Huang et al., 2017). On the other hand, persistent activation of HIF-1α promotes cardiac hypertrophy in hypertension (Kumar et al., 2018) and increased HIF-1α suppresses mitochondrial function (Kim et al., 2006; Papandreou et al., 2006). Considering these facts together we endeavored to explore whether there was a link between miR-18a-5p and HIF-1α in NG-HTN. Our *in silico* analysis predicted that miR-18a-5p targets HIF-1α. Our data demonstrated that when miR-18a-5p is downregulated the levels of HIF-1α protein is increased in the hearts of rats with NG-HTN, concomitantly. Moreover, increased HIF-1α is associated with hypertrophy in the hearts and cultured neonatal rat cardiac myocytes, which is consistent with the role of HIF-1α in the heart for hypertension-induced hypertrophic cardiac remodeling *via* mitochondrial suppression (Kumar et al., 2019). HIF-1α promotes glycolytic activation and suppresses mitochondrial function (Kim et al., 2006; Papandreou et al., 2006). In addition, our *in vitro* data using cardiomyocyte cultures clearly demonstrated that direct application of NE causes a decrease in miR-18a-5p with a concomitant increase in HIF-1α and induced molecular markers of cardiomyocyte hypertrophy and mitochondrial dysfunction. These results demonstrate an inverse relationship between levels of miR-18a-5p and levels of HIF-1α suggesting that conceivably miR-18a-5p inhibits HIF-1α.

These result supports the overall hypothesis that NE reduces the levels of miR-18a-5p which in turn allows for an increase in the levels of HIF-1α which in turn involved in suppressed mitochondrial function in cardiac myocytes. Our data show that NG-HTN reduces miR-18a-5p levels and at the same time increases cardiac HIF-1α. In addition, we have shown that miR-18a-5p targets HIF-1α 3′UTR and binds to HIF-1α 3′UTR seed sequence to regulate its function using miRNA 3′URT dual-luciferase assay and miRNA–mRNA EMSA assays as well. Furthermore, miR-18a-5p overexpression blunted norepinephrine-induced HIF-1α increase in cardiomyocytes, and lack of miR-18a-5p in *in vitro* H9c2 cardiomyocytes increased mitochondrial fragmentation. These results further suggesting that the levels of miR-18a-5p regulate levels of HIF-1α and thus hypertrophic cardiac remodeling *via* mitochondrial suppression (Kumar et al., 2019).

In conclusion, we have demonstrated that chronic Ang II (ICV) infusion induces exaggerated sympatho-excitation mediated NG-HTN in rats. Our study has identified a critical neural link operating *via* ROS, metabolism, and miRNA signaling pathway that produces mitochondrial stress leading to cardiac hypertrophy, fibrosis, and progression to cardiomyopathy/heart failure in our rat model of NG-HTN. The relationship between mitochondrial dynamics and mitochondrial stress in hypertensive cardiac hypertrophy is presented in the study. A stimulation of the adrenergic receptors by enhanced noradrenergic tone perhaps leads to an increase in mitochondrial calcium and OXPHOS overload and associated mitochondrial UPR^{mt} dysfunctions. Our results identify a new potential therapeutic target for the prevention of pathological hypertensive hypertrophy *via* targeting mitochondria. We showed that norepinephrine promotes mitochondrial fission *via* mitochondrial ROS, proteotoxicity, dynamics alteration, and by shifted metabolism. Possibly, a balance between mitochondrial fission, fusion, biogenesis, mitophagy, and altered NE→reduced UPR^{mt}→ROS and miR-18a-5p/HIF-1α→ROS axis may be sufficient to prevent cardiomyocyte hypertrophy and hypertension cardiomyopathy. The understanding of these fundamental molecular mechanisms provides us critical insight into the possible development of novel therapeutics for alleviating the cardiac abnormality commonly observed in hypertensive heart disease in the future.

LIMITATIONS

1. The results shown with this NG-HTN model are unique and novel since they delineate the effect of sympto-excitation specifically on cardiac mitochondrial function and cardiac remodeling. Although clinically all hypertensives patients have some neural contribution, there are potentially other factors that may also play a role.

2. It could be argued that sympatho-excitation may cause an increase in peripheral Ang II which in turn may induce the production of mitochondrial reactive oxygen species. Nevertheless, it is safe to assume that direct effects of cardio-neuronal mechanisms are primarily responsible for cardiac remodeling in the current model. We studied the NG-HTN induced changes with 14 days of Ang II infusion, however, an infusion study over longer period of time remains to be examined.
3. Contribution of vascular constriction, dysfunction, and/or a systemic inflammation mechanism in response to NG-HTN may contribute to the changes in cardiac abnormalities. These factors remain to examined.
4. We proposed an impairment of mitochondrial OXPHOS shift in the heart of rat with NG-HTN, which provokes cardiac remodeling. However, it is acknowledged that this mechanism is not directly tested in this study.
5. Our *in vitro* results validated that miR-18a-5p functionally targets HIF-1α and is directly involved in regulating mitochondrial structures. However, the contribution of miR-18a-5p/HIF-1α axis relevance to mitochondrial UPR *in vivo* remains to be examined in gain or loss of function models.

FUTURE PERSPECTIVE

Mitochondrial abnormalities is commonly reported in the hearts of patients with hypertension. However, the source of what elicits this cardiac mitochondrial impairments leading to heart failure remains to be explored. Present study demonstrated that neurogenic hypertension reduced cardiac miRNA-18a-5p and increased HIF-1α, with concomitant mitochondrial proteinopathy, UPR^{mt} stress, mitochondrial structural abnormalities, increased mitochondrial ROS, altered oxidative phosphorylation and reduced mitochondrial biogenesis and fusion, but increased fission. This study suggests that chronic sympathoexcitation to the heart contributes to pathological cardiac remodeling *via* NE→miR-18a-5p/HIF-1α axis and UPR^{mt} to alter mitochondrial function. Targeting this pathway therapeutically would provide a novel approach.

DATA AVAILABILITY STATEMENT

The raw data supporting the conclusions of this article will be made available by the authors, without undue reservation.

ETHICS STATEMENT

The animal study was reviewed and approved by all experimental protocols were approved by the Institutional Animal Care and Use Committee, University of Nebraska Medical Center, and all protocols/methods were conducted in accordance with the relevant guidelines and regulations of our institution, the American Physiological Society, and the National Institutes of Health Guide for the Care and Use of Laboratory Animals.

AUTHOR CONTRIBUTIONS

SN conceived, designed, and co-ordinated the research plans, performed surgeries, generated and interpreted the data, wrote and edited the manuscript. SN and KK contributed to the hemodynamics analyses. SM performed EM studies. KP supervised all aspects of the study and the manuscript. All authors contributed to the article and approved the submitted version.

FUNDING

This work was supported by the American Heart Association Career Development Grant (19CDA34490029 to SN), and National Institutes of Health Grants (R01-DK-114663, P01-HL-62222, and endowed McIntyre Professorship fund to KP). SM was supported by grants from the Veterans Affairs (I01 BX003934).

REFERENCES

Almela, P., Cuenca-Bermejo, L., Yuste, J. E., Estrada, C., de Pablos, V., Bautista-Hernández, V., et al. (2020). Cardiac Noradrenaline Turnover and Heat Shock Protein 27 Phosphorylation in Dyskinetic Monkeys. *Mov. Disord.* 35, 698–703. doi: 10.1002/mds.27958

Barki-Harrington, L., Perrino, C., and Rockman, H. A. (2004). Network integration of the adrenergic system in cardiac hypertrophy. *Cardiovasc. Res.* 63, 391–402. doi: 10.1016/j.cardiores.2004.03.011

Boyman, L., Greiser, M., and Lederer, W. J. (2021). Calcium influx through the mitochondrial calcium uniporter holocomplex, MCUcx. *J. Mol. Cell Cardiol.* 151, 145–154. doi: 10.1016/j.yjmcc.2020.10.015

Brown, D. A., Perry, J. B., Allen, M. E., Sabbah, H. N., Stauffer, B. L., Shaikh, S. R., et al. (2017). Expert consensus document: Mitochondrial function as a therapeutic target in heart failure. *Nat. Rev. Cardiol.* 14, 238–250. doi: 10.1038/nrcardio.2016.203

Chen, L., Gong, Q., Stice, J. P., and Knowlton, A. A. (2009). Mitochondrial OPA1, apoptosis, and heart failure. *Cardiovasc. Res.* 84, 91–99. doi: 10.1093/cvr/cvp181

Chu, W., Wan, L., Zhao, D., Qu, X., Cai, F., Huo, R., et al. (2012). Mild hypoxia-induced cardiomyocyte hypertrophy via up-regulation of HIF-1alpha-mediated TRPC signalling. *J. Cell Mol. Med.* 16, 2022–2034. doi: 10.1111/j.1582-4934.2011.01497.x

Dai, D. F., Johnson, S. C., Villarin, J. J., Chin, M. T., Nieves-Cintrón, M., Chen, T., et al. (2011). Mitochondrial oxidative stress mediates angiotensin II-induced cardiac hypertrophy and Galphaq overexpression-induced heart failure. *Circ. Res.* 108, 837–846. doi: 10.1161/CIRCRESAHA.110.232306

Dikalov, S. I., and Dikalova, A. E. (2016). Contribution of mitochondrial oxidative stress to hypertension. *Curr. Opin. Nephrol. Hypertens.* 25, 73–80. doi: 10.1097/MNH.0000000000000198

Drazner, M. H. (2011). The progression of hypertensive heart disease. *Circulation* 123, 327–334. doi: 10.1161/CIRCULATIONAHA.108.845792

Eirin, A., Lerman, A., and Lerman, L. O. (2014). Mitochondrial injury and dysfunction in hypertension-induced cardiac damage. *Eur. Heart J.* 35, 3258–3266. doi: 10.1093/eurheartj/ehu436

Eirin, A., Lerman, A., and Lerman, L. O. (2018). Enhancing Mitochondrial Health to Treat Hypertension. *Curr. Hypertens. Rep.* 20:89. doi: 10.1007/s11906-018-0889-4

Fiorese, C. J., Schulz, A. M., Lin, Y. F., Rosin, N., Pellegrino, M. W., and Haynes, C. M. (2016). The Transcription Factor ATF5 Mediates a Mammalian Mitochondrial UPR. *Curr. Biol.* 26, 2037–2043. doi: 10.1016/j.cub.2016.06.002

Fukai, K., Nakamura, A., Hoshino, A., Nakanishi, N., Okawa, Y., Ariyoshi, M., et al. (2015). Pyk2 aggravates hypoxia-induced pulmonary hypertension by activating HIF-1alpha. *Am. J. Physiol. Heart Circ. Physiol.* 308, H951–H959. doi: 10.1152/ajpheart.00770.2014

Garcia-Diaz, L., Coserria, F., and Antinolo, G. (2013). Hypertrophic Cardiomyopathy due to Mitochondrial Disease: Prenatal Diagnosis, Management, and Outcome. *Case Rep. Obstet. Gynecol.* 2013:472356. doi: 10.1155/2013/472356

Givvimani, S., Munjal, C., Tyagi, N., Sen, U., Metreveli, N., and Tyagi, S. C. (2012). Mitochondrial division/mitophagy inhibitor (Mdivi) ameliorates pressure overload induced heart failure. *PLoS One* 7:e32388. doi: 10.1371/journal.pone.0032388

Holmgren, D., Wahlander, H., Eriksson, B. O., Oldfors, A., Holme, E., and Tulinius, M. (2003). Cardiomyopathy in children with mitochondrial disease; clinical course and cardiological findings. *Eur. Heart J.* 24, 280–288. doi: 10.1016/S0195-668X(02)00387-1

Hölscher, M., Schäfer, K., Krull, S., Farhat, K., Hesse, A., Silter, M., et al. (2012). Unfavourable consequences of chronic cardiac HIF-1alpha stabilization. *Cardiovasc. Res.* 94, 77–86. doi: 10.1093/cvr/cvs014

Huang, C. Y., Pai, P. Y., Kuo, C. H., Ho, T. J., Lin, J. Y., Lin, D. Y., et al. (2017). p53-mediated miR-18 repression activates HSF2 for IGF-IIR-dependent myocyte hypertrophy in hypertension-induced heart failure. *Cell Death Dis.* 8:e2990. doi: 10.1038/cddis.2017.320

Igarashi, N., Nozawa, T., Fujii, N., Suzuki, T., Matsuki, A., Nakadate, T., et al. (2006). Influence of beta-adrenoceptor blockade on the myocardial accumulation of fatty acid tracer and its intracellular metabolism in the heart after ischemia-reperfusion injury. *Circ. J.* 70, 1509–1514. doi: 10.1253/circj.70.1509

Ikeda, Y., Shirakabe, A., Maejima, Y., Zhai, P., Sciarretta, S., Toli, J., et al. (2015). Endogenous Drp1 mediates mitochondrial autophagy and protects the heart against energy stress. *Circ. Res.* 116, 264–278. doi: 10.1161/CIRCRESAHA.116.303356

Javadov, S., Karmazyn, M., and Escobales, N. (2009). Mitochondrial permeability transition pore opening as a promising therapeutic target in cardiac diseases. *J. Pharmacol. Exp. Ther.* 330, 670–678. doi: 10.1124/jpet.109.153213

Javadov, S., Rajapurohitam, V., Kilić, A., Hunter, J. C., Zeidan, A., Said Faruq, N., et al. (2011). Expression of mitochondrial fusion-fission proteins during post-infarction remodeling: the effect of NHE-1 inhibition. *Basic Res. Cardiol.* 106, 99–109. doi: 10.1007/s00395-010-0122-3

Kim, J. W., Tchernyshyov, I., Semenza, G. L., and Dang, C. V. (2006). HIF-1-mediated expression of pyruvate dehydrogenase kinase: a metabolic switch required for cellular adaptation to hypoxia. *Cell Metab.* 3, 177–185. doi: 10.1016/j.cmet.2006.02.002

Kline, R. L., Patel, K. P., Ciriello, J., and Mercer, P. F. (1983). Effect of renal denervation on arterial pressure in rats with aortic nerve transection. *Hypertension* 5, 468–475. doi: 10.1161/01.HYP.5.4.468

Krishnan, J., Suter, M., Windak, R., Krebs, T., Felley, A., Montessuit, C., et al. (2009). Activation of a HIF1alpha-PPARgamma axis underlies the integration of glycolytic and lipid anabolic pathways in pathologic cardiac hypertrophy. *Cell Metab.* 9, 512–524. doi: 10.1016/j.cmet.2009.05.005

Kumar, S., Wang, G., Liu, W., Ding, W., Dong, M., Zheng, N., et al. (2018). Hypoxia-Induced Mitogenic Factor Promotes Cardiac Hypertrophy via Calcium-Dependent and Hypoxia-Inducible Factor-1alpha Mechanisms. *Hypertension* 72, 331–342. doi: 10.1161/HYPERTENSIONAHA.118.10845

Kumar, V., Ak, A., Sanawar, R., Jaleel, A., Kumar, T. R. S., and Kartha, C. C. (2019). Chronic Pressure Overload Results in Deficiency of Mitochondrial Membrane Transporter ABCB7 Which Contributes to Iron Overload, Mitochondrial Dysfunction, Metabolic Shift and Worsens Cardiac Function. *Sci. Rep.* 9:13170. doi: 10.1038/s41598-019-49666-0

Lee, S., Choi, E., Cha, M. J., Park, A. J., Yoon, C., and Hwang, K. C. (2015). Impact of miRNAs on cardiovascular aging. *J. Geriatr. Cardiol.* 12, 569–574.

Li, H., Zhang, X., Wang, F., Zhou, L., Yin, Z., Fan, J., et al. (2016). MicroRNA-21 Lowers Blood Pressure in Spontaneous Hypertensive Rats by Upregulating Mitochondrial Translation. *Circulation* 134, 734–751. doi: 10.1161/CIRCULATIONAHA.116.023926

Lionakis, N., Mendrinos, D., Sanidas, E., Favatas, G., and Georgopoulou, M. (2012). Hypertension in the elderly. *World J. Cardiol.* 4, 135–147. doi: 10.4330/wjc.v4.i5.135

Melber, A., and Haynes, C. M. (2018). UPR(mt) regulation and output: a stress response mediated by mitochondrial-nuclear communication. *Cell Res.* 28, 281–295. doi: 10.1038/cr.2018.16

Montoya, M. M., Maul, J., Singh, P. B., Pua, H. H., Dahlström, F., Wu, N., et al. (2017). A Distinct Inhibitory Function for miR-18a in Th17 Cell Differentiation. *J. Immunol.* 199, 559–569. doi: 10.4049/jimmunol.1700170

Nadruz, W. (2015). Myocardial remodeling in hypertension. *J. Hum. Hypertens.* 29, 1–6. doi: 10.1038/jhh.2014.36

Nandi, S. S., and Mishra, P. K. (2015). Harnessing fetal and adult genetic reprograming for therapy of heart disease. *J. Nat. Sci.* 1:e71.

Nandi, S. S., and Mishra, P. K. (2017). H2S and homocysteine control a novel feedback regulation of cystathionine beta synthase and cystathionine gamma lyase in cardiomyocytes. *Sci. Rep.* 7:3639. doi: 10.1038/s41598-017-03776-9

Nandi, S. S., and Mishra, P. K. (2018). Targeting miRNA for Therapy of Juvenile and Adult Diabetic Cardiomyopathy. *Adv. Exp. Med. Biol.* 1056, 47–59. doi: 10.1007/978-3-319-74470-4_4

Nandi, S. S., Duryee, M. J., Shahshahan, H. R., Thiele, G. M., Anderson, D. R., and Mishra, P. K. (2015). Induction of autophagy markers is associated with attenuation of miR-133a in diabetic heart failure patients undergoing mechanical unloading. *Am. J. Transl. Res.* 7, 683–696.

Nandi, S. S., Katsurada, K., Sharma, N. M., Anderson, D. R., Mahata, S. K., and Patel, K. P. (2020a). MMP9 inhibition increases autophagic flux in chronic heart failure. *Am. J. Physiol. Heart Circ. Physiol.* 319, H1414–H1437. doi: 10.1152/ajpheart.00032.2020

Nandi, S. S., Katsurada, K., Sharma, N. M., Mahata, S. K., and Patel, K. P. (2020b). Abstract 15288: Mitochondrial Injury in Cardiomyopathy of Neurogenic Hypertension: Role of MiR-18a-5p/HIF-1a Axis. *Circulation* 142, A15288–A. doi: 10.1161/circ.142.suppl_3.15288

Nandi, S. S., Shahshahan, H. R., Shang, Q., Kutty, S., Boska, M., and Mishra, P. K. (2018). MiR-133a Mimic Alleviates T1DM-Induced Systolic Dysfunction in Akita: An MRI-Based Study. *Front. Physiol.* 9:1275. doi: 10.3389/fphys.2018.01275

Nandi, S. S., Zheng, H., Sharma, N. M., Shahshahan, H. R., Patel, K. P., and Mishra, P. K. (2016). Lack of miR-133a Decreases Contractility of Diabetic Hearts: A Role for Novel Cross Talk Between Tyrosine Aminotransferase and Tyrosine Hydroxylase. *Diabetes* 65, 3075–3090. doi: 10.2337/db16-0023

Nanki, M., Itoh, K., Matsubara, T., Nishimura, K., Kambe, T., Sugiyama, S., et al. (1987). Evaluation of the effect of metoprolol on energy metabolism in the ischaemic myocardium in relation to regional myocardial blood flow. *Cardiovasc. Res.* 21, 660–667. doi: 10.1093/cvr/21.9.660

Nargund, A. M., Pellegrino, M. W., Fiorese, C. J., Baker, B. M., and Haynes, C. M. (2012). Mitochondrial import efficiency of ATFS-1 regulates mitochondrial UPR activation. *Science* 337, 587–590. doi: 10.1126/science.1223560

Nikami, H., Nedergaard, J., and Fredriksson, J. M. (2005). Norepinephrine but not hypoxia stimulates HIF-1alpha gene expression in brown adipocytes. *Biochem. Biophys. Res. Commun.* 337, 121–126. doi: 10.1016/j.bbrc.2005.09.011

Ong, S. B., Subrayan, S., Lim, S. Y., Yellon, D. M., Davidson, S. M., and Hausenloy, D. J. (2010). Inhibiting mitochondrial fission protects the heart against ischemia/reperfusion injury. *Circulation* 121, 2012–2022. doi: 10.1161/CIRCULATIONAHA.109.906610

Papandreou, I., Cairns, R. A., Fontana, L., Lim, A. L., and Denko, N. C. (2006). HIF-1 mediates adaptation to hypoxia by actively downregulating mitochondrial oxygen consumption. *Cell Metab.* 3, 187–197. doi: 10.1016/j.cmet.2006.01.012

Papanicolaou, K. N., Khairallah, R. J., Ngoh, G. A., Chikando, A., Luptak, I., O'Shea, K. M., et al. (2011). Mitofusin-2 maintains mitochondrial structure and contributes to stress-induced permeability transition in cardiac myocytes. *Mol. Cell Biol.* 31, 1309–1328. doi: 10.1128/MCB.00911-10

Patel, K. P., Xu, B., Liu, X., Sharma, N. M., and Zheng, H. (2016). Renal Denervation Improves Exaggerated Sympathoexcitation in Rats With Heart Failure: A Role for Neuronal Nitric Oxide Synthase in the Paraventricular

Nucleus. *Hypertension* 68, 175–184. doi: 10.1161/HYPERTENSIONAHA.115.06794

Paxinos, G., and Watson, C. (2005). *The Rat Brain in Stereotaxic Coordinates. Compact 6th Edn.* Academic Press, New York, 400

Pellegrino, M. W., Nargund, A. M., and Haynes, C. M. (2013). Signaling the mitochondrial unfolded protein response. *Biochim. Biophys. Acta* 1833, 410–416. doi: 10.1016/j.bbamcr.2012.02.019

Pennanen, C., Parra, V., López-Crisosto, C., Morales, P. E., Del Campo, A., Gutierrez, T., et al. (2014). Mitochondrial fission is required for cardiomyocyte hypertrophy mediated by a Ca2+-calcineurin signaling pathway. *J. Cell Sci.* 127, 2659–2671. doi: 10.1242/jcs.139394

Power, A. S., Pham, T., Loiselle, D. S., Crossman, D. H., Ward, M. L., and Hickey, A. J. (2016). Impaired ADP channeling to mitochondria and elevated reactive oxygen species in hypertensive hearts. *Am. J. Physiol. Heart Circ. Physiol.* 310, H1649–H1657. doi: 10.1152/ajpheart.00050.2016

Rainbolt, T. K., Atanassova, N., Genereux, J. C., and Wiseman, R. L. (2013). Stress-regulated translational attenuation adapts mitochondrial protein import through Tim17A degradation. *Cell Metab.* 18, 908–919. doi: 10.1016/j.cmet.2013.11.006

Rolland, S. G., Schneid, S., Schwarz, M., Rackles, E., Fischer, C., Haeussler, S., et al. (2019). Compromised Mitochondrial Protein Import Acts as a Signal for UPR(mt). *Cell Rep.* 28, 1659–69e5. doi: 10.1016/j.celrep.2019.07.049

Schmidt, O., Pfanner, N., and Meisinger, C. (2010). Mitochondrial protein import: from proteomics to functional mechanisms. *Nat. Rev. Mol. Cell Biol.* 11, 655–667. doi: 10.1038/nrm2959

Seeger, T., and Boon, R. A. (2016). MicroRNAs in cardiovascular ageing. *J. Physiol.* 594, 2085–2094. doi: 10.1113/JP270557

Sharp, W. W., Fang, Y. H., Han, M., Zhang, H. J., Hong, Z., Banathy, A., et al. (2014). Dynamin-related protein 1 (Drp1)-mediated diastolic dysfunction in myocardial ischemia-reperfusion injury: therapeutic benefits of Drp1 inhibition to reduce mitochondrial fission. *FASEB J.* 28, 316–326. doi: 10.1096/fj.12-226225

Shirakabe, A., Zhai, P., Ikeda, Y., Saito, T., Maejima, Y., Hsu, C. P., et al. (2016). Drp1-Dependent Mitochondrial Autophagy Plays a Protective Role Against Pressure Overload-Induced Mitochondrial Dysfunction and Heart Failure. *Circulation* 133, 1249–1263. doi: 10.1161/CIRCULATIONAHA.115.020502

Shpilka, T., and Haynes, C. M. (2018). The mitochondrial UPR: mechanisms, physiological functions and implications in ageing. *Nat. Rev. Mol. Cell Biol.* 19, 109–120. doi: 10.1038/nrm.2017.110

Shpilka, T., Du, Y., Yang, Q., Melber, A., Uma Naresh, N., Lavelle, J., et al. (2021). UPR(mt) scales mitochondrial network expansion with protein synthesis via mitochondrial import in Caenorhabditis elegans. *Nat. Commun.* 12:479. doi: 10.1038/s41467-020-20784-y

Stiburek, L., Cesnekova, J., Kostkova, O., Fornuskova, D., Vinsova, K., Wenchich, L., et al. (2012). YME1L controls the accumulation of respiratory chain subunits and is required for apoptotic resistance, cristae morphogenesis, and cell proliferation. *Mol. Biol. Cell* 23, 1010–1023. doi: 10.1091/mbc.e11-08-0674

Tam, M. C., Lee, R., Cascino, T. M., Konerman, M. C., and Hummel, S. L. (2017). Current Perspectives on Systemic Hypertension in Heart Failure with Preserved Ejection Fraction. *Curr. Hypertens. Rep.* 19:12. doi: 10.1007/s11906-017-0709-2

van Almen, G. C., Verhesen, W., van Leeuwen, R. E., van de Vrie, M., Eurlings, C., Schellings, M. W., et al. (2011). MicroRNA-18 and microRNA-19 regulate CTGF and TSP-1 expression in age-related heart failure. *Aging Cell* 10, 769–779. doi: /10.1111/j.1474-9726.2011.00714.x

Volpe, M., Santolamazza, C., and Tocci, G. (2016). Hypertension in Patients with Heart Failure with Reduced Ejection Fraction. *Curr. Cardiol. Rep.* 18:127. doi: 10.1007/s11886-016-0807-9

Wang, Z. V., Rothermel, B. A., and Hill, J. A. (2010). Autophagy in hypertensive heart disease. *J. Biol. Chem.* 285, 8509–8514. doi: 10.1074/jbc.R109.025023

Wei, T., Huang, G., Gao, J., Huang, C., Sun, M., Wu, J., et al. (2017). Sirtuin 3 Deficiency Accelerates Hypertensive Cardiac Remodeling by Impairing Angiogenesis. *J. Am. Heart Assoc.* 6:e006114. doi: 10.1161/JAHA.117.006114

Wrobel, L., Topf, U., Bragoszewski, P., Wiese, S., Sztolsztener, M. E., Oeljeklaus, S., et al. (2015). Mistargeted mitochondrial proteins activate a proteostatic response in the cytosol. *Nature* 524, 485–488. doi: 10.1038/nature14951

Zhu, G. Q., Patel, K. P., Zucker, I. H., and Wang, W. (2002). Microinjection of ANG II into paraventricular nucleus enhances cardiac sympathetic afferent reflex in rats. *Am. J. Physiol. Heart Circ. Physiol.* 282, H2039–H2045. doi: 10.1152/ajpheart.00854.2001

Zucker, I. H., Wang, W., Pliquett, R. U., Liu, J. L., and Patel, K. P. (2001). The regulation of sympathetic outflow in heart failure. The roles of angiotensin II, nitric oxide, and exercise training. *Ann. N Y. Acad. Sci.* 940, 431–443. doi: 10.1111/j.1749-6632.2001.tb03696.x

Conflict of Interest: The authors declare that the research was conducted in the absence of any commercial or financial relationships that could be construed as a potential conflict of interest.

frontiers in Physiology

BRIEF RESEARCH REPORT
published: 04 February 2022
doi: 10.3389/fphys.2021.805005

COVID-19 and Mitochondrial Non-Coding RNAs: New Insights From Published Data

*Andrea Pozzi**

Graduate School of Life Sciences, Tohoku University, Sendai, Japan

Scientists all around the world are working to investigate new ways to prevent and treat COVID-19, and recent research has been focusing on the effects of a syndrome commonly called "long COVID." People affected by this syndrome usually suffer from symptoms like the ones observed in several types of fatigue syndrome. As these syndromes are often linked to mitochondrial dysfunction, researchers hypothesized that a dysfunction in the mitochondrial metabolism might be part of the causes of long COVID. However, while there are a few studies investigating the effect of SARS-CoV-2 infection on mitochondrial metabolism, the effect on the transcription of mitochondrial non-coding RNAs has not been investigated yet. Thus, using publicly available data, I explored the effect of SARS-CoV-2 on the expression of several mitochondrial non-coding RNAs in patients recovering from COVID-19. No change in the expression of long non-coding RNAs was detected at any stage of the infection, but up to 43 small mitochondrial RNAs have their expression altered during the recovery from COVID-19. This result suggests that the SARS-CoV-2 infection somehow affected the metabolism of small mitochondrial RNAs specifically without altering the overall mitochondrial transcription. Despite these being only preliminary results on a small cohort, the analyses clearly showed that individuals infected by SARS-CoV-2 retain an altered expression of these small RNAs. This persistent alteration in the expression of small mitochondrial RNAs might be involved in the long COVID syndrome and further studies are needed to confirm the possibility.

Keywords: non-coding RNAs, mitochondria, mitochondrial metabolism, COVID-19, long COVID, SARS-CoV-2

OPEN ACCESS

Edited by:
Eleonora Leucci,
KU Leuven, Belgium

Reviewed by:
Iain P. Hargreaves,
Liverpool John Moores University, United Kingdom
Afshin Beheshti,
Space Biosciences Research of NASA Ames Research Center, United States

***Correspondence:**
Andrea Pozzi
andrea.pozzi.d2@tohoku.ac.jp

Specialty section:
This article was submitted to Mitochondrial Research, a section of the journal Frontiers in Physiology

Received: *29 October 2021*
Accepted: *31 December 2021*
Published: *04 February 2022*

Citation:
Pozzi A (2022) COVID-19 and Mitochondrial Non-Coding RNAs: New Insights From Published Data. Front. Physiol. 12:805005. doi: 10.3389/fphys.2021.805005

INTRODUCTION

Although the majority of individuals fully recover from SARS-CoV-2 infections, sometimes a subgroup of patients develops a condition generally known as "long COVID syndrome" where the patient still has lingering symptoms from the infection. Although the full clinical features of the "long COVID syndrome" are not known yet (Komaroff and Bateman, 2020), many of its symptoms generally overlap with the ones observed in myalgic encephalomyelitis/chronic fatigue syndrome (ME/CFS; Paul et al., 2021). ME/CFS is a long-term debilitating illness that causes multiple symptoms, including extreme tiredness, sleep problems, and muscle pain. Although ME/CFS cause is unknown, a wide range of risk factors such as allergies or anxiety disorders (Hempel et al., 2008; Lievesley et al., 2014) has been identified. Among those, the oldest known

potential cause of these symptoms is a viral infection. Indeed, when symptoms similar to the ME/CFS manifest after a viral infection, the condition is usually called "postviral fatigue syndrome," or other names such as Iceland disease or Royal Free disease (Behan and Behan, 1988; Eriksen, 2018). The postviral fatigue syndrome matches what is observed seen in people suffering from long COVID syndrome, suggesting that long COVID syndrome might simply be the most recent case of postviral fatigue syndrome.

While the postviral fatigue syndrome has been known for decades, the mechanism used by viruses to cause this syndrome is still unknown. However, a few studies identified the disruption of the mitochondria metabolic pathway as one of the possible causes of the syndrome (Behan et al., 1991; Tomas et al., 2017). These studies led researchers to hypothesize that the SARS-CoV-2 infection might lead to a redox imbalance, similar to what was observed in postviral fatigue syndrome, thus causing the symptoms observed in the "long COVID" syndrome (Komaroff and Bateman, 2020; Paul et al., 2021). A few recent studies support this hypothesis. For example, researchers found that SARS-CoV-2 infection can lower the expression of nuclear-encoded genes related to the mitochondrial Complex I (Miller et al., 2021), thus disrupting the mitochondrial function in a similar way to what was observed in patients suffering from postviral fatigue syndrome (Behan et al., 1991). However, the mechanism used by SARS-CoV-2 to disrupt mitochondrial metabolism is unknown. One possible mechanism used could be to alter the expression of genes encoded in the mitochondrial genome. This possibility has been already partially investigated, and a recent study showed that the expression of canonical mitochondrial genes (i.e., protein-coding genes involved in ATP production) is not impaired during COVID-19 (Miller et al., 2021). Nonetheless, this study focused on the canonical mitochondrial genes while not reporting on the expression of non-canonical genes encoded within the mitochondrial genome.

Most genes encoded within the human mitochondrial genome have been known for decades, however, a few new genes have been discovered only in the last decade. The well-known genes, here called "canonical genes," are involved in ATP production (13 protein-coding genes, 22 tRNAs, and 2 rRNAs), while the newly discovered genes, here called "non-canonical genes," are a mix of small peptides and non-coding RNAs which biogenesis and function are still not fully understood. Despite their recent discovery, some information is already known for a few non-canonical genes. For example, a recent study showed that double-stranded mitochondrial RNAs trigger antiviral signaling in humans and that this signaling is partially regulated by proteins such as PNPase and SUV3 (Dhir et al., 2018). Similarly, several long non-coding RNAs (mt-lncRNAs) encoded within the mitochondrial genome, encoded in the protein-coding genes CYTB, ND5, and ND6, are likely involved in mitochondrial metabolism and have been shown to be part of known RNA-biogenesis pathways (Rackham et al., 2011; Zhao et al., 2018; Statello et al., 2021). Another group of non-canonical mitochondrial genes that might be relevant for human health is small RNAs (mt-sRNAs), which presence and tissue-specific expression have been demonstrated across multiple organisms, ranging from clam to humans (Mercer et al., 2011; Ro et al., 2013; Pozzi et al., 2017; Pozzi and Dowling, 2019; Riggs et al., 2019). These small RNAs (25–35 nt) function is unknown, however, researchers hypothesized that they might influence gene expression of both nuclear and mitochondrial genes (Pozzi and Dowling, 2021). Despite not being well characterized, it is known that at least one group of the non-canonical mitochondrial genes is involved in the immune response again viruses (double-stranded RNAs) thus making it plausible for other types of mitochondrial non-coding RNAs to be involved as well (Dhir et al., 2018). In order to obtain some preliminary results on whether other non-canonical mitochondrial genes are involved in immune response and if these genes could be linked to the long COVID syndrome, I analyzed the data from a published study using samples from patients at different stages of COVID-19 recovery (Zheng et al., 2020).

A previously published RNA dataset was analyzed to investigate the role of non-canonical mitochondrial genes in long COVID, in this dataset both long and small RNAs have been sampled from the same 18 individuals of Chinese ethnicity during their recovery from a SARS-CoV-2 infection (Zheng et al., 2020). In the published study, the researchers split the patients into three categories during their COVID-19 recovery, treatment, convalescence, and rehabilitation. Their research focused on understanding the changes in expression of known micro RNAs and nuclear mRNAs, while not reporting on mitochondrial sequences. Thus, this study will be complementary, as it will focus only on mitochondrial sequences. As studies publishing samples with double-stranded RNAs from patients infected with COVID-19 are not available, this study focuses only on long and small RNAs (mt-lncRNAs and mt-sRNAs). The hypothesis is that because of SARS-CoV-2 on mitochondrial metabolism (Miller et al., 2021), mitochondria non-canonical genes expression might be disrupted at some stage of the infection. To test this hypothesis, the following rationale will be used. Usually, changes in the expression of a gene of interest during a specific event, such as an infection, can be explained either by the gene being involved in that event, such as immune response, or that the gene expression is disrupted because of the event. Furthermore, to verify if the changes in mitochondrial non-canonical genes are reliable, another small RNA dataset from a European population has been used, where a comparison between individuals suffering from COVID-19 and healthy individuals. By using the datasets available, it can be tested if mt-lncRNAs and mt-sRNAs expression changes at any, or all, stages of COVID-19 recovery, which would suggest that these genes are either involved in the response to SARS-CoV-2 infection or disrupted by its presence (or both), thus suggesting a possible link to long COVID-19 syndrome. Furthermore, by performing these tests, it is possible to obtain several insights into the effect of SARS-CoV-2 infection on mitochondrial expression.

RESULTS

The first analysis focused on the general expression of the mitochondrial canonical genes across the three groups of patients

(**Figure 1A**). These genes clustered in four expression clusters, with most mt-tRNAs staying in the two clusters with very low expression levels. This is expected, as the RNA library used for this analysis focuses mostly on longer RNAs (200 nt >) while mt-tRNAs are usually relatively short (∼70 nt). Similarly, the cluster with the highest expression includes the genes we expected to see: the two rRNAs and most protein-coding genes. However, the cluster with a moderate level of transcription includes a mix of genes, including regions without genes (D-Loop), a mt-tRNA (Asparagine), and a few protein-coding genes. Importantly, apart from MT-ND6, none of the canonical genes is differentially expressed across the three groups of patients (**Figure 1B**). Contrary to the others, the transcription of MT-ND6 seems stable during the first two clinical stages (treatment

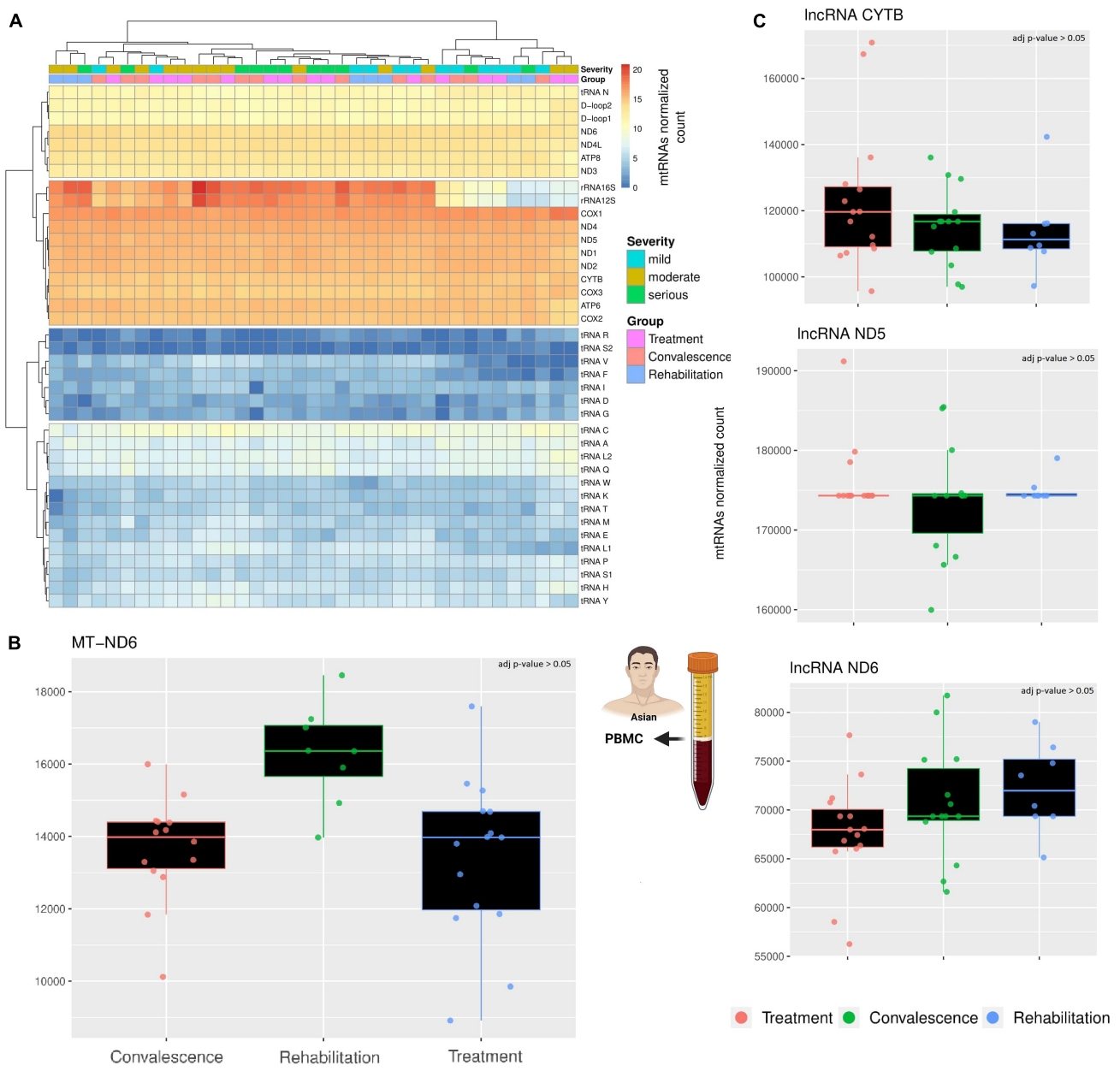

FIGURE 1 | A comparison across three clinical stages of long RNAs expression. **(A)** The heatmap compare the expression of canonical genes encoded on the mitochondrial genome. The rows represent mitochondrial genes, while the columns are individuals. Each individual has annotated the severity of the COVID-19 infection and the stage when their blood sample was taken. According to the different level of expression, ranging from blue to red, four clusters can be identified. Both columns and rows have been clustered. **(B)** The barplot compare the expression of MT-ND6 mRNA across three clinical stages. Each datapoint in a single clinical stage (e.g., Treatment) represent a different patient, furthermore, the patients are the same across the three clinical stages. **(C)** The barplots compare the expression of three lncRNAs across three clinical stages using the same criteria of the previous barplot. The icons in the figure highlights from which population and type of sample the data are generated. The icons have been made using Biorender.

and convalescence) but is significantly upregulated during the rehabilitation stage (p-value < 0.05, Wald test adjusted with Benjamin-Hochberg correction). While these results mostly align with previously observed as we did not observe a change in mRNAs for most genes (Miller et al., 2021), the upregulation of ND6 after the infection has not been observed before and it supports the hypothesis that mitochondrial metabolism might be present in patients with long COVID (Komaroff and Bateman, 2020; Paul et al., 2021).

Like the canonical genes, the transcriptional profile of the three chosen lncRNAs is stable across clinical stages (**Figure 1C**). Indeed, a differential expression analysis confirmed the absence of any significant difference among the three clinical stages (p-value > 0.05, Wald test adjusted with Benjamin-Hochberg correction). Interestingly, the gene MT-ND6 harbor both a canonical gene (protein ND6) and a non-canonical gene (lncRNA ND6), but only the canonical gene is differentially expressed across the clinical stages. This difference suggests that the SARS-CoV-2 infection affects the different classes of mitochondrial RNAs independently.

After analyzing the longer RNAs, the focus of the analysis shifted on the other non-canonical genes, the small mitochondrial RNAs (mt-sRNAs). However, contrary to the mt-lncRNAs, it was not possible to choose mt-sRNAs previously characterized to analyze, considering that human mt-sRNA with known function or biogenesis are not known. Thus, the relevant mt-sRNAs were identified using a computational pipeline that create an assembly of these mt-sRNAs and then cluster partially overlapping RNAs into clusters. For simplicity, these clusters will be referred as "mtRNA" followed by an arbitrary number. Despite the clusters including slightly different sequences, each mtRNA has a "most expressed sequence" that can be found in the material and methods section. To visualize if these mt-sRNA clusters are different across the three clinical stages, a PCA analysis was performed (**Figure 2A**). The PCA analysis clustered together with the individuals during the treatment and convalescence but separated most of the individuals during the rehabilitation stage. This is particularly evident on the first component (PC1 31%) where eight of 12 individuals cluster together. Surprisingly, while rehabilitation is more distant temporarily from the treatment stage than to the convalescence stage, the PCA analysis shows that the expression profiles of patients in the rehabilitation and treatment are more similar than rehabilitation and convalescence. The differences across mt-sRNA clusters and stages become evident when performing a differential expression analysis (**Figure 2B**). The analysis includes a total of 75 mtRNAs (mt-sRNA clusters) which were selected with arbitrary parameters (having at least 50 reads in four different samples) meant to limit the number of clusters with very low expression or high expression only in one patient. Comparing the expression of the cluster across different degrees of COVID-19 infection severity (mild, moderate, and serious) did not yield any significant results. Statistics of the comparisons between clinical stages and sexes are available in **Supplementary Table 1**. Similarly, the comparison across different ages did not yield any significant results, potentially because most of the individuals were over 50 with only a few outliers (2 male children). However, when comparing these 75 mtRNAs across the three clinical stages, and across sexes, it became obvious that some mt-sRNA clusters have differential expression. In the comparison between males and females 19 mtRNAs are differentially expressed (p-value < 0.05, Wald test adjusted with Benjamin-Hochberg correction), although it is possible that the difference in age distribution across the two sexes might have affected the result. Likewise, across the three clinical stages, there are nine are differentially expressed between the stages of treatment/convalescence, while 33 and 43 mtRNAs are differentially expressed between the stage of treatment/rehabilitation and convalescence/rehabilitation, respectively (p-value < 0.05, Wald test adjusted with Benjamin-Hochberg correction). The mtRNAs changes in expression are different across the mtRNAs, with some being upregulated and some downregulated, suggesting that the increase in mtDNA copy number is not the cause of these changes. For example, the mtRNAs 144, 57, and 104 are upregulated during the rehabilitation stage, while others like mtRNA 1 are lower during the same stage. This mixed pattern suggests that these changes are caused by a specific regulatory pathway that affects these mtRNAs rather than a simple increase or decrease of mtDNA copy number, and this process might be linked to sex-specific differences. Indeed, some mtRNAs (including the three just mentioned) are significantly enriched in one of the sexes, suggesting that some of these RNAs might have sex-specific expression. Despite the number of differentially expressed mtRNAs being different across the clinical stages, most of these clusters overlap across the clinical stages, with six of them having a very reliable difference in their expression ($p < 0.0001$ with Wald test corrected using Benjamini and Hochberg method). These mtRNAs are mtRNA1, 33 nt long and encoded within the gene mt-tRNA Glutamic acid; mtRNA2, 32 nt long encoded within the gene mt-rRNA 12 S; mtRNA8 and mtRNA9 are isoforms of the same mt-sRNA with 3 nt of difference, 26–29 nt long and both encoded within the gene mt-tRNA Serine 2 (AGU/C); mtRNA16, 38 nt long encoded within the gene mt-tRNA Lysine; mtRNA57, 37 nt long encoded within the gene mt-COX2.

Although the six mtRNAs change in expression from the two initial clinical stages to the last is always significant, the type of change is not the same clusters (**Figures 2C,D**). Furthermore, only one of these RNA clusters was significantly different across sexes, while the others were unaffected. The first cluster, mtRNA1, shows a consistent decreasing trend that goes from being the highest during the treatment stage to intermediate value during the convalescence stage, and finally reaches the lowest during the rehabilitation stage. This suggests that somehow the SARS-CoV-2 infection can lower the expression of this mtRNA even after the infection is gone. The second cluster, mtRNA2, has similar expression during the first two stages, but it is upregulated during the last clinical stage, showing an opposite regulation from mtRNA1. Likewise, the clusters mtRNAs 16 and 57 are relatively stable during treatment and convalescence but upregulated during the rehabilitation stage. Interestingly, the type of gene (i.e., rRNA and protein-coding genes) where an mtRNA is encoded does not seem to affect whether it will be down- or upregulated

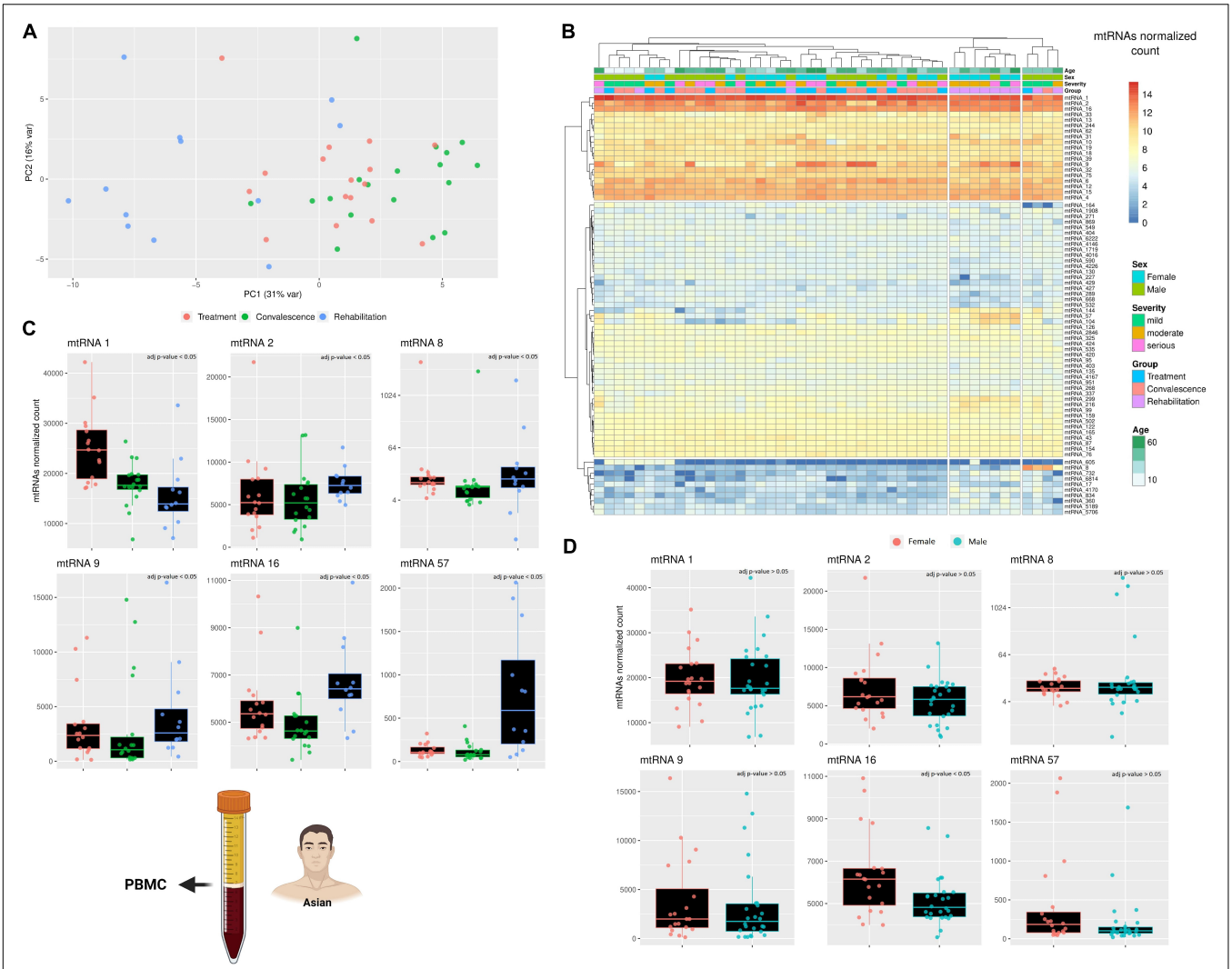

FIGURE 2 | A comparison across three clinical stages of small RNAs expression. **(A)** The PCA shows how the differences in the small mitochondrial RNAs expression cluster the patients during the rehabilitation stages away from the other two clinical stages. This effect is evident already on the PC1, suggesting that only a small number of small mitochondrial RNAs is driving this effect. The variability of each principal component is in the axis label. **(B)** The heatmap compare the expression of small RNAs encoded on the mitochondrial genome. The rows represent clusters of small RNAs (mtRNAs), while the columns are individuals. Each individual has annotated the severity of the COVID-19 infection and the stage when their blood sample was taken, its age, and its sex (male/female). The different level of expression, ranging from blue to red. **(C,D)** The barplot compare the expression of several mtRNAs that are differentially transcribed across the three clinical stages **(C)** and across sexes **(D)**. Each datapoint in a single clinical stage (e.g., Rehabilitation) represent a different patient, furthermore, the patients are the same across the three clinical stages. Full stats can be found in **Supplementary Table 1**. Due to the presence of an outlier with very high expression, only mtRNA8 has its Y-axis in Log scale. The icons in the figure on the left-side highlights from which population and type of sample the data are generated. The icons have been made using Biorender.

during the rehabilitation stage. Nonetheless, clusters such as mtRNA 8 and 9, encoded within the same mt-tRNA, have similar patterns of expression. Indeed, as they differ only of 3 nucleotides, we can see that both downregulate only during the convalescence stage and have the highest expression at the rehabilitation stage. These results clearly suggest that the SARS-CoV-2 effect on the mitochondrial transcription is specific to singular mt-sRNAs rather than general.

Due to the limited amount of data, the results presented so far lack reliability, as we could only focus on a limited cohort and use only one sample type (PBMC). To try increasing the reliability of this study, a further dataset exploring the expression of small mitochondrial RNAs from a different sample type was included (Farr et al., 2021). This small RNA dataset includes plasma samples from 10 individuals positive for COVID-19 and 10 age-matched individuals negative for COVID-19, however, there is no information regarding the disease progression or severity. A PCA analysis was performed to verify if there is any small mitochondrial RNA able to discern between the two states (positive/negative), however, there was no clustering across

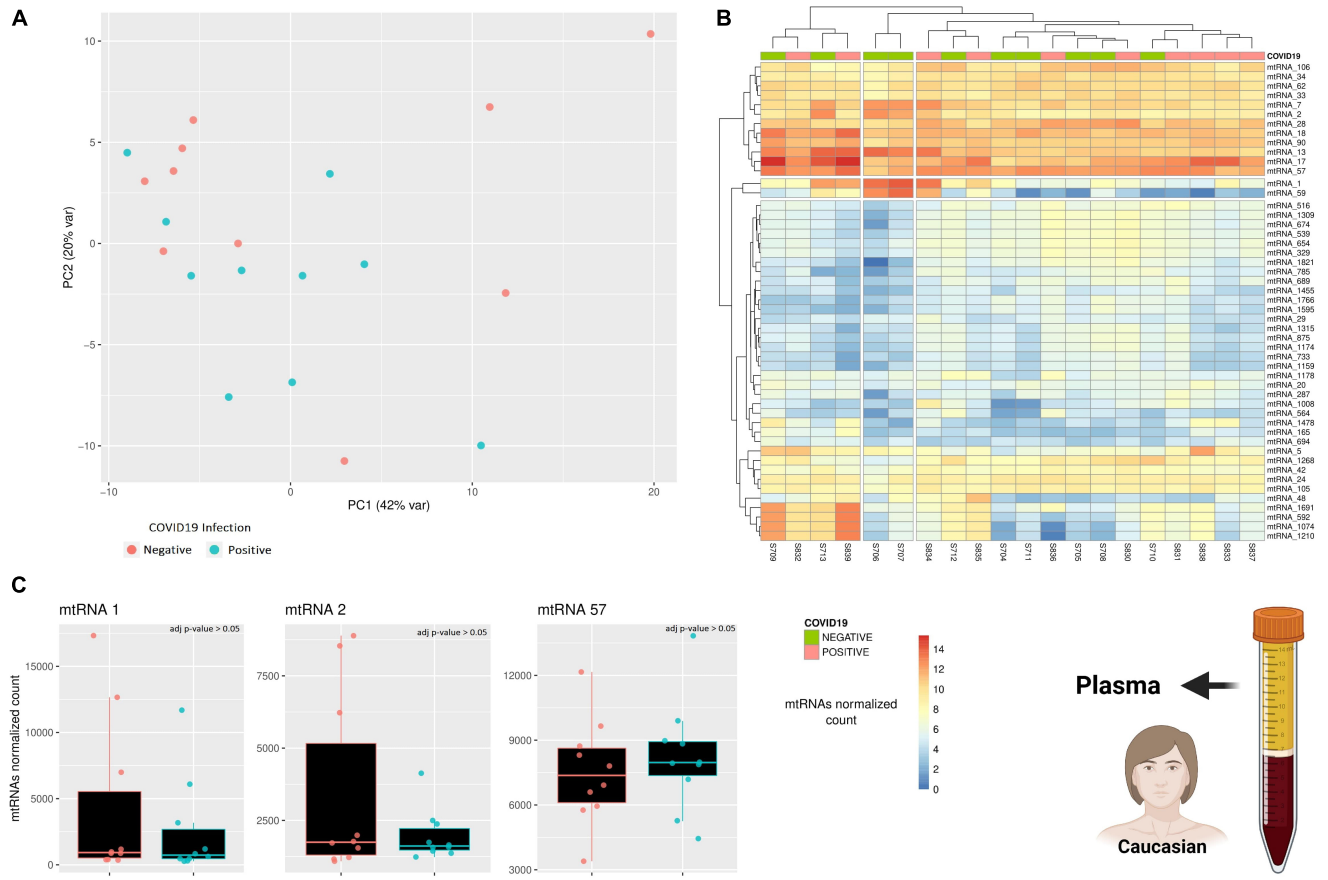

FIGURE 3 | A comparison across of small RNAs expression between COVID-19 patients and age-matched healthy individuals. **(A)** The PCA shows how similar is the general small mitochondrial RNAs expression across patients and healthy individuals. The variability of each principal component is in the axis label. **(B)** The heatmap compare the expression of small RNAs encoded on the mitochondrial genome. The rows represent clusters of small RNAs (mtRNAs), while the columns are individuals. **(C)** The barplot compare the expression of several mtRNAs that are differentially transcribed across the three clinical stages. Each datapoint represent a different patient or healthy individual. The icons in the figure on the right-side highlights from which population and type of sample the data are generated. The icons have been made using Biorender.

the samples (**Figure 3A**). Similarly, performing a differential expression analysis showed that none of the small mitochondrial RNAs expression was significantly different in the individual infected (**Figure 3B**), suggesting that pooling together different stages of the infection—and recovery—can hide the changes in expression caused by the infection. Nonetheless, it is possible that the lack of significance in the small mitochondrial RNAs might be due to the change in sample type. Indeed, three of the six small mitochondrial RNAs mentioned in the previous paragraph are absent in these plasma samples (**Figure 3C**), suggesting an important role for tissue-specific regulation on the expression of these RNAs. The three small mitochondrial RNAs present in the sample have thousands of copies, like what was observed in the dataset, however, a direct comparison could be misleading. Indeed, the different protocols for the library preparation, the sequencing depth, and the initial amount of RNA would all be strong confounding factors. Nonetheless, these results suggest that the small mitochondrial RNAs of interest might be diverse across tissues and that separating COVID-19 patients according to their different stages of recovery would help to identify small mitochondrial RNAs of interest.

DISCUSSION

Considering together the results from canonical and non-canonical genes it can be concluded that SARS-CoV-2 infection does not affect general mitochondrial transcription but, rather, affects the biogenesis pathways of specific mitochondrial products. This effect seems to be more marked on the mt-sRNAs rather than longer ones, although the reason for such a pattern can only be speculated at this stage. Nonetheless, the analysis shows that the initial hypothesis was only partially correct. Indeed, while the differential expression analysis clearly shows that some mitochondrial non-canonical genes are disrupted by the SARS-CoV-2 infection, the disruption seems limited to a specific class of genes (mt-sRNAs) and is not extended to all mitochondrial canonical and non-canonical genes. Furthermore,

the disruption detected in the first dataset was not confirmed in the second dataset, suggesting a more complex scenario.

The second dataset was included to verify if a similar disruption in the small mitochondrial RNAs expression would be present in a different sample type, thus testing if the RNAs of interest identified (e.g., mtRNA1 and 2) are likely to be upregulated through the body or only in the PBMC. However, plasma from the same samples is not available, and the second dataset changes multiple factors from the first. Indeed, in the second dataset, most individuals are women (60%) and, contrary to the previous cohort, they were recruited in central Europe, thus likely being of different ethnicity from the first dataset (Caucasian rather than Asian). Furthermore, different materials and methods were used to collect the samples and create the dataset. Thus, the two datasets differ in population, sampling and sequencing method, and tissue type, making it rather hard to know why the small mitochondrial RNAs expression is similar across COVID-19 patients and healthy individuals. However, the comparison between the datasets provides a different kind of insight.

As the data is limited, this study can only be preliminary, however, the results shown here can be used to find insights that can guide future experiments, where, hopefully, more definitive evidence can be found. The first insight we can gather by the comparison of the two small RNAs datasets is that the time of COVID-19 infection should be noted when comparing the samples, as mixing people at different stages might give misleading results. The second insight is that despite the tissue-specific expression of small mitochondrial RNAs, some of them is conserved across tissues (such as mtRNA1 and 2), thus it could be possible to easily test their abundance in many samples by qPCR and without needing to perform sequencing of each and every sample. Along the same lines, the third insight we can gather from the results is that due to the tissue-specific nature of these samples it would be important to gather samples from the tissue that better match the biology of the problem. For example, to study long COVID syndrome, having data from muscle tissues would be ideal, and if they were available, they would have been included in this study. The fourth insight we can gather is that sex might be an important variant in the expression of mitochondrial non-canonical genes, as being male or female affects the expression of some small mitochondrial RNAs in the small cohort here analyzed. The last insight that we can gather is that populations effects might be particularly relevant when studying the disruption of mitochondrial genes expression, as different mitochondria haplotypes might have different expression (as seen in fruit flies before). In conclusion, despite having only preliminary results, and in need of further experiments, it can be concluded that the mt-sRNAs expression can change during the recovery from COVID-19, making these relatively unknown RNAs good candidates for further studies into their role in long COVID.

MATERIALS AND METHODS

The long RNA datasets were downloaded from the NCBI database and then aligned to the known sequences of the three mt-lncRNAs using the aligner Bowtie2 (Langmead and Salzberg, 2013) using the –local setting, thus not requiring any adapter trimming. The count of each mt-lncRNA was computed using the tool featureCounts (Liao et al., 2014) ignoring multi-mapping reads (there were no multi-mapping reads). I used the gene count output to analyze the expression of mt-lncRNA through the package DEseq2 in R (Love et al., 2014). Similarly, all statistical tests were performed using DEseq2, which involves testing the differences across samples through a Wald test and correcting for multiple testing by using Benjamini and Hochberg method.

The small RNA datasets were downloaded from the NCBI database and then aligned to the mitochondrial reference genome (NC_012920.1) using the aligner Bowtie2 (Langmead and Salzberg, 2013) using the –local setting, thus not requiring any adapter trimming. The alignment files (.bam) were used to generate a sequence file (.fasta) including all the reads from the small RNA datasets that could be aligned to the mitochondrial genome. This file was then used to generate an assembly of all the small RNAs in the dataset by using Inchworm, the first tool of the Trinity package (Grabherr et al., 2011). Inchworm is a tool meant to be used on mRNA data, thus it tries to create an assembly with longer RNAs rather than short ones, so using this tool creates an assembly of small RNAs clusters, rather than identifying single small RNAs. Although not optimal, this approach should be accurate enough to enable at least a comparison between small RNA clusters (Bermúdez-Barrientos et al., 2020). The assembly of small RNA clusters was then used to map all the small RNAs mapping to the mitochondrial genome using the program ShortStack, which then computed the gene counts for each mt-sRNA cluster. I used the gene count output to analyze the expression of mt-lncRNA through the package DEseq2 in R (Love et al., 2014). Similarly, all statistical tests were performed using DEseq2, which involves testing the differences across samples through a Wald test and correcting for multiple testing by using Benjamini and Hochberg method. Statistics of the comparisons between clinical stages and sexes are available in **Supplementary Table 1**.

The differentially expressed mtRNAs mentioned sequences are the following:

mtRNA_1 UUGGUCGUGGUUGUAGUCCGUGCGAGAAUACCA;

mtRNA_2 AUAGGUUUGGUCCUAGCCUUUCUAUUAGCUCU;

mtRNA_8 GAGAAAGCUCACAAGAACUGCUAACU;

mtRNA_9 ACGAAAGUGGCUUUAACAUAUCUGAACA;

mtRNA_16 CACUGUAAAGCUAACUUAGCAUUAACCUUUUUAAGUUAA;

mtRNA_57 AGUAGCGUCUUGUAGACCUACUUGCGCUGCACCACCA;

DATA AVAILABILITY STATEMENT

The data used in the first part of this study are available under the accession PRJNA662985 in the NCBI database (https://www.ncbi.nlm.nih.gov/bioproject). There are 85

samples in the dataset, gathered from 18 individuals and separated into small and long RNA data. All the patients were hospitalized and enrolled between January-17-2020 and April-09-2020. All RNA samples were extracted from peripheral blood mononuclear cells (PBMC). Further information regarding the patients and the ethics of the study can be found in the article that first described the data (Zheng et al., 2020).

ETHICS STATEMENT

The data used were already available online and validated by the human ethics committee of the university that first generated the data. The patients/participants provided their written informed consent to participate in this study.

AUTHOR CONTRIBUTIONS

AP conceived the study, performed all the analyses, made the figures, wrote, and reviewed the manuscript.

FUNDING

This study was funded by the Japan Society for the Promotion of Science grant ID 21F20082.

ACKNOWLEDGMENTS

I thank Maruyama Shinichiro and Kawata Masakado for their comments and suggestion to earlier drafts of this manuscript.

SUPPLEMENTARY MATERIAL

The Supplementary Material for this article can be found online at: https://www.frontiersin.org/articles/10.3389/fphys.2021.805005/full#supplementary-material

REFERENCES

Behan, P. O., and Behan, W. M. (1988). Postviral fatigue syndrome. *Crit. Rev. Neurobiol.* 4, 157–178.

Behan, W. M., More, I. A., and Behan, P. O. (1991). Mitochondrial abnormalities in the postviral fatigue syndrome. *Acta Neuropathol.* 83, 61–65. doi: 10.1007/BF00294431

Bermúdez-Barrientos, J. R., Ramírez-Sánchez, O., Chow, F. W.-N., Buck, A. H., and Abreu-Goodger, C. (2020). Disentangling sRNA-Seq data to study RNA communication between species. *Nucleic Acids Res.* 48:e21. doi: 10.1093/nar/gkz1198

Dhir, A., Dhir, S., Borowski, L. S., Jimenez, L., Teitell, M., Rötig, A., et al. (2018). Mitochondrial double-stranded RNA triggers antiviral signalling in humans. *Nature* 560, 238–242. doi: 10.1038/s41586-018-0363-0

Eriksen, W. (2018). ME/CFS, case definition, and serological response to Epstein-Barr virus. A systematic literature review. *Fatigue* 6, 220–234. doi: 10.1080/21641846.2018.1503125

Farr, R. J., Rootes, C. L., Rowntree, L. C., Nguyen, T. H. O., Hensen, L., Kedzierski, L., et al. (2021). Altered microRNA expression in COVID-19 patients enables identification of SARS-CoV-2 infection. *PLoS Pathog.* 17:e1009759. doi: 10.1371/journal.ppat.1009759

Grabherr, M. G., Haas, B. J., Yassour, M., Levin, J. Z., Thompson, D. A., Amit, I., et al. (2011). Full-length transcriptome assembly from RNA-Seq data without a reference genome. *Nat. Biotechnol.* 29, 644–652. doi: 10.1038/nbt.1883

Hempel, S., Chambers, D., Bagnall, A.-M., and Forbes, C. (2008). Risk factors for chronic fatigue syndrome/myalgic encephalomyelitis: a systematic scoping review of multiple predictor studies. *Psychol. Med.* 38, 915–926. doi: 10.1017/S0033291707001602

Komaroff, A. L., and Bateman, L. (2020). Will COVID-19 Lead to Myalgic Encephalomyelitis/Chronic Fatigue Syndrome? *Front. Med.* 7:606824. doi: 10.3389/fmed.2020.606824

Langmead, B., and Salzberg, S. L. (2013). Fast gapped-read alignment with Bowtie 2. *Nat. Methods* 9, 357–359.

Liao, Y., Smyth, G. K., and Shi, W. (2014). featureCounts: an efficient general purpose program for assigning sequence reads to genomic features. *Bioinformatics* 30, 923–930. doi: 10.1093/bioinformatics/btt656

Lievesley, K., Rimes, K. A., and Chalder, T. (2014). A review of the predisposing, precipitating and perpetuating factors in Chronic Fatigue Syndrome in children and adolescents. *Clin. Psychol. Rev.* 34, 233–248. doi: 10.1016/j.cpr.2014.02.002

Love, M. I., Huber, W., and Anders, S. (2014). Moderated estimation of fold change and dispersion for RNA-seq data with DESeq2. *Genome Biol.* 15:550.

Mercer, T. R., Neph, S., Dinger, M. E., Crawford, J., Smith, M. A., Shearwood, A.-M. J., et al. (2011). The human mitochondrial transcriptome. *Cell* 146, 645–658. doi: 10.1016/j.cell.2011.06.051

Miller, B., Silverstein, A., Flores, M., Cao, K., Kumagai, H., Mehta, H. H., et al. (2021). Host mitochondrial transcriptome response to SARS-CoV-2 in multiple cell models and clinical samples. *Sci. Rep.* 11:3. doi: 10.1038/s41598-020-79552-z

Paul, B. D., Lemle, M. D., Komaroff, A. L., and Snyder, S. H. (2021). Redox imbalance links COVID-19 and myalgic encephalomyelitis/chronic fatigue syndrome. *Proc. Natl. Acad. Sci. U.S.A.* 118:e2024358118. doi: 10.1073/pnas.2024358118

Pozzi, A., and Dowling, D. K. (2019). The Genomic Origins of Small Mitochondrial RNAs: Are They Transcribed by the Mitochondrial DNA or by Mitochondrial Pseudogenes within the Nucleus (NUMTs)? *Genome Biol. Evol.* 11, 1883–1896. doi: 10.1093/gbe/evz132

Pozzi, A., and Dowling, D. K. (2021). Small mitochondrial RNAs as mediators of nuclear gene regulation, and potential implications for human health. *Bioessays* 43:e2000265. doi: 10.1002/bies.202000265

Pozzi, A., Plazzi, F., Milani, L., Ghiselli, F., and Passamonti, M. (2017). SmithRNAs: Could Mitochondria "Bend" Nuclear Regulation? *Mol. Biol. Evol.* 34, 1960–1973. doi: 10.1093/molbev/msx140

Rackham, O., Shearwood, A.-M. J., Mercer, T. R., Davies, S. M. K., Mattick, J. S., and Filipovska, A. (2011). Long noncoding RNAs are generated from the mitochondrial genome and regulated by nuclear-encoded proteins. *RNA* 17, 2085–2093. doi: 10.1261/rna.029405.111

Riggs, C. L., Woll, S. C., and Podrabsky, J. E. (2019). MitosRNAs and extreme anoxia tolerance in embryos of the annual killifish *Austrofundulus limnaeus*. *Sci. Rep.* 9:19812.

Ro, S., Ma, H.-Y., Park, C., Ortogero, N., Song, R., Hennig, G. W., et al. (2013). The mitochondrial genome encodes abundant small noncoding RNAs. *Cell Res.* 23, 759–774. doi: 10.1038/cr.2013.37

Statello, L., Guo, C.-J., Chen, L.-L., and Huarte, M. (2021). Gene regulation by long non-coding RNAs and its biological functions. *Nat. Rev. Mol. Cell Biol.* 22, 96–118.

Tomas, C., Brown, A., Strassheim, V., Elson, J. L., Newton, J., and Manning, P. (2017). Cellular bioenergetics is impaired in patients with chronic fatigue syndrome. *PLoS One* 12:e0186802. doi: 10.1371/journal.pone.0186802

Zhao, Y., Sun, L., Wang, R. R., Hu, J.-F., and Cui, J. (2018). The effects of mitochondria-associated long noncoding RNAs in cancer mitochondria: new players in an old arena. *Crit. Rev. Oncol. Hematol.* 131, 76–82. doi: 10.1016/j.critrevonc.2018.08.005

Zheng, H.-Y., Xu, M., Yang, C.-X., Tian, R.-R., Zhang, M., Li, J.-J., et al. (2020). Longitudinal transcriptome analyses show robust T cell immunity during recovery from COVID-19. *Signal Transduct. Target. Ther.* 5:294.

Conflict of Interest: The author declares that the research was conducted in the absence of any commercial or financial relationships that could be construed as a potential conflict of interest.

Publisher's Note: All claims expressed in this article are solely those of the authors and do not necessarily represent those of their affiliated organizations, or those of the publisher, the editors and the reviewers. Any product that may be evaluated in this article, or claim that may be made by its manufacturer, is not guaranteed or endorsed by the publisher.

frontiers in Physiology

BRIEF RESEARCH REPORT
published: 22 February 2022
doi: 10.3389/fphys.2022.800171

mt tRFs, New Players in MELAS Disease

Salvador Meseguer and Mari-Paz Rubio*

Molecular and Cellular Immunology Laboratory, Centro de Investigación Príncipe Felipe (CIPF), Valencia, Spain

MELAS (mitochondrial encephalomyopathy, lactic acidosis, and stroke-like episodes) is an OXPHOS disease mostly caused by the m.3243A>G mutation in the mitochondrial $tRNA^{Leu(UUR)}$ gene. Recently, we have shown that the mutation significantly changes the expression pattern of several mitochondrial tRNA-derived small RNAs (mt tsRNAs or mt tRFs) in a cybrid model of MELAS and in fibroblasts from MELAS patients versus control cells. Among them are those derived from mt tRNA LeuUUR containing or not the m.3243A>G mutation (mt 5′-tRF LeuUUR-m.3243A>G and mt 5′-tRF LeuUUR), whose expression levels are, respectively, increased and decreased in both MELAS cybrids and fibroblasts. Here, we asked whether mt 5′-tRF LeuUUR and mt 5′-tRF LeuUUR-m.3243A>G are biologically relevant and whether these mt tRFs are detected in diverse patient samples. Treatment with a mimic oligonucleotide of mt tRNA LeuUUR fragment (mt 5′-tRF LeuUUR) showed a therapeutic potential since it partially restored mitochondrial respiration in MELAS cybrids. Moreover, these mt tRFs could be detected in biofluids like urine and blood. We also investigated the participation of miRNA pathway components Dicer and Ago2 in the mt tRFs biogenesis process. We found that Dicer and Ago2 localize in the mitochondria of MELAS cybrids and that immunoprecipitation of these proteins in cytoplasm and mitochondria fractions revealed an increased mt tRF/mt tRNA ratio in MELAS condition compared to WT. These preliminary results suggest an involvement of Dicer and Ago2 in the mechanism of mt tRF biogenesis and action.

Keywords: sncRNAs, tRF and tiRNA, tRNA fragment, mitochondrial dysfunction, retrograde signaling

OPEN ACCESS

Edited by:
Samarjit Das,
Johns Hopkins University,
United States

Reviewed by:
Shirin Elizabeth Khorsandi,
The Roger Williams Institute of Hepatology,
United Kingdom
Kei Akiyoshi,
Johns Hopkins Medicine,
United States

****Correspondence:***
Salvador Meseguer
smeseguer@cipf.es

Specialty section:
This article was submitted to Mitochondrial Research, a section of the journal Frontiers in Physiology

Received: *22 October 2021*
Accepted: *20 January 2022*
Published: *22 February 2022*

Citation:
Meseguer S and Rubio M-P (2022) mt tRFs, New Players in MELAS Disease. Front. Physiol. 13:800171. doi: 10.3389/fphys.2022.800171

INTRODUCTION

Mitochondria activity is genetically controlled by both mitochondrial and nuclear genomes. Mutations in those DNAs can lead to diseases owing to OXPHOS deficiency, which are accompanied with extremely variable clinical manifestations (Rotig, 2011; DiMauro et al., 2013; Boczonadi and Horvath, 2014). Mitochondria–nucleus communication influences mitochondrial disease expression and is considered an important contributor to such extreme variability (Reinecke et al., 2009; Varabyova et al., 2013; Dogan et al., 2014; Picard et al., 2014; Cagin and Enriquez, 2015; Chen et al., 2015). Small non-coding RNAs (sncRNAs) are recently emerging as players in mitonuclear cross-talk (Vendramin et al., 2017; Meseguer, 2021). Several studies have addressed the engagement of microRNAs (miRNAs) in the cell response to mitochondrial dysfunction (Meseguer et al., 2015, 2017, 2018; Wang et al., 2017); however, they seem not to be the unique type of sncRNAs that participate in the mitochondria–nucleus communication

(Vendramin et al., 2017; Meseguer et al., 2019; Meseguer, 2021). tRNA-derived small fragments (tRFs or tsRNAs; ~16–35 nucleotides (nts) in length) are derived from nuclear- and mitochondrial-encoded mature and precursor tRNA sequences (Ro et al., 2013; Telonis et al., 2015; Olvedy et al., 2016; Pliatsika et al., 2016, 2018) and are generated constitutively or/and under certain conditions including cellular stress (Thompson et al., 2008; Thompson and Parker, 2009; Haussecker et al., 2010; Pederson, 2010; Garcia-Silva et al., 2012; Saikia et al., 2012; Gebetsberger and Polacek, 2013; Wang et al., 2013; Honda et al., 2015; Telonis et al., 2015; Megel et al., 2019). tRFs are arranged in major structural categories based on their sequence alignment respect to (a) the parental mature tRNA sequence: tRF-5s (also called 5′-tRFs), i-tRFs, tRF-2s, tRF-3s (or 3′-tRFs), 5′-tRNA halves (also known as 5′-tRHs or 5′-tiRNAs), and 3′-tRNA halves (3′-tRHs or 3′-tiRNAs) or (b) to the precursor tRNA in the 5′ leader (5′U-tRFs) or 3′ trailer (tRF-1s or 3′U-tRFs) sequences (Pliatsika et al., 2016; Loher et al., 2017; Xie et al., 2020). At present, there is not a full knowledge of the tRF biogenesis pathways operating in the cell, but some of the RNases reported for cytosolic tRFs are Angiogenin, RNase T2, Dicer, and RNaseZ/ELAC2 (Cole et al., 2009; Haussecker et al., 2010; Ivanov et al., 2011; Diebel et al., 2016; Megel et al., 2019; Su et al., 2019). Moreover, the function of tRFs is not yet clear. Since they can interact with various Argonaute (AGO) proteins and form biologically active complexes (Burroughs et al., 2011; Wang et al., 2013; Kuscu et al., 2018), tRFs could act as negative post-transcriptional regulators of specific mRNAs, as miRNAs do (Yeung et al., 2009; Kuscu et al., 2018).

Based on recent studies, mitochondrial tRFs differ from nuclear tRFs in terms of sequence and size (Telonis et al., 2015; Loher et al., 2018). New sensitive and specific methods like MINTmap take into consideration the existence of plenty of sequences in the nuclear genome matching mitochondrially encoded tRNAs ("mitochondrial tRNA-looklikes") among other particularities of the tRNA sequences during the mapping of the RNA-seq data (Loher et al., 2017). Although there are several *in silico* studies, so far, there are few works providing experimental evidence about the mitochondrial origin and function of tRFs (Loher et al., 2017, 2018; Magee et al., 2018; Telonis and Rigoutsos, 2018; Meseguer et al., 2019; Londin et al., 2020).

In a previous study, we used a cybrid model of MELAS (mitochondrial encephalomyopathy, lactic acidosis, and stroke-like episodes) to demonstrate that the MELAS m.3243A>G mutation in the mitochondrial tRNALeu(UUR) gene, which is associated with OXPHOS dysfunction, significantly changes the production of specific mt tRFs in comparison to controls (Meseguer et al., 2019). The analysis of small RNA-seq data by MINTmap provided a list of differentially expressed mt tRFs in the comparison MELAS cybrids versus controls, some of which had unequivocal mitochondrial origin in basis of their sequence alignment on mtDNA, while that of others was considered uncertain because of their additional matching to several regions in the nuclear genome. Among the last group of ambiguous mt tRFs, there were two derived from the 5′-end of mt tRNA LeuUUR, containing or not the m.3243A>G mutation (mt 5′-tRF LeuUUR-m.3243A>G and mt 5′-tRF LeuUUR), whose expression levels were found, respectively, increased and decreased in MELAS cybrids and in fibroblasts from MELAS patients. Two other ambiguous mt tRFs studied were derived from the 3′-end of the mt tRNA ValUAC (mt 3′-tRF ValUAC) and from the internal region of mt tRNA GluUUC (mt i-tRF GluUUC). They followed the same expression pattern as mt 5′-tRF LeuUUR-m.3243A>G. Despite their ambiguous origin, they were verified as true mitochondrial products since (i) they were mainly detected in mitochondria after performing subfraction experiments which included an RNase treatment to eliminate any RNA anchored to the mitochondrial outer membrane and (ii) they had null expression in cells depleted of mtDNA but with the same background as MELAS cells (143B Rho0 cells).

Moreover, we reported that the levels of these selected mt tRFs were diminished after knocking down of Dicer and Argonaute 2, key components in the miRNA pathway. Following the hypothesis that some mt tRFs act as miRNAs, a tool for miRNA target prediction was used to identify potential mt tRFs targets. The functional analysis of these genes revealed connection between mt tRFs and processes involving the most common affected tissues in MELAS (neurological-, cardiac-, and muscular-related processes). However, we took a step beyond the *in silico* study and biological relevance of one of the mt tRFs (mt i-tRF GluUUC) was analyzed in the cybrid cells. In particular, we found that mt i-tRF GluUUC downregulates the expression of the mitochondrial pyruvate carrier 1 (MPC1) in MELAS cybrids, promoting the accumulation of extracellular lactate. Interestingly, levels of mt i-tRF GluUUC were dependent on mt tRNA modifying enzymes operating at wobble uridine position (U34) of the parental mt tRNA, mt tRNA GluUUC (GTPBP3, MTO1, and TRMU). MELAS cells exhibited increased levels of mt i-tRF GluUUC, at least in part due to downregulation of the mt tRNA modification enzymes by the post-transcriptional repressor activity of miR-9/9*, a stress-sensitive microRNA.

In the present work, we wanted to provide preliminary data on the biogenesis mechanism of mt tRFs, as well as new evidence of their biological relevance and their therapeutic/diagnostic potential. In particular, we determined whether Dicer and Ago2 are present in the mitochondria of the WT and MELAS cybrids. Furthermore, we wondered whether it is possible to detect mt tRNA and specific mt tRFs in the Dicer and Ago2 immunoprecipitates and, if so, if their levels change in the MELAS versus control comparison. We also studied whether restoring 5′-mt-tRFLeuUUR levels in MELAS cybrids could be of biological relevance by studying its possible effects on mitochondrial respiration. Finally, we tested the levels of a selected group of mt tRFs in a small cohort of MELAS samples of different types.

MATERIALS AND METHODS

Materials

Oligonucleotides (**Supplementary Table S1**) were purchased from Sigma or Thermo Fisher.

Cell Culture

Transmitochondrial cytoplasmic hybrids (cybrids) were prepared by fusing platelets derived from a patient carrying the m.3243A>G mutation with human osteosarcoma 143B cells lacking mtDNA (TK-; ρ0 cells) as previously described (Chomyn, 1996). They were cultured in high glucose Dulbecco's modified Eagle medium (Gibco) containing 10% Fetal Bovine Serum (FBS), 1 mM sodium pyruvate, 100 U/ml penicillin, 100 µg/ml streptomycin, 2 mM glutamine, and 1 mM non-essential amino acids. They were kept at 37°C in a humidified atmosphere with 5% CO_2.

Ethics Statement

Muscle biopsies were provided by Telethon Network of Genetic Biobanks (Italy) and urine, plasma, and peripheral blood mononuclear cells (PBMCs) by Ciberer Biobank (Valencia, Spain). All samples were collected from patients with MELAS disease or from healthy subjects, and written informed consent was obtained from the participants. All procedures were approved by the Ethics Committee of Milano Area 2, Fondazione IRCCS Ca′ Granda Ospedale Maggiore Policlinico (Milan, Italy) and the Ethics Committee of Foundation for the Promotion of Health and Biomedical Research of Valencia Region, FISABIO (Valencia, Spain) and performed in accordance with the guidelines set forth by the Declaration of Helsinki.

Fluorescence Microscopy

Cybrid cells were cultured on coverslips in 24-well plates. Twenty-four hour post-seeding, cells were rinsed with PBS, fixed with 4% paraformaldehyde–PBS for 20 min at room temperature (RT), washed with PBS, permeabilized with 0.3% Triton X-100 in PBS for 15 min and washed again with PBS. Then, unreacted paraformaldehyde was quenched in 100 mM NH_4Cl, 150 mM glycine in PBS for 10 min, washed with PBS, and blocked with a solution containing 2% BSA and 0.05% Triton X-100 in PBS for 30 min at RT. Then, cells were incubated with 1:100-diluted anti-Ago2 (Sigma, SAB4200085-200UL) and anti-ATP5A1 (Thermo Fisher, 43-9800) or anti-Dicer (Abcam, ab14601) and anti-CLPP (Abcam, ab124822) antibodies in blocking solution overnight at 4°C. Upon washing with blocking solution, bound antibodies were detected by incubation, as appropriate, with 1:150-diluted Alexa Fluor 594-conjugated anti-rat (Invitrogen, A11007), Alexa Fluor 594-conjugated anti-mouse (A11020, Invitrogen), Alexa Fluor 488-conjugated anti-rabbit (Invitrogen, A11008), and Alexa Fluor 488-conjugated anti-mouse (A11001, Invitrogen) secondary antibodies in blocking solution for 1 h at 37°C. Slides were mounted in Prolong Gold antifade reagent with DAPI (Molecular Probes, 936,576), and images were obtained with Apotome-equipped Axio Observer Z1 microscope (Carl Zeiss AG).

Subcellular Fractionation

$3\text{-}5{\cdot}10^7$ cybrid cells were harvested with trypsin–EDTA solution, washed with PBS, and resuspended in 1 ml ice-cold lysis buffer (0.6 M manitol, 1 mM EDTA, 10 mM pH 6.7 PIPES, 0.3% BSA) supplemented with 1 µg/ml PMSF and 1 µg/ml leupeptin. Cells were disrupted with a nitrogen cavitation pump (2.5 bar, 10 min), and cell lysate was passed through a glass Teflon Dounce homogenizer, ~20-times. Then, the cell lysate was subjected to centrifugation at 1,500 rpm for 5 min at 4°C. The supernatant (containing cytoplasm membrane and mitochondria) and pellet (containing nuclei and undisrupted cells) were separated, and the supernatant was further centrifuged at 20,000 *g* for 20 min. The clarified supernatant (cytoplasm and membrane fraction) and pellet (mitochondria) were separated. Supernatant was re-centrifuged at 20,000 *g* for 20 min to purify the cytoplasm fraction. Mitochondria pellet was kept in ice and treated with 100 µl of 4 mg/ml Digitonin in PBS for 10 min to remove the mitochondrial outer membrane and to obtain mitoplasts. Then, PBS was added up to 1.5 ml and centrifuged at 20,000 *g* for 20 min. Pellet was washed once with PBS. Cell extracts (nuclei + undisrupted cells, mitoplasts, and cytoplasm) were prepared in RIPA buffer (150 mM NaCl, 1% Nonidet P40, 0.5% sodium deoxycholate, 0.1% SDS, and 50 mM Tris–HCl pH 8.0), containing 0.1 mM leupeptin and 1 mM PMSF. Proteins (50 µg) from the various lysates were separated by SDS/PAGE (10% acrylamide) and transferred to PVDF membranes (GE Healthcare, Amersham Biosciences). For immunodetection, we used commercial antibodies: anti-Ago2 (Sigma, SAB4200085-200UL), anti-Dicer (Abcam, ab14601), anti-RNApol II (Santa Cruz, sc-899), anti-SDHA (Abcam, ab14715), and anti-vinculin (Santa Cruz, sc-73,614). Anti-rabbit (A6154), anti-rat (A5795), and anti-mouse (A4416) IgG-horseradish peroxidase-conjugated secondary antibodies were obtained from Sigma.

Cell Culture Transfections

Cybrid cells were seeded at 1,500,000 cells/100 mm dish. After 24 h, they were transfected with antisense oligonucleotides targeting mt 5′-tRF LeuUUR-m.3243A>G (anti-mt 5′-tRF LeuUUR-m.3243A>G; custom mirVana miRNA inhibitor; Thermo Fisher), mimic molecules of mt 5′-tRF LeuUUR (pre-mt 5′-tRF LeuUUR; custom mirVana miRNA mimic; Thermo Fisher) or their respective negative Controls NC; mirVana™ miRNA Inhibitor, Negative Control #1 (NC-anti-mt tRF; 4464076; Thermo Fisher) and mirVana miRNA Mimic, Negative Control #1 (NC-pre-mt tRF; 4464058; Thermo Fisher) at a final concentration of 50 nM, using Lipofectamine 2000 reagent (Invitrogen) and Opti-MEM medium according to manufacturer's instructions. The medium was replaced by fresh growth medium 6 h after transfection, and cells were collected 48 h after transfection.

RNA Isolation and qRT-PCR

Total RNA from PBMCs, muscle samples, and MELAS cells transfected with mt 5′-tRF LeuUUR mimic or the control was isolated using TRIzol reagent (Invitrogen) and from plasma and urine samples using miRNeasy Serum/Plasma Kit (Qiagen) following the manufacturer's protocol. For mt tRF quantification, 10 ng of total RNA were reverse-transcribed in 15 µl total reaction volume using the MultiScribe reverse transcriptase and custom miRNA specific stem-loop RT primers (Thermo Fisher). Then, 1.33 µl of the reverse transcription reaction was subjected to a custom TaqMan miRNA assay (Thermo Fisher), in a total reaction volume of 12 µl using

specific primers and probes for the selected human mt tRFs and U6 snRNA, according to the manufacturer's protocol. Expression values were calculated using the comparative CT method and U6 snRNA as an endogenous control. In case of plasma samples, the combination of miR-16, −191, and 484 was used as endogenous control. To quantify mitochondrial DNA-encoded transcripts, one-step qRT-PCRs were performed in an Applied Biosystems Step-One Real-Time PCR System. 5 µl of 1/10 diluted RNA samples were reverse-transcribed and amplified by qPCR in 12 µl of total volume reaction containing specific primers (Sigma; **Supplementary Table S1**), Power SYBR Green PCR Master Mix, MultiScribe Reverse Transcriptase, and RNase Inhibitor (all from Applied Biosystems), according to manufacturer's instructions. Amplification efficiency values were very close to 100%. Expression values were calculated using the comparative CT method and 16S rRNA as an endogenous control.

Dicer and Ago2 Immunoprecipitation

3-5·10^7 cybrid cells were harvested with trypsin–EDTA solution, washed with PBS, and resuspended in growth medium with 1% formaldehyde. Cell suspensions were incubated at room temperature for 10 min on rocker. Unreacted formaldehyde was quenched by addition of Glycine to a final concentration of 141 mM and incubation at room temperature for 5 min on rocker. To pellet the cells, samples were centrifuged at 1,500 rpm for 5 min at 4°C. Medium was removed, and the pellet was washed with 2 ml cold PBS containing 0.1 mM leupeptin, 1 mM PMSF, and 20 U/ml RNase Inhibitor and resuspended in mitobuffer (0.6 M manitol, 1 mM EDTA, 10 mM PIPES pH 6.7, 0.3% BSA, 0.1 mM leupeptin, 1 mM PMSF, and 20 U/ml RNase Inhibitor). Cells were disrupted with a nitrogen cavitation pump (2.5 bar, 10 min), and cell lysates were passed through a glass Teflon Dounce homogenizer, ~20-times. Then, cell lysates were subjected to centrifugation at 1,500 rpm for 5 min at 4°C. The supernatant (containing cytoplasm membrane and mitochondria) and pellet (containing nuclei and undisrupted cells) were separated, and the supernatant was further centrifuged at 20,000 *g* for 20 min. The clarified supernatant (cytoplasm and membrane fraction) and pellet (mitochondria) were separated. Supernatant was re-centrifuged at 20,000 *g* for 20 min to purify the cytoplasm fraction. To eliminate the RNA anchored to mitochondria, mitochondria pellets were treated with 20 µg/ml RNaseA in 10 mM Tris pH 7.5 for 15 min at 37°C and washed with PBS containing 0.1 mM leupeptin, 1 mM PMSF, and 20 U/ml RNase Inhibitor. Mitochondria were resuspended in 1 ml mitochondria lysis buffer (25 mM HEPES-KOH pH 7.6, 10% Glycerol, 5 mM $MgCl_2$, 0.5 mM EDTA, 0.5% Tween 20, 0.15 M KCl, 0.1 mM leupeptin, 1 mM PMSF, and 20 U/ml RNase Inhibitor). After a 30 min incubation on ice, immunoprecipitation (IP) of crosslinked Protein/RNA was performed. For each immunoprecipitation (Ago2, Dicer, and IgG), 2 ml microfuge tubes containing 200 µl of mitochondrial lysates or cytoplasm fractions and 1.8 ml dilution buffer (16.7 mM Tris–HCl pH 8, 1.2 mM EDTA, 0.01% SDS, 1.1% Triton X-100, 165 mM NaCl, 0.1 mM leupeptin, 1 mM PMSF, and 20 U/ml RNase Inhibitor) were prepared. 20 µl Protein A Dynabeads (Invitrogen, 10002D) was added to each IP, and tubes were incubated for 2 h at 4°C with rotation. Dynabeads were pelleted using a magnet, and supernatants were transferred into new 2 ml microfuge tubes. Antibodies (10 µg) were added for each immunoprecipitation [IgG (Cell Signaling, 2729S), Ago2, and Dicer], and tubes were kept overnight at 4°C with rotation. Next day, 30 µl Protein A Dynabeads was added to each tube to collect the antibody/antigen/RNA complexes using the magnet. They were washed by resuspension in 1 ml of the following cold buffers in the order listed, low salt immune complex wash buffer (20 mM Tris–HCl pH 8, 150 mM NaCl, 1% Triton X-100, 2 mM EDTA, and 0.01% SDS), high salt immune complex wash buffer (20 mM Tris–HCl pH 8, 500 mM NaCl, 1% Triton X-100, 2 mM EDTA, and 0.01% SDS), LiCl immune complex wash buffer (10 mM Tris–HCl pH 8, 0.25 M LiCl, 1% NP40, 1 mM EDTA, and 1% deoxycholic acid), and TE buffer (10 mM Tris–HCl pH 8 and 1 mM EDTA). After the washes, antibody/antigen/RNA complexes were eluted by adding 250 µl elution buffer (100 mM $NaHCO_3$ and 1% SDS) to each tube and tubes were incubated at RT mixing at 300 rpm for 15 min. Then, supernatants with antibody/antigen/RNA complexes were separated from beads with the magnet and transferred to 1.5 ml microfuge tubes. 750 µl TRIzol reagent was added to each tube, and RNA isolation was performed according to the manufacturer's protocol. RNA pellets were resuspended in 30 µL RNase-, DNase-free water. To quantify mt tRNA levels, one-step qRT-PCRs were performed in an Applied Biosystems Step-One Real-Time PCR System. 5 µl of 1/10 diluted RNA samples were reverse-transcribed and amplified by qPCR in 12 µl of total volume reaction containing specific primers (Sigma; **Supplementary Table S1**), Power SYBR Green PCR Master Mix, MultiScribe Reverse Transcriptase, and RNase Inhibitor (all from Applied Biosystems), according to manufacturer's instructions. Amplification efficiency values were very close to 100%. To quantify mt tRFs levels, 5 µl of 1/10 diluted RNA samples were reverse-transcribed and amplified by qPCR as described in section "RNA Isolation and qRT-PCR". Relative quantitation of mt tRNAs and mt tRFs levels in mitochondria and cytoplasm fractions was calculated by the fold enrichment method 2^-[Ct(Protein)-Ct(IgG)].

High-Resolution Respirometry in Intact Cells Using Oxygraph-2K (Oroboros)

Oxygen consumption rate (OCR) in oligonucleotides-transfected and non-transfected cybrid cells was measured using a high-resolution respirometer (Oxygraph-2k, Oroboros Instruments, Innsbruck, Austria). 80% confluent cells were detached at 37°C with trypsin–EDTA and resuspended in fresh growth media at a concentration of 2,000,000 cells/mL. Each cell type was analyzed in a 2 ml Oxygraph chamber. A real-time measurement of the oxygen consumption rate (OCR) was performed at 37C° in each chamber at basal conditions and after sequential addition of inhibitors for the different mitochondrial respiratory complexes: oligomycin (2.5 µg/ml) to inhibit complex V (to assess ATP-linked respiration and leak rate), carbonyl cyanide p-trifluoromethoxyphenylhydrazone (CCCP) uncoupler with stepwise titration in 2.5 to 1.5 µM

increments (to assess maximal electron transport system respiratory capacity rate and reserve capacity), rotenone (0.5 μM) to inhibit complex I, and antimycin A (2.5 μM) to inhibit complex III (to assess non-mitochondrial respiratory capacity). Data were analyzed using DatLab7 (Oroboros, Austria) software.

Statistical Analysis

Statistical analysis was performed using Student's *t*-test and was conducted using GraphPad Prism 8 (GraphPad Software, Inc., San Diego, CA). The statistically significant differences between the means were indicated by asterisks ($*p < 0.05$, $**p < 0.01$ or $***p < 0.001$) and non-significant differences by n.s.

RESULTS

The miRNA Pathway Components Dicer and Ago2 Are present in Mitochondria of WT and MELAS Cybrids

Given that we previously reported (i) a dependence of mt tRF levels on the components of miRNA pathway Dicer and Ago2 and (ii) a major accumulation of mt tRFs in mitochondria from osteosarcoma 143B (WT and MELAS) cybrids (Meseguer et al., 2019), we decided to investigate whether those proteins are located within mitochondria of these cells. We performed immunofluorescence staining in WT and MELAS cybrids using antibodies against Ago2 and Dicer, together with antibodies against the mitochondrial proteins ATP5A1 and CLPP, and we visualized the cells by Apotome microscopy. The confocal-like images showed a partial localization of Ago2 (**Figure 1A**, top panels) and Dicer (**Figure 1A**, below panels) to mitochondria in both WT and MELAS cybrids. To further investigate the location of Dicer and Ago2 within the cell, we also completed subcellular fractionation experiments. To evaluate an internal mitochondrial localization, a Digitonin treatment of the mitochondria-enriched fraction was included in the protocol, since this non-ionic detergent is able to solubilize proteins in the mitochondrial outer membrane (MOM), providing a mitoplast (mitochondrial inner membrane (MIM) + Matrix) enriched fraction. Purity of cytosolic and mitoplast fractions was monitored by immunodetection of the cytoplasm marker vinculin and the mitochondrial marker SDHA (**Figure 1B**). In these experiments, we detected both Dicer and Ago2 not only in the cytoplasm but also in mitoplasts of WT and MELAS cybrid cells.

Therefore, we confirmed by two experimental approaches the presence of both proteins inside the mitochondria in osteosarcoma 143B cybrid cells.

Dicer and Ago2 May Interact With Mitochondrial tRNAs and tRFs

Similar to other studies using different cell lines (Bandiera et al., 2011a,b; Das et al., 2012; Sripada et al., 2012; Tattikota et al., 2013; Zhang et al., 2014; Wang et al., 2015; Bose et al., 2020), we found that both components of the miRNA pathway, Dicer and Ago2, can be located in the mitochondria of osteosarcoma 143B cybrids. Furthermore, we had previously shown that silencing of Dicer and Ago2 in cybrids reduced the expression of the tested mt tRFs (Meseguer et al., 2019). The next step was to provide more evidence on whether these proteins participate in mt tRF biogenesis and in which cellular compartment/s this could take place. To this end, we immunoprecipitated Dicer and Ago2 from the cytosolic and mitochondrial fractions of WT and MELAS cybrids and analyzed whether selected mt tRNAs (mt tRNA LeuUUR and GluUUC) and their derivative mt tRFs species (mt 5′-tRF LeuUUR and mt i-GluUUC) were bound to these proteins. RT-qPCR analysis of cytosolic fractions showed lower levels of mt tRNA LeuUUR bound to Dicer in MELAS than in WT cybrids (**Figure 2A**, left panel). Although mt tRNAs LeuUUR bound to Dicer were less detectable in mitochondrial fractions, we also observed a decrease in MELAS versus WT cells. Interestingly, the opposite result was observed when mt 5′-tRFs LeuUUR were evaluated in both cellular fractions. With respect to the levels of mt tRNA GluUUC and its derivative mt tRF specie (mt i-GluUUC), they showed an equivalent pattern to mt tRNA LeuUUR and mt 5′-tRF LeuUUR in cytosolic fractions but in mitochondria there were no significant differences (**Figure 2A**, right panel). On the other hand, Ago2 immunoprecipitations were less effective since the fold enrichment respect to IgG was low in almost all cases (**Figure 2B**). Even so, a pattern similar to that of Dicer immunoprecipitates was observed for mt tRNA LeuUUR and mt 5′-tRF LeuUUR (**Figure 2B**, left panel). All together, we found a general increase of the mt tRF/mt tRNA ratio in the Dicer and Ago2 immunoprecipitates from both fractions in favor of MELAS (**Figure 2C**). The different mt tRF/mt tRNA ratio between WT and MELAS cells indicate a differential recruitment of mt tRNAs versus mt tRFs by Dicer and Ago2 and could be the result of the stimulation of the biogenesis process of the mt tRFs in the MELAS condition: (i) the increase of Dicer-dependent digestion of mt tRNAs in MELAS cells would reduce their presence in Dicer's immunoprecipitates from these cells while increasing the presence of their mt tRF derivatives, (ii) if Ago2 were facilitating the transfer of mt tRNAs to Dicer and/or the reception of mt tRF derivatives from digestion, a stimulated biogenesis would also shift the mt tRNA-mt tRF equilibrium in favor of mt tRFs. Thus it would explain the increase of mt tRFs in Ago2 immunoprecipitates in MELAS compared to WT. However, other experimental approaches including knock out and knock in cybrids for Dicer and Ago2 are needed to validate this hypothesis.

The Treatment With a 5′-tRF LeuUUR Mimic Partially Restores Mitochondrial Respiration in MELAS Cybrids

mt tRFs may be biologically relevant as we have previously demonstrated that one of them (mt i-tRF GluUUC) downregulates the expression of its target (MPC1) and, accordingly, has an effect on a phenotypic trait of the disease (the accumulation of extracellular lactate; Meseguer et al., 2019).

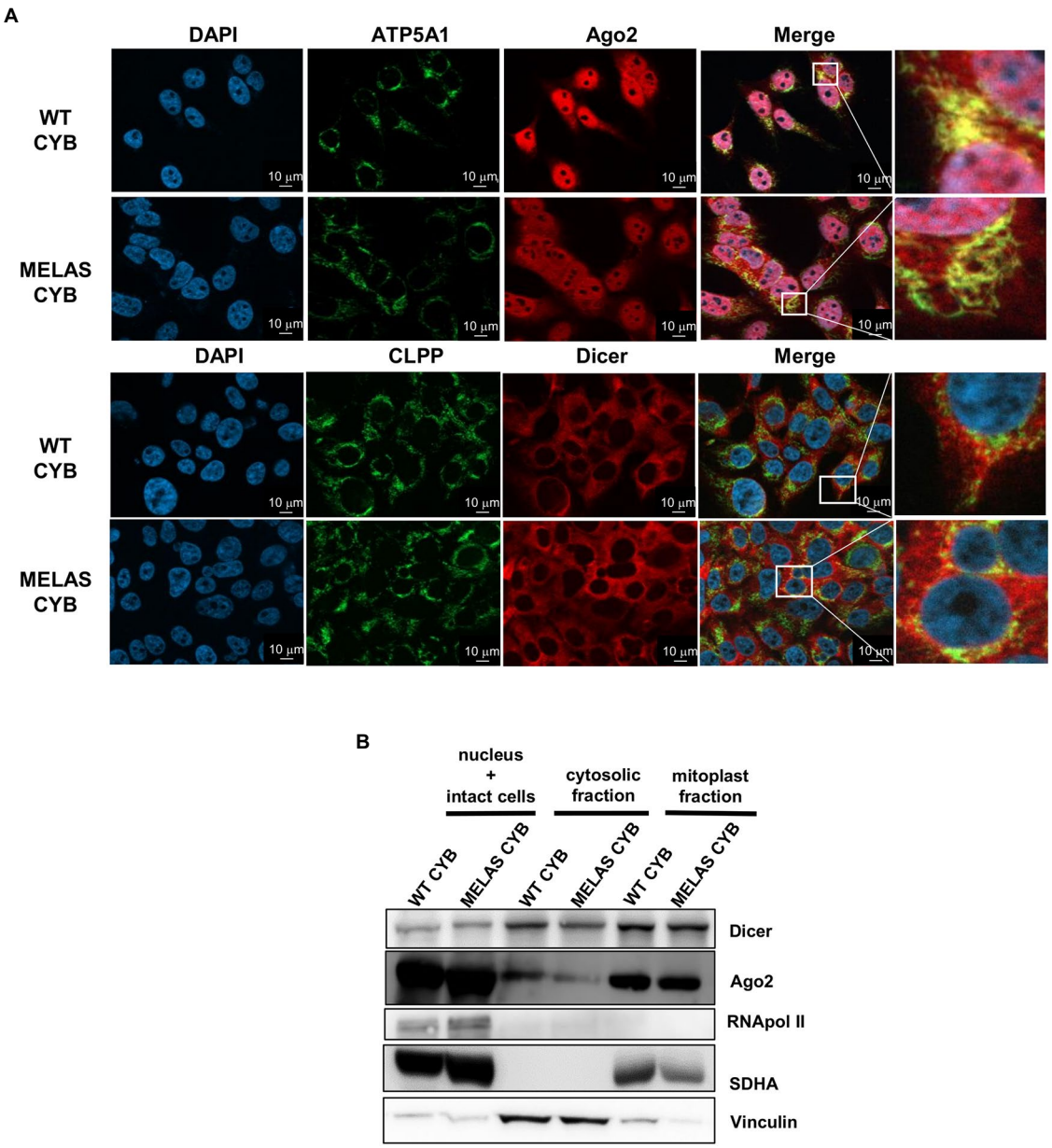

FIGURE 1 | Partial localization of Dicer and Ago2 in the mitochondrial fraction of WT and MELAS cybrid cells. **(A)** Immunofluorescence microscopy analysis of endogenous Dicer and Ago2 subcellular localization in WT and MELAS cybrid cells. Nuclei were stained with DAPI (blue), and mitochondria were immunodetected with anti-ATP5A1 (OXPHOS Complex V subunit) or anti-CLPP (a serine protease located in the mitochondrial matrix). Scale bars, 10 μm. **(B)** Representative immunoblots of Dicer and Ago2 in subcellular fractions of WT and MELAS cybrid cells. Dicer and Ago2 levels were determined in nucleus and intact cells, cytosol and mitoplasts enriched fractions together with respective markers (Pol II (nucleus), Vinculin (cytoplasm), and SDHA (mitochondria)).

In that work we also found that two significantly altered mt tRFs are derived from the mt tRNA affected by the MELAS mutation (m.3243A>G), mt 5′-tRF LeuUUR, and mt 5′-tRF LeuUUR-m.3243A>G. Here, we decided to evaluate the effect of modulating the levels of those mt tRFs, by treatment with specific oligonucleotides, on another important phenotypic characteristic of MELAS cells, a defective mitochondrial respiration. To this end, we transfected MELAS cybrids with one of the following: a mimic oligonucleotide of the wild-type mt tRNA LeuUUR fragment (pre-mt 5′-tRF LeuUUR), an antisense oligonucleotide of mutant mt tRNA LeuUUR fragment (anti-mt 5′-tRF LeuUUR-m.3243A>G) or their respective negative controls. The oxygen consumption rate (OCR) was monitored in intact cells by the High-resolution respirometer Oroboros instrument, in basal conditions and using a combination of inhibitors to analyze different respiratory states. We found that basal, ATP-linked, proton leak, reserve capacity, and maximal OCR were

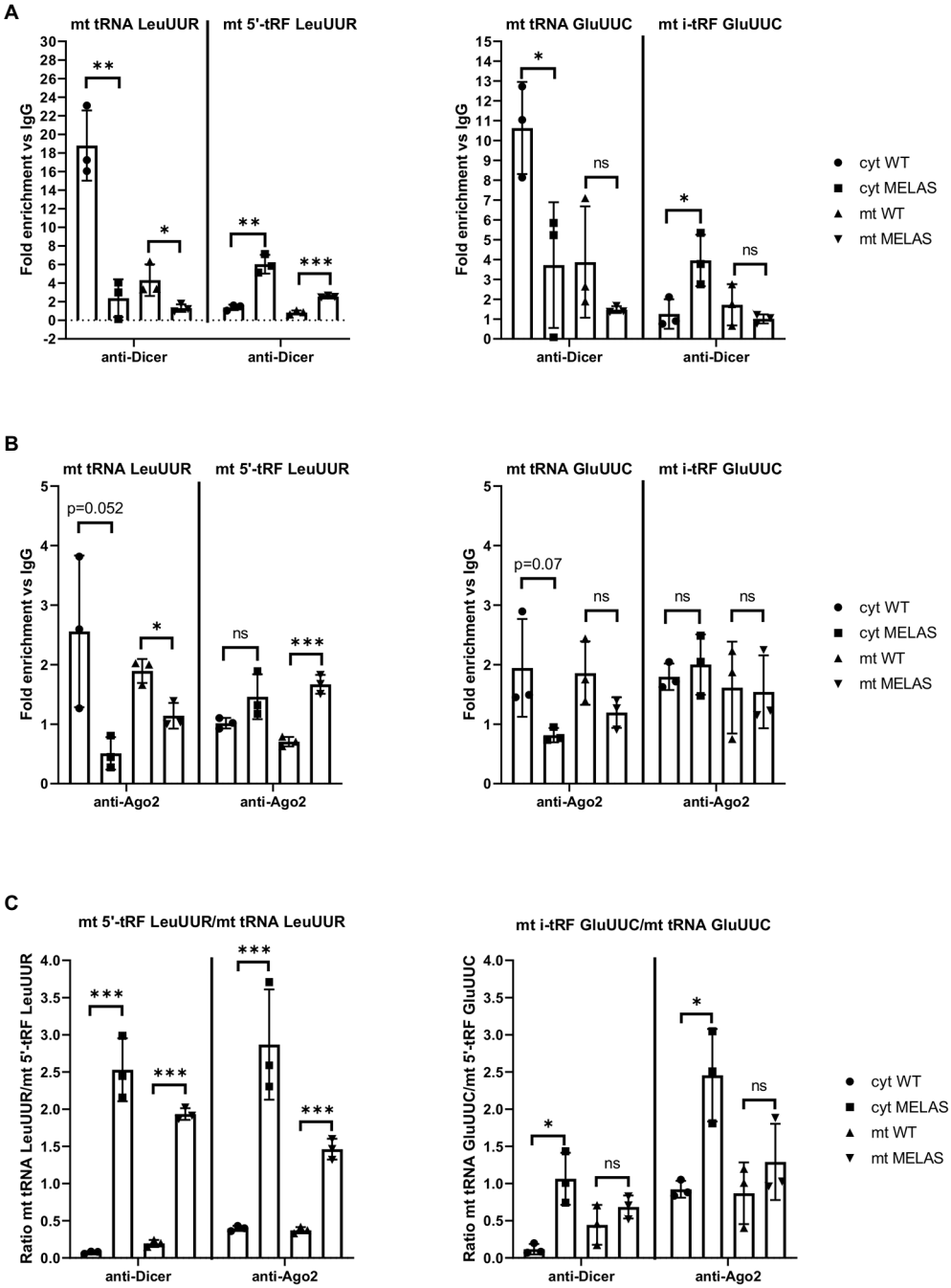

FIGURE 2 | mt tRNAs may recruit Dicer and Ago2. (A and B) RT-qPCR analysis of the expression of mt tRNAs LeuUUR, and GluUUC and mt tRFs, mt 5′-tRF LeuUUR and mt i-tRF GluUUC in Dicer **(A)** and Ago2 **(B)** immunoprecipitates from cytosolic and mitochondrial fractions of WT and MELAS cybrids. Data are represented as fold change respect to values from IgG immunoprecipitates. **(C)** Ratio between fold enrichment values for a mt tRF and its parental mt tRNA in Dicer and Ago2 immunoprecipitates from cytosolic and mitochondrial fractions of WT and MELAS cybrids. Differences from control values were found to be statistically significant at $*p<0.05$, $**p<0.01$, $***p<0.001$.

significantly increased in MELAS cells transfected with the mt-tRF LeuUUR mimic with respect to negative control-transfected cells (**Figure 3A**). However, we did not observe any effect after transfecting the cells with the anti-mt 5′-tRF LeuUUR-m.3243A>G as compared with its negative control. These results demonstrate that the mt 5′-tRF LeuUUR has also a biological relevance since its levels affect the mitochondrial respiration.

According to literature, tRFs can act as post-transcriptional regulators of specific mRNAs, as miRNAs do (Yeung et al., 2009;

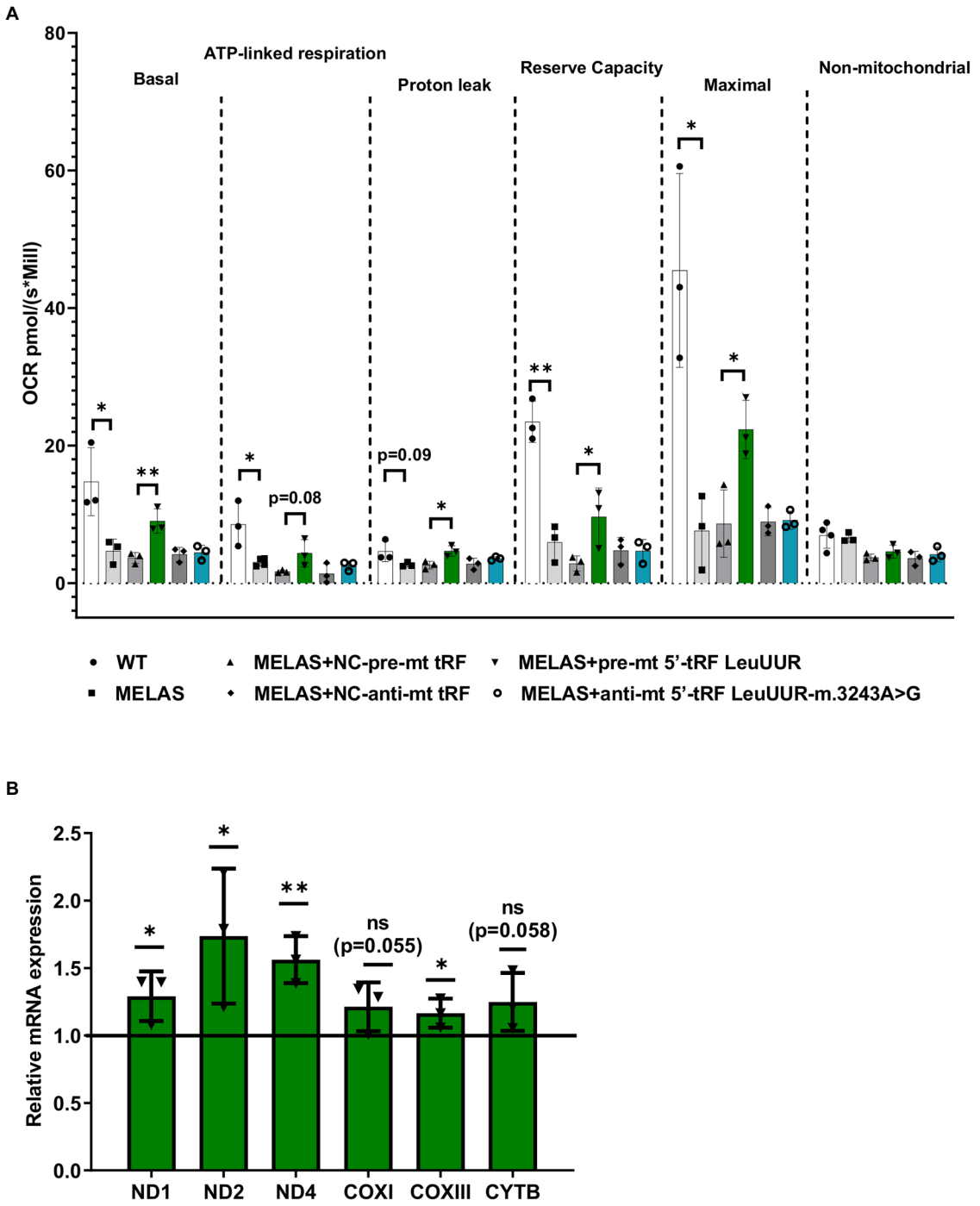

FIGURE 3 | Over-expression of mt tRNA LeuUUR fragment (mt 5′-tRF LeuUUR) increases mitochondrial respiration in MELAS cybrids. **(A)** Analysis of oxygen consumption rate (OCR) of WT and MELAS cybrids, and MELAS cybrids transfected with an oligonucleotide mimic of mt-tRNA LeuUUR fragment (mt 5′-tRF LeuUUR), an oligonucleotide antisense against mt-tRNA LeuUUR-m.3243A>G fragment (mt 5′-tRF LeuUUR-m.3243A>G) and their respective controls. OCR was measured under basal conditions and after sequential addition of different OXPHOS inhibitors: oligomycin, carbonyl cyanide p-trifluoromethoxyphenylhydrazone (CCCP), rotenone, and antimycin A. The scatter plot shows basal OCR (determined as the difference between OCR before oligomycin and OCR after rotenone/antimycin incorporation A), ATP-linked OCR (difference between OCR before and after oligomycin), proton leak (difference between basal OCR and ATP-linked OCR), reserve capacity (difference between the CCCP-stimulated rate and basal OCR), non-mitochondrial OCR (OCR after rotenone and antimycin A treatment), and maximal OCR (difference between OCR after CCCP and non-mitochondrial OCR). **(B)** RT-qPCR analysis of the expression of *ND1*, *ND2*, *ND4, COXI, COXIII*, and *CYTB* mRNAs in MELAS cybrids transfected with an oligonucleotide mimic of mt-tRNA LeuUUR fragment (mt 5′-tRF LeuUUR) with respect to negative control-transfected cells. Data are represented as fold change respect to values from control samples. The horizontal bar represents the media value for control samples. Differences from control values were found to be statistically significant at $*p < 0.05$ and $**p < 0.01$.

Kuscu et al., 2018). It has also been reported that sncRNAs encoded by mtDNA may affect mitochondrial gene expression (Ro et al., 2013). Using RNAhybrid, a prediction tool of microRNA/target RNA duplexes, we studied the putative binding sites to mtDNA-encoded genes for the mt 5′-tRF LeuUUR. We found at least 100 interactions along mtDNA (**Supplementary Figure S1A**), almost 50% of which were located in mt mRNAs codifying for OXPHOS subunits (**Supplementary Figure S1B**). We next examined the levels of several mt mRNAs in MELAS cells transfected with the mt 5′-tRF LeuUUR mimic and compared them to those of MELAS cells transfected with the control mimic. We found that some mitochondrial transcripts, mainly those encoding for Complex I subunits, increased significantly (**Figure 3B**) when the levels of the wild-type fragment were enhanced (**Supplementary Figure S2**). These results support the idea that mt 5′-tRF LeuUUR participates in the regulation of the expression of mt DNA-encoded genes. However, we cannot exclude an indirect regulation by a nuclear-encoded target of mt 5′-tRF LeuUUR.

MT TRFS ARE DETECTED IN DIFFERENT MELAS PATIENT SAMPLES

Considering that the levels of mt i-tRF GluUUC, mt 5′-tRF LeuUUR-m.3243A>G, and mt 3′-tRF ValUAC are increased in MELAS cybrids and fibroblasts compared to controls and those of mt 5′- tRF LeuUUR (the wild-type version of the fragment) are reduced (Meseguer et al., 2019), we wanted to study whether it is possible to detect this tRF signature in different types of MELAS samples. We evaluated the levels of those mt tRFs in a small but diverse cohort of MELAS and control samples, specifically, biofluids, such as urine and plasma from one MELAS and two control individuals, PBMCs from four MELAS and two control individuals, and muscle tissue from five MELAS and two control individuals. RT-qPCR analysis showed that in MELAS the expression of mt 5′-tRF LeuUUR-m.3243A>G, mt i-tRF GluUUC, and mt 3′-tRF ValUAC was increased in urine, plasma, and PBMCs (**Figure 4**). Interestingly, mt 5′- tRF LeuUUR levels were reduced in urine (**Figure 4A**) similarly to what was found in MELAS cybrids and fibroblasts (Meseguer et al., 2019) but were increased in plasma and PBMCs (**Figures 4B,C**). Due to the limited amount of RNA isolated from muscle tissue samples, we were only able to analyze mt 5′-tRF LeuUUR-m.3243A>G and mt 5′-tRF LeuUUR. We found low levels of mt 5′-tRF LeuUUR in muscles, and only one sample showed high levels of mt 5′-tRF LeuUUR-m.3243A>G (**Figure 4D**).

These results, despite the limited number of individuals in the study, hint that the tRF signature found in cybrids and fibroblasts can also be present in other MELAS samples, including biofluids, suggesting that these elements are good non-invasive biomarker candidates to be explored in depth in a study with a larger cohort. Furthermore, blood samples (plasma and PBMCs) showed increased levels of mt 5′-tRF LeuUUR in MELAS patients, a fact that could be interesting to analyze in more detail.

DISCUSSION

In this study, we demonstrated that the components of miRNA pathway Dicer and Ago2 are located in a fraction of mitochondria from WT and MELAS cybrids. Previously, other groups had also found Dicer and Ago2 in these organelles from other cell lines (Bandiera et al., 2011a,b; Das et al., 2012; Sripada et al., 2012; Tattikota et al., 2013; Zhang et al., 2014; Wang et al., 2015; Bose et al., 2020). However, this finding has not always been confirmed (Das et al., 2012; Ro et al., 2013), probably due to differences in the cell type and/or the preparation of the sample used in those other studies. The immunoprecipitation of Dicer in cytosolic and mitochondrial fractions provided mt tRNA and tRFs among the RNA pool bound to Dicer. In these *in vitro* experiments, tested mt tRNAs were more abundant in Dicer immunoprecipitates from WT fractions than from MELAS, while the opposite occurred for their derived tRFs. Although further experiments are needed to confirm whether (i) this is a direct interaction and (ii) this occurs *in vivo*, it is tentative to speculate that Dicer participates in the biogenesis of mt tRFs and that its activity is specially stimulated in the MELAS condition in basis of the increased ratio mt tRF/mt tRNA compared to WT. The immunoprecipitation of Ago2 did not provide results as clear as Dicer's but a similar tendency was observed at least for mt tRNA LeuUUR and its derived mt tRF. In the previous work, we postulated two putative mechanisms for mt tRF biogenesis which depended on Dicer and Ago2 localization within the cell. In case there were only cytosolic Dicer and Ago2 proteins, we suggested that mt tRNA molecules would be exported out of the mitochondria and processed by Dicer in the cytoplasm to generate mt tRFs. A cytosolic fraction of mt tRFs would be loaded onto Ago2 for the silencing of nuclear-encoded genes, like MPC1. In a mechanism that considers a mitochondrial fraction of Dicer and Ago2, we proposed that mt tRNAs could be processed by Dicer within the mitochondria to generate mt tRFs that would be loaded onto mt Ago2 proteins. These RNA-Ago2 complexes could participate in the regulation of the expression of mt DNA-encoded genes and/or a fraction of the mitochondrially processed mt tRFs could be transported to the cytoplasm for the regulation of nuclear-encoded genes. Our results from Dicer immunoprecipitations suggest that this enzyme operates both in the cytoplasm and inside the mitochondria, providing mt tRFs that could be participating in the post-transcriptional regulation of nDNA- and mtDNA-encoded gene expression, respectively (**Supplementary Figure S3**). The idea of a mt tRF biogenesis mechanism that functions according to the target origin is supported by the fact that mt i-tRF GluUUC, which regulates the expression of a nuclear-encoded gene (MPC1), was only detectable in the cytosolic fraction of MELAS in detrimental of its parental

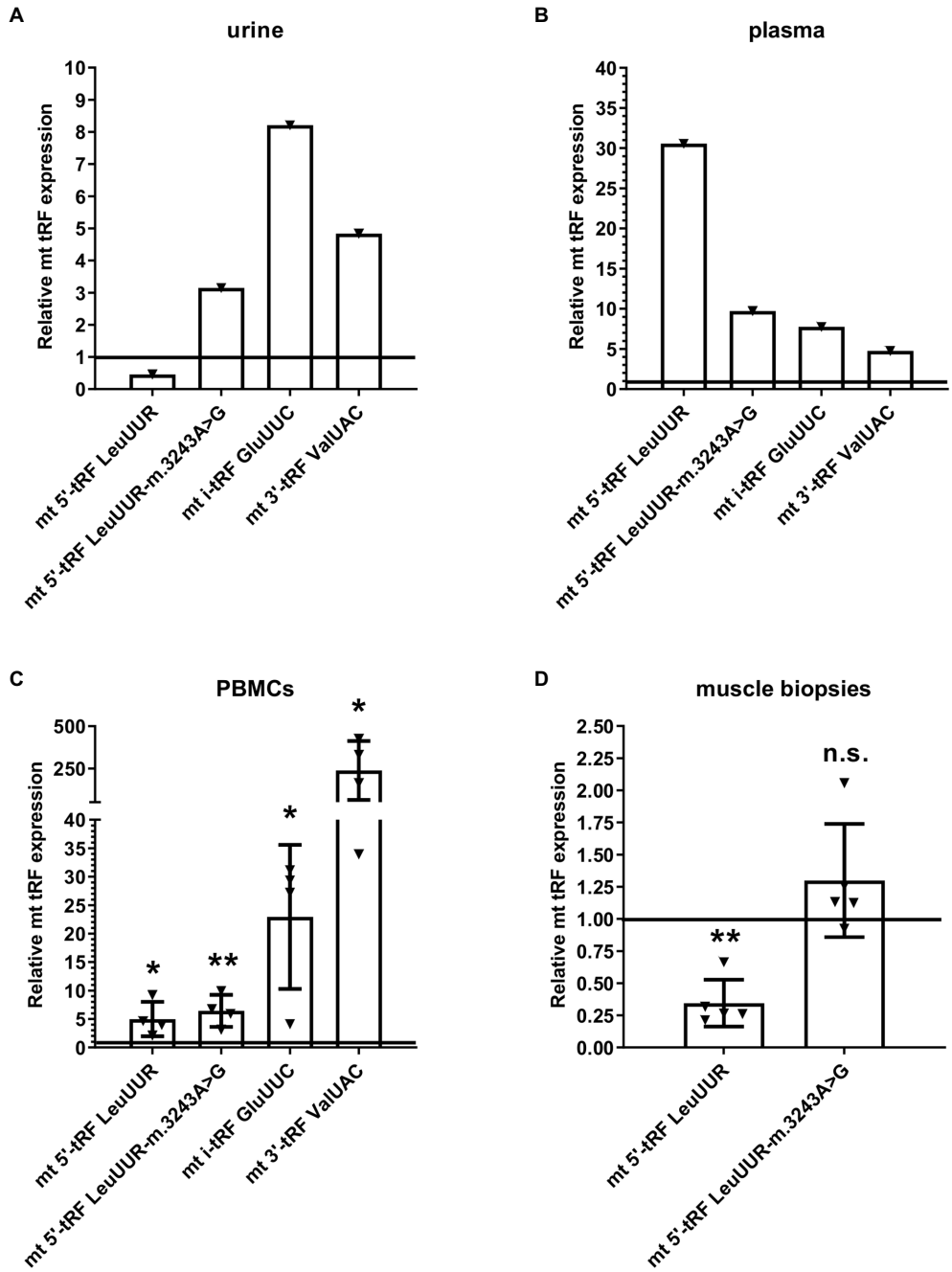

FIGURE 4 | Expression profile of mt 5′-tRF LeuUUR, mt 5′-tRF LeuUUR-m.3243A>G, mt i-tRF GluUUC, and mt 3′-tRF ValUAC in a small cohort of diverse samples from MELAS patients and controls. RT-qPCR analysis of the expression of mt 5′-tRF LeuUUR, mt 5′-tRF LeuUUR-m.3243A>G, mt i-tRF GluUUC and mt 3′-tRF ValUAC in biofluids (urine and plasma), PBMCs, and muscle tissues from MELAS patients as compared to controls. Data are represented as fold change respect to values from control samples. Each triangle represents an individual and the horizontal bar the media value for control group. Differences from control values were found to be statistically significant at $^{*}p < 0.05$ and $^{**}p < 0.01$.

mt tRNA in the same fraction. Further experiments are needed to demonstrate whether the proposed biogenesis mechanism is correct.

We also explored the therapeutic strategy of administering a mt 5′-tRF LeuUUR mimic and mt 5′-tRF LeuUUR-m.3243A>G antagonist oligonucleotides to MELAS cells. We found that treatment with the mt 5′-tRF LeuUUR mimic improved the mitochondrial respiration, a phenotypic trait of the disease, and that it was accompanied by an increase of the expression of some mitochondrial transcripts,

mainly those encoding for Complex I subunits. These results support the idea that mt 5′-tRF LeuUUR participates in the regulation of the expression of mt DNA-encoded genes and, consequently, has an effect on mitochondrial respiration. Perhaps, it would be interesting to analyze whether the mitochondrial respiration improvement increases when the mitochondrial internalization of the mt 5′-tRF LeuUUR is enhanced, using a mitochondrial deliver system like mitoPORTER (Yamada et al., 2008, 2020).

Finally, we explored the potential of mt tRFs as non-invasive biomarkers of MELAS disease. In particular, we analyzed whether the tRF signature observed in MELAS cybrids and fibroblasts [increased levels of mt i-tRF GluUUC, mt 5′-tRF LeuUUR-m.3243A>G, and mt 3′-tRF ValUAC and reduced levels of mt 5′- tRF LeuUUR (the wild-type version of the fragment) compared to controls] was also exhibited by a small group of diverse samples from MELAS patients including biofluids like urine and plasma. The urine sample showed the same tRF signature as MELAS cybrids and fibroblasts while blood samples (PBMCs and plasma) differed only in mt 5′- tRF LeuUUR levels, which were increased in these MELAS specimens. Based on these results, it would be interesting to explore in a study with a larger cohort of MELAS samples whether mt tRFs detection in biofluids could be an effective non-invasive diagnostic system.

In summary, this short study provides preliminary data on the biogenesis mechanism of mt tRFs and highlights the necessity to keep exploring the biological relevance and the therapeutic and diagnostic potential of mt tRFs.

DATA AVAILABILITY STATEMENT

The raw data supporting the conclusions of this article will be made available by the authors, without undue reservation.

ETHICS STATEMENT

The studies involving human participants were reviewed and approved by Ethics Committee of Foundation for the Promotion of Health and Biomedical Research of Valencia Region, FISABIO (Valencia, Spain) and Committee of Milano Area 2, Fondazione IRCCS Ca′ Granda Ospedale Maggiore Policlinico (Milan, Italy). The patients/participants provided their written informed consent to participate in this study.

AUTHOR CONTRIBUTIONS

SM designed the study and wrote the paper. SM and M-PR performed the experiments. All authors reviewed the manuscript. All authors contributed to the article and approved the submitted version.

FUNDING

This work has been supported by grant GV/2020/191 from the Valencian Ministry of Innovation, Universities, Science and Digital Society to Salvador Meseguer.

ACKNOWLEDGMENTS

The authors thank C. Aguado (Ciberer Biobank, Valencia, Spain) and Giacomo Pietro Comi (University of Milan) for providing MELAS samples.

SUPPLEMENTARY MATERIAL

The Supplementary Material for this article can be found online at: https://www.frontiersin.org/articles/10.3389/fphys.2022.800171/full#supplementary-material

Supplementary Table S1 | Oligonucleotides used in this work.

Supplementary Figure S1 | Potential binding sites of mt 5′-tRF LeuUUR to the mitochondrial DNA-encoded transcripts. **(A)** Binding sites for the mt 5′-tRF LeuUUR along the mitochondrial DNA and the minimum free energy of these hybridizations provided by RNAhybrid using a threshold of -15Kcal/mol. **(B)** Number of binding sites per mitochondrial transcript encoding for an OXPHOS subunit.

Supplementary Figure S2 | Levels of mt 5′-tRF LeuUUR in MELAS cells transfected with the mt-tRF LeuUUR mimic. RT-qPCR analysis of the expression of mt 5′-tRF LeuUUR in MELAS cells transfected with the mt-tRF LeuUUR mimic with respect to negative control-transfected cells. Data are represented as fold change respect to values from control samples. Differences from control values were found to be statistically significant at $^{*}p < 0.001$.

Supplementary Figure S3 | Proposed model of mt tRF biogenesis. (I) mt tRNA molecules would be exported out of the mitochondria and processed by Dicer in the cytoplasm to generate mt tRFs. Mitochondrial and cytoplasmic fractions of Ago2 proteins could be involved in the transport of mt tRNAs from mitochondria to cytosolic Dicer and mt tRFs generated in the cytoplasm would be loaded onto cytosolic Ago2 for the silencing of nuclear-encoded genes (OXPHOS subunits and/or other mitochondrial-related proteins). (II) mt tRNAs could be processed by Dicer within the mitochondria to generate mt tRFs that would be loaded onto mt Ago2 proteins. These mt tRF-Ago2 complexes could participate in the regulation of the expression of mt DNA-encoded genes (OXPHOS subunits).

REFERENCES

Bandiera, S., Hanein, S., Lyonnet, S., and Henrion-Caude, A. (2011a). Mitochondria as novel players of the cellular RNA interference. *J. Biol. Chem.* 286:le19. doi: 10.1074/jbc.L111.240259

Bandiera, S., Ruberg, S., Girard, M., Cagnard, N., Hanein, S., Chretien, D., et al. (2011b). Nuclear outsourcing of RNA interference components to human mitochondria. *PLoS One* 6:e20746. doi: 10.1371/journal.pone.0020746

Boczonadi, V., and Horvath, R. (2014). Mitochondria: impaired mitochondrial translation in human disease. *Int. J. Biochem. Cell Biol.* 48, 77–84. doi: 10.1016/j.biocel.2013.12.011

Bose, M., Chatterjee, S., Chakrabarty, Y., Barman, B., and Bhattacharyya, S. N. (2020). Retrograde trafficking of Argonaute 2 acts as a rate-limiting step for de novo miRNP formation on endoplasmic reticulum-attached polysomes in mammalian cells. *Life Sci. Alliance.* 3:e201800161. doi: 10.26508/lsa.201800161

Burroughs, A. M., Ando, Y., de Hoon, M. J., Tomaru, Y., Suzuki, H., Hayashizaki, Y., et al. (2011). Deep-sequencing of human Argonaute-associated small RNAs provides insight into miRNA sorting and reveals Argonaute association with RNA fragments of diverse origin. *RNA Biol.* 8, 158–177. doi: 10.4161/rna.8.1.14300

Cagin, U., and Enriquez, J. A. (2015). The complex crosstalk between mitochondria and the nucleus: what goes in between? *Int. J. Biochem. Cell Biol.* 63, 10–15. doi: 10.1016/j.biocel.2015.01.026

Chen, C., Chen, Y., and Guan, M. X. (2015). A peep into mitochondrial disorder: multifaceted from mitochondrial DNA mutations to nuclear gene modulation. *Protein Cell* 6, 862–870. doi: 10.1007/s13238-015-0175-z

Chomyn, A. (1996). Platelet-mediated transformation of human mitochondrial DNA-less cells. *Methods Enzymol.* 264, 334–339. doi: 10.1016/S0076-6879(96)64031-2

Cole, C., Sobala, A., Lu, C., Thatcher, S. R., Bowman, A., Brown, J. W., et al. (2009). Filtering of deep sequencing data reveals the existence of abundant dicer-dependent small RNAs derived from tRNAs. *RNA* 15, 2147–2160. doi: 10.1261/rna.1738409

Das, S., Ferlito, M., Kent, O. A., Fox-Talbot, K., Wang, R., Liu, D., et al. (2012). Nuclear miRNA regulates the mitochondrial genome in the heart. *Circ. Res.* 110, 1596–1603. doi: 10.1161/CIRCRESAHA.112.267732

Diebel, K. W., Zhou, K., Clarke, A. B., and Bemis, L. T. (2016). Beyond the ribosome: extra-translational functions of tRNA fragments. *Biomark. Insights* 11, 1–8. doi: 10.4137/BMI.S35904

DiMauro, S., Schon, E. A., Carelli, V., and Hirano, M. (2013). The clinical maze of mitochondrial neurology. *Nat. Rev. Neurol.* 9, 429–444. doi: 10.1038/nrneurol.2013.126

Dogan, S. A., Pujol, C., Maiti, P., Kukat, A., Wang, S., Hermans, S., et al. (2014). Tissue-specific loss of DARS2 activates stress responses independently of respiratory chain deficiency in the heart. *Cell Metab.* 19, 458–469. doi: 10.1016/j.cmet.2014.02.004

Garcia-Silva, M. R., Cabrera-Cabrera, F., Guida, M. C., and Cayota, A. (2012). Hints of tRNA-derived small RNAs role in RNA silencing mechanisms. *Genes* 3, 603–614. doi: 10.3390/genes3040603

Gebetsberger, J., and Polacek, N. (2013). Slicing tRNAs to boost functional ncRNA diversity. *RNA Biol.* 10, 1798–1806. doi: 10.4161/rna.27177

Haussecker, D., Huang, Y., Lau, A., Parameswaran, P., Fire, A. Z., and Kay, M. A. (2010). Human tRNA-derived small RNAs in the global regulation of RNA silencing. *RNA* 16, 673–695. doi: 10.1261/rna.2000810

Honda, S., Loher, P., Shigematsu, M., Palazzo, J. P., Suzuki, R., Imoto, I., et al. (2015). Sex hormone-dependent tRNA halves enhance cell proliferation in breast and prostate cancers. *Proc. Natl. Acad. Sci. U. S. A.* 112, E3816–E3825. doi: 10.1073/pnas.1510077112

Ivanov, P., Emara, M. M., Villen, J., Gygi, S. P., and Anderson, P. (2011). Angiogenin-induced tRNA fragments inhibit translation initiation. *Mol. Cell* 43, 613–623. doi: 10.1016/j.molcel.2011.06.022

Kuscu, C., Kumar, P., Kiran, M., Su, Z., Malik, A., and Dutta, A. (2018). tRNA fragments (tRFs) guide ago to regulate gene expression post-transcriptionally in a dicer independent manner. *RNA* 24, 1093–1105. doi: 10.1261/rna.066126.118

Loher, P., Telonis, A. G., and Rigoutsos, I. (2017). MINTmap: fast and exhaustive profiling of nuclear and mitochondrial tRNA fragments from short RNA-seq data. *Sci. Rep.* 7, 41184. doi: 10.1038/srep41184

Loher, P., Telonis, A. G., and Rigoutsos, I. (2018). Accurate profiling and quantification of tRNA fragments from RNA-Seq data: a vade mecum for MINTmap. *Methods Mol. Biol.* 1680, 237–255. doi: 10.1007/978-1-4939-7339-2_16

Londin, E., Magee, R., Shields, C. L., Lally, S. E., Sato, T., and Rigoutsos, I. (2020). IsomiRs and tRNA-derived fragments are associated with metastasis and patient survival in uveal melanoma. *Pigment Cell Melanoma Res.* 33, 52–62. doi: 10.1111/pcmr.12810

Magee, R. G., Telonis, A. G., Loher, P., Londin, E., and Rigoutsos, I. (2018). Profiles of miRNA isoforms and tRNA fragments in prostate cancer. *Sci. Rep.* 8:5314. doi: 10.1038/s41598-018-22488-2

Megel, C., Hummel, G., Lalande, S., Ubrig, E., Cognat, V., Morelle, G., et al. (2019). Plant RNases T2, but not dicer-like proteins, are major players of tRNA-derived fragments biogenesis. *Nucleic Acids Res.* 47, 941–952. doi: 10.1093/nar/gky1156

Meseguer, S. (2021). MicroRNAs and tRNA-derived small fragments: key messengers in nuclear-mitochondrial communication. *Front. Mol. Biosci.* 8:643575. doi: 10.3389/fmolb.2021.643575

Meseguer, S., Boix, O., Navarro-Gonzalez, C., Villarroya, M., Boutoual, R., Emperador, S., et al. (2017). microRNA-mediated differential expression of TRMU, GTPBP3 and MTO1 in cell models of mitochondrial-DNA diseases. *Sci. Rep.* 7:6209. doi: 10.1038/s41598-017-06553-w

Meseguer, S., Martinez-Zamora, A., Garcia-Arumi, E., Andreu, A. L., and Armengod, M. E. (2015). The ROS-sensitive microRNA-9/9* controls the expression of mitochondrial tRNA-modifying enzymes and is involved in the molecular mechanism of MELAS syndrome. *Hum. Mol. Genet.* 24, 167–184. doi: 10.1093/hmg/ddu427

Meseguer, S., Navarro-González, C., Panadero, J., Villarroya, M., Boutoual, R., Sánchez-Alcázar, J. A., et al. (2019). The MELAS mutation m.3243A>G alters the expression of mitochondrial tRNA fragments. *Biochim Biophys Acta Mol. Cell Res.* 1866, 1433–1449. doi: 10.1016/j.bbamcr.2019.06.004

Meseguer, S., Panadero, J., Navarro-Gonzalez, C., Villarroya, M., Boutoual, R., Comi, G. P., et al. (2018). The MELAS mutation m.3243A>G promotes reactivation of fetal cardiac genes and an epithelial-mesenchymal transition-like program via dysregulation of miRNAs. *Biochim. Biophys. Acta* 1864, 3022–3037. doi: 10.1016/j.bbadis.2018.06.014

Olvedy, M., Scaravilli, M., Hoogstrate, Y., Visakorpi, T., Jenster, G., and Martens-Uzunova, E. S. (2016). A comprehensive repertoire of tRNA-derived fragments in prostate cancer. *Oncotarget* 7, 24766–24777. doi: 10.18632/oncotarget.8293

Pederson, T. (2010). Regulatory RNAs derived from transfer RNA? *RNA* 16, 1865–1869. doi: 10.1261/rna.2266510

Picard, M., Zhang, J., Hancock, S., Derbeneva, O., Golhar, R., Golik, P., et al. (2014). Progressive increase in mtDNA 3243A>G heteroplasmy causes abrupt transcriptional reprogramming. *Proc. Natl. Acad. Sci. U. S. A.* 111, E4033–E4042. doi: 10.1073/pnas.1414028111

Pliatsika, V., Loher, P., Magee, R., Telonis, A. G., Londin, E., Shigematsu, M., et al. (2018). MINTbase v2.0: a comprehensive database for tRNA-derived fragments that includes nuclear and mitochondrial fragments from all the cancer genome atlas projects. *Nucleic Acids Res.* 46, D152–D159. doi: 10.1093/nar/gkx1075

Pliatsika, V., Loher, P., Telonis, A. G., and Rigoutsos, I. (2016). MINTbase: a framework for the interactive exploration of mitochondrial and nuclear tRNA fragments. *Bioinformatics* 32, 2481–2489. doi: 10.1093/bioinformatics/btw194

Reinecke, F., Smeitink, J. A., and van der Westhuizen, F. H. (2009). OXPHOS gene expression and control in mitochondrial disorders. *Biochim. Biophys. Acta* 1792, 1113–1121. doi: 10.1016/j.bbadis.2009.04.003

Ro, S., Ma, H. Y., Park, C., Ortogero, N., Song, R., Hennig, G. W., et al. (2013). The mitochondrial genome encodes abundant small noncoding RNAs. *Cell Res.* 23, 759–774. doi: 10.1038/cr.2013.37

Rotig, A. (2011). Human diseases with impaired mitochondrial protein synthesis. *Biochim. Biophys. Acta* 1807, 1198–1205. doi: 10.1016/j.bbabio.2011.06.010

Saikia, M., Krokowski, D., Guan, B. J., Ivanov, P., Parisien, M., Hu, G. F., et al. (2012). Genome-wide identification and quantitative analysis of cleaved tRNA fragments induced by cellular stress. *J. Biol. Chem.* 287, 42708–42725. doi: 10.1074/jbc.M112.371799

Sripada, L., Tomar, D., Prajapati, P., Singh, R., and Singh, A. K. (2012). Systematic analysis of small RNAs associated with human mitochondria by deep sequencing: detailed analysis of mitochondrial associated miRNA. *PLoS One* 7:e44873. doi: 10.1371/journal.pone.0044873

Su, Z., Kuscu, C., Malik, A., Shibata, E., and Dutta, A. (2019). Angiogenin generates specific stress-induced tRNA halves and is not involved in tRF-3-mediated gene silencing. *J. Biol. Chem.* 294, 16930–16941. doi: 10.1074/jbc.RA119.009272

Tattikota, S. G., Sury, M. D., Rathjen, T., Wessels, H. H., Pandey, A. K., You, X., et al. (2013). Argonaute2 regulates the pancreatic β-cell secretome. *Mol. Cell. Proteomics* 12, 1214–1225. doi: 10.1074/mcp.M112.024786

Telonis, A. G., Loher, P., Honda, S., Jing, Y., Palazzo, J., Kirino, Y., et al. (2015). Dissecting tRNA-derived fragment complexities using personalized transcriptomes reveals novel fragment classes and unexpected dependencies. *Oncotarget* 6, 24797–24822. doi: 10.18632/oncotarget.4695

Telonis, A. G., and Rigoutsos, I. (2018). Race disparities in the contribution of miRNA isoforms and tRNA-derived fragments to triple-negative breast cancer. *Cancer Res.* 78, 1140–1154. doi: 10.1158/0008-5472.CAN-17-1947

Thompson, D. M., Lu, C., Green, P. J., and Parker, R. (2008). tRNA cleavage is a conserved response to oxidative stress in eukaryotes. *RNA* 14, 2095–2103. doi: 10.1261/rna.1232808

Thompson, D. M., and Parker, R. (2009). Stressing out over tRNA cleavage. *Cell* 138, 215–219. doi: 10.1016/j.cell.2009.07.001

Varabyova, A., Stojanovski, D., and Chacinska, A. (2013). Mitochondrial protein homeostasis. *IUBMB Life* 65, 191–201. doi: 10.1002/iub.1122

Vendramin, R., Marine, J. C., and Leucci, E. (2017). Non-coding RNAs: the dark side of nuclear-mitochondrial communication. *EMBO J.* 36, 1123–1133. doi: 10.15252/embj.201695546

Wang, Q., Lee, I., Ren, J., Ajay, S. S., Lee, Y. S., and Bao, X. (2013). Identification and functional characterization of tRNA-derived RNA fragments (tRFs) in respiratory syncytial virus infection. *Mol. Ther.* 21, 368–379. doi: 10.1038/mt.2012.237

Wang, W. X., Visavadiya, N. P., Pandya, J. D., Nelson, P. T., Sullivan, P. G., and Springer, J. E. (2015). Mitochondria-associated microRNAs in rat hippocampus following traumatic brain injury. *Exp. Neurol.* 265, 84–93. doi: 10.1016/j.expneurol.2014.12.018

Wang, W., Zhuang, Q., Ji, K., Wen, B., Lin, P., Zhao, Y., et al. (2017). Identification of miRNA, lncRNA and mRNA-associated ceRNA networks and potential biomarker for MELAS with mitochondrial DNA A3243G mutation. *Sci. Rep.* 7:41639. doi: 10.1038/srep41639

Xie, Y., Yao, L., Yu, X., Ruan, Y., Li, Z., and Guo, J. (2020). Action mechanisms and research methods of tRNA-derived small RNAs. *Signal Transduct. Target. Ther.* 5:109. doi: 10.1038/s41392-020-00217-4

Yamada, Y., Akita, H., Kamiya, H., Kogure, K., Yamamoto, T., Shinohara, Y., et al. (2008). MITO-Porter: A liposome-based carrier system for delivery of macromolecules into mitochondria via membrane fusion. *Biochim. Biophys. Acta* 1778, 423–432. doi: 10.1016/j.bbamem.2007.11.002

Yamada, Y., Maruyama, M., Kita, T., Usami, S. I., Kitajiri, S. I., and Harashima, H. (2020). The use of a MITO-Porter to deliver exogenous therapeutic RNA to a mitochondrial disease's cell with a A1555G mutation in the mitochondrial 12S rRNA gene results in an increase in mitochondrial respiratory activity. *Mitochondrion* 55, 134–144. doi: 10.1016/j.mito.2020.09.008

Yeung, M. L., Bennasser, Y., Watashi, K., Le, S. Y., Houzet, L., and Jeang, K. T. (2009). Pyrosequencing of small non-coding RNAs in HIV-1 infected cells: evidence for the processing of a viral-cellular double-stranded RNA hybrid. *Nucleic Acids Res.* 37, 6575–6586. doi: 10.1093/nar/gkp707

Zhang, X., Zuo, X., Yang, B., Li, Z., Xue, Y., Zhou, Y., et al. (2014). MicroRNA directly enhances mitochondrial translation during muscle differentiation. *Cell* 158, 607–619. doi: 10.1016/j.cell.2014.05.047

Conflict of Interest: The authors declare that the research was conducted in the absence of any commercial or financial relationships that could be construed as a potential conflict of interest.

Publisher's Note: All claims expressed in this article are solely those of the authors and do not necessarily represent those of their affiliated organizations, or those of the publisher, the editors and the reviewers. Any product that may be evaluated in this article, or claim that may be made by its manufacturer, is not guaranteed or endorsed by the publisher.

frontiers | Frontiers in Physiology

ORIGINAL RESEARCH
published: 06 April 2022
doi: 10.3389/fphys.2022.772313

A Synthetic Small RNA Homologous to the D-Loop Transcript of mtDNA Enhances Mitochondrial Bioenergetics

Theodore L. Mathuram[1], Danyelle M. Townsend[2], Vincent J. Lynch[3], Ilya Bederman[4], Zhi-Wei Ye[2], Jie Zhang[2], Wade J. Sigurdson[5], Erin Prendergast[4], Raul Jobava[4], Jonathan P. Ferruzza[1], Mary R. D'Angelo[1], Maria Hatzoglou[4], Yaron Perry[6†] and Anna Blumental-Perry[1†]*

[1] Department of Biochemistry, Jacobs School of Medicine and Biomedical Sciences, University at Buffalo, State University of New York, Buffalo, NY, United States, [2] Department of Drug Discovery & Biomedical Sciences, College of Pharmacy, Medical University of South Carolina, Charleston, SC, United States, [3] Department of Biological Sciences, College of Arts and Sciences, University at Buffalo, State University of New York, Buffalo, NY, United States, [4] Department of Genetics and Genome Sciences, School of Medicine, Case Western Reserve University, Cleveland, OH, United States, [5] Department of Medicine, Confocal Microscope and Flow Cytometry Facility, Jacobs School of Medicine and Biomedical Sciences, University at Buffalo, State University of New York, Buffalo, NY, United States, [6] Division of Thoracic Surgery, Department of Surgery, Jacobs School of Medicine and Biomedical Sciences, University at Buffalo, State University of New York, Buffalo, NY, United States

Mitochondrial malfunction is a hallmark of many diseases, including neurodegenerative disorders, cardiovascular and lung diseases, and cancers. We previously found that alveolar progenitor cells, which are more resistant to cigarette smoke-induced injury than the other cells of the lung parenchyma, upregulate the mtDNA-encoded small non-coding RNA mito-ncR-805 after exposure to smoke. The mito-ncR-805 acts as a retrograde signal between the mitochondria and the nucleus. Here, we identified a region of mito-ncR-805 that is conserved in the mammalian mitochondrial genomes and generated shorter versions of mouse and human transcripts (mmu-CR805 and hsa-LDL1, respectively), which differ in a few nucleotides and which we refer to as the "functional bit". Overexpression of mouse and human functional bits in either the mouse or the human lung epithelial cells led to an increase in the activity of the Krebs cycle and oxidative phosphorylation, stabilized the mitochondrial potential, conferred faster cell division, and lowered the levels of proapoptotic pseudokinase, TRIB3. Both oligos, mmu-CR805 and hsa-LDL1 conferred cross-species beneficial effects. Our data indicate a high degree of evolutionary conservation of retrograde signaling *via* a functional bit of the D-loop transcript, mito-ncR-805, in the mammals. This emphasizes the importance of the pathway and suggests a potential to develop this functional bit into a therapeutic agent that enhances mitochondrial bioenergetics.

Keywords: mitochondria, mitochondria-to-nucleus retrograde signaling, small ncRNA, Krebs cycle, OxPhos, D-loop transcripts

OPEN ACCESS

Edited by:
Veronica Andrea Burzio, Andres Bello University, Chile

Reviewed by:
Constantinos Stathopoulos, University of Patras, Greece
Ge Shan, University of Science and Technology of China, China
Maria Rita Rippo, Marche Polytechnic University, Italy
Jaime Villegas, Andrés Bello University, Chile

***Correspondence:**
Anna Blumental-Perry
annablum@buffalo.edu

†These authors share senior authorship

Specialty section:
This article was submitted to Mitochondrial Research, a section of the journal Frontiers in Physiology

Received: *07 September 2021*
Accepted: *24 February 2022*
Published: *06 April 2022*

Citation:
Mathuram TL, Townsend DM, Lynch VJ, Bederman I, Ye Z-W, Zhang J, Sigurdson WJ, Prendergast E, Jobava R, Ferruzza JP, D'Angelo MR, Hatzoglou M, Perry Y and Blumental-Perry A (2022) A Synthetic Small RNA Homologous to the D-Loop Transcript of mtDNA Enhances Mitochondrial Bioenergetics. Front. Physiol. 13:772313. doi: 10.3389/fphys.2022.772313

INTRODUCTION

Mitochondria are an integral part of eukaryotic cells. They have their own genome, which in mammals is approximately 16.6 kb, encoding 13 mitochondrial proteins of the electron transport chain (ETC) and harboring 22 tRNAs and 2 ribosomal subunit RNAs (Shadel and Clayton, 1997; Fernandez-Silva et al., 2003). The rest of the mitochondrial proteins, including proteins of tricarboxylic acid (TCA) or Krebs cycle) and ETC complexes, are encoded by nuclear genes, and are imported into the organelle (Scarpulla, 2008). Thus, signaling between the two organelles is necessary for mitochondrial integrity and cellular homeostasis. This signaling cascade is achieved through bidirectional communication between the nucleus and the mitochondria (Quiros et al., 2016; Vendramin et al., 2017). Nucleus-to-mitochondrion anterograde signaling is mediated by well-studied nuclear transcription factors, and many aspects of it are well characterized (Scarpulla, 2008). It is thought that anterograde signaling adjusts the functioning of healthy mitochondria to the cellular needs. When a cell faces stressful challenges, mitochondrial function may be compromised (Grek and Townsend, 2014; Zhang et al., 2019; Costiniti et al., 2020). Sometimes, the mitochondria can mitigate the damage caused by the stress, but sometimes that damage is irreversible. In either adaptive or maladaptive stress responses, the mitochondria need to convey their status to the nucleus, and often the composition and the function of the organelles need to be altered for cell survival (Scarpulla, 2008; Quiros et al., 2016; Vendramin et al., 2017). Retrograde mitochondrion-to-nucleus signaling is achieved through common metabolite intermediates, such as Ca^{2+} ions and TCA cycle metabolites (Quiros et al., 2016).

Nuclear genes that encode mitochondrial proteins (neMITO) monitor mitochondrial status. For example, the mitochondrial unfolded protein response (mito-UPR) is regulated by activating transcription factor associated with stress/activation transcription factor 5 (ATFS-1/ATF5). The ATFS-1 (or ATF5 in the mammals) is imported into the healthy mitochondria *via* its mitochondrion-targeting sequence (MTS). The ATFS-1/ATF5 that cannot be imported due to the effects of stress is transported into the nucleus to activate the genes to relieve that stress (Shpilka and Haynes, 2018; Munoz-Carvajal and Sanhueza, 2020). Another protein with mitochondrial localization, the DELE1, communicates with the mitochondrial stress to the integrated stress response *via* its relocation to cytosol (Fessler et al., 2020; Guo et al., 2020) to restore the mitochondrial function. Other neMITO proteins, such as the mitochondrial isomer of transcriptional coactivator G-protein pathway suppressor 2 (GPS2), act during physiological stresses (Cardamone et al., 2018; Kim K. H. et al., 2018). Nuclear translocation of GPS2 results in the synthesis of other neMITOs that change the composition and function of the mitochondria in a way that supports cell survival (Scarpulla, 2008).

The mitochondrial genome has recently shown to produce short mitochondrion-encoded peptides, such as MOTC-s and short humanin-like peptides (SHLPs), which are encoded in the 16S and 12S ribosomal RNA regions, respectively, of the mitochondrial genome (Yen et al., 2013; Cobb et al., 2016; Lee et al., 2016). The MOTC-s translocates into the nucleus to regulate the expression of the genes to optimize cellular metabolism, with implications in aging and muscle function (Reynolds et al., 2021). Other SHLPs may also act as important retrograde signaling molecules (Nashine et al., 2018; Nashine and Kenney, 2020).

In addition to protein factors, multiple non-coding RNAs have been shown to reside in mitochondria (Ro et al., 2013; Liang et al., 2021; Liu and Shan, 2021). These mito-ncRNAs are encoded either by the nuclear genome imported into the mitochondria or by the mitochondrial genome directly. An example of a nuclear genome-encoded mito-ncRNA is miR-146a-5p. In a brain injury model, the levels of miR146a-5p are decreased in the mitochondria and increased in the cytosol, where they regulate the uncontrolled activation of the NF-κB pathway (Wang et al., 2021). The mito-ncRNAs are not only encoded by the mitochondrial genome function within the mitochondria but also elsewhere, such as in the exosomes (Liang et al., 2021; Liu and Shan, 2021). Although their functions are not completely understood, they may regulate the maturation of mitochondrial transcripts (Ro et al., 2013). Circular mtDNA-encoded RNAs facilitate the import of nuclear-encoded proteins from both the sides of the organelle (Liu et al., 2020). The mtDNA-encoded long non-coding RNAs, sense non-coding mitochondrial RNA (SncmtRNA), and antisense non-coding mitochondrial RNA (ASncmtRNA), are generated from the transcripts derived from 12S and 16S mitochondrial rRNA genes. The SncmtRNA and ASncmtRNA exit into the cytosol, where they oppose each other to regulate the cell cycle progression and growth (Burzio et al., 2009; Borgna et al., 2017; Farfan et al., 2021). There is also evidence that mitochondrion-encoded tRNA-derived small fragments exit from the mitochondria under certain conditions, including cellular stress, and participate in different signaling pathways that operate between the mitochondria and the host cell (Liu et al., 2021; Meseguer, 2021). Two novel lncRNAs from the D-loop region were identified in the mammalian mitochondria: the H-strand transcript mitochondrial D-Loop (MDL1) and L-strand transcript MDL1AS. These were suggested to regulate some aspects of mtDNA replication but may also be processed into small RNAs with as-yet-unknown biological roles (Gao et al., 2018).

Therefore, accumulated evidence suggests that mitochondrion-localized factors, including mtDNA-encoded RNAs, are exported to convey mitochondrial status to the cell and the nucleus, leading to changes in the nuclear gene expression (Wen et al., 2019). We recently identified mtDNA-encoded small non-coding RNA, mmu-mito-ncR-805, which is generated from the D-loop of the L strand of the mitochondrial genome. The mmu-mito-ncR-805 is an abundant transcript that is stored in a granular form in the mitochondria under normal homeostasis and acts as a retrograde signal by translocating into the nucleus in certain cell types during the adaptive response to stress (Blumental-Perry et al., 2020). An increase in its nuclear localization correlates with an increase in the intermediates of the Krebs cycle and mitochondrial respiration and in the improved mitochondrial potential and function. It is to be noted that the SHLP2 and SHLP3 have biological effects similar to

those of mmu-mito-ncR-805, suggesting that multiple retrograde signaling molecules, including mtDNA-encoded ncRNAs, modulate and fine-tune mitochondrial function under different physiological conditions and stresses (Nashine et al., 2018; Nashine and Kenney, 2020).

This work explores the feasibility of using mmu-mito-ncR-805 retrograde signaling pathways to enhance mitochondrial bioenergetics. To this end, short synthetic versions of an evolutionarily conserved region (CR) of mmu-mito-ncR-805, mmu-CR805, and a human ortholog of the CR, light-strand D-loop small non-coding transcript-1 (hsa-LDL1) (Ro et al., 2013) were tested for their ability to improve the mitochondrial energy production.

MATERIALS AND METHODS

Cell Model

Immortalized mouse lung epithelial 12 (MLE12) and non-cancerous human bronchial epithelial immortalized with Ad12-SV40 2B (BEAS-2B) cell lines were purchased from the American Type Culture Collection and cultured as per their instructions (Wikenheiser et al., 1993) (US patent 4,885,238, dated December 05, 1989). The MLE12 cells were cultured in RPMI 1640 medium (Gibco, cat. #11875085) and BEAS-2B cells were cultured in DMEM/F-12 (Gibco, cat. #11320033), both supplemented with 4% of fetal bovine serum (Serum International, Laval, QC, Canada), insulin-transferrin-selenous acid (ITS) premix (BD Biosciences, San Jose, CA, United States), 10 nM of hydrocortisone (Sigma-Aldrich), 10 nM of estradiol (Sigma-Aldrich), 10 mM of 4-(2-hydroxyethyl)-1-piperazineethanesulfonic acid (HEPES), 2 mM of glutamine (CellGro), 100 U/ml of penicillin, and 100 g/ml of streptomycin. The BEAS-2B cells were grown using plates precoated overnight at 37°C with a mixture of 0.01 mg/ml of fibronectin (Sigma-Aldrich, cat. #F2006-5MG), 0.03 mg/ml of bovine collagen type I (Advanced Biomatrix, cat. #5005-100 ml), and 0.01 mg/ml of bovine serum albumin (heat shock fraction) with the pH of 5.2 (Sigma-Aldrich, cat. #A8022-100G) dissolved in Dulbecco's Modified Eagle Medium (DMEM) (Corning, cat. #10-013-CM). All experiments were performed on cells between passages 2 and 12 (Kenche et al., 2013, 2016).

Bioinformatics Analysis

We used the first 20 nt of mmu-mito-ncR-805 as a seed region (GAATTGATCAGGACATAGGG) in a BLAT search against the human nuclear and mitochondrial genomes (hg19 and NC_012920) and identified human mitochondrial homolog sequence, 16516-GAAGTAGGAACCAGATGTCG-16497. This human sequence was used to extend the species distribution analysis *via* the Multiz alignment algorithm available at the UCSC Genome Browser (Blanchette et al., 2004).

Transfection Procedure

The MLE12 or BEAS-2B cells were seeded at the desired density (10,000 cells/well of 96-well plates, 40,000 cells/well of 24-well plates, and 150,000 cells/well of 6-well plates) in their respective media and left to adhere for 6–8 h. The medium was removed and replaced with OptiMEM. After 12 h, the cells were transfected with siPORT NeoFX (Life Technologies, Thermo Fisher Scientific) transfection reagent with 5 nM of RNA oligos (**Table 1**).

Similar conditions were used for siRNAs targeting TRIB3, which was purchased from Ambion: Silencer Select predesigned siRNA of TRIB3 silencer (cat. #4390771, siRNA ID s105984 targeting RefSeq NM_175093.2 at 2 exons on location 256)[1]. A negative control oligo (Ambion, cat. #4390843) was used for siRNA control, as per the manufacturer's instructions. After 6 h, the transfection complexes were removed, and the cells were incubated in their regular medium for further analysis.

RNA Fluorescent *in situ* Hybridization

Probe Design and RNA-Fluorescent *in situ* Hybridization

To derive and detect mito-ncR-805, a 1ZZ probe (BA-Mm-mt-D-loop-O1-1zz) targeting 16,131–16,188 of NC_005089.1 was generated by ACD *via* ACD probe design software. The RNA-FISH was performed using the BaseScope Detection Red v2 assay (ACD, Inc.) according to the manufacturer's protocol. The cells were seeded on coverslips (Fisherbrand, cat. #12-545-82 12CIR-1D) at a density of 40,000 cells/well, transfected or not with mmu-CR805, grown for 24 h, washed with phosphate-buffered saline (PBS), and fixed in 3.8% paraformaldehyde for 30 min at room temperature. Fixed cells were permeabilized, dehydrated in an ethanol series with PBS (50, 70, and 100% ethanol) for 1 min each at room temperature, and stored at −20°C until further use. The cells were treated with a 1:15 dilution of protease III provided with the kit for 7 min at room temperature. The cells were then hybridized with the probe, and amplification steps were performed according to the manufacturer's instructions. The cells were then incubated with Hoechst solution (1 mg/ml in water; Sigma-Aldrich) to counterstain nuclei and mounted on a microscope slide. FastRed pigment was introduced into the amplification tree as a visual identifier of probe binding to enable both fluorescence and chromogenic detection.

Fluorescence Confocal Microscopy

For fluorescence detection, imaging was performed using a Leica SP8-HyVolution laser scanning confocal microscope (Leica Microsystems, Heidelberg, GmbH) equipped with an HCX PL APO 63×/1.4 oil immersion lens objective, HyD detectors, and Leica Application Suite X software. The mito-ncR-805-labeled and CR805-labeled structures were excited at 561 nm, with fluorescence emission collected from 570 to 630nm. Images were acquired at 1,256 pixels × 1,256 pixels and a step size of 0.15 μm. All images were acquired using identical microscope settings. Images were further processed using FIJI (ImageJ) for Mac version 2.1.0/1.53k (build 5f23140693) and Adobe Photoshop CS5.1 software.

[1]https://www.thermofisher.com/order/genome-database/details/sirna/s105984?CID=&ICID=&subtype=#assay-details-section

TABLE 1 | List of oligos used in the study.

Oligo name	Oligo sequence (5′→3′), if available[a]	Source, cat. #, and reference
Non-targeting RNA 1	Random sequence Pre-miR molecule extensively tested in human cell lines and tissues and validated to produce no identifiable effects on known miRNA function	Invitrogen, AM17110
Non-targeting RNA 2	GC medium-content oligos without homology to any known genes	Invitrogen, Universal control, 46-2001
Mmu-CR805	mG*mA*mA*UUGAUCAGGACAUAmG*mG*mG	Genscript
Mmu-ncR-805^{FL}	mG*mA*mA*UUGAUCAGGACAUAGGGUUU-GAUAGUUAAUAUUAUAUGUCUUUCAAGUUC-UUAGUGUUUUUGGG*mG*mU*mU	Genscript, (Blumental-Perry et al., 2020)
Hsa-LDL1	GAAGUAGGAACCAGAUGUCG; mG*mA*mA*GUAGGAACCAGAUG*mU*mC*mG	Genscript
AI805	CCCUAUGUCCUGAUCAAUUC	Ambion, AM11866, (Blumental-Perry et al., 2020)
Mmu-CR805 FAM labelled	mG*mA*mA*UUGAUCAGGACAUAmG*mG*mG-6-FAM-3′	Genscript

[a]*Some oligos were stabilized by modifications and additions to 5′ and 3′ termini, where "m" stands for 2-O-methyl-RNA and "*" stands for phosphorothioate.*

Localization Analysis

To assess the localization of mmu-CR805 in different subcellular compartments, single planes were chosen for each image. The chosen plane contained the CR805 signals of the strongest intensities using the line scan function of FIJI (ImageJ). Line scans were obtained manually from multiple representative regions under each condition (specified in the figure legends). The Line scans were created using straight line and freehand line tools in FIJI software across the regions of interest: through the cytoplasm, through outlines of mito-ncR-805 areas, which were localized by proximity/partial colocalization with mitochondrial marker Tom20 (Blumental-Perry et al., 2020), and through the nucleus. The plot profile tool was used to determine the fluorescence intensities for the red channel along the line scan. Values were imported into Microsoft Excel, plotted as the function of distance in pixels (x-axis) and intensities (y-axis).

Immunofluorescence Staining

The cells were seeded on coverslips at a density of 40,000 cells/well and transfected with FAM-labeled mmu-CR805 as described above. Twenty-four hours after transfection, the cells were fixed with 3.8% of paraformaldehyde for 20 min at room temperature, washed three times with PBS, and permeabilized with 0.05% of saponin-PBS. Non-specific staining was blocked by incubation with 5% of goat serum in 0.05% of saponin-PBS for 30 min at room temperature before incubating the cells for 2 h at room temperature with anti-Tom20 antibodies (Cell Signaling Technology, cat. #CS42406, at dilution 1:300). The cells were again washed three times, incubated with secondary antibodies conjugated to Alexa Fluor 568 (Invitrogen, cat. #A-11004, at dilution 1:500) for 1 h at room temperature, and washed twice with 0.05% of saponin-PBS. Nuclei were stained with Hoechst 33258 (Sigma-Aldrich, cat. #14530), and the cells were washed once with 0.05% of saponin-PBS and once with PBS and mounted on slides using Gold Antifade mounting medium (Thermo Fisher, cat. #P36930).

Confocal Microscopy

Z-stack optical sections of 0.364 μm were acquired at a magnification of 100 times and zoom of 3.37 times using a Leica TCS SP8 (Leica Microsystems) equipped with an HC PL APO CS2 100×/1.4 oil immersion lens objective and hybrid detectors controlled by LAS X 3.5.7.23225 software. Tom20-labeled structures were excited at 578 nm, with an emission peak at 603 nm. FAM-labeled mmu-CR805 was excited at 495 nm, with an emission peak at 520 nm. Lightning Wizard was used for the acquisition of images, and for subsequent deconvolution processing of the images using Leica Lightning GPU-accelerated deconvolution. Green fluorescent carboxylate-modified microspheres, (505/515), 100 nm in diameter (Thermo Fisher, Invitrogen, cat. # F8888) were imaged at the identical conditions, and were used to calculate achieved resolution *via* full width at half maximum of the central peak of the intensity profile. The achieved resolution was calculated as 135 ± 16 nm. Individual experiments were performed with identical laser output levels, exposure times, and scaling.

Line Scan Analysis

The line scan function of LAS X 3.5.7.23225 software was used to further determine the spatial proximity of green (FAM-labeled mmu-CR805) and red (Tom20) signals. Line scans were obtained manually from multiple representative regions under each condition (specified in the figure legends). The fluorescence intensities along the line scan for red and green channels and for green and blue (Hoechst) were imported into Microsoft Excel, plotted as a function of distance (nm) and intensities (**Supplementary Table 1**). Colocalization was confirmed when the intensity peaks of the green channel coincided with the intensity peaks of the red channel.

RNA Extraction and Detection

RNA was extracted from MLE12 cells using an miRNeasy kit (Qiagen), which enriches the small non-coding RNAs, as per the manufacturer's protocol. Northern blot analysis was performed using Signosis High Sensitive miRNA Northern blot assay kit (cat. #NB-1001 and 1002; Signosis, Inc., Santa Clara, CA, United States). Probes were 5′-biotin-CCCTATGTCCTGATCAATTC-3′ for the detection of mito-ncR-805 and 5′-biotin-ATCGTTCCAATTTTA GTATATGTGCTGCCGAAGCGAGCAC-3′for U6 (Signosis,

cat. #MP-0512). Northern blots were probed with mito-ncR-805, stripped by incubating in 0.5% of sodium dodecyl sulfate (SDS) at 60°C for 60 min, and reprobed with U6 probe for a loading control.

Real-Time RT-qPCR

Complementary DNA (cDNA) synthesis was performed using a high-capacity cDNA reverse transcription kit (Applied Biosystems, Foster City, CA, United States) on a T100 thermal cycler (Bio-Rad, cat. #186-1096). The following program was used for random primers cDNA synthesis: 25°C for 10 min, followed by 37°C for 2 h, and 85°C for 5 min. TaqMan® miRNA Looped Primer cDNA synthesis was carried out using the same kit, using the following program: 16°C for 30 min, followed by 42°C for 30 min, and 85°C for 5 min. Primers were from TaqMan assays (Life Technologies and Thermo Fisher Scientific): for the transcripts containing CR of mito-ncR-$805^{1-20\ nt}$, cat. #4427975, the assay ID 002045 was used; for sno55 to normalize the expression levels of small RNAs, cat. #4427975, the assay ID 001228 was used; for TRIB3, Mm00454879-m1 was used; for RNR2, Mm04260181_s1 was used; and for GAPDH, Mm99999915_g1 (cytosolic marker and as a normalization of TRIB3 data) was used. All TaqMan assay qPCRs were performed using TaqMan Universal Master Mix II, no UNG, from Life Technologies (cat. #4440040) and a C1000 Touch Thermal Cycler chassis (Bio-Rad, cat. #1841100) equipped with a CFX96 real-time PCR detection system (Bio-Rad, cat. #1845097) and controlled by CFX Maestro software (Bio-Rad, cat. #12004110). The manufacturer's standard program 10 min at 95°C, then 40 cycles for 15 s at 95°C, and 1 min at 60°C was used. Real time PCR results were compared using comparative $C(T)$ methods and calculated as folds $2^{-\Delta\Delta Ct}$ (Schmittgen and Livak, 2008). The relative abundance of mmu-CR805 in different fraction was calculated using identical inputs of RNA as $Ct^{fractiontransfected} - Ct^{fractiontotal}$ (Wang et al., 2020).

Subcellular Fractionation

Separation of mitochondrial and cytosolic fractions was performed using a mitochondrial isolation kit from Sigma-Aldrich (cat. #MITOISO2) according to the manufacturer's instructions for the isolation of the mitochondria from the cells with modifications. Briefly, the cells grown on plates were washed twice with PBS, scraped into lysis buffer, which is 1 time extraction buffer supplemented with protease inhibitory cocktail (Sigma-Aldrich Roche Biochemical Reagents) and 1:200 dilution of cell lysis solution, incubated 5 min on ice, and diluted with two volumes of 1 time extraction buffer. Lysates were centrifuged at 600 × *g* for 10 min at 4°C. One-third of the supernatant was removed for the analysis of the total fraction, which was further divided for protein analysis and RNA extraction. The remainder of the lysates were centrifuged at 11,000 × *g* for 10 min at 4°C. The supernatant was carefully removed and saved for further analysis as the cytosolic fraction, which was divided for protein and RNA analyses. Mitochondrial pellets were considered crude mitochondria and further purified by resuspension in 16% Percoll-PBS using the following Percoll gradient: 2 ml of 40% Percoll at the bottom, overlayed with 2 ml of 23% Percoll, followed by 16% of Percoll containing crude mitochondria. Percoll gradients were prepared using 1 time storage buffer provided in the mitochondrial isolation kit from Sigma-Aldrich as per the manufacturer's instructions. The gradient was separated using SW41 Ti swinging bucket rotor 3,33,790 at 31,000 × *g* for 8 min at 4°C in a Beckman Coulter Optima XPN-100 ultracentrifuge.

The mitochondrial band was harvested at the lowest interface, diluted with four volumes of ice-cold 1 time storage buffer, and centrifuged in a fixed-angle Sorvall Legend RT centrifuge at 17,000 × *g* at 4°C for 10 min. The purified mitochondria were resuspended in 150 μl of 1 times storage buffer and treated with RNase I (Ambion, cat. #AM2294, 250 U/150 μl) at 4°C for 1 h to eliminate cytosolic RNAs. The treated mitochondria were suspended in Trizol for further RNA extraction and analysis.

Nuclear Extracts and Nuclear RNA Preparation

The nuclear extracts were prepared by modification of the protocol by Wang et al. (2000). Briefly, MLE12 cells, collected by trypsinization, were resuspended in 10 mM of HEPES (pH 7.9), 10 mM of KCl, 1.5 mM of $MgCl_2$, and 0.5 mM of dithiothreitol supplemented with protease inhibitory tablet (Sigma-Aldrich Roche Biochemical Reagents), incubated for 15 min on ice, followed by the addition of Non-idet P-40 to a final concentration of 0.325%. The cells were allowed to swell 10 min on ice with occasional shaking. Nuclear pellets were separated by centrifugation at 2,500 rpm for 4 min at 4°C. The nuclear pellets were washed once in the lysis buffer and resuspended in 20 mM of HEPES (pH 7.9), 0.45 M of NaCl, 1 mM of ethylenediaminetetraacetic acid (EDTA), 0.5 mM of dithiothreitol, 0.3 U/μl of RNase inhibitor (RNaseOUT recombinant ribonuclease inhibitor; Thermo, cat. #10777019), and 1 protease inhibitor tablet (cOmplete mini, EDTA free; Sigma-Aldrich Roche Biochemical Reagents) per 10 ml of lysis buffer. The nuclei were incubated with rocking at 4°C for 30 min. The nuclear extracts were cleared by centrifugation at 12,000 rpm for 10 min. The supernatant was divided for Western blot analysis and for RNA extraction and analysis. To eliminate cytosolic RNAs, the nuclear pellets were resuspended in the lysis buffer supplemented with 0.3 M of sorbitol and treated with RNase I (Ambion, cat. #AM2294, 100 U/100 μl) at 4°C for 1 h and suspended in Trizol for further RNA analysis.

Protein Lysate Preparation and Western Blot Analysis

Western blotting was performed as described by Kenche et al. (2013). Briefly, the cells were either lysed in RIPA buffer (150 mM of NaCl, 1.0% of Non-idet P-40 or 0.1% of Triton X-100, 0.5% of sodium deoxycholate, 0.1% of SDS, 50 mM of Tris-HCl, pH 8.0) or the subcellular fractions were obtained as described above. Proteins were resolved by SDS-PAGE and transferred to nitrocellulose membranes (Bio-Rad, cat. #162-0115) by using a *Trans*-Blot Turbo transfer system (Bio-Rad, cat. #1704150) in *Trans*-Blot Turbo 5 times transfer buffer (Bio-Rad, cat. #10026938). High-molecular-weight proteins run using

1.5-mm of SDS gels were transferred using the setting of 25 V, 1.3 A constant, for 15 min (10 min for H3). Membranes were blocked in Tris-buffered saline (TBS) with 0.1% of Tween (TBST) supplemented with 5% of non-fat dry milk (Blotto; Santa Cruz Biotechnology, cat. #sc-2324) for 1 h at room temperature, washed with TBST twice, and incubated with primary antibodies in either TBST with 5% of bovine serum albumin or 5% of milk overnight at 4°C. The primary antibodies against the following were used: lactate dehydrogenase A (LDHA; Cell Signaling, cat. #2012, 1:1,000), succinate dehydrogenase subunit A (SDHA; Abcam, cat. #ab14715, 1:1,000), H3 (Cell Signaling, cat. #9715, 1:4,000), nucleophosmin (Abcam, cat. #ab10530 [FC82291], 1:1,000), β-actin (Abcam, cat. #ab6276, 1:10,000), TRIB3 (LSBio, LifeSpan BioSciences, cat. #LS-C164592, 1:250), and phospho-Akt (Trh308) (Cell Signaling, cat. #2965, 1:500). The blots were washed three times in TBST for 5 min each, incubated in TBST supplemented with 5% of milk with secondary antibodies for 1–2 h at room temperature, washed three times with TBST, and developed using Pierce ECL Western blotting substrate (Thermo Scientific, cat. #32106). The secondary antibodies included were goat anti-mouse IgG horseradish peroxidase (Thermo Fisher Scientific, cat. #31430, 1:5,000) and goat anti-rabbit IgG horseradish peroxidase (Thermo Fisher Scientific, cat. #31460, 1:5,000). Probed membranes were imaged using ChemiDoc MP imaging system (Bio-Rad, cat. #17001402) equipped with a blot/UV/stain-free sample tray for ChemiDoc MP/ChemiDoc imaging systems (Bio-Rad, cat. #12003028) and processed using Bio-Rad Image Lab version 6.1.0 (build 7 SE for Mac).

Metabolic Labeling

The MLE12 cells were transfected with either CR805 or a non-targeting sequence; 30 h post-transfection, the cells were exposed to 20 mM [U-^{13}C]glucose for 12 h and harvested. Metabolic flux was determined following ^{13}C label incorporation into various metabolites. After incubation, 0.5 ml of removed medium was saved from one well of each condition and from each plate. The cells were washed while attached on the plates with PBS (three times, at room temperature wash, moving to 10°C, and completed with ice-cold PBS wash), fixed by adding 1 ml of 80% ethanol cooled at −20°C, collected by scraping and placing on dry ice ethanol bath, and stored at −80°C for further analysis.

Assay of Medium [U-^{13}C]Glucose Enrichment

Glucose isotopic enrichment was determined according to Gao et al. (2015) with modifications. Briefly, the glucose was extracted by the addition of 500 μl of ice-cold ethanol into 50 μl of a medium. Samples were mixed and incubated on ice for 30 min. The samples were centrifuged at 4°C for 10 min at 14,000 rpm, and ethanol was transferred to GC/MS vials and evaporated to dryness in a SpeedVac evaporator. Glucose was converted into its pentaacetate derivative by its reaction with 150 μl of acetic anhydride in pyridine (2:1 [vol/vol]) at 60°C for 30 min. The samples were evaporated to dryness, and the glucose derivative was reconstituted in 80 μl of ethyl acetate and transferred to a GC/MS insert. The samples were injected in duplicates, and the masses 331–337, containing M0–M5 isotopomers, were monitored. Enrichment was determined as a ratio of M5 to Σ_{M0-M5}.

Metabolite Extraction

The MLE12 cells were treated as previously described (Yang et al., 2008). Briefly, cell extract was vortexed and sonicated using an ultrasonicator alternating 30 s on 30 s off for 10 min. The cells were pelleted by centrifugation at 4°C for 10 min at 14,000 rpm. The supernatant was transferred to GC/MS vials and evaporated to dryness under a gentle stream of nitrogen. Keto and aldehyde groups were reduced by the addition of 10 μl of 1 N NaOH and 15 μl of NaB_2H_4 (prepared as 10 mg/ml in 50 mM of NaOH). After mixing, the samples were incubated at room temperature for 1 h, acidified by 55 μl of 1 N HCl (dropping the acid slowly), and evaporated to dryness. Fifty microliters of methanol were added to precipitate boric acid. Internal standard was added (10 μl of 17:0 formic acid, 0.1 mg/ml). The samples were evaporated to dryness and reacted with 40 μl of pyridine and 60 μl of *tert*-butylbis(dimethylsilyl) trifluoroacetamide with 10% trimethylchlorosilane (Regisil) *tert*-butyl(dimethylsilyl) at 60°C for 1 h. Resulting *tert*-butyl(dimethylsilyl) derivatives were injected into the GC/MS equipment.

GC/MS Conditions

Analyses were carried out on an Agilent 5973 mass spectrometer equipped with a 6890 Gas Chromatograph. An HP-5MS capillary column (60 m × 0.25 mm × 0.25 μm) was used in all the assays, with a helium flow of 1 ml/min. The samples were analyzed in selected ion- monitoring mode using electron impact ionization. Ion dwell time was set to 10 ms. The following metabolites were detected: α-ketoglutarate, alanine, aspartate, citrate, fumarate, glutamate, lactate, malate, oxaloacetate, pyruvate, serine, and succinate.

Calculations

Fractional metabolic flux was determined according to the relationship between the precursor ([U-^{13}C]glucose) and the product ([^{13}C]-labeled metabolites). Molar percent enrichment (MPE) of the metabolites was determined in the same manner as for glucose (refer to GC/MS conditions). Fractional metabolic flux was calculated as follows: $MPE_{product}/MPE_{precursor}$. The absolute metabolic rate shown in **Figures 4A–C** was determined as a product of the fractional metabolic flux and pool size, i.e., the relative concentration of the metabolite of interest (**Supplementary Table 2**).

Mitochondrial Bioenergetics Analysis

The MLE12 cells were seeded at 10,000 cells/well (80 μl) and transfected with either CR805 or a negative control as described above. Forty hours after transfection and 1 h before the measurements, RPMI medium was changed to unbuffered DMEM (Seahorse Bioscience, United States) supplemented with 1% of fetal bovine serum, 4 mM of glutamine (Sigma-Aldrich), 2 mM of sodium pyruvate (Gibco), 10 mM of glucose (Sigma-Aldrich), 100 μM of insulin (Sigma-Aldrich), and mitochondrial bioenergetics were measured using a Seahorse XFe96 extracellular flux analyzer and the XF Cell Mito Stress

kit (Seahorse Bioscience) as described before (Zhang et al., 2018). Real-time measurement of oxygen consumption rate was obtained as per the manufacturer's instructions by sequential treatment with 1 μM of oligomycin, 1 μM of carbonyl cyanide *p*-trifluoromethoxyphenylhydrazone (FCCP), and 1 μM mixture of rotenone/antimycin A, and normalized to total protein amount measured by a Pierce BCA protein assay kit (Thermo Scientific). Basal respiration was calculated as the average of the first three readings before the addition of oligomycin minus the average of the last 3 readings after the addition of rotenone addition. Proton leak was calculated as the average from three readings after the addition of oligomycin minus the average of the last three readings. ATP production was calculated as basal respiration minus the proton leak. Maximal respiration was calculated as the average of the three readings after FCCP stimulation minus the average of the last three readings. Spare respiratory capacity was calculated as the maximal respiration minus the basal respiration. Coupling efficiency was calculated as 100× ATP production/non-mitochondrial respiration, where the non-mitochondrial respiration was the average of the last three readings after the addition of rotenone and antimycin A (**Supplementary Table 3**).

Mitochondrial Membrane Potential Assays

Mitochondrial membrane potential was measured using a JC-10 mitochondrial membrane potential assay kit (Abcam, cat. #ab112134) according to the manufacturer's instructions. The results were read by a BioTek Synergy HT spectrophotometer.

Preparation of Cigarette Smoke Extract

The cigarette smoke extract (CSE) was prepared using the method described by Kenche et al. (2013). Research-grade 1R5F cigarettes (Kentucky Tobacco and Health Research Institute, Lexington, KY, United States) were used to prepare the CSE. The CSE was made fresh for each experiment by bubbling the smoke from 1 cigarette through 5 ml of serum-free medium in a 15-ml conical tube and filtering it through a 0.22-μm of filter to remove large particles and to maintain the sterility. This solution was designated 100% CSE and diluted in a culture medium to yield the concentrations specified for each experiment.

Cigarette Smoke Extract Growth After Stress

Cells were plated at 50,000 cells/ml in 24-well plates. The cells were transfected as previously described; 20 h post-transfection, cells were exposed to 10% of CSE for 30 min. The medium was removed, the cells were washed twice with PBS, and fresh medium was added. The Cells were counted at time points specified in the figure legends.

Statistical Analyses

Unless specified in text, data are expressed as means and standard deviations from at least three independent experiments. Fold-change for qPCR was determined using the $2^{\Delta\Delta CT}$ method (Livak and Schmittgen, 2001; Schmittgen and Livak, 2008). Student's *t*-tests were used to determine the *P*-values. *P*-values of ≤ 0.05 were considered statistically significant. ANOVAs were used to determine whether multiple groups differed from each other.

RESULTS

The first 20 nt of mmu-mito-ncR-805 are evolutionarily conserved, and the corresponding synthetic oligos are detected in multiple cellular compartments in the transfected cells. Our previous work demonstrated that the amount of mmu-mito-ncR-805 in the nucleus increased almost 10-fold in CSE-exposed cells. This increase coincided with the recovery from stress (Blumental-Perry et al., 2020). An antisense inhibitor of mito-ncR-805, AI805, revealed a positive regulation of a subset of neMITO genes and energy metabolism by mito-ncR-805 (Blumental-Perry et al., 2020). Accordingly, overexpression of a synthetic oligo corresponding to the full-length mmu-mito-ncR-805 (mmu-ncR-805^{FL}) increased the expression of a few neMITO genes and had a beneficial impact on the intermediates of the Krebs cycle (Blumental-Perry et al., 2020). We therefore wanted to employ a forced overexpression system to test if we can improve the bioenergetics of the cells transfected with ncRNA.

The 70-nt mmu-mito-ncR-805 transcript is mouse-specific. To identify a possible human homolog, we analyzed the sequence and found that the first 20 nt were unique to the mitochondrial genome; the rest of the transcript shares short stretches of homology with two nuclear genes, ZFP280c and Adams9 (Blumental-Perry et al., 2020). We performed a BLAST analysis with the 20-nt region against the human mitochondrial genome and searched the existing databases for previously identified human transcripts that are generated from the D-loop of the L strand of the human mitochondrial DNA that shares a homology with the mito-ncR-805. The transcript, hsa-mitosRNA-L-DL-1 (**Figure 1A**) shares a high degree of homology with the first 20 nt of mito-ncR-805 (Ro et al., 2013). We therefore investigated whether there is any evolutionary conservation of this region in the mammalian mitochondrial genomes by using Multiz analysis, which demonstrated that the 20-nt sequence is conserved in the mammalian mitochondria (**Figure 1A**). Whether those homologous sequences are able to generate transcripts in other species is not known, but the conservation within the mitochondrial non-coding sequences is strongly suggestive of a functional importance of those transcripts. We therefore hypothesized that the first 20 nt of mmu-mito-ncR-805 may be critical for its function. The first 20 nt of mmu-mito-ncR-805 was introduced into the cells in the form of the single-stranded RNA oligo, mmu-conserved region 805 (mmu-CR805), titrated to transfect at least 80% of the cells (5 nM). Northern blot analysis confirmed the presence of the 20 nt of mmu-mito-ncR-805 in the transfected cells (**Supplementary Figure 1A**).

We next wanted to observe the intracellular distribution of the transfected oligo. Since our previous data suggested that mmu-mito-ncR-805 has a nuclear function, we first evaluated if the mmu-CR805 oligo is found in the nuclei of the transfected cells. **Figure 1B** demonstrates that the isolated nuclear pellets

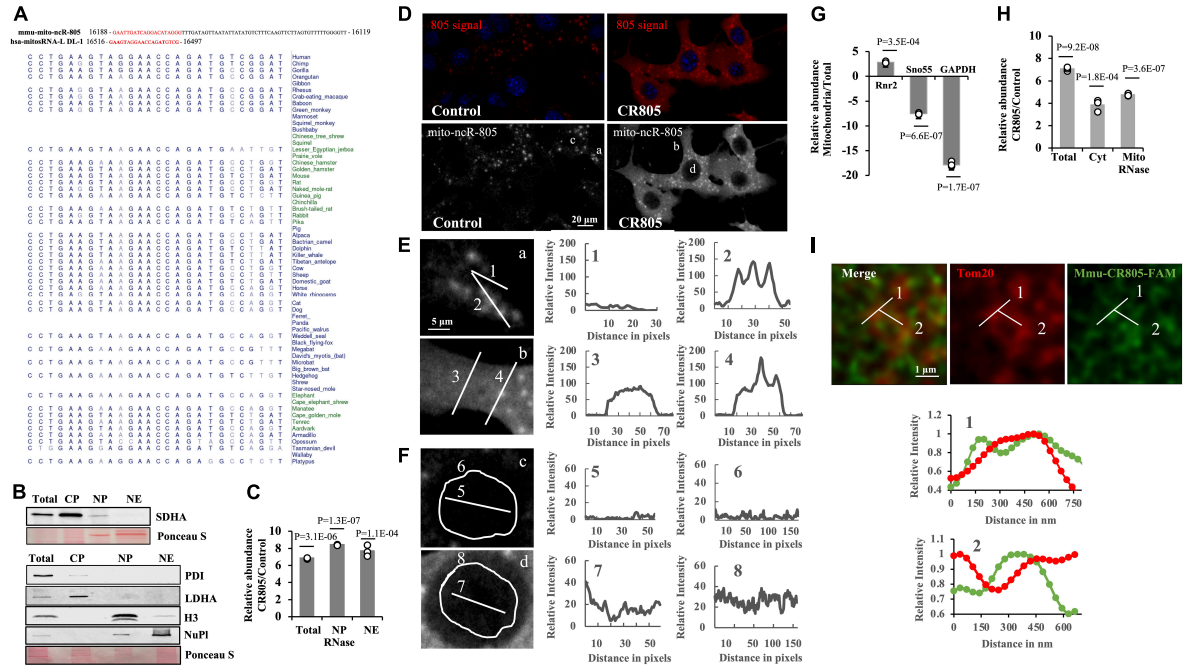

FIGURE 1 | The first 20 nt of mito-ncR-805 is evolutionarily conserved in the mammals. **(A)** Alignment of mmu-mito-ncR-805 (accession number MI0005204) and hsa-mito-RNA-L-DL-1, which maps to the D-loop of the control region (Ro et al., 2013). Multiz alignment of hsa-mito-RNA-L-DL-1 with sequences from 100 vertebrates. The evolutionarily conserved region is shown in red. **(B–H)** Subcellular distribution of transfected mmu-CR805 (or control) in MLE12 cells. **(B,C)** Total, cytoplasmic (CP), nuclear pellet (NP), and nuclear extract (NE) fractions were prepared. NPs were treated with RNase I. **(B)** Purity of the fractions was assessed by the presence of the cytosolic protein, LDHA, mitochondrial protein SDHA, endoplasmic reticulum protein PDI, nuclear chromatin protein H3, and nucleoplasm protein nucleoplasmin *via* Western blot analysis. Ponceau S staining is shown as a loading control. **(C)** Small RNAs were extracted from generated fractions and analyzed for the expression levels of transcripts containing the conserved region of mito-ncR-805 by RT-qPCR. **(D)** MLE12 cells transfected with control or mmu-CR805 were grown on slides, fixed, and hybridized with a mito-ncR-805-specific probe. Images were acquired at 63 times magnification on a Leica DM IRE2 Leica SP8 laser confocal microscope. **(E,F)** Enlarged areas from Panel **(D)** are shown on the left. Graphs on the right show relative red channel fluorescence intensity through the line-scanned regions. **(E)** Line-scans drawn through cytoplasm (1 and 3) and structures positive for mmu-mito-ncR-805 and/or mmu-CR805 (2 and 4). **(F)** Line scans drawn through and around the perimeter of nuclei of cells transfected with non-targeting RNA (top image) and mmu-CR805 (bottom image). **(G,H)** MLE12 cells transfected with mmu-CR805 or non-targeting RNA oligos were lysed and analyzed (total fraction). Cytosolic fractions (Cyt) were obtained by separating the crude mitochondria, which were further purified using Percoll gradient and treated with RNase I to remove non-mitochondrial RNAs. The RNAs were isolated from the obtained fractions. **(G)** Purity of the fractions was evaluated by comparing the expression levels of mtDNA-encoded mRNA of Rnr2, nucleus-encoded and localized Sno55-RNA, and cytosolic GAPDH mRNA. Graph shows the difference between C_T levels relative to the total lysates and with identical RNA inputs. **(H)** Expression levels of transcripts containing the mmu-CR805 sequence in different fractions as evaluated by RT-qPCR. Graph shows the difference in C_T values between the control and mmu-CR805-transfected cells. **(I)** The MLE12 cells were transfected with FAM-labeled mmu-CR805, fixed, and stained for Tom20. Images were acquired at a magnification of 100 times and zoom of 3.37 times on a Leica TCS SP8 microscope with accelerated deconvolution (entire images are provided in **Supplementary Figure 2**). Line scans were drawn through Tom20-labeled structures. Graphs show relative red and green channel fluorescence intensity through the line-scanned regions.

treated with RNase had small amounts of detectable SDHA, as expected, whereas the nuclear extracts did not. Both the RNase-treated nuclear pellets and the extracts from the transfected cells demonstrated a significant increase in mmu-CR805 signal (**Figure 1C**). Since fractionation involves enrichment, we verified these findings using a microscopy in two different ways. First, we used FISH and demonstrated an increase in the signal following the forced expression of mmu-CR805 (**Figure 1D**). Line scan analysis showed increasing red signal intensity (from 10–25 relative units in the background to 45–85 in the transfected cells), mostly in the cytosol of the transfected cells (**Figure 1E**, 1 and 3, and **Supplementary Table 1**). Our previous work demonstrated that the endogenous mmu-mito-ncR-805 localized into the structures that partially overlap with mitochondrial marker Tom20 and hence their presence requires intact mitochondria (Blumental-Perry et al., 2020). The signal intensity of those structures increased only slightly in the transfected cells (compare **Figure 1E**, 3 and 4). This may be due to the signal saturation and it was addressed in experiments presented below. **Figure 1F** demonstrates that endogenous levels of mmu-mito-ncR-805 in the nucleus are below FISH detection in the cells transfected with a non-targeting oligo (**Figure 1F**, c, 5 and 6), whereas mmu-CR805 was detectable (**Figure 1F**, d, 7 and 8) and its signal increased from 15 (background) to 45–50 units, suggesting that the mmu-CR805 oligo entered the nucleus. Similar results were obtained using fluorescently labeled mmu-CR805 oligos (**Supplementary Figures 2D,E**). Therefore, these data provide strong evidence in support of the nuclear localization of the transfected mmu-CR-805.

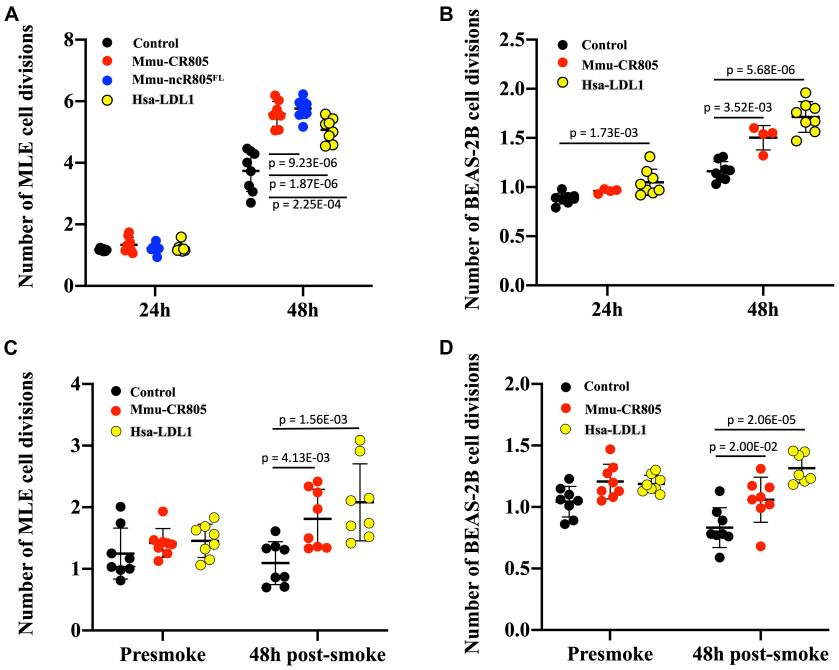

FIGURE 2 | RNA oligos containing the conserved regions of mouse and human orthologs (mmu-CR805 and hsa-LDL1, respectively) demonstrate biological activity similar to that of the full-length ncR-805 in MLE12 and BEAS-2B cells. The MLE12 **(A,C)** and BEAS-2B **(B,D)** cells were transfected with non-targeting RNA, mmu-CR805, or hsa-LDL1. The MLE12 cells were also transfected with mmu-ncR-805^{FL}. **(A,B)** Growth rates of cells 24 and 48 h post-transfection. **(C,D)** Growth rates of cells post-stress. Twenty-four hours post-transfection, the cell numbers were counted and the cells were exposed to 10% of CSE for 30 min, washed, and allowed to recover in their respected fresh media. Forty-eight hours post-exposure, the cell numbers were counted again.

To further assess the ability of mmu-CR805 to enter into different cellular compartments, we isolated cytosolic and enriched (purified on Percoll gradient and RNase treated) mitochondrial fractions (refer to **Figure 1G** and **Supplementary Figure 1B** for the fraction purity). The mitochondrial fraction demonstrated very low RT-qPCR signal for the nuclear marker, sno55, whereas there was a significant increase in the mmu-CR805 signal (**Figure 1H**). We next used accelerated deconvolution confocal microscopy to gain sufficient resolution of 120-150 nm to determine if Tom20 and FAM-labeled mmu-CR805 oligo signals overlap. Imaging demonstrates multiple yellow dots, and Line Scan analysis demonstrates a complete overlap between Tom20 and CR805 for the stretches of at least 250–300 nm at multiple sites (**Figure 1I** and **Supplementary Figure 2**). Our data suggest that some mmu-CR805 oligos were localized into the mitochondrial structures labeled by Tom20. Nevertheless, the forced expression of RNA oligos, such as mmu-CR805 represent a good system to study the consequences of non-mitochondrial evolutionarily conserved functional bits of mmu-mito-ncR-805.

RNA Oligos Containing Conserved Region of Mito-ncR-805 Are Biologically Active

Since we focused on the delivery of a "functional bit" of mmu-mito-ncR-805 and its human ortholog, we wanted to see if those oligos have any biological activity in the transfected cells. According to our previous research (Blumental-Perry et al., 2020), the mmu-mito-ncR-805 accelerates the repopulation of cells lost after the stress from smoke, presumably due to the higher bioenergetics of cells with high levels of mmu-mito-ncR-805 and their ability to divide faster (Blumental-Perry et al., 2020). We therefore introduced mmu-CR805, its human ortholog hsa-LDL1, and the full-length ncR-805^{FL} into MLE12 cells and mmu-CR805 and hsa-LDL1 into BEAS-2B cells and compared their growth rates with and without stress. **Figures 2A,B** demonstrate that over 48 h, all the mmu-mito-ncR-805 derivatives and the human orthologs induced faster cell division of MLE12 and BEAS-2B cells, with respective orthologs being slightly less efficient than species-specific oligos but still significantly different from cells transfected with non-targeting oligos. Importantly, the growth rates of MLE12 cells carrying the functional bit oligo, mmu-CR805, and the full-length synthetic transcript, ncR-805^{FL}, were the same, supporting the idea that the 20-nt conserved region of mmu-mito-ncR-805 is indeed a functional bit. Next, the MLE12 and BEAS-2B cells were stressed by short-term exposure to CSE (30 min, 10% of CSE). This exposure was titrated to cause the death of approximately 50% of the cell population. Both the mouse and human orthologs conferred faster cell division following stress (**Figures 2C,D**). Therefore, we concluded that the first 20-nt segments of mmu-mito-ncR-805 and its human orthologous transcript are biologically active and function similarly to mito-ncR-805, which justified the functional studies that follow.

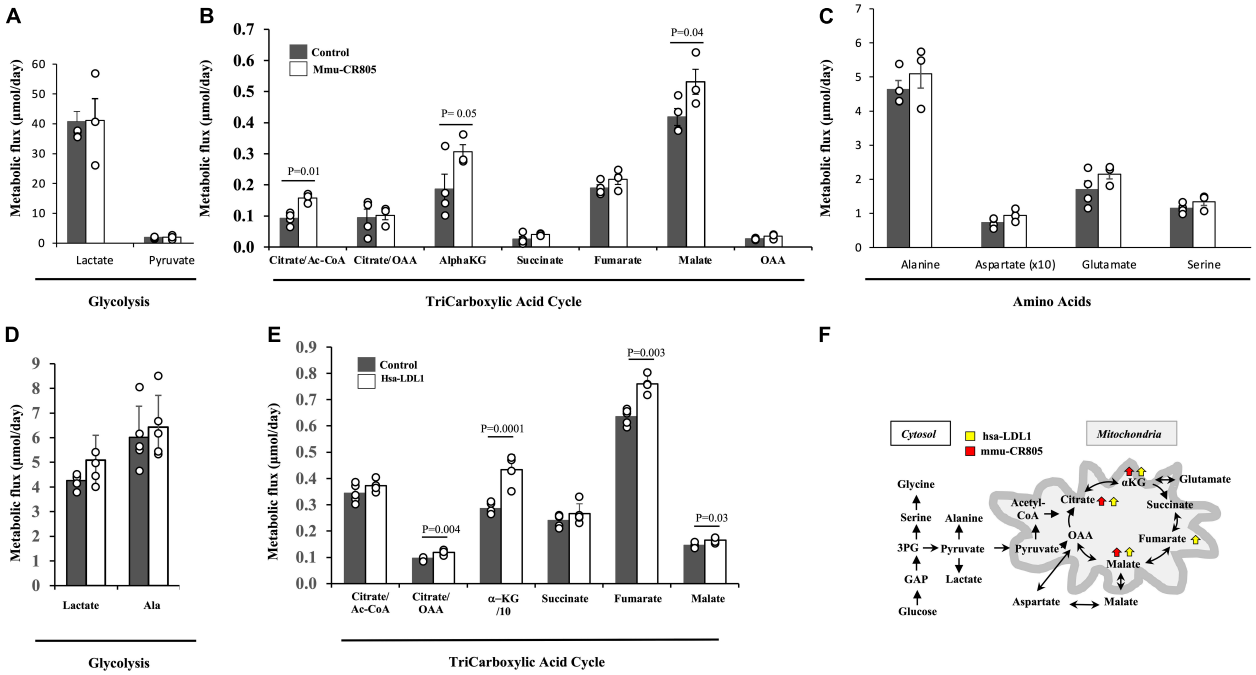

FIGURE 3 | mmu-CR805 and hsa-LDL1 increase the TCA cycle activity. **(A–C)** The MLE12 cells were transfected with either 12 nM mmu-CR805 or a non-targeting sequence. **(D,E)** The BEAS-2B cells were transfected with either hsa-LDL1 or a non-targeting sequence. At 30 h post-transfection, the cells were exposed to 20 mM of [U-^{13}C]glucose for 12 h and harvested, and the metabolic flux was determined according to ^{13}C label incorporation into various metabolites. Metabolic flux of glycolysis **(A,D)**, TCA cycle activity **(B,E)**, and amino acid turnover **(C)**. Metabolic flux was determined as a product of fractional flux multiplied by the concentration (pool size) of a metabolite. Fractional flux was calculated as ^{13}C enrichment of a product metabolite over the [^{13}C] enrichment of the precursor, i.e., [U-^{13}C]glucose. All quantifications are presented as means from at least four independent experiments ± S.E.M (**Supplementary Table 2**). Graphs are representative of at least two independent biological experiments of four replicates. **(F)** Schematic representation of the major findings on the glucose metabolic flux regulated by the forced overexpression of mmu-CR805 and hsa-LDL1.

CR805 Increases Tricarboxylic Acid Cycle Intermediates

We previously demonstrated that mmu-mito-ncR-805 can be found in the nuclei of cells recovering from stress and is associated with an increase in the mRNA levels of genes for multiple subunits of ETC complexes and metabolic enzymes, including the enzymes of the TCA cycle and related pathways (Blumental-Perry et al., 2020). We therefore examined the metabolic flux of the TCA intermediates in MLE12 and BEAS-2B cells transfected with mmu-CR805 and hsa-LDL1, respectively, by direct measurements of metabolic flux using stable isotope incorporation and mass isotopomer analyses. Neither mmu-CR805 nor hsa-LDL1 affected the glycolytic flux, as seen from the small changes in alanine and lactate (**Figures 3A,C,D**); however, they increased the absolute flux of TCA intermediates (**Figures 3B,E**, and **Supplementary Table 2**). Moreover, the significant increase in fumarate/malate is indicative of further channeling of energy to increase pyruvate production *via* the so-called mitochondrial gas pedal (Gellerich et al., 2013). This corresponds to the same response we previously characterized in the MLE12 cells recovered from CSE exposure (Blumental-Perry et al., 2020). Therefore, the transfection with 20 nucleotides of mito-ncRNA-805 is sufficient to promote a metabolic response (**Figure 3F**).

CR805 Increases Mitochondrial Bioenergetics Activity

We next used the XF Cell Mito Stress kit to measure the mitochondrial oxygen consumption rate in MLE12 cells at baseline and in response to the overexpression of different mmu-mito-ncR-805 oligos or their human orthologs of the functional bits (**Figure 4A**). We found that all tested oligos increased the maximal mitochondrial respiration and spared the respiratory capacity (**Figures 4B,C** and **Supplementary Table 3**). The rates of non-mitochondrial respiration were not affected, which was in agreement with the metabolomic data from the previous section, and demonstrated that it is not influenced by mmu-CR805 or by hsa-LDL1 (**Figures 3**, **4A**).

High activity of the enzymes of the TCA cycle, reflected in our metabolomic data, and ETC, as indicated by the Mito Stress test results, should result in a higher mitochondrial membrane potential ($\Delta\Psi$m). We therefore measured $\Delta\Psi$m using a JC-10 assay (Reers et al., 1991) and found that the MLE12 cells expressing mmu-CR805 or hsa-LDL1 had lower depolarization of the mitochondrial membrane (higher $\Delta\Psi$m) (**Figure 4D**). A similar analysis was performed in BEAS-2B cells either transfected with or not with mmu-ncR-805^{FL}, mmu-CR805, or hsa-LDL1. The mmu-ncR-805^{FL}, mmu-CR805, and hsa-LDL1 increased the maximal

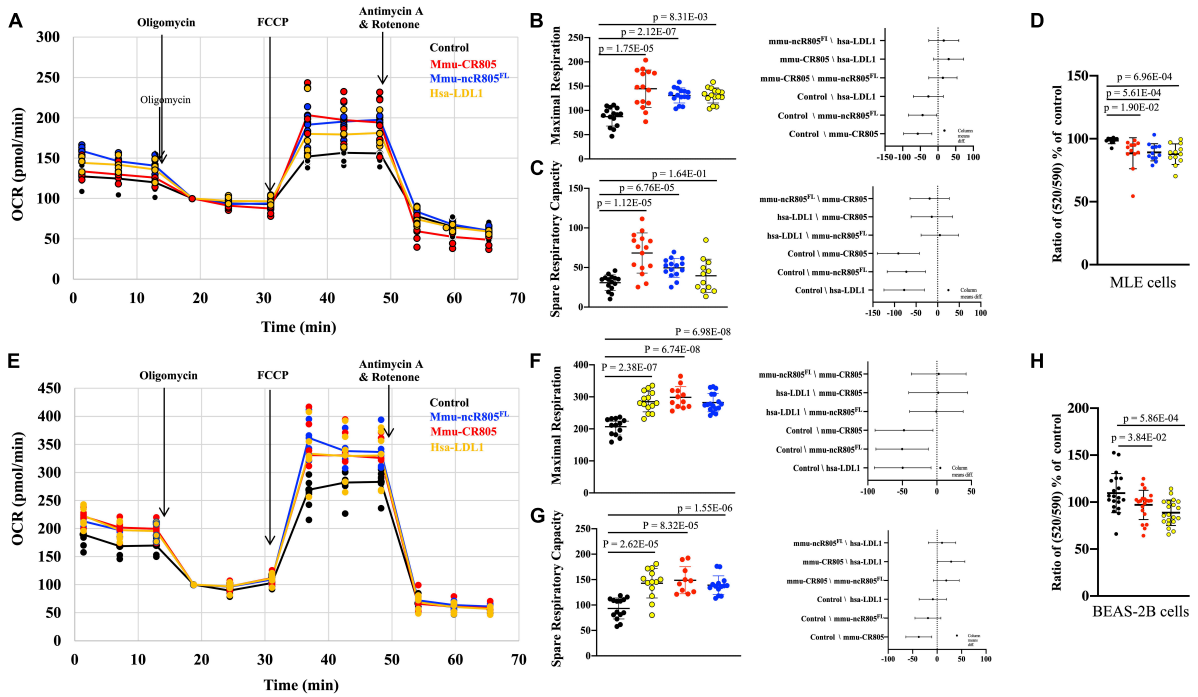

FIGURE 4 | mmu-CR805 and hsa-LDL1 increase mitochondrial bioenergetics. The MLE12 **(A–D)** and BEAS-2B **(E–H)** cells were transfected with indicated CR805-containing RNA oligos or non-targeting RNA; at 48 h post-transfection, bioenergetics were measured using a Seahorse XFe96 extracellular flux analyzer, and mitochondrial membrane potential was measured using JC-10 assay. Oxygen consumption rate (OCR) was measured at the basal level and with subsequent and sequential additions of oligomycin (1 μM), FCCP (1 μM), and rotenone (1 μM) + antimycin A (1 μM) in MLE12 **(A)** and BEAS-2B **(E)** cells. Graphs are representative of experiments with at least three biological repetitions (**Supplementary Table 3**). Graphs of maximal mitochondrial respiration in MLE12 **(B)** and BEAS-2B **(F)** cells and spare respiratory capacity for MLE12 **(C)** and BEAS-2B **(G)** cells. Results from ANOVAs of differences between the groups are shown. **(D,H)** Mitochondrial membrane potential determined by a JC-10 assay, where monomer/aggregate ratios specify the depolarization of the mitochondrial membrane. All constructs containing CR805 or its human ortholog region had a lower monomer/aggregate ratio and increased $\Delta\Psi m$.

mitochondrial respiration, spared the respiratory capacity and the mitochondrial membrane potential (**Figures 4E–H**). In conclusion, both the mitochondrial respiration and the membrane polarization are increased by forced overexpression of the CR of mmu-mito-ncR-805 or its human ortholog in both the murine and human alveolar epithelial cells.

High Levels of mmu-CR805 Result in Low mRNA and Protein Levels of Pro-apoptotic Pseudokinase TRIB3

Akt1 kinase is activated during the stress of smoking (Nakayama et al., 2002; Nicoletti-Carvalho et al., 2010). The Akt1 stress-related activation is not a common feature of stress response, where downregulation of prosurvival Akt1 activity is expected, but a response is specific to the stress from smoke and nicotine exposure. It can have numerous effects, including but not limited to increased mitochondrial bioenergetics (Li et al., 2013). We previously found that a decrease in the mRNA levels of the Akt1 inhibitor pseudokinase, TRIB3 (Nicoletti-Carvalho et al., 2010; Mondal et al., 2016) coincides with the recovery of cells from the stress due to smoke and with an increase in the levels of mmu-mito-ncR-805 in MLE12 cells (**Figure 5A**) (Blumental-Perry et al., 2020). We therefore asked if the bioenergetic effect of mmu-CR805 may culminate in the lower levels of TRIB3 mRNA. Forced expression of mmu-CR805 indeed resulted in a decrease in the levels of TRIB3 mRNA and protein as well as an increase in Akt1 phosphorylation (**Figures 5B–E**). Depletion of mmu-mito-ncRNA-805 with antisense inhibitor, AI805 [refer **Supplementary Figure 3** and (Blumental-Perry et al., 2020)] caused an increase in the expression of TRIB3 mRNA, but only in the stressed cells (**Figure 5B**). Without stress, the cells were able to function with lowered levels of mmu-ncR-805 without any correlation with TRIB3 levels (**Figures 5C,D** and **Supplementary Figure 3**).

We compared the recovery after acute CSE exposure of MLE12 cells transfected with non-targeting RNA, mmu-CR805, siRNA-TRIB3 (**Figures 5C–H**), and AI805. Both mmu-CR805 and siRNA-TRIB3 promoted post-stress cell growth, with mmu-CR805 being more efficient (**Figure 5I**), supporting the idea that mmu-CR805 has broader downregulation than that of the effects of TRIB3 mRNA. As expected, cells carrying AI805 grew slower after stress (**Figure 5I**). Therefore, one of the actions of mito-ncR-805 may culminate in the downregulation of TRIB3 expression, which in turn promotes higher activity of the Akt1 (Mondal et al., 2016) and cell health.

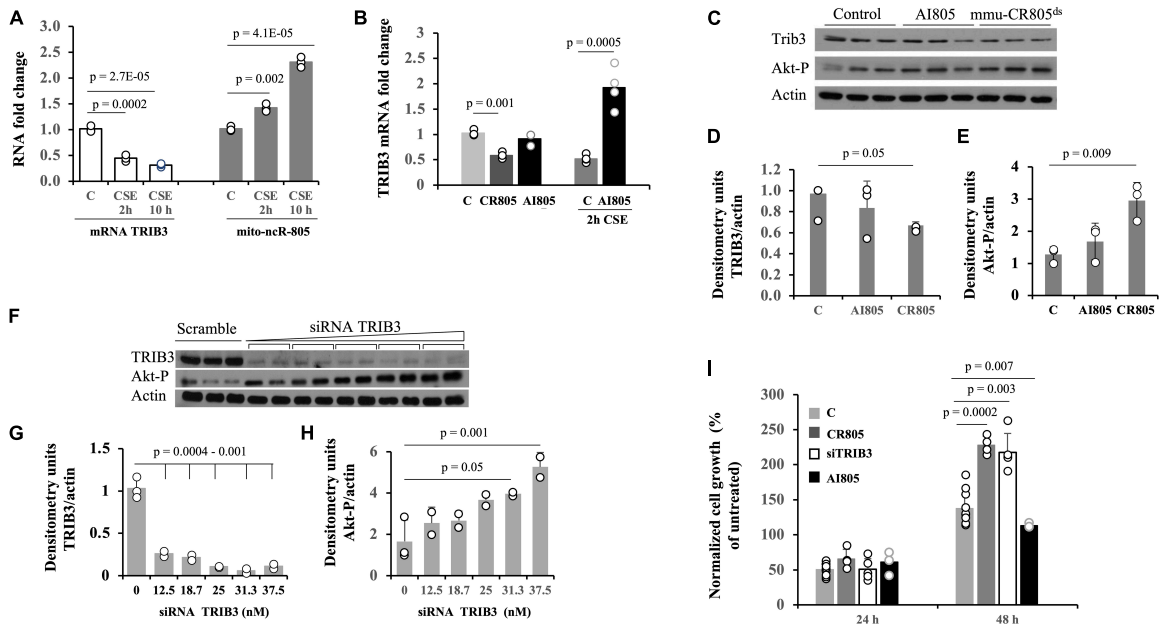

FIGURE 5 | Forced expression of mmu-CR805 results in lower abundance of Akt kinase inhibitor, TRIB3 mRNA. **(A)** The MLE12 cells were either exposed or not exposed to CSE, the RNA was extracted, and the expressions of TRIB3 and mmu-mito-ncR-805 were tested by RT-qPCR. **(B–E)** The MLE12 cells were transfected with mmu-CR805, AI805, or non-targeting RNA and were either stressed or not on exposure to CSE, and RNA or proteins were extracted to assess the expression of TRIB3. **(B)** Levels of TRIB3 mRNA as evaluated by RT-qPCR. **(C)** Levels of TRIB3 protein and Akt1 phosphorylation as evaluated by Western blotting. Graphs represent quantification of TRIB3 protein levels **(D)** and Akt1 phosphorylation **(E)**. **(F–H)** The MLE12 cells were transfected with either increasing concentrations of siRNA against TRIB3 (in duplicates [TRIB3 Silencer Select S105984]) or with non-targeting siRNA, and the efficiency of TRIB3 depletion was tested by evaluating TRIB3 protein levels *via* Western blotting. Since TRIB3 inhibits the activation of prosurvival kinase Akt1, the Akt kinase activation/phosphorylation was used as an additional parameter to evaluate TRIB3 downregulation. Actin was used as a loading control. Graphs represent quantification of TRIB3 protein levels **(G)** and Akt1 phosphorylation **(H)**; 25 μM of siRNA against TRIB3 was chosen for further experiments. **(I)** The MLE12 cells were transfected with mmu-CR805, siRNA-TRIB3, AI805, or non-targeting RNA; 24 h post-transfection, the cell numbers were counted to ensure that pre-smoke cell numbers did not differ between the groups. No significant changes were observed, as expected from the data presented in **Figure 2A**. Twenty-four hours post-transfection, the cells were either exposed or not to 10% of CSE for 30 min, washed, and returned to grow in their regular medium; the cell counts were recorded 24 and 48 h after exposure to CSE. All experiments are representative of three independent experiments performed with triplicate samples.

DISCUSSION

Mitochondrial stress and malfunction are common features of multiple human diseases, including cardiovascular, pulmonary, and neurodegenerative diseases (Mizumura et al., 2014; Galluzzi et al., 2016; Annesley and Fisher, 2019; Bader and Winklhofer, 2020; Jusic et al., 2020). Here, we demonstrated that the forced expression of the evolutionarily conserved fragments of mtDNA-encoded mmu-mito-ncR-805, mmu-CR805, and its human ortholog, hsa-LDL1, improves the mitochondrial metabolism and bioenergetics. Our findings suggest that mitochondrial ncRNAs, which were proposed to act as a communicator between different cellular compartments, can be considered as a potential therapeutic target in the restoration of mitochondrial function (Liang et al., 2021).

Many efforts were and are directed toward improving the mitochondrial function in multiple diseased states and during aging (Corona and Duchen, 2016; Brown et al., 2017; Tampaki et al., 2018; Zhang et al., 2020). These efforts can be summarized in a simplified way as the ones that improve mitochondrial function, such as small molecules and ligands that can activate transcription factors for anterograde signaling, such as NRF1 and PPARα, Ca^{2+} ion modulators, and cardiolipin targeting and protecting compounds (inner mitochondrial membrane-specific lipid cardiolipin is needed for the correct assembly and function of ETC complexes). Some of them are reported to be safe, but their efficacy needs further investigation and improvement. The other class of mitochondrion-targeting compounds includes ones that inhibit mitophagy, mito-fission, and the mitochondrial permeability transition pore (Brown et al., 2017). Attempts to use those to prevent mitochondrial loss produced controversial results, probably due to the physiological corrections of malfunctioning mitochondria, and more research is needed to assess their potential use.

Retrograde signaling molecules that are generated in and released from the mitochondria during mitochondrial stress can lead to adjustment and, at proper circumstances, lead to a successful restoration of mitochondrial function. Recent discoveries support this notion (Landerer et al., 2011; Kim K. H. et al., 2018; Kim S. J. et al., 2018; Blumental-Perry et al., 2020). Those molecules input the functional state of mitochondria into the cellular homeostasis network by activating the mechanisms outside the mitochondria. It

is to be noted that the open reading frames of such molecules, including mitochondrial ORF of the 12S rRNA type-c (MOTS-c) peptide, as well as SHLPs, are embedded within the mitochondrial RNR genes, the expression of which is tightly regulated and influences many aspects of the transcription and translation of the mitochondrial genome. Those peptides are currently in use as food supplements to prevent mitochondrial decline (Reynolds et al., 2021). The mito-ncR-805 is generated from the control region of the D-loop of the L strand of mtDNA, and SncmtRNAs and ASncmtRNAs are the recombined products of RNR genes (Landerer et al., 2011). Few up-to-date discovered retrograde signaling molecules are generated from the regulatory regions of the mitochondrial genome, strongly implying their governing function and importance in the communication between the genomes.

Small regulatory ncRNAs encoded by the mitochondrial genome (Rackham et al., 2011; Vendramin et al., 2017; Larriba et al., 2018) were suggested to be involved in communication between the mitochondria and the nucleus (Liang et al., 2021). For example, the mito-lncRNA, SncmtRNA, is observed in both the mitochondria and the nucleus and is shown to function in retrograde signaling (Landerer et al., 2011). We recently identified mito-ncR-805, which is generated from the light-strand promoter (LSP) in the D-loop regulatory region of mtDNA and relocates to the nucleus during adaptive stress. Conservation of non-coding sequences of the mitochondrial genome is low (Jansen, 2000; Zardoya, 2020). Accordingly, we found that an entire 70-nt mmu-mito-ncR-805 transcript is mouse-specific, but its first 20 nt demonstrates evolutionary conservation in the mitochondria of mammals. We therefore suggest that the 20 nt represents a functional bit, whereas the rest of the sequence has other functions, which are not conserved at the level of the sequence. To initiate studies into the possible function of the conserved region of mito-ncR-805, we overexpressed the CR of the mouse sequence as well as its human ortholog in both the mouse and the human cells, and evaluated the activity of the Krebs cycle, mitochondrial respiration, and the mitochondrial membrane potential. The forced expression of either mmu-CR805 or hsa-LDL1 increased those parameters in both the mouse and the human cells, although the ortholog oligos were somewhat less efficient than the species-specific ones. It is to be noted that when forcedly overexpressed, the magnitude of the effect of the full-length mouse transcript was very similar to that of the biological effects of its functional bit, mmu-CR805. On the basis of this observation, we concluded that the rest of the transcript may have either regulatory or stabilizing functions. Future research is needed to interrogate this hypothesis. Our findings support the idea that this region has functional significance and provide justification for future studies on the precise mechanism of the action of those functional bits in the mouse and human cells.

The forced overexpression system used in the present study did not enable us to determine the cellular compartment where the transfected oligo was active, because we detected it in the cytosol, the nucleus, and in some mitochondria. However, our previous data provided strong supporting evidence that mito-ncR-805 acts as a retrograde signaling molecule during stress from smoke, and its nuclear presence leads to changes in the expression of nuclear genes that encode mitochondrial proteins (Blumental-Perry et al., 2020). Indeed, the transcript levels of at least 14 nuclear genes that encode mitochondrial proteins were affected by the levels of mmu-mito-ncR-805. Those genes mostly encode the subunits of ETC complexes. Their induction by mmu-mito-ncR-805 and the subsequent increase in proteins they encode in the mitochondria can potentially explain the increase in the mitochondrial bioenergetics observed as a biological consequence of forced expression of functional bits of mmu-mito-ncR-805 or of its human ortholog, hsa-LDL1. Alternatively, there is a possibility that the transfected oligos are active in some mitochondrial compartment. We have not observed significant effects of the inhibition of mmu-mito-ncR-805 by AI805 on mtDNA replication or steady-state mitochondrial transcription or translation (Blumental-Perry et al., 2020). Nevertheless, the mmu-CR805 or its ortholog can potentially influence the activity of the ETC or affect the rates of transcription. Future research is needed to address this possibility.

The molecular mechanisms of CR805 function are unknown and need further investigation. Exposure to cigarette smoke is known to increase Akt1 activation (Nakayama et al., 2002). We associated the high levels of mito-ncR-805 with low expression of the pseudokinase TRIB3. We therefore, used TRIB3 levels as read out of CR805 activity. The TRIB3 is a multifunctional scaffolding protein that has been shown to coordinate multiple cellular signaling systems in a content-specific manner that can determine cellular fate (Ord and Ord, 2017; Stefanovska et al., 2021). We tested if a possible cellular outcome of high mmu-ncR-805 and CR805 is a low abundance of TRIB3 mRNA and protein. Indeed, high levels of CR805 resulted in lower levels of TRIB3. Cells with forced expression of CR805 had higher maximal respiration and spare respiratory capacity and grew faster than the control cells. Therefore, low TRIB3 mRNA is likely a result of a favorable cellular bioenergetic state induced by high levels of mmu-CR805. Cells with lowered levels of mito-ncR-805 (*via* the AI805 antisense inhibitor) had the same TRIB3 levels under unstressed conditions as cells with normal levels of mito-ncR-805. But low expression of mito-ncR-805 results in low maximal and spare respiratory capacities (Blumental-Perry et al., 2020), indicative of cells being close to their bioenergetics limit (Wang et al., 2018). When such cells experience stress, the levels of TRIB3 are significantly induced. Therefore, the action of mito-ncR-805 via its CR likely culminates in the coordination with other cellular systems important for mitochondrial function.

Interestingly, one of the TRIB3 functions is to inhibit Akt activation (Nicoletti-Carvalho et al., 2010). Akt1, when phosphorylated and activated in some systems, translocates into mitochondria and localizes within their membranes, where it can phosphorylate a number of mitochondrial residence proteins, including the α and β subunits of ATP synthase (Li et al., 2013). It would be interesting to see if mmu-CR805 contributes to

increased mitochondrial respiration by reducing TRIB3 mRNA and thus enabling Akt1 to increase the activity of ETC complexes.

In summary, it is tempting to suggest that mito-ncR-805 serves as a mitochondrion-derived signaling molecule that has evolved to trigger adaptive cellular responses through increased bioenergetics. We speculate that this adaptive pro-energy molecule might be used to mitigate mitochondrial malfunction common to multiple human diseases.

DATA AVAILABILITY STATEMENT

The original contributions presented in the study are included in the article/**Supplementary Material**, further inquiries can be directed to the corresponding author/s.

AUTHOR CONTRIBUTIONS

TM participated in the design of the experiments, performed fractionation, western blot analysis, transfections, cell counting, some seahorse experiments, participated in analysis of the images, and in the preparation of the manuscript. DT, Z-WY, and JZ conceived and analyzed bioenergetic experiments. VL performed evolutional conservation analysis. WS designed, performed, and participated in the analysis of high-resolution imaging. IB and EP performed metabolomics analysis. RJ completed Northern blot analysis and participated in the interpretation of the results. JF performed RT-qPCR analysis. MD'A performed the titration of the transfection efficiency. MH and YP participated in the project design and interpreted multiple results and participated in writing and editing of the manuscript. AB-P conceived, designed, and coordinated the research project, performed multiple experiments, generated and interpreted the data, supervised all aspects of the study and the manuscript. All authors contributed to the article and approved the submitted version.

FUNDING

This project was supported by a funding from the UBT Research Foundation to AB-P, the Gainard Golz research fund to YP, the National Institutes of Health grants R37-DK60596 and R01-DK53307 to MH, NCRR P20RR024485 to DT, and the American Cancer Society Institutional research grant #IRG-19-137-20 to JZ.

ACKNOWLEDGMENTS

We thank Andrew L. Degar for providing technical assistance in the initial stages of this project, Amber Worral (Multispectral Imaging Suite, Jacobs School of Medicine and Biomedical Sciences, University at Buffalo) for help with imaging, and Karen Dietz (Research and Graduate Education, Jacobs School of Medicine and Biomedical Sciences, University at Buffalo) for the editorial help.

SUPPLEMENTARY MATERIAL

The Supplementary Material for this article can be found online at: https://www.frontiersin.org/articles/10.3389/fphys.2022.772313/full#supplementary-material

Supplementary Figure 1 | (A) The RNA enriched with small RNAs was isolated, resolved on 15% of urea gels, and hybridized with probes complementary to the conserved region of mmu-mito-ncR-805. The MTHe membrane was stripped and reprobed with a U6-specific probe as a loading control. **(B)** The MLE12 cells were transfected with mmu-CR805 or non-targeting RNA and lysed, and the lysates were analyzed (total). Cytosolic fractions were obtained by separating crude mitochondria, which were further purified using Percoll gradient and treated with RNase I to remove non-mitochondrial RNAs. The RNAs were isolated from obtained fractions. Purity of the fractions was evaluated by comparing the relative expression levels of mtDNA-encoded mRNA of Rnr2, nucleus-encoded and localized Sno55-RNA, and cytosolic GAPDH mRNA with identical RNA inputs.

Supplementary Figure 2 | The MLE12 cells were transfected with FAM-labeled mmu-CR805, fixed, and stained for Tom20. Images were acquired at a magnification of 100 times and zoom of 3.37 times on a Leica TCS SP8 microscope with accelerated deconvolution. **(A)** Single plane of representative cell images, with two boxed areas that contain Tom20-labeled structures (1–2 and 3) and one boxed area through the nucleus (4). **(B)** Enlarged area 3 from **(A)**. **(C)** Graphs of relative red and green channel fluorescence intensity through the line-scanned region shown in **(B)**. **(D)** Enlarged area 4. **(E)** Graphs of a relative blue and green channel fluorescence intensity through the line-scanned region shown in **(D)**. **(F)** Line scans 5a–c were drawn to obtain the relative green channel intensity (FAM-labeled mmu-CR805) through cytoplasmic regions.

Supplementary Figure 3 | Efficiency of inhibition by AI805. The MLE12 cells were transfected with AI805 or non-targeting RNA; 24 h post-transfection, the RNA was extracted and analyzed for the expression levels of mmu-CR805 containing transcripts.

Supplementary Table 1 | Linescan analysis of green FAM-labelled mmu-CR805 and red (Tom20) signals.

Supplementary Table 2 | Metabolic analysis of TCA intermediates.

Supplementary Table 3 | Mitochondrial stress test kit data analysis.

REFERENCES

Annesley, S. J., and Fisher, P. R. (2019). Mitochondria in health and disease. *Cells* 8:680.

Bader, V., and Winklhofer, K. F. (2020). Mitochondria at the interface between neurodegeneration and neuroinflammation. *Semin. Cell Dev. Biol.* 99, 163–171. doi: 10.1016/j.semcdb.2019.05.028

Blanchette, M., Kent, W. J., Riemer, C., Elnitski, L., Smit, A. F. A., Roskin, K. M. et al. (2004). Aligning multiple genomic sequences with the threaded blockset aligner. *Genome Res.* 14, 708–715. doi: 10.1101/gr.1933104

Blumental-Perry, A., Jobava, R., Bederman, I., Degar, A. J., Kenche, H., Guan, B. J., et al. (2020). Retrograde signaling by a mtDNA-encoded non-coding RNA preserves mitochondrial bioenergetics. *Commun. Biol.* 3:626. doi: 10.1038/s42003-020-01322-4

Borgna, V., Villegas, J., Burzio, V. A., Belmar, S., Araya, M., Jeldes, E., et al. (2017). Mitochondrial ASncmtRNA-1 and ASncmtRNA-2 as potent targets to inhibit tumor growth and metastasis in the RenCa murine renal adenocarcinoma model. *Oncotarget* 8, 43692–43708. doi: 10.18632/oncotarget.18460

Brown, D. A., Perry, J. B., Allen, M. E., Sabbah, H. N., Stauffer, B. L., Shaikh, S. R., et al. (2017). Expert consensus document: mitochondrial function as a

therapeutic target in heart failure. *Nat. Rev. Cardiol.* 14, 238–250. doi: 10.1038/nrcardio.2016.203

Burzio, V. A., Villota, C., Villegas, J., Landerer, E., Boccardo, E., Villa, L. L., et al. (2009). Expression of a family of noncoding mitochondrial RNAs distinguishes normal from cancer cells. *Proc. Natl. Acad. Sci. U.S.A.* 106, 9430–9434. doi: 10.1073/pnas.0903086106

Cardamone, M. D., Tanasa, B., Cederquist, C. T., Huang, J., Mahdaviani, K., Li, W., et al. (2018). Mitochondrial retrograde signaling in mammals is mediated by the transcriptional cofactor GPS2 via direct mitochondria-to-nucleus translocation. *Mol. Cell* 69, 757–772. doi: 10.1016/j.molcel.2018.01.037

Cobb, L. J., Lee, C., Xiao, J., Yen, K., Wong, R. G., Nakamura, H. K., et al. (2016). Naturally occurring mitochondrial-derived peptides are age-dependent regulators of apoptosis, insulin sensitivity, and inflammatory markers. *Aging* 8, 796–809. doi: 10.18632/aging.100943

Corona, J. C., and Duchen, M. R. (2016). PPARgamma as a therapeutic target to rescue mitochondrial function in neurological disease. *Free Radic Biol. Med.* 100, 153–163. doi: 10.1016/j.freeradbiomed.2016.06.023

Costiniti, V., Bomfim, G. H., Li, Y., Mitaishvili, E., Ye, Z. W., Zhang, J., et al. (2020). Mitochondrial function in enamel development. *Front. Physiol.* 11:538. doi: 10.3389/fphys.2020.00538

Farfan, N., Sanhueza, N., Briones, M., Burzio, L. O., and Burzio, V. A. (2021). Antisense noncoding mitochondrial RNA-2 gives rise to miR-4485-3p by Dicer processing in vitro. *Biol. Res.* 54:33. doi: 10.1186/s40659-021-00356-0

Fernandez-Silva, P., Enriquez, J. A., and Montoya, J. (2003). Replication and transcription of mammalian mitochondrial DNA. *Exp. Physiol.* 88, 41–56.

Fessler, E., Eckl, E. M., Schmitt, S. I, Mancilla, A., Meyer-Bender, M. F., Hanf, M., et al. (2020). A pathway coordinated by DELE1 relays mitochondrial stress to the cytosol. *Nature* 579, 433–437. doi: 10.1038/s41586-020-2076-4

Galluzzi, L., Kepp, O., and Kroemer, G. (2016). Mitochondrial regulation of cell death: a phylogenetically conserved control. *Microb. Cell* 3, 101–108. doi: 10.15698/mic2016.03.483

Gao, S., Tian, X., Chang, H., Sun, Y., Wu, Z., Cheng, Z., et al. (2018). Two novel lncRNAs discovered in human mitochondrial DNA using PacBio full-length transcriptome data. *Mitochondrion* 38, 41–47. doi: 10.1016/j.mito.2017.08.002

Gao, X. H., Krokowski, D., Guan, B. J., Bederman, I., Majumder, M., Parisien, M., et al. (2015). Quantitative H2S-mediated protein sulfhydration reveals metabolic reprogramming during the integrated stress response. *Elife* 4:e10067. doi: 10.7554/eLife.10067

Gellerich, F. N., Gizatullina, Z., Gainutdinov, T., Muth, K., Seppet, E., Orynbayeva, Z., et al. (2013). The control of brain mitochondrial energization by cytosolic calcium: the mitochondrial gas pedal. *IUBMB Life* 65, 180–190. doi: 10.1002/iub.1131

Grek, C., and Townsend, D. M. (2014). Protein disulfide isomerase superfamily in disease and the regulation of apoptosis. *Endoplasmic Reticulum Stress Dis.* 1, 4–17. doi: 10.2478/ersc-2013-0001

Guo, X., Aviles, G., Liu, Y., Tian, R., Unger, B. A., Lin, Y. T., et al. (2020). Mitochondrial stress is relayed to the cytosol by an OMA1-DELE1-HRI pathway. *Nature* 579, 427–432. doi: 10.1038/s41586-020-2078-2

Jansen, R. P. (2000). Origin and persistence of the mitochondrial genome. *Hum. Reprod.* 15(Suppl. 2), 1–10.

Jusic, A., Devaux, Y., and Action, E. U.-C. C. (2020). Mitochondrial noncoding RNA-regulatory network in cardiovascular disease. *Basic Res. Cardiol.* 115:23. doi: 10.1007/s00395-020-0783-5

Kenche, H., Baty, C. J., Vedagiri, K., Shapiro, S. D., and Blumental-Perry, A. (2013). Cigarette smoking affects oxidative protein folding in endoplasmic reticulum by modifying protein disulfide isomerase. *FASEB J.* 27, 965–977. doi: 10.1096/fj.12-216234

Kenche, H., Ye, Z. W., Vedagiri, K., Richards, D. M., Gao, X. H., Tew, K. D., et al. (2016). Adverse outcomes associated with cigarette smoke radicals related to damage to protein-disulfide isomerase. *J. Biol. Chem.* 291, 4763–4778. doi: 10.1074/jbc.M115.712331

Kim, K. H., Son, J. M., Benayoun, B. A., and Lee, B. (2018). The mitochondrial-encoded peptide MOTS-c translocates to the nucleus to regulate nuclear gene expression in response to metabolic stress. *Cell Metab.* 28, 516–524. doi: 10.1016/j.cmet.2018.06.008

Kim, S. J., Mehta, H. H., Wan, J., Kuehnemann, C., Chen, J., Hu, J. F., et al. (2018). Mitochondrial peptides modulate mitochondrial function during cellular senescence. *Aging* 10, 1239–1256. doi: 10.18632/aging.101463

Landerer, E., Villegas, J., Burzio, V. A., Oliveira, L., Villota, C., Lopez, C., et al. (2011). Nuclear localization of the mitochondrial ncRNAs in normal and cancer cells. *Cell Oncol.* 34, 297–305. doi: 10.1007/s13402-011-0018-8

Larriba, E., Rial, E., and Del Mazo, J. (2018). The landscape of mitochondrial small non-coding RNAs in the PGCs of male mice, spermatogonia, gametes and in zygotes. *BMC Genomics* 19:634. doi: 10.1186/s12864-018-5020-3

Lee, C., Kim, K. H., and Cohen, P. (2016). MOTS-c: a novel mitochondrial-derived peptide regulating muscle and fat metabolism. *Free Radic Biol. Med.* 100, 182–187. doi: 10.1016/j.freeradbiomed.2016.05.015

Li, C., Li, Y., He, L., Agarwal, A. R., Zeng, N., Cadenas, E., et al. (2013). PI3K/AKT signaling regulates bioenergetics in immortalized hepatocytes. *Free Radic Biol. Med.* 60, 29–40. doi: 10.1016/j.freeradbiomed.2013.01.013

Liang, H., Liu, J., Su, S., and Zhao, Q. (2021). Mitochondrial noncoding RNAs: new wine in an old bottle. *RNA Biol.* 18, 2168–2182. doi: 10.1080/15476286.2021.1935572

Liu, B., Cao, J., Wang, X., Guo, C., Liu, Y., and Wang, T. (2021). Deciphering the tRNA-derived small RNAs: origin, development, and future. *Cell Death Dis.* 13:24. doi: 10.1038/s41419-021-04472-3

Liu, X., and Shan, G. (2021). Mitochondria encoded non-coding RNAs in cell physiology. *Front. Cell Dev. Biol.* 9:713729. doi: 10.3389/fcell.2021.713729

Liu, X., Wang, X., Li, J., Hu, S., Deng, Y., Yin, H., et al. (2020). Identification of mecciRNAs and their roles in the mitochondrial entry of proteins. *Sci. China Life Sci.* 63, 1429–1449. doi: 10.1007/s11427-020-1631-9

Livak, K. J., and Schmittgen, T. D. (2001). Analysis of relative gene expression data using real-time quantitative PCR and the 2(-Delta Delta C(T)) Method. *Methods* 25, 402–408. doi: 10.1006/meth.2001.1262

Meseguer, S. (2021). MicroRNAs and tRNA-Derived small fragments: key messengers in nuclear-mitochondrial communication. *Front. Mol. Biosci.* 8:643575. doi: 10.3389/fmolb.2021.643575

Mizumura, K., Cloonan, S. M., Nakahira, K., Bhashyam, A. R., Cervo, M., Kitada, T., et al. (2014). Mitophagy-dependent necroptosis contributes to the pathogenesis of COPD. *J. Clin. Invest.* 124, 3987–4003. doi: 10.1172/JCI74985

Mondal, D., Mathur, A., and Chandra, P. (2016). Tripping on TRIB3 at the junction of health, metabolic dysfunction and cancer. *Biochimie* 124, 34–52. doi: 10.1016/j.biochi.2016.02.005

Munoz-Carvajal, F., and Sanhueza, M. (2020). The mitochondrial unfolded protein response: a hinge between healthy and pathological aging. *Front. Aging Neurosci.* 12:581849. doi: 10.3389/fnagi.2020.581849

Nakayama, H., Numakawa, T., and Ikeuchi, T. (2002). Nicotine-induced phosphorylation of Akt through epidermal growth factor receptor and Src in PC12h cells. *J. Neurochem.* 83, 1372–1379. doi: 10.1046/j.1471-4159.2002.01248.x

Nashine, S., and Kenney, M. C. (2020). Effects of mitochondrial-derived peptides (MDPs) on mitochondrial and cellular health in AMD. *Cells* 9:1102. doi: 10.3390/cells9051102

Nashine, S., Cohen, P., Nesburn, A. B., Kuppermann, B. D., and Kenney, M. C. (2018). Characterizing the protective effects of SHLP2, a mitochondrial-derived peptide, in macular degeneration. *Sci. Rep.* 8:15175. doi: 10.1038/s41598-018-33290-5

Nicoletti-Carvalho, J. E., Nogueira, T. C., Gorjao, R., Bromati, C. R., Yamanaka, T. S., Boschero, A. C., et al. (2010). UPR-mediated TRIB3 expression correlates with reduced AKT phosphorylation and inability of interleukin 6 to overcome palmitate-induced apoptosis in RINm5F cells. *J. Endocrinol.* 206, 183–193. doi: 10.1677/JOE-09-0356

Ord, T., and Ord, T. (2017). Mammalian Pseudokinase TRIB3 in normal physiology and disease: charting the progress in old and new avenues. *Curr. Protein Pept. Sci.* 18, 819–842. doi: 10.2174/1389203718666170406124547

Quiros, P. M., Mottis, A., and Auwerx, J. (2016). Mitonuclear communication in homeostasis and stress. *Nat. Rev. Mol. Cell Biol.* 17, 213–226. doi: 10.1038/nrm.2016.23

Rackham, O., Shearwood, A. M., Mercer, T. R., Davies, S. M., Mattick, J. S., and Filipovska, A. (2011). Long noncoding RNAs are generated from the mitochondrial genome and regulated by nuclear-encoded proteins. *RNA* 17, 2085–2093. doi: 10.1261/rna.029405.111

Reers, M., Smith, T. W., and Chen, L. B. (1991). J-aggregate formation of a carbocyanine as a quantitative fluorescent indicator of membrane potential. *Biochemistry* 30, 4480–4486. doi: 10.1021/bi00232a015

Reynolds, J. C., Lai, R. W., Woodhead, J. S. T., Joly, J. H., Mitchell, C. J., Cameron-Smith, D., et al. (2021). MOTS-c is an exercise-induced mitochondrial-encoded regulator of age-dependent physical decline and muscle homeostasis. *Nat. Commun.* 12:470. doi: 10.1038/s41467-020-20790-0

Ro, S., Ma, H. Y., Park, C., Ortogero, N., Song, R., Hennig, G. W., et al. (2013). The mitochondrial genome encodes abundant small noncoding RNAs. *Cell Res.* 23, 759–774. doi: 10.1038/cr.2013.37

Scarpulla, R. C. (2008). Transcriptional paradigms in mammalian mitochondrial biogenesis and function. *Physiol. Rev.* 88, 611–638. doi: 10.1152/physrev.00025.2007

Schmittgen, T. D., and Livak, K. J. (2008). Analyzing real-time PCR data by the comparative C(T) method. *Nat. Protoc.* 3, 1101–1108. doi: 10.1038/nprot.2008.73

Shadel, G. S., and Clayton, D. A. (1997). Mitochondrial DNA maintenance in vertebrates. *Annu. Rev. Biochem.* 66, 409–435. doi: 10.1146/annurev.biochem.66.1.409

Shpilka, T., and Haynes, C. M. (2018). The mitochondrial UPR: mechanisms, physiological functions and implications in ageing. *Nat. Rev. Mol. Cell Biol.* 19, 109–120. doi: 10.1038/nrm.2017.110

Stefanovska, B., Andre, F., and Fromigue, O. (2021). Tribbles pseudokinase 3 regulation and contribution to cancer. *Cancers (Basel)* 13:1822. doi: 10.3390/cancers13081822

Tampaki, E. C., Tampakis, A., Droeser, R., Patsouris, E., and Kouraklis, G. (2018). Cabozantinib and Vandetanib in medullary thyroid carcinoma: mitochondrial function and its potential as a therapeutic target towards novel strategies to design anti-CSCs drugs. *Cancer Biol. Ther.* 19, 847–849. doi: 10.1080/15384047.2018.1433495

Vendramin, R., Marine, J. C., and Leucci, E. (2017). Non-coding RNAs: the dark side of nuclear-mitochondrial communication. *EMBO J.* 36, 1123–1133. doi: 10.15252/embj.201695546

Wang, S., Shi, X., Wei, S., Ma, D., Oyinlade, O., Lv, S. Q., et al. (2018). Kruppel-like factor 4 (KLF4) induces mitochondrial fusion and increases spare respiratory capacity of human glioblastoma cells. *J. Biol. Chem.* 293, 6544–6555. doi: 10.1074/jbc.RA117.001323

Wang, W. X., Prajapati, P., Nelson, P. T., and Springer, J. E. (2020). The mitochondria-associated ER membranes are novel subcellular locations enriched for inflammatory-responsive microRNAs. *Mol. Neurobiol.* 57, 2996–3013. doi: 10.1007/s12035-020-01937-y

Wang, W. X., Prajapati, P., Vekaria, H. J., Spry, M., Cloud, A. L., Sullivan, P. G., et al. (2021). Temporal changes in inflammatory mitochondria-enriched microRNAs following traumatic brain injury and effects of miR-146a nanoparticle delivery. *Neural Regen. Res.* 16, 514–522. doi: 10.4103/1673-5374.293149

Wang, W., Furneaux, H., Cheng, H., Caldwell, M. C., Hutter, D., Liu, Y., et al. (2000). HuR regulates p21 mRNA stabilization by UV light. *Mol. Cell Biol.* 20, 760–769. doi: 10.1128/MCB.20.3.760-769.2000

Wen, Y. A., Xiong, X., Scott, T., Li, A. T., Wang, C., Weiss, H. L., et al. (2019). The mitochondrial retrograde signaling regulates Wnt signaling to promote tumorigenesis in colon cancer. *Cell Death Differ.* 26, 1955–1969. doi: 10.1038/s41418-018-0265-6

Wikenheiser, K. A., Vorbroker, D. K., Rice, W. R., Clark, J. C., Bachurski, C. J., Oie, H. K., et al. (1993). Production of immortalized distal respiratory epithelial cell lines from surfactant protein C/simian virus 40 large tumor antigen transgenic mice. *Proc. Natl. Acad. Sci. U.S.A.* 90, 11029–11033. doi: 10.1073/pnas.90.23.11029

Yang, L., Kombu, R. S., Kasumov, T., Zhu, S. H., Cendrowski, A. V., David, F., et al. (2008). Metabolomic and mass isotopomer analysis of liver gluconeogenesis and citric acid cycle. I. Interrelation between gluconeogenesis and cataplerosis; formation of methoxamates from aminooxyacetate and ketoacids. *J. Biol. Chem.* 283, 21978–21987. doi: 10.1074/jbc.M803454200

Yen, K., Lee, C., Mehta, H., and Cohen, P. (2013). The emerging role of the mitochondrial-derived peptide humanin in stress resistance. *J. Mol. Endocrinol.* 50, R11–R19. doi: 10.1530/JME-12-0203

Zardoya, R. (2020). Recent advances in understanding mitochondrial genome diversity. *F1000Res.* 9:F1000 Faculty Rev-270. doi: 10.12688/f1000research.21490.1

Zhang, J., Xiang, H., Liu, J., Chen, Y., He, R. R., and Liu, B. (2020). Mitochondrial Sirtuin 3: new emerging biological function and therapeutic target. *Theranostics* 10, 8315–8342. doi: 10.7150/thno.45922

Zhang, J., Ye, Z. W., Chen, W., Manevich, Y., Mehrotra, S., Ball, L., et al. (2018). S-Glutathionylation of estrogen receptor alpha affects dendritic cell function. *J. Biol. Chem.* 293, 4366–4380. doi: 10.1074/jbc.M117.814327

Zhang, L., Zhang, J., Ye, Z., Manevich, Y., Ball, L. E., Bethard, J. R., et al. (2019). Isoflavone ME-344 Disrupts Redox Homeostasis and Mitochondrial Function by Targeting Heme Oxygenase 1. *Cancer Res.* 79, 4072–4085.

Conflict of Interest: The authors declare that the research was conducted in the absence of any commercial or financial relationships that could be construed as a potential conflict of interest.

Publisher's Note: All claims expressed in this article are solely those of the authors and do not necessarily represent those of their affiliated organizations, or those of the publisher, the editors and the reviewers. Any product that may be evaluated in this article, or claim that may be made by its manufacturer, is not guaranteed or endorsed by the publisher.

Advantages of publishing in Frontiers

OPEN ACCESS
Articles are free to read for greatest visibility and readership

FAST PUBLICATION
Around 90 days from submission to decision

HIGH QUALITY PEER-REVIEW
Rigorous, collaborative, and constructive peer-review

TRANSPARENT PEER-REVIEW
Editors and reviewers acknowledged by name on published articles

Frontiers
Avenue du Tribunal-Fédéral 34
1005 Lausanne | Switzerland

Visit us: www.frontiersin.org
Contact us: frontiersin.org/about/contact

REPRODUCIBILITY OF RESEARCH
Support open data and methods to enhance research reproducibility

DIGITAL PUBLISHING
Articles designed for optimal readership across devices

FOLLOW US
@frontiersin

IMPACT METRICS
Advanced article metrics track visibility across digital media

EXTENSIVE PROMOTION
Marketing and promotion of impactful research

LOOP RESEARCH NETWORK
Our network increases your article's readership